INFRA-RED STUDIES OF CARBON MONOXIDE CHEMISORBED ON IRON TRIAD ELEMENTS.

A Thesis

Presented to the

UNIVERSITY OF CAPE TOWN

For

The Degree of

DOCTOR OF PHILOSOPHY

By

LEONARDUS CORNELIUS FERREIRA
B.Sc. (Stell.), B.Sc. (HONS.)(S.A.), M.Sc. (O.F.S.)

Department of Chemistry,
University of Cape Town,
April, 1970.

TO MY WIFE.

CONTENTS

		Page Number
ACKNOWLEDGEMENTS		(ix)
SUMMARY		1
GENERAL INTRODUCTION		3
REFERENCES		5
UNITS USED IN ABSORPTION SPECTROSCOPY		7
REFERENCES		7
	CHAPTER 1.	
1.1	MOLECULAR SPECTRA	8
1.1.1	Introduction	8
1.1.2	The Mathematical Formulation of the Theory	12
1.1.3	The Rotator and Rotational Spectra	14
1.1.4	Vibrational Spectra	20
1.1.5	The Heisenberg Uncertainty Principle	25
1.1.6	The Probability of Transitions	26
1.1.7	Vibration - Rotation Spectra	28
1.1.7.1	Linear Polyatomic Molecules	30
1.1.7.2	Symmetrical Top Molecules	31
1.1.7.3	Spherical Top Molecules	33
1.1.7.4	Asymmetrical Top Molecules	33
1.2	MOLECULAR SYMMETRY	34
1.3	SPECTROSCOPICAL ANALYSIS	36
1.3.1	Qualitative Analysis	36
1.3.2	Quantitative Analysis	37
1.3.2.1	The Beer-Lambert Law	37
1.3.2.2	Deviations from Beer-Lambert's Law	38
1.3.2.2.1	Effects of Finite Slit Widths	38
1.3.2.2.2	Pressure Broadening Effects	39
REFERENCES		40

CHAPTER 2.

THE INFRA-RED SPECTRA OF ADSORBED MOLECULES (CO IN PARTICULAR) ON METALS.

		Page Number
2.1	INTRODUCTION	42
2.2	A LITERATURE REVIEW	42
2.3	SPECTRA OF CHEMISORBED CARBON MONOXIDE ON SUPPORTED NICKEL	43
2.4	SPECTRA OF CHEMISORBED CARBON MONOXIDE ON UNSUPPORTED NICKEL	47
2.5	SPECTRA OF CHEMISORBED CARBON MONOXIDE ON COBALT	49
2.6	SPECTRA OF CHEMISORBED CARBON MONOXIDE ON IRON	49
2.7	CONCLUSIONS	50
REFERENCES		92

CHAPTER 3.

THE INFRA-RED SPECTRA OF CARBON MONOXIDE ADSORBED ON NICKEL, COBALT, IRON AND NICKEL, COBALT AND IRON OXIDE SURFACES SUPPORTED ON COLLOIDAL SILICA — EXPERIMENTAL.

3.1	INTRODUCTION	51
3.2	APPARATUS	51
3.2.1	The Infra-red Spectrometer	51
3.2.2	Miscellaneous Equipment	52
3.2.3	The Die	52
3.2.4	An All Glass High Temperature Infra-red Cell	53

		Page Number
3.3	GAS PREPARATION	55
3.3.1	Purification of Hydrogen and Helium	55
3.3.2	Purification of Carbon Monoxide	55
3.3.3	General	55
3.4	ADSORBENT PREPARATION	55
3.4.1	Silica-Supported Nickel Catalysts	55
3.4.1.1	Type I	55
3.4.1.2	Type II	56
3.4.1.3	Type III	58
3.4.1.4	Potassium Promoted Silica-Supported Nickel Samples	59
3.4.2	Silica-Supported Cobalt Catalysts	59
3.4.2.1	Type I	59
3.4.2.2	Type III	59
3.4.2.3	Potassium Promoted Silica-Supported Cobalt Samples	60
3.4.3	Silica-Supported Iron Catalysts	60
3.5	THE SPECTRA	60
3.5.1	Recording The Spectra	60
3.5.2	Classifying The Spectra	61
3.5.2.1	Nickel	62
3.5.2.2	Cobalt	62
3.5.3	The Effects, on the Spectra, of the Method of Preparing the Discs.	62
3.5.3.1	Nickel	62
3.5.3.2	Cobalt	63
3.5.4	The Effects, on the Spectra, of Carbon Monoxide Pressure	
A:	On the Intensities of the Bands	64
3.5.4.A1	Nickel	64
3.5.4.B2	Cobalt	65
B:	On the Wave Numbers of the Bands	65
3.5.4.B1	Nickel	65
3.5.4.B2	Cobalt	65
3.5.5	The Effects, on the Spectra, of Temperature	66
3.5.5.1	Nickel — Unpromoted Samples	66
3.5.5.2	Nickel — Promoted Samples	66

		Page Number
3.5.6	The Effects, on the Spectra, of the Presence of Potassium in the Discs	66
3.5.6.1	Nickel	66
3.5.6.2	Cobalt	67
3.5.6	The Effects, on the Spectra, of adding Hydrogen	68
3.5.7.1	Nickel — Unpromoted Samples	68
3.5.7.2	Nickel — Promoted Samples	68
REFERENCES		92

CHAPTER 4.

DISCUSSION OF THE SPECTRA

4.1		INTRODUCTION AND THEORY	70
4.1.1		Terminal Ligands	70
4.1.2		Bridged Ligands	71
4.1.3		Chemisorption and Infra-red Frequencies	73
4.2		THE ASSIGNMENT OF THE INFRA-RED BANDS OBSERVED FOR CARBON MONOXIDE CHEMISORBED ON SILICA-SUPPORTED NICKEL AND COBALT	74
4.2.1		Nickel Spectra	75
4.2.1.1		Bridged Ligands	75
4.2.1.2		Terminal Ligands	76
	(1)	One Ligand per Site	76
	(2)	More Than One Ligand per Site	79
	(3)	Ligands Attached to Oxide Lattices	80
4.2.1.3		The Assignment of a Band at 1620 cm^{-1}	82
4.2.2		Cobalt Spectra	82
4.2.2.1		Bridged Ligands	82
4.2.2.2		Terminal Ligands	84
4.3		EFFECTS OF POTASSIUM	
	A:	On the Spectra Attributed to Metal Surfaces	84
	B:	On the Spectra Attributed to Metal Oxide Surfaces	86
4.3.B1		Nickel Oxide	86
4.3.B2		Cobalt Oxide	87

		Page Number
4.4	THE INTERACTION BETWEEN CHEMISORBED CARBON MONOXIDE AND HYDROGEN ON NICKEL SURFACES	88
4.4.1	Unpromoted Samples	88
4.4.2	Promoted Samples	89
4.4.3	Possible Reaction Mechanisms	89
REFERENCES		92
TABLE I		67
TABLE II		68
TABLE III		69
TABLE IV		108

APPENDIX 1.

Improving the Activity of Silica-Supported Nickel Type I. 96

APPENDIX 2.

On the Distribution of the Metal on the Surface of the Silica. 97

APPENDIX 3.

(A) The Preparation of Nickel Tetracarbonyl. 97

(B) The Infra-red Spectrum of Nickel Tetracarbonyl. 98

APPENDIX 4.

The Combined Influence of Carbon Monoxide Pressure and Time of Contact on the Spectra of CO Chemisorbed on Silica-Supported Nickel 98

APPENDIX 5.

(A) Carbon Monoxide Chemisorbed on Silica-Supported Nickel Type I. 99

(B) Carbon Monoxide Chemisorbed on Silica-Supported Nickel Type II. 100

APPENDIX 6.

Page Number

The Origin of Band C (Nickel)

(A) Experimental. 103

(B) Discussion. 104

APPENDIX 7.

On Which Band Appears First (Nickel). 105

APPENDIX 8.

The Influence of Temperature on the Bands ascribed to Chemisorbed Species (Nickel). 106

APPENDIX 9.

The Influence of Temperature and Hydrogen on the Chemisorbed CO Species. 107

APPENDIX 10.

Carbon Monoxide Chemisorption on Nickel Oxide. 111

APPENDIX 11.

Carbon Monoxide Chemisorbed on Potassium Promoted Nickel 112

APPENDIX 12.

The Effect of Temperature on Chemisorbed CO on Potassium Promoted Nickel. 113

APPENDIX 13.

The Interaction of Hydrogen and Carbon Monoxide on Potassium Promoted Silica-Supported Nickel. 113

Page Number

APPENDIX 14.

Carbon Monoxide Chemisorption on Cobalt Oxide.
Unpromoted Samples. 115
Promoted Samples. 116

APPENDIX 15.

(A) Carbon Monoxide Chemisorbed on Silica-Supported Cobalt Type I. 116

(B) Carbon Monoxide Chemisorbed on Silica-Supported Cobalt Type III. 117

APPENDIX 16.

Carbon Monoxide Chemisorbed on Potassium Promoted Cobalt. 117

REFERENCES 92

FIGURES

Fig. Number:	Follow on Page Number:
1	46
2	52
3	53
4	54
5	61
6	64
7	65
8	66
9 to 11	67
12	75
13 and 14	80
15 to 17	98
18 to 20	99
21 and 22	100
23 to 27	101
28 and 29	102

Fig. Number:	Follow on Page Number:
30	103
31 and 32	104
33	105
34 and 35	106
36 and 37	107
38 and 39	108
40 and 41	109
42	111
43 to 45	112
46 to 48	113
49 and 50	114
51	115
52 and 53	116
54 to 57	117

ACKNOWLEDGEMENTS

The author wishes to express his sincere appreciation to Messrs. The South African Coal, Oil and Gas Corporation Limited, Sasolburg, for the award of a Fellowship and other financial support and the University of Cape Town for providing the necessary academic and laboratory environment and equipment; in particular the staff of the Department of Chemistry, University of Cape Town, including his supervisor Dr. E.C. Leisegang, Professor of Theoretical and Inorganic Chemistry.

S U M M A R Y.

1. The infra-red spectra of carbon monoxide species chemisorbed on nickel and cobalt and on their oxides were observed and "measured"; leading to the following findings:-

(a) Carbon monoxide chemisorbed on nickel.

Band A: A broad band, 1700 to 2000 cm^{-1}, with main inflection points at about 1950 and 1820 cm^{-1}; ascribed to single carbon monoxide molecules adsorbed onto two nickel atoms in a bridged fashion.

Band B: Found at 2035 to 2050 cm^{-1}, but very often at 2040 cm^{-1}; ascribed to a single carbon monoxide molecule adsorbed onto a nickel atom in an edge or corner site, or in the 110 plane of the crystal.

Band C: Always found at 2058 cm^{-1}; ascribed to more than one carbon monoxide molecule on a single nickel atom.

Band D: Found between 2060 and 2090 cm^{-1}; ascribed to single carbon monoxide molecules adsorbed onto nickel atoms in planes, e.g. the 100 plane.

Band E: Found at 2100 to 2130 cm^{-1}; ascribed to single carbon monoxide molecules adsorbed onto single nickel ions in nickel oxide lattices.

Band F: Found at 2165 to 2195 cm^{-1}; ascribed to single carbon monoxide molecules adsorbed onto oxygen ions in nickel oxide lattices.

(b) Carbon monoxide chemisorbed on cobalt:

As (a) above, but with the following wave numbers:-

Band A: A broad band lying between 1800 and 2040 cm^{-1}; main inflection point found between 2015 and 2033 cm^{-1}, with minor inflection points at about 1960 and 1850 cm^{-1}.

Band B: Found between 2060 and 2073 cm^{-1}.

Band C: Found at about 2070 cm^{-1}, on top of Band B.

Band D: Found between 2090 and 2100 cm^{-1}.

2/.. .. .. ..

Band E: Found at about 2130 cm^{-1}.

Band F: Found at about 2180 cm^{-1}.

There exist well reasoned arguments for the above assignments of infra-red data to structural species.

2. Furthermore, the following factors were investigated:

(a) The addition of potassium to the metal, in the role of "promoter". Very significant shifts to lower wave numbers, especially for the most strongly held species (A, B and D in 1(a) and 1(b), above), were observed; showing that the presence of potassium decreased the bond order of the carbon to oxygen linkage with consequent increase, according to the theory, of the bond order of the carbon to metal linkage. Concentrations of potassium in excess of about 10% by weight led to decreased band intensities.

(b) The addition of potassium to the metal oxide. Small concentrations of potassium salts increase the activity with respect to chemisorption of carbon monoxide on nickel oxide; probably by producing surface defects which have the power of adsorbing carbon monoxide and oxidising it to carbon dioxide which can then be desorbed. A mechanism for the production of these defects is postulated. Above 2:100 K:Ni the potassium appears to poison the sites.

In the case of cobalt oxide the presence of potassium salts appears to poison the sites normally active for carbon monoxide chemisorption. However, in addition new active sites were formed, as evidenced by the appearance of a band.

(c) The addition of hydrogen with the carbon monoxide.
Hydrogen appears to interact with adsorbed carbon monoxide in mechanisms in which (i) the hydrogen must first be in the adsorbed state on B sites with some exclusion of linearly held B site carbon monoxide (thus the bridged A site carbonyl species abundance is relatively greater) and (ii) adsorbed hydrogen interacts with bridged carbonyl species forming methane; perhaps <u>via</u> a surface carbide intermediate. The presence of potassium inhibits methane formation perhaps because:

(i) The bridged species become more firmly bonded to the lattice and

(ii) The potassium inhibits hydrogen capture.

3. Carbon monoxide chemisorption on iron and iron oxide were very disappointing in that no infra-red bands were observed.

3/.. .. .. ..

GENERAL INTRODUCTION

Techniques involving heterogeneous catalysis are among the most important industrial processes known. The interaction of carbon monoxide and hydrogen on an iron catalyst to synthesise hydrocarbons, generally known as the FISCHER - TROPSCH process *1, is of particular interest.

* The FISCHER - TROPSCH process can occur at low pressure, about one atmosphere, but the synthesis process in general use is performed at a medium pressure, about 20 atmospheres. The latter was developed by FISCHER and PICHLER[2], and is therefore more correctly named the FISCHER - PICHLER process.

The South African Coal, Oil and Gas Corporation, Limited, Sasolburg, Orange Free State, Republic of South Africa, is the only company in the world to synthesise oil on a large scale, using low grade coal as the primary starting material. The raw materials used are water (source of hydrogen), air (oxygen) and coal (carbon). The coal is gassified by reaction with steam and oxygen at very high pressure and temperature (380 lb/in^2 and 1300 °C). This reaction is:

$$5C(s) + 4\,H_2O(g) + 2\,O_2(g) \longrightarrow 2CO + 4\,H_2 + 3CO_2 \quad -104 \text{ K. Cal. (+ other by products).}$$

The gas is purified according to techniques described elsewhere[1]. The synthesis (FISCHER - TROPSCH or FISCHER - PICHLER) reaction may be represented:

$$CO + H_2 + Fe \text{ (catalyst)} \longrightarrow \text{paraffinic and olefinic hydrocarbons, carbon dioxide and water.}$$

While these are the main reaction products, other hydrocarbons such as cyclic compounds and diolefins are produced in smaller concentrations[1].

The efficiency of the synthesis process is determined by factors of the kind:

(1) reactor design,

(2) temperature,

(3) pressure,

4/.. .. .. ..

(4) the ratio H_2 : CO,

(5) the concentrations of impurities,

(6) catalyst composition and its physical condition as a function, say, of prehistory, etc.

Nevertheless it is the gas-solid adsorption process that is of prime importance. For this reason it was found necessary, in setting up the process at SASOL, to make a study of the catalyst. SASOL has thus played a leading role in this field of research; in particular, the effects of chemical and structural promoters on the hydrogenation of carbon monoxide in the presence of iron catalysts were investigated by the Sasol Research Laboratory[9].

The synthesis process has been the subject of many studies; including kinetic, radioactive tracer, and gas adsorption investigations[3]. The study of the adsorption of gases on metals has provided many interesting results. Among the many techniques that have provided particularly useful and interesting results are: gas volumetric analysis in the determination of surface areas and pore sizes, electron microscopy, mass spectrometry, magnetic susceptibility measurements, field emission, conductivity, and spectroscopy[4]. However, few of these techniques furnish direct information about the structure of the chemisorbed species. In spite of a large number of chemisorption experiments reported in the literature, there still exists a challenging research field concerning the mechanism of the synthesis reaction. As will be seen in the next chapters, infrared spectroscopy has proven to be of some use in the determination of the structure of species existing at the gas-solid interphase.

Some of the previous workers[5] in the field of the chemisorption of carbon monoxide on metal surfaces claimed that at room temperature carbonyl ligands exist only as terminal groups, whereas other workers[6,7] supported the idea that both terminal and bridged carbonyl surface groups are adsorbed.

In consequence of this disagreement one of the main objectives of this research was to establish with greater confidence the structures of carbon monoxide species chemisorbed on metal surfaces at room and at elevated temperatures. Stable carbonyl species found at one temperature may be unstable at higher temperatures. Thus spectra taken at room temperature alone may lead to incorrect conclusions regarding the reaction mechanisms involved in the synthesis.

5/.. .. .. ..

On the other hand it is necessary to determine the structures of species existing at elevated temperatures for the reason that the synthesis reaction is performed at high temperatures. Since the chemisorption of carbon monoxide on metals is exothermic it may be expected that only the most strongly held species might be observed at elevated temperatures.

On the other hand carbonyl species held weakly to the metal surface at room temperature and not observed at high temperatures makes it necessary to study room temperature phenomena in order to avoid missing information possibly valuable in the elucidation of reaction mechanisms.

For the above reasons a thorough study was made first of the carbonyl species found at room temperature. Factors such as the effect of method of adsorbent preparation and carbon monoxide pressure on the spectra were studied and similar studies were continued at elevated temperatures.

It has been stated[8] that it is not possible to tell whether chemisorbed carbon monoxide, while on the surface, is able to react with hydrogen to form hydrocarbons. A second objective was therefore to determine the reaction mechanism involved in the hydrogenation of carbon monoxide in the presence of a metal catalyst. Positive results were obtained, making it possible to postulate reaction mechanisms for the formation of methane and carbon dioxide on the surface.

In the industrial synthesis process the effects of a chemical promoter, such as potassium, on the spectrum of hydrocarbon products, are well-known[1]. The nature of the chemical reactions which cause these effects are however, obscure. Thus, a third objective was to investigate the influence of potassium on the spectra and on the interaction between carbon monoxide and hydrogen. The results led to a better understanding of the role of a chemical promoter and gave greater confidence to the structural assignments made for carbonyl species chemisorbed on metal surfaces.

REFERENCES:

1. H.H. Storch, N. Golumbic and R.B. Anderson, The Fischer-Tropsch and Related Syntheses, John Wiley and Sons, Inc., New York, 1951.

2. O.G. Malan, J.D. Louw and L.C. Ferreira, Brennstoff-Chemie, No. 7, 209 - 212 (1961).

3. G. Blyholder and L.D. Neff, J. Phys. Chem., 66,1664 (1962).

6/.. .. .. ..

4. R.A. Gardner and R.H. Petrucci, J. Am. Chem. Soc., 82, 5051 (1960).

5. G. Blyholder, J. Phys. Chem., 68, 2772 (1964).

6. J.T. Yates, Jr., and C.W. Garland, ibid, 65, 617 (1961).

7. R.P. Eischens and W.A. Pliskin, Adv. in Cat., Vol. X, 2, Academic Press, Inc., New York, 1958.

8. G. Blyholder and L.D. Neff, J. Cat., 2, 138 (1963).

9. M.E. Dry, Brennstoff-Chemie, No. 7, 193-224 (1969).

UNITS USED IN ABSORPTION SPECTROSCOPY[1].

In order to prevent the text from becoming tedious, units have been omitted; where applicable these are included in the lists given below:

WAVE NUMBER UNIT:

Reciprocal centimetre or wave number is defined:

$$\nu = \frac{1}{\lambda} = \frac{\nu'}{c} \quad \text{cm}^{-1}$$

where λ is the wave length in cm ,

ν' is the frequency, i.e. the number of complete oscillations per second,

and c is the velocity of light ($c = 2.99793 \times 10^{10}$ cm sec.$^{-1}$ in "free" space).

In some expressions the rotational term value, $F_J = E_{J/hc}$ cm^{-1}, is used.

where E_J is the rotational energy in erg,

h is Planck's constant ($h = 6.6252 \times 10^{-27}$ erg sec.),

and J is the rotational quantum number (values of 0, 1, 2, ...).

The vibrational term value is given by, $G_v = E_{v/hc}$ cm^{-1},

where E_v is the vibrational energy in erg,

and v is the vibrational quantum number (values of 0, 1, 2 .....).

The vibrational - rotational term value, T (v,r), is expressed, in a first approximation, as the sum of the vibrational and rotational values (see the text) and, accordingly, has the units of cm^{-1}.

WAVE LENGTH UNITS:

1 Å	= 10^{-8} cm	(Å = Angström unit)
1 mμ	= 10^{-7} cm	(mμ = millimicron)
1 μ	= 10^{4} Å	(μ = micron)

ENERGY UNITS:

The most commonly used energy unit is the electron volt (e.v.):

1 e.v. = 1.60186×10^{-12} erg,

equivalent to 8065.98 cm^{-1}.

REFERENCE:

1. R.E. Dodd, Chemical Spectroscopy, Elsevier Publishing Co., Amsterdam, 1962.

CHAPTER I.

1.1 MOLECULAR SPECTRA

1.1.1 Introduction:

Chemical compounds interact with electromagnetic radiation, or emit radiation, so giving rise to molecular spectra; thus many display colour. In chemical spectroscopy, therefore, the radiation transmitted by (adsorption spectra), or emitted by (emission spectra), materials is analysed by means of an optical spectroscope or spectrometer, and the observations are correlated with matters of interest to the chemist. Spectrometers may be sensitive to radiation in almost any region of the spectrum, from X-rays through the ultra-violet and visible regions, to the infra-red and microwave regions. In addition electron spin and nuclear magnetic spectrometry have been developed as have Raman spectroscopy (observation of radiation emitted at right angles to the source of radiation) and spectro-polarimetry.

The present work is concerned with near infra-red absorption spectroscopy, i.e. the region of the spectrum immediately beyond the red. The technique is simply that of irradiating the sample with the broad band continuous radiation emitted by a hot body (e.g. Nernst filament or Globar) and analysing the transmitted radiation by means of prism and/or grating monochromation and suitable radiation detection (Golay cell, thermocouple, photo-conductive cell, etc.). In this way the intensities of different parts of the eletromagnetic spectrum may be compared and it can be observed precisely in what manner the sample absorbs electromagnetic energy.

The theory of spectroscopy remained a complete mystery until the advent (1900) of Planck's quantum theory and its application, side by side with Rutherford's work on the atom and the rapidly growing knowledge of atomic and molecular structure; viz. Bohr (1913) and others. At the same time recognition must be given to the experimentalists (Balmer (1885), Ritz (1908) and others) who had observed and measured atomic line spectra and related phenomena; and to the well established and generalised body of theoretical work termed "classical mechanics".

Bohr, Sommerfeld, etc. formulated the "old" quantum theory, representing a very revolutionary advance on classical mechanics. The older laws of mechanics, formulated by Newton, were found to be inadequate and were extended in order to encompass sub-atomic phenomena. Thereafter the modern theory of quantum mechanics was developed, starting in the late "twenties".

9/...Cl...C.1

It provides a completely radical generalisation of the mechanical properties of matter, including classical mechanics as a "special" case" as it were. There exist many excellent works (e.g. Pauling and Wilson's Introduction to Quantum Mechanics) on the subject and it would be out of place, here, to attempt more than to show an appreciation of those concepts considered of immediate relevance.

Thus we may, for the sake of not becoming involved in unnecessary detail, in the first instance, restrict our attention to brief consideration of absorption spectra in the region from the ultra-violet to the far infra-red.

Line spectra arise from the emission or absorption of discrete quanta of radiation corresponding to transitions between definite energy levels of matter. In an atom, such energy levels represent the different allowed states for the orbital electrons. Molecules too, absorb and emit energy in transitions between discrete electronic energy levels associated with molecular orbitals. There are further ways in which molecules can change their energy (which do not occur for atoms); namely intramolecular vibration and rotation of the molecule as a whole. Vibrational and rotational energies, like electronic, are quantized; so that only certain discrete levels are allowed.

The total energy of a molecule, excluding translational energy and neglecting gravitation, nuclear transitions, electron spin, etc., may thus be approximately expressed simply as the sum of the electronic, vibrational, and rotational contributions respectively, i.e.:

$$E = E_e + E_v + E_r \qquad 1.1.$$

The complete separation of the energy into three distinct, non-interacting categories is not always a good approximation to the truth. For example, the atoms in a rapidly rotating molecule are repelled from one another by centrifugal forces which can affect the character of their vibrations and anharmonic vibration operates on the rotational energy. However, the summation of the three different energies is very often valid to a good first approximation and the adoption of this simplification very often explains many of the observed characteristics of molecular spectra, so leading to valuable qualitative and quantitative information.

10/.. .. .. ..

Max Planck most brilliantly discovered the law whereby the phenomenon of the interactions between radiation and matter was placed upon a quantitative basis. An aspect of this quantum theory may be set out as follows:

On placing a molecule in an electromagnetic radiation field, a transfer of energy from the field to the molecule may occur if certain conditions are fulfilled; whereby the molecule may pass from one quantized state, E", to another E', with the gain of energy ΔE at the expense of radiation energy of frequency ν', such that

$$E' - E'' = \Delta E = h\nu' = hc/\lambda = hc\nu \qquad 1.2$$

where h is Planck's constant, λ and ν are the wave length and wave number, respectively, of the radiation, and c is the velocity of light.

When a molecule in the ground state absorbs radiation of frequency ν' it is said to be elevated to an excited state. Conversely, an excited molecule may revert to a lower state; losing energy ΔE which appears as radiation of frequency ν', and the molecule is said then to emit a photon of radiation of this frequency.

Equation 1.1 may be written as

$$(E' - E'') = (E'_e - E''_e) + (E'_v - E''_v) + (E'_r - E''_r) \qquad 1.3.$$

$$\therefore \quad \nu' = \nu'_e + \nu'_v + \nu'_r$$

where ν'_e, ν'_v, and ν'_r are the electronic, vibrational, and rotational frequency components of the absorption line in the electronic spectrum.

Gaseous molecules with permanent dipole moments are observed to exhibit line spectra in the far infra-red and microwave regions of the spectrum. These are assigned to energy changes between rotational levels of the molecule. Because they are line spectra the experimental evidence is in accord with Planck's concept that the energy levels must be discrete (*viz.* Bohr's postulate of the existence of stationary (energy states). If we consider a molecule of medium mass, by way of example, a rotational line is observed at about 20 cm^{-1} (*ca* 10^{-3} e.v.) and a number of further lines appear at higher wave numbers, spaced by about 20 cm^{-1}. The theory quantitatively relates, as will be seen later, the wave numbers of the lines to the moments of inertia of molecules. Thus, knowing the atomic masses (from mass spectrometry), interatomic distances and bond angles may in principle be calculated. As the complexity of molecular structure increases, however, the number of established

11/.. .. .. ..

entities tends to be insufficient for the calculation of all the molecular parameters, a disadvantage which may be minimised on consideration of molecular symmetry and by comparing the data for the isotopic derivatives of the same molecule; bond properties not being significantly sensitive to isotopic substitution. The accurate measurement of rotation spectra, mainly by precise microwave techniques, discloses second order effects to do with the non-rigidity of chemical bonds and related to the strength of the chemical bond.

In the nearer infra-red region of the spectrum intramolecular vibrational energies are excited. These correspond to the wave number region approximately 300 to 3,000 cm^{-1} (ca 0.04 to 0.4 e.v.). In the case of freely rotating gaseous molecules a rotational fine structure is evident in the vibration bands. Thus the spectra tend to yield the same information as do pure rotational spectra. However, it is no longer necessary that the molecule should have a permanent dipole in order to interact with radiation and the near infra-red technique thus yields data on a larger population of species. In order to excite vibrational transitions it is necessary that the vibration should be accompanied by a changing bond moment. Thus homopolar diatomic molecules, such as those of the gases H_2, N_2, O_2, do not yield near infra-red spectra. The measurement and analysis of vibrational spectra yield not only structural data, but accurate thermodynamic information on bond strengths.

Consider an N-atomic molecule. It will have 3N degrees of freedom of motion of which 3 are translational and generally 3 are rotational. Thus there will be 3N - 6 fundamental vibrational modes which characterise or "fingerprint" the species. Linear molecules have but 2 rotational modes so there are 3N - 5 vibrational degrees of freedom.

Molecular orbitals may be excited by even larger quanta of energies in the approximate range 2 to 10 e.v., corresponding to the visible and ultra-violet regions of the spectrum. Electronic spectra generally have vibrational bands which in turn, may display rotational fine structures.

Raman spectra also display pure rotational and vibration/rotation structures, and are complementary to absorption spectra in the sense that infra-red vibration bands are intense for polar bonds while Raman spectra are most intense for non-polar bonds.

Vibrational spectra are of particular interest in this work. Thus we see that if the molecules are free to rotate, as in gases, the

12/.. .. .. ..

vibration bands will have rotational fine structures, provided sufficiently high resolving power is used. These observations were found most useful in distinguishing between free gaseous species and similar species in the adsorbed state.

1.1.2 The Mathematical Formulation of the Theory:

While the most powerful mathematical methods of quantum mechanics employ a sophisticated algebra (see, for example the Methuen Monograph, "The General Principles of Quantum Theory" by G. Temple, 1934.) these techniques yield but a poor descriptive picture of the system of interest. Wave mechanics is possibly more readily grasped and is adequate to a good appreciation of the simpler systems. The quantum theoretical laws may be formulated in terms of a series of axioms leading to a procedure for applying the method of wave mechanics to atoms and molecules. The system is first described in classical terms, as a number of point masses, their coordinates and the operative forces. The total energy is written down as the sum of the kinetic energy, T, of the particles and of its potential energy, V. V is a function of the coordinates of the particles and involves electrostatic or other forces.

In the next step of the procedure the kinetic energies are written in the Hamiltonian form. In order to illustrate this point consider a single particle of mass, m, and velocity v_x in the x direction. The kinetic energy may be written $\frac{1}{2} mv_x^2$; i.e. as a function of velocity. The momentum of the particle, in the x direction, is defined by $p_x = mv_x$. Writing the kinetic energy in the Hamiltonian form simply involves the manipulation: $T = \frac{1}{2} mv_x^2 = (\frac{1}{2} m) (mv_x)^2 = p_x^2/2m$. The complete Hamiltonian function is simply the summation of the kinetic and potential energies, T + V, with the kinetic energy in the Hamiltonian form.

Now the Hamiltonian function is transformed into the appropriate Hamiltonian operator. This is accomplished by substituting a differential operator wherever momentum appears. For example the momentum p_x is replaced by $(-ih/2\pi)\, d/dx$, in which i is the square root of minus one and h is Planck's constant. Thus the Hamiltonian function $p_x^2/2m = V(x)$ becomes the operator $H = (-h^2/8\pi^2 m)\, d^2/dx^2 + V(x)$.

If the same procedure as above be applied to a particle of mass, m, free to move in all directions, its velocity, v, may be resolved into the three components, v_x, v_y and v_z in the directions, respectively, of a set of Cartesian coordinates. Extension of Pythagora's theorem

13/.. .. .. ..

shows, since velocity is a vector quantity, that $v^2 = v_x^2 + v_y^2 + v_z^2$. Hence the kinetic energy is given by $p^2/2m = \frac{1}{2} mv^2 = \frac{1}{2m} (v_x^2 + v_y^2 + v_z^2)$ $= (p_x^2 + p_y^2 + p_z^2)/2m$; in which p is the "overall" momentum and p_x, p_y and p_z are the components along the three axes of space. In this instance it follows that the appropriate Hamiltonian operator will be

$$H = (-h^2/8\pi^2 m) \nabla^2 + V(x, y, z), \text{ in which}$$
$$\nabla^2 = (\partial^2/\partial x^2 + \partial^2/\partial y^2 + \partial^2/\partial z^2).$$

The objective of the exercise is to discover the properties of the Hamiltonian operator and to interpret the results as appropriate to the system under study. This is done by solving Schrödinger's first or amplitude equation, namely:

$$H\psi = E\psi$$

where ψ or $\psi(x, y, z)$, called a "wave function" or <u>eigenfunction,</u> is a function of the coordinates of the system and its square (or better $\psi\psi^*$, where ψ^* is the complex conjugate of ψ — i.e. wherever i appears in ψ it is replaced by -i) represents the probability distribution, i.e. the shape of the system.

$\Psi(x, y, z, t)$, where t is time, is given by the product of the two factors $\psi(x, y, z,)$ and $\phi(t)$. $\phi(t) = e^{-2\pi i\nu t} = e^{-2\pi iEt/h}$ represents one of the axioms. A knowledge of the form of Ψ, and of the way in which electromagnetic radiation may perturb the system, enables the calculation of the probability of photon capture or of photon emission.

E, in Schrödinger's equation, and above is the "real" energy of the system, accessible to experimental measurement. E values are called <u>eigenvalues</u>.

Schrödinger's equation is a second order differential equation, generally yielding an infinite number of solutions. In order for the method to be useful the solutions have to be restricted to well behaved wave functions or eigenfunctions, i.e. ψ must be finite and single valued for all permitted values of the coordinates. Such solutions are said to belong to the appropriate energy eigenvalues.

Naturally the method is more elaborate and sophisticated than indicated here, but the intention was simply to outline the main elements of the first principles of the procedure. However, before proceeding, a number of concepts must be mentioned. The probability of existence, within the interval dx, of a one dimensional system is $\psi^*\psi dx$.

More generally, since the total probability of a system must be unity,

$$\int_{\text{all space}} \psi^{*} \psi \, dx dy dz = 1.$$

This is the normalising condition and permits the calculation of the absolute magnitude of wave functions.

Furthermore Heisenberg Uncertainty Principle and the matter of Schrödinger's second, time dependent, equation and the question of the probabilities of energy transitions require to be considered. These concepts are best left till a little later.

1.1.3 The Rotator and Rotational Spectra:

We may first consider the simple case of a diatomic molecule. In order to gain ready appreciation of the main quantum mechanical considerations, it is customary to first consider the "rigid rotator" approximation, i.e. a system comprised of two mass points m_1 and m_2 (the atomic masses of the diatomic molecule), separated by the fixed distance, r_o.

Since atomic nuclei are relatively very small and contain the greater part of the atomic mass, and because the electron density is mostly symmetrically disposed about the atomic centre, the point mass approximation is a very good one.

In order to simplify the mathematics the above dumbbell model may be replaced by a reduced mass point (μ) model in which this single mass point, given by $\mu = m_1 m_2/(m_1 + m_2)$, rotates at a fixed distance, r_e from the fixed origin. Thus the moment of inertia of the system, about any axis passing through the centre of mass of the dumbbell model, and perpendicular to its axis, is given by:

$$I = \mu r^2 \qquad 1.4.$$

The classical energy of such a rotator is purely kinetic (i.e. zero potential energy); viz.:

$$E_{\text{classical}} = \tfrac{1}{2} \mu v^2 = \tfrac{1}{2} \mu r^2 w^2 \qquad 1.5$$

where v = tangential velocity (in a circular orbit), r = radius of orbit and $w = v/r$ = angular velocity. Incidentally, the frequency of rotation will be $\nu'_{\text{classical}} = v/2\pi r \ \text{sec}^{-1}$ (since each rotation generates 2π radians) so that $w = 2\pi \nu'_{\text{classical}}$.

15/.. .. .. ..

The angular momentum of the system will be $p = Iw$ and, in order to write the classical energy in Hamiltonian form we rearrange the algebra as follows:-

$$E_{classical} = \tfrac{1}{2} Iw^2 = (1/2\ I)\ (I\ w)^2 = p^2/2\ I \qquad 1.6.$$

Let θ be the angular coordinate of μ, rotating in a plane. Now we are in a position to transform the result into the appropriate Hamiltonian operator, by substituting $-\ i\ h/2\pi \cdot d/d\theta$ for p, i.e.

$$H = -\frac{h}{8\pi^2 I}\frac{d^2}{d\theta^2} \qquad 1.7.$$

The Schrödinger equation is thus:

$$\left(-\frac{h^2}{8\pi^2 I}\frac{d^2}{d\theta^2}\right)\ \psi(\theta) = E\psi$$

Solving this, $\psi = Ne^{-iM\theta}$ in which $M = \pm 2\pi\sqrt{2IE}/h$. being confined to the limits 0 to 2π, and in order that ψ be single valued, $e^{iM\theta} = e^{iM(\theta + 2\pi)}$. Hence

$e^{i2\pi M} = 1$, which is only true if M is a positive or negative integer, ... $-2, -1, 0, 1, 2,$ ..... .

Thus $E = (h^2/8\pi^2 I)M^2$

In the above, N is the normalization factor and can be evaluated by considering that the probability for the existence of the system somewhere in space must be unity, namely:

$$\int_0^{2\pi} \psi^* \psi\ d\theta = N^2 \int_0^{2\pi} d\theta = 1$$

Hence $N = (1/2\pi\ )^{\frac{1}{2}}$.

The above conclusions were reached on the basis of the "old" quantum theory. However, as will be seen now, more sophisticated theoretical considerations give the correct eigenvalues.

More generally, in three dimensions, $d^2/d\theta^2$ (in equation 1.7) may be replaced by ∇^2 (the square of the three dimensional operator), so that the Schrödinger equation, using the polar coordinates of the reduced mass, will be:

16/.. .. .. ..

$$\frac{\partial^2\psi}{\partial r^2} + \frac{2}{r}\frac{\partial\psi}{\partial r} + \frac{1}{r^2\sin\theta}\frac{\partial}{\partial\theta}\left(\sin\theta\frac{\partial\psi}{\partial\theta}\right) + \frac{1}{r^2\sin^2\theta}\frac{\partial^2\psi}{\partial\phi^2} + \frac{8\pi^2\mu E\psi}{h^2} = 0 \qquad 1.8.$$

On solving the above equation the permissible rotational energy are found to be:

$$E_J = \frac{h^2}{8\pi^2 I} \cdot J(J+1) \qquad 1.9$$

in which J is defined as the rotational quantum number and may have the integral values 0,1,2,3, ... etc.

The energy difference between two energy states E' and E" is given by 1.2, namely:

$$\Delta E = E' - E'' = hc\nu$$

From equation 1.9, therefore:

$$\Delta E = \frac{h^2}{8\pi^2 I}\left[J'(J'+1) - J''(J''+1)\right] \qquad 1.10.$$

Combination of 1.2 and 1.10 gives the wave number

$$\nu_r = B\left[J'(J'+1) - J''(J''+1)\right] \qquad 1.11$$

where B is called the rotational constant and has the value $h/8\pi^2 Ic$.

The selection rules which apply to pure rotational transitions are that the change in the rotational quantum number ΔJ be ± 1, but only for molecules which have permanent dipole moments. For molecules which do not have permanent dipole moments, the selection rule is, $\Delta J = 0$, and consequently such molecules do not display pure rotational spectra, as is confirmed by experiment.

The selection rule for diatomic molecules undergoing purely rotational changes is therefore $\Delta J = \pm 1$. Simplifying 1.11 by putting $J' = J + 1$ and $J'' = J$, we have:

$$\nu_r = 2B(J+1), \quad J = 0,1,2, \ldots\ldots \qquad 1.12.$$

This equation applies to absorption rotational spectra.

The separation between lines is obviously given by:

$$\Delta\nu_r = 2B \qquad 1.13.$$

17/.. .. .. ..

From equation 1.13 it follows that the pure rotational spectrum furnishes a means of measuring the moment of inertia and hence, the internuclear separation of the diatomic molecule. This is achieved in the technique of far infra-red spectroscopy or, better (because of the very high precision of measurement), in microwave spectroscopy.

The moment of inertia of a rigid polyatomic molecule about any axis passing through the centre of mass is defined by

$$I = \sum_{i=1}^{i=n} m_i r_i^2 \qquad 1.14$$

where r_i is the perpendicular distance of the i th nucleus from the centre of mass of the system comprised of n atoms. This means that three different moments of inertia are in general possible in the directions of the principal axes of the molecule, a, b and c; thus the moments may be symbolised as I_a, I_b and I_c respectively. Polyatomic molecules may be classified into four groups, according to their symmetry properties, namely:

(i) Asymmetric top molecules, for which $I_a \neq I_b \neq I_c$

(ii) Symmetric top molecules, for which $I_a = I_b \neq I_c$ (I_a and $I_c \neq 0$)

(iii) Spherical top molecules, for which $I_a = I_b = I_c$

(iv) Linear molecules, for which $I_a = I_b$ and $I_c = 0$.

Equation 1.9 is also valid for linear polyatomic molecules and for spherical top rotators which each have only one numerical value for their moments of inertia. Spherical top molecules do not generally, because of their high symmetry, have permanent dipole moments and hence, have no observable rotational spectra.

According to 1.12, pure rotational spectra should consist of equidistantly spaced lines. In practice this is not found for there is a convergence of the lines with increasing J. It was found empirically that an equation of the form

$$\nu_r = a\,m - f\,m^3 \qquad 1.15$$

fitted the wave numbers of experimentally observed lines. An expression of the form of 1.15 is obtained when a non-rigid rotator model is assumed. Actually, no real molecule can be considered to be rigid, and equation 1.9 is not valid. Theory shows that the rotational term for linear molecules is given to a far better approximation,

18/.. .. .. ..

sufficient for the interpretation of the most accurate experimental measurements, by:

$$F(J) = BJ(J+1) - D_J J^2 (J+1)^2 \qquad 1.16.$$

The last term in this expression provides for the centrifugal distortion effects, i.e., account is taken of a slight dependence of the moment of inertia upon J. In classical terms this means that I increases slightly as the molecule rotates more rapidly. The centrifugal distortion coefficient, D_J, is very small relative to the magnitude of the rotational constant, B, and the last term of 1.16 may often be neglected for small J values. As may be expected the magnitude of the constant, D_J, depends upon the vibration frequency, ν' , of the molecule, and if the harmonic oscillator model is used:

$$D_J = 4B^3/(\nu')^2 \qquad 1.17.$$

The selection rule $\Delta J = \pm 1$ still applies with rigidity to the non-rigid rotator, so that putting $J \longrightarrow J+1$ (this being the only change which gives rise to absorption of radiation in the case of linear molecules), the rotational wave numbers (using 1.16 and Planck's law) are:

$$\nu_r = 2B(J+1) - 4D_J (J+1)^3 \qquad 1.18.$$

The theory is thus in excellent agreement with the empirical finding of 1.15. The lowest rotational wave number occurs for J" = J = 0, namely $2B - 4D_J$ cm^{-1}. The lines of the rotational spectrum are separated by approximately 2 B. The even spacing is however, destroyed by the centrifugal stretching term $4D_J (J+1)^3$, which is small for low J values, but becomes significant usually for J values above ten.

Consideration of the eigenfunctions shows that the degeneracy of a rotational level of a linear molecule is (2 J + 1). Expression 1.16, for a linear molecule, is also valid for a spherical top, but in place of the (2 J + 1) degeneracy there is a degeneracy of $(2J+1)^2$. This arises because in addition to the (2 J + 1) space degeneracy of J there is a (2 J + 1) degeneracy with respect to a fixed direction in the molecule as a result of its high symmetry.

For symmetrical tops a second moment of inertia, and a second angular quantum number, K, must of course be introduced and 1.9 is no longer adequate. J now determines the total angular momentum and K determines its component along the unique axis of the molecule.

The eigenfunctions may be expressed, to a first approximation, in the form:

$$F_{JK} = BJ(J+1) + (A - B)K^2 \text{ cm}^{-1} \qquad 1.19$$

where $J = 0,1,2 \ldots\ldots$, $K = 0,1,2 \ldots\ldots\ldots J$,

$$A = \frac{h}{8\pi^2 c I_a} \quad \text{and} \quad B = \frac{h}{8\pi^2 c I_b}$$

For $J \longrightarrow J+1$ the wave numbers of absorption lines are again given by $\nu = 2B(J+1)$.

Equation 1.19 again corresponds to the assumption of a rigid molecule and additional terms must be introduced to account for the effects of centrifugal stretching, when:

$$F_{JK} = BJ(J+1) + (A - B)K^2 - D_{JJ}J^2(J+1)^2 - D_{JK}J(J+1)K^2 - D_{KK}K^4 \qquad 1.20$$

and the wave number of the lines in the rotational spectrum are:

$$\nu = 2B(J+1) - 4D_J(J+1)^3 - 2D_{JK}(J+1)K^2.$$

The last term in the above shows a splitting of each line into $(J+1)$ components, increasing with increasing J and K.

For asymmetric tops, all three principal moments of inertia are different. The classical motion of such a body is very complicated and no simple formula can be given for the energy levels and only two limiting cases will be discussed.

Let the three principal moments of inertia be I_a, I_b and I_c in order of increasing magnitude.

In one limiting case, in which $I_b = I_c$ (prolate symmetric top), the eigenvalues may be expressed as before namely:

$$F_{JK} = BJ(J+1) + (A - B)K^2 \qquad 1.19a$$

In the second limiting case, in which $I_b = I_a$ (oblate symmetric top), C replaces A and:

$$F_{JK} = BJ(J+1) + (C - B)K^2 \qquad 1.21$$

where $C = \frac{h}{8\pi^2 c I_c}$.

In 1.19 and 1.21, $J = 0,1,2,\ldots\ldots\ldots$, and $K = 0,1,2,\ldots\ldots\ldots J$.

Instead of the (J + 1) degeneracy as in the case of the symmetric top, there are now (2J + 1) different energy levels. This arises because in passing from the symmetric top to the asymmetric top there is no longer a preferred direction in the molecule which carries out a simple rotation about J.

The energy levels for the prolate and oblate symmetric tops may be plotted on the extreme left and right of a graph, respectively. The energy levels in the intermediate cases (asymmetric tops) may be obtained to a rough approximation, simply by connecting by smooth curves the levels of a given J on the left, without intersection, with corresponding levels on the righthand side.

1.1.4 Vibrational Spectra:

The dumbbell model of the diatomic molecule, simplified to the reduced mass model, may also be used as a basis for understanding vibration. We are now concerned with the two atoms of the molecule oscillating along the molecular axis, i.e. with the reduced mass point, $\mu = m_1 m_2/(m_1 + m_2)$ vibrating in the x direction. Assuming simple harmonic motion, i.e. a sine wave oscillating, is the same as assuming Hooke's law, namely that the restoring force will oppose displacement (negative sign) and its magnitude will be proportional to displacement, viz.:

$$F = - kx$$

where F = force, k = force constant and x = displacement.

According to classical mechanics, force is given by the product of mass and acceleration so that:

$$- kx = m. \, d^2x/dt^2$$

where t is time. The well known solution of this second order differential equation is:

$$x = x_o \sin 2\pi \nu' t$$

where x_o is the amplitude of oscillation and ν' its classical vibration frequency. It follows that:

$$\nu' = (1/2\pi) (k/\mu)^{\frac{1}{2}} \qquad 1.22.$$

Force, being the negative differential of the potential energy, V(x), the potential energy of the system is given by:

$$V = \tfrac{1}{2} k x^2 = 2\pi^2 \nu'^2 x^2 \qquad 1.23.$$

21/.. .. .. ..

The total classical energy of this conservative system must therefore be $\frac{1}{2}\mu v^2 + \frac{1}{2} k x^2 = p^2/2\mu + \frac{1}{2} k x^2$, where p (or p_x) = μv is the x momentum of the reduced mass particle. It follows that the Hamiltonian operator is $-(h^2/8\pi^2\mu)\, d^2/d x^2 + \frac{1}{2} k x^2$ and that the appropriate Schrödinger equation will be:

$$\left(-\frac{h}{8\pi^2\mu}\frac{d}{dx^2} + \frac{1}{2} k x^2\right)\psi(x) = E\psi(x) \qquad 1.24.$$

Solution of this equation yields the appropriate eigenfunctions as a function of the vibrational quantum number v = 0,1,2 .... and with three factors, namely normalizing constants, Hermite polynomials of order v and an exponential factor. These belong to the eigenvalues:

$$E_v = (v + \tfrac{1}{2})\, h\nu' \qquad 1.25.$$

in which ν' is the classical frequency of vibration, and in which v = 0,1,2,3 ..... and is termed the vibrational quantum number.

It follows that the zero point vibrational energy is not zero, but $\frac{1}{2} h\nu'$ and that the separation of successive energy levels is $h\nu'$. According to these results the lines of a pure vibrational spectrum should be equidistantly spaced; however, the approximation is but a poor one as the motion is anharmonic.

As the heteronuclear diatomic molecule vibrates, its dipole moment vector also changes with the same frequency. Thus if it be bathed in electromagnetic radiation, the vibrating dipole moment vector will tend to interact with the oscillating electric vector of that radiation having the same frequency. Energy may then pass from the radiation field to the molecule. As plausible as these thoughts may be they are nevertheless somewhat classical and perhaps classical analogy can be carried too far. By coincidence, in order to excite the molecule from level v to v + 1, the energy increment is approximately $h\nu'$ (as shown above), i.e. in "sympathy" with the vibration frequency. Homonuclear diatomic molecules have no changing dipole moment to interact with radiation and hence do not display infra-red spectra.

Let the time dependent eigenfunctions of the simple harmonic oscillator be given by

$$\psi(x, t) = \psi(v) \cdot \phi(t) \qquad 1.26$$

where $\psi(v)$ are amplitude functions, dependent on x only and of order v, and the factor $\phi(t)$, a function of time, t, only, may be written

$$e^{-i2\pi Et/h}, \qquad \nu' = E/h.$$

22/.. .. .. ..

We represent the capture of a photon in the terms $\Psi_n + h\nu' \longrightarrow \Psi_m$ in which n and m designate two different states of the oscillator.

The potential energy of the system ($V = \frac{1}{2} k x^2$) will be perturbed by the presence of radiation and may now be written V + v, where v is a small potential supplied by the radiation. The total eigenfunction may now be written $\Psi = c_n\Psi_n + c_m\Psi_m$, in which the coefficients are functions of time. If it is assumed that the perturbation is small, i.e. $V \gg v$, Schrödinger's second equation reduces to:

$$\left(-\frac{h^2}{8\pi^2\mu} \cdot \frac{\partial}{\partial x^2} + V\right)\Psi + v\Psi = \frac{ih}{2\pi} \cdot \frac{\partial\Psi}{\partial t}.$$

Mathematical operations now yield the result:

$$\frac{dc_m}{dt} = \frac{-i2\pi}{h}\left(c_n\int\Psi_m^* v\,\Psi_n\,dx + c_m\int\Psi_m^* v\,\Psi_m\,dx\right)$$

in which the symbol $\int$ signifies integration over the whole space accessible and v is the perturbing potential operator. dc_m/dt provides a measure of the rate of transfer from the lower (n) to the upper (m) state. Initially, when $c_m = 0$, it is clear that transition cannot occur unless $v \neq o$.

If $v = E_x ex$, where e is an electric charge and E_x has the form $2 E_o \cos 2\pi\nu' t$, dc_m/dt may be expanded and c_m evaluated. It is then readily seen that the transition $E_n \longrightarrow E_m$ can only occur when $E_m - E_n = h\nu'$, i.e. when Planck's law or the "Bohr frequency condition" is obeyed. Furthermore the probability of transitions proves proportional to time of irradiation, to the intensity (E_o^2) of the radiation and to the transition moment $M_x = e\int\Psi_m x\,\Psi_n\,dx$, where x is the "displacement operator". The selection rule for the simple harmonic oscillator may be shown to be, $\Delta v = \pm 1$.

Rewriting 1.25 in order to define the value of the vibrational term,

$$G(v) = (v + \tfrac{1}{2})\ \nu_o\ cm^{-1}$$

where $\nu_o = \nu'/c$ and v = 0,1,2 .....

and combining this with the selection rule ($\Delta v = +1$) for adsorption, the absorption spectrum of the heteronuclear diatomic molecule will consist of one line of wave number given by:

$$\nu = G(v = v + 1) - G(v = v) = \nu_o \qquad 1.27.$$

23/.. .. .. ..

From equation 1.27 it is possible to interpret spectra in terms of molecular energy levels and the theory gives quantitative information on the restoring force constant of the molecule, i.e. the strength of the chemical bond.

The selection rule $\Delta v = \pm 1$ is derived on the assumption that the vibrations are harmonic and that they are free from the disturbing effects of neighbouring molecules. This is not strictly the case and consideration of the anharmonic oscillator model shows that Δv may take any integral value, but as $\Delta v = \pm 2, \pm 3$, etc. the probability of transition falls very rapidly. When $\Delta v = 1$ we speak of the fundamental transition, $\Delta v = 2$ defines the first overtone or second harmonic, $\Delta v = 3$ the second overtone or third harmonic, etc. In fact, as will be seen presently, the frequencies of these overtones is not exactly 2,3, ... times that of the fundamental as the energy levels converge with increasing v.

In addition there are combination bands, i.e. sums and differences of two or more fundamentals. The intensities of combination and overtone bands are generally much lower than those of fundamentals.

Generally speaking, at ordinary temperatures only the $v = 0$ level is significantly populated so that the fundamental $v = 0 \longrightarrow v = 1$ is the only transition readily observed and the overtones and combination bands have relatively very small intensities. This is of course because separations of vibrational energy levels are relatively large compared with thermal energies. At elevated temperatures, however, and when the vibrational states happen to be unusually closely spaced, transitions from excited vibrational states (so-called "hot" bands) appear, sometimes with relatively large intensity.

The appearance of combination and overtone bands indicates that the assumption made previously, viz.: of the simple harmonic oscillator mode, is not justified. Account must therefore be taken of the anharmonic nature of the vibrations.

It is well known in chemistry that bond compression is far more difficult than bond stretching and Hooke's law is but a poor approximation to the truth. On adding higher order terms to the potential energy expression 1.23 (i.e. by adding terms such as $l x^3 + m x^4 + \ldots$, in which $k >> l >> m$, and so on) the eigenvalues become:

24/.. .. .. ..

$$E_v = (v + \tfrac{1}{2})\, h\nu' - (v + \tfrac{1}{2})^2\, x\, h\nu' + (v + \tfrac{1}{2})^3 yh\nu' + \ldots. \quad 1.28$$

where x , y, etc., are called anharmonieity constants; $1 \gg x \gg y$ and so on.

Thus the vibrational term is modified to:

$$G(v) = (v + \tfrac{1}{2})\, \nu_e - (v + \tfrac{1}{2})^2\, x\, \nu_e + (v + \tfrac{1}{2})^3 y\, \nu_e + \ldots\ldots \quad 1.29$$

where the quantity ν_e is the hypothetically vibrationless wave number for the molecule, i.e. for infinitesimal amplitudes. From equations 1.28 to 1.29 it is quite clear that the vibrational levels will converge with increasing vibrational quantum number, v.

Except in the most accurate work the cubic and higher order terms may be neglected and the fundamental wave number is given by:

$$\begin{aligned} \overline{\nu_v} &= G\,(v = 1) - G\,(v = 0) \\ &= \left[(v + \tfrac{1}{2})\, \nu_e - (v + \tfrac{1}{2})^2 x \nu_e\right] - \left[(\tfrac{1}{2})\, \nu_e - (\tfrac{1}{2})^2 x\, \nu_e\right] \\ &= v\, \nu_e - x \nu_e\, v\,(v + 1) \qquad\qquad 1.30. \end{aligned}$$

The vibrational spectra of polyatomic molecules are exceedingly complicated. The complexity occurs not only because there are in general 3n - 6 fundamental vibrational degrees of freedom (see below) (n = number of atoms in the molecule) and a host of combinations and overtones, but also because the interactions among the atoms cause motion of any one to excite motion on the part of the other atoms of which the molecule is composed. Polyatomic molecules therefore lend themselves to study with the help of molecular symmetry. In order to grasp vibrational spectra it is very helpful indeed to study the symmetry of normal vibrations as the forms of these are strongly dependent upon symmetry.

If a molecule consists of n atoms, the motions of the system can be described in terms of the motion of the n, nearly independent, individual atoms. Three coordinates are necessary to specify the location of each atom so that 3n coordinates will be required to describe the system, i.e. the molecules has 3n degrees of freedom of motion. Certain combinations of changes of these 3n coordinates correspond to motions of the molecule as a whole, such that the positions of the atoms relative to one another remain unchanged. Of these, three govern the translational motion of the molecule as a whole and three are components of rotational motion (except for linear molecules when there are only two rotational degrees of freedom) of the molecule

as a whole about the three axis of inertia. Thus for a n-atomic molecule there will be, for a linear molecule, (3n-5), or for a non-linear molecule (3n-6) genuine or normal vibrational motions. The frequencies or wave numbers associated with these are termed fundamental. Symmetry may lead to degeneracy, i.e. coinciding energy levels (Degenerate eigenvalues have more than one eigenfunction).

1.1.5 The Heisenberg Uncertainty Principle:

Inherent in the quantum mechanical formulation of states in terms of probability there are limitations to the accuracy with which certain quantities can be simultaneously measured, or meaningfully specified.

Restricting attention to a one dimensional system, the average value of a dynamical variable q is:

$$\bar{q} = \int \psi^{*} Q \psi \, dx$$

in which Q is the operator associated with q and $\int$ indicates that the integration is performed over the whole of the accessible range of the coordinate system. In the case of the linear harmonic oscillator the average value of the displacement will be given by

$$\overline{x_v} = \int \psi_v^{*} x \psi_v \, dx \quad .$$

For v even, on reflexion (substituting $-x$ for x) leaves ψ_v unchanged in magnitude and sign; whereas for v odd, the operation leaves ψ_v unaltered in magnitude, but changes its sign. ψ (v even) are said to be symmetric in x and ψ (v odd) antisymmetric in x. In the above integrand ψ_v^{*} and ψ_v are either both symmetric or both antisymmetric; x is antisymmetric. Therefore the integrand must change its sign on reflection. Since the limits of integration are symmetrical about $x = 0$ ($-\infty$ to $+\infty$), the magnitude of the integral must be independent of reflection and is therefore zero, i.e. $\overline{x} = 0$. The same argument applies to the average momentum, since the momentum operator $P = -(ih/2\pi)\, d/dx$, like x, is antisymmetric. $\overline{x^2}$ and $\overline{p^2}$, however, are found, for $v = o$, to have the respective values $r^2/2$ and $h^2/8\pi^2 r^2$; $r = \sqrt[4]{h^2/4\pi^2 k\mu}$. Comparing the above four results it is clear that there is a discrepancy between the time average values of the dynamical variable and of the average of its square.

26/.. .. .. ..

It is accepted in the first principles of elementary statistics that error is given by:

$$\Delta q = \sqrt{\overline{q^2} \quad -(\bar{q})^2}$$

On this basis $\Delta x = r/\sqrt{2}$ and $\Delta p = \sqrt{2}\, h/r$, no matter how often "the experiment" be performed! While from a statistical point of view we are accustomed to accepting the idea of "error of measurement", the concept that Nature is fundamentally erratic is most novel and revolutionary, as are the whole of quantum mechanics, except perhaps to those who are familiar with wave motion, e.g. in electronics.

To generalise we consider the product of Δx and Δp ($v = 0$), namely $h/4\pi$. This represents the Uncertainity Principle in a particular case and more generally it establishes a relationship between any pair of canonically conjugate variables, q and s, of the same system, namely $\Delta q . \Delta s \sim h$.

In this case the potential energy of the simple harmonic oscillator is zero for zero displacement, implying that $x = 0$, $p = 0$ simultaneously. This is contrary to Heisenberg's Principle, but in fact (as was seen a little earlier) the lowest eigenvalue is given by putting $v = 0$ in $(v + \frac{1}{2})\nu$, viz.: the non zero, zero-point value $G_o = \nu/2$.

1.1.6 The Probability of Transitions:

In the application of the quantum-mechanical theory to the topics under discussion (i.e. to infra-red spectra only), the magnitude of the radiant energy emitted or absorbed depends upon the value of the transition moment of the system, i.e.

$$\mu = \int \psi_i \, O \, \psi_f \, d\tau$$

where O is an operator, specific to the transition mechanism of the molecule. O can be a dipole or higher moment, polarizability (i.e. interactions of electric or magnetic moments), etc.

ψ_i is the eigenfunction of the lower state and
ψ_f is the eigenfunction of the excited state.

Thus the transition moment represents the probability that an oscillator in a state ψ_i will undergo a transition to a higher state ψ_f. $d\tau$ is a volume element and the integration is carried out over all space available to the system participating in the transition.

27/.. .. .. ..

The intensity of absorption or emission is proportional to $\left|\psi_i \, 0 \, \psi_f \, d\tau\right|^2$.

This "transition probability" (which can be determined experimentally) must, in order to be non-zero, be "independent of the coordinate system". The square of the transition moment, $\left|\int \psi_i \, 0 \, \psi_f \, d\tau\right|^2$, must then remain unchanged on re-numbering of the particles of the system. This means that either $\int \psi_i \, 0 \, \psi_f \, d\tau$ remains unchanged or, at most, that it changes sign during a symmetry operation. (If ψ^* and ψ are either symmetric or antisymmetric in the coordinates (i.e. they either do not, or do, respectively, change sign on reflection at the centre), two cases arise: (a) if 0 is symmetric the integral can be non-zero, or (b) if 0 is antisymmetric and if the integration is symmetrical about the origin, the integrand must be zero). If the integral undergoes a sign change during a symmetry operation it must have an equivalent, but opposite, value in another part of the space. The integral of the total space will be zero under these conditions. It is therefore necessary that the transition moment $\mu = \int \psi_i \, 0 \, \psi_f \, d\tau$ does not change during a symmetry operation, i.e. $\mu \neq 0$, if there is to be a transition.

The fact that the integral for the transition moment must be different from zero for a transition, means that all transitions between states, even though the states themselves are possible, are not necessarily allowed. The restrictions imposed upon transfers are known as selection rules. These determine whether transitions are allowed (infra-red active) or forbidden (infra-red inactive).

The theoretical treatment is greatly simplified on neglecting interactions between electronic, vibrational and rotational energy levels. In the simple case of the diatomic molecule it follows that two independent models may be considered, whereby the vibrational mode, without rotation, may be discussed in terms of a simple harmonic oscillator (section 1.1.4) and rotation may be considered in terms of a rigid model, (section 1.1.3). It requires but small modifications to these approximate models in order to account for observed rotational and vibration - rotation spectra to a high degree of accuracy.

28/.. .. .. ..

1.1.7 Vibration - Rotation Spectra:

Provided the molecule is free to rotate, it is found that rotational transitions always occur simultaneously with vibrational transitions so that the vibrational spectra of gases display rotational fine structure. In the liquid phase no well defined rotational energy levels exist, and rotational fine structure is not observed. (The incidence of centrifugal stretching is, in a sense, an interaction with vibration. A change of I in going from one J level to the next implies a change in internuclear distance, allied to the concept of vibration).

From equations 1.16 and 1.29, the total of the vibrational and rotational energies of a diatomic molecule (expressed in cm^{-1}) may be given to a first approximation by their sum, $G(v) + F_v(J)$, considered in the first approximation to be independent of one another, except in so far as $F_v(J)$ contains rotational constants which depend upon the strength of the chemical bond.

The new rotational term, however, introduce an additional concept, namely that of the dependence of F not only on J, but also on the vibrational level. We are agreed that the vibration are anharmonic so that the average moment of inertia (vibration being in general much faster than rotation) will depend upon the vibrational state. In general the bond distance, r_v, will increase with v so that r' $(v = 1) > r''$ $(v = 0) > r_e$ (vibrationless equilibrium bond length). Hence $I' > I'' > I_e$, so that $B' < B'' < B_e$. This generalisation is not always followed, however, as in some instances the distortion of a bond strengthens it. It is clearly necessary to re-define the rotational term and, in case of the vibrator, clearly distinguish rotational constants according to the vibrational state. We now write:

$$F_v(J) = B_v J(J+1) - D_v J^2 (J+1)^2 \qquad 1.31$$

where $B_v = B_e - \alpha_e (v + \frac{1}{2}) + \ldots\ldots$

and $D_v = D_e + \beta_e (v + \frac{1}{2}) + \ldots\ldots$

α_e and β_e are small, respectively, compared with B_e and D_e.

The selection rules are still $\Delta v = \pm (1,2,3 \ldots.)$, with rapidly decreasing probability as Δv increases, and $\Delta J = \pm 1$. Since we need consider only the transitions $\Delta v = +1$ (fundamental, absorption band) and $\Delta J = \pm 1$, the wave numbers of the rotational lines comprising the fine structure of the vibration band will be given by:

29/.. .. .. .

$$\nu = G'(v = 1) + F'(J \pm 1) - (G''(v = 0) + F''(J))$$

$$= \nu_0 + F'(J \pm 1) - F''(J) \qquad 1.32.$$

where ν_0 is termed the vibrational band centre.

At higher wave numbers than ν_0 the lines of the R branch of the band are generated when $\Delta J = +1$ and $J = 0,1,2 \ldots\ldots$. These lines are given by:

$$\nu(R) = \nu_0 + (B' + B'')(J + 1) + (B' - B'' - (D' - D''))(J + 1)^2 - 2(D' + D'')(J + 1)^3 - (D' - D'')(J + 1)^4 \qquad 1.33(a).$$

At lower wave numbers than the band centre the P branch is generated according to $\Delta J = -1$ and $J = 1,2,3,\ldots\ldots$ ($J \neq 0$ since $J = 0 \not\rightarrow J = -1$), so that:

$$\nu(P) = \nu_0 - (B' + B'')J + (B' - B'' - (D' - D''))J^2 + 2(D' + D'')J^3 - (D' - D'')J^4 \qquad 1.33(b).$$

Both expressions may be written :

$$\nu = \nu_0 + (B' + B'')m + (B' - B'' - (D' - D''))m^2 - 2(D' + D'')m^3 - (D' - D'')m^4 \qquad 1.34.$$

in which $m = \pm (1,2,3,\ldots\ldots)$ and $m = J + 1$ for the R branch and $m = -J$ for the P branch. This is in fact the empirical expression resulting from analyses of measured spectra, so that the theory is in very excellent agreement with experiment.

Of great importance, therefore in interpreting experimental measurement in terms of the theory, B", B', D" and D' may be estimated, and hence α_e, β_e, I_e, r_e, and so forth, and the data may be extrapolated in order to include higher vibrational states. Furthermore, ν_0 may be calculated with high accuracy, so that bond strengths may be compared. But it must be remembered that the above is applicable to heteronuclear diatomic molecules, and treatment must go further.

It will be noted that in the "normal" case the rotational lines converge with increasing wave number since B" is normally greater than B' and the quadratic term thus opposes the linear term. If there are enough rotational lines in the band, and/or if B" — B' is not very much smaller than B" + B', a band head may form at the high wave number end of the R branch.

30/.. .. .. ..

The treatment for diatomic molecules may be extended to linear molecules, with the difference that there will now generally be more than one vibrational fundamental, each with its rotational fine structure if the compound is a gas. In general it may sometimes be possible (see below) for ΔJ to be zero (as well as ± 1) in which case the lines of a Q branch are generated. These are generally very closely spaced and appear as a line like absorption peak at the band centre (if a Q branch is absent there is a doubly spaced, "zero gap", identifying the band centre).

For polyatomic molecules the total energy can be expressed as the sum of two terms, as follows:

$$T(v,r) = G(v_1,v_2,....) + F_v(J,K) \qquad 1.35$$

where the term $G(v_1,v_2,...)$ is a general expression for the vibrational levels of the molecule and $F_v(J,K)$ are the rotational levels associated with each vibrational state. v_1, v_2, ... are the vibrational quantum numbers of the individual modes and J and K are rotational quantum numbers. In polyatomic molecules the rotational constant is unique for each vibrational level since there is an value assigned to each normal mode. Thus

$$B(v_1,v_2,...) = Be - \alpha_1(v_1 + \tfrac{1}{2}) - \alpha_2(v_2 + \tfrac{1}{2}) + ...$$

and $B(v_1 = 0, v_2 = 0, ...) = Be - \frac{1}{2}(\alpha_1 + \alpha_2 + ...)$

α is usually positive for stretching vibrations and negative for bending modes.

Degenerate vibrational terms (ignoring the anharmonic nature of the modes) are given by:

$$G(v_1, v_2, ...) = \sum_i \nu_i \left(v_i + \frac{d_i}{2}\right)$$

where ν_i is the fundamental vibration frequency of the i-th normal mode and d_i is the degree of degeneracy. If the mode is doubly degenerate (species E) its contribution to B_v is $-\alpha(v + 1)$; and if triply degenerate (species F) its contribution is $-\alpha(v + 3/2)$, and so on.

1.1.7.1 Linear Polyatomic Molecules:

For linear polyatomic molecules the normal vibration modes may be divided into two types, namely:

(a) normal modes in which the dipole oscillates parallel to the molecular axis; termed parallel vibrations for which the selection

rule $\Delta J = \pm 1$ operates and

(b) vibrations which produce oscillating dipoles perpendicular to the internuclear axis with the selection rule $\Delta J = 0, \pm 1$.

The two kinds of vibration, (a) and (b), respectively give rise to the so-called parallel vibration-rotation bands, with P and R branches (and no Q branch) and perpendicular bands with P, Q, and R branches. There is one exceptional instance in which a linear molecule does exhibit a Q branch in the parallel vibration, viz. the case of the NO molecule. This is because the molecule have an odd electron in its ground state, with the result that there is a resultant electronic angular momentum about the internuclear axis.

Diatomic and linear polyatomic molecules yield the same expressions for their rotational levels and the same general conclusions apply. Neglecting centrifugal distortion, 1.32 may be expanded to:

$$\nu = \nu_0 + B' J' (J' + 1) - B'' J'' (J'' + 1) \qquad 1.36.$$

With the selection rule $\Delta J = \pm 1$ the expression for the parallel band now becomes for $\Delta J = +1$ (i.e. $J \longrightarrow J + 1$).

$$\nu(R) = \nu_0 + 2B' (J + 1) + (B' - B'') J (J + 1), \qquad J = 0,1,2,\ldots \qquad 1.37.$$

and $\Delta J = -1$ (i.e. $J \longrightarrow J - 1$)

$$\nu(P) = \nu_0 - (B' + B'') + (B' - B'') J^2 \qquad J = 1,2,\ldots\ldots \qquad 1.38.$$

For the perpendicular band the selection rule $\Delta J = 0, \pm 1$ applies so that we may add $\Delta J = 0$ (i.e. $J \longrightarrow J$ transitions).

$$\nu(Q) = \nu_0 + (B' - B'') J + (B' - B'') J^2, \qquad J = 0,1,2\ldots\ldots \qquad 1.39.$$

1.1.7.2 Symmetrical Top Molecules:

The energy levels of a rigid symmetric top molecule in a non-degenerate vibrational state, according to equations 1.19 and 1.35, will be:

$$T(v,r) = E_{v,r}/hc = G(v_1, v_2, \ldots) + B_v J (J + 1) + (A_v - B_v) K^2 \qquad 1.40.$$

The vibrations of symmetric top molecules may also divide into parallel and perpendicular fundamentals. Vibrations that lead to parallel bands have the rotational selection rules:

32/.. .. .. ..

$\Delta K = 0, \quad \Delta J = \pm 1 \quad \text{if} \quad K = 0$
and $\Delta K = 0, \quad \Delta J = 0, \pm 1 \text{ if } K \neq 0.$

The rotational transitions for a particular K level (except the K = 0 level) with $\Delta J = 0, \pm 1$ and $\Delta K = 0$ form the P, Q and R branches in the sub-bands; each K value giving rise to a sub-band. The complete parallel band is the result of the superposition of the set of sub-bands. All the lines tend to coincide and the bands generally resemble the perpendicular bands of linear molecules, i.e. with P, Q and R fine structures.

For vibrations whose transition moment is perpendicular to the top axis, the rotational selection rules are:

$\Delta K = \pm 1$ and $J = 0, \pm 1.$

Perpendicular fundamentals occur by transition from the non-degenerate ground state to the doubly degenerate first vibrational level. For every value of K and ΔK a sub-band is obtained, each consisting of its own P, Q and R structures, but with different sub-origins depending upon the value of K. Thus K = 0 gives rise to one sub-band and when $K \neq 0$, there are two sub-bands corresponding to $\Delta K = +1$ and $\Delta K = -1$. The complete perpendicular bands are thus in general more complex than those of linear molecules and can only be understood in terms of a summation of sub-bands. The resultant usually has the appearance of a number of fairly evenly spaced Q branches, while the P and R structures form a jumble of unresolved background. There are, however, important exceptions.

It is further found in a detailed investigation of the perpendicular bands of a molecule, that the Q branch spacing is not necessarily the same in the different bands. This is the result of Coriolis forces which arise when a molecule is simultaneously rotating and vibrating. Coupling between doubly degenerate vibrations as a result of Coriolis forces may lead to additional vibrational angular momentum $\zeta_i h/2\pi$ about the symmetry axis (where ζ_i is the Coriolis constant). As a result of this angular momentum each $K > 0$ rotational level is split into two sub-levels. This splitting increases with K. Accordingly a quantity of $\mp 2 A_v \zeta_i K$ must be added to the rotational term value of a symmetric top molecule (equation 1.40) in which one degenerate vibration is singly excited.

33/.. .. .. ..

1.1.7.3 Spherical Top Molecules:

The three principal moments of inertia of a spherical top molecule are all equal so that A = B in equation 1.40. The rotational energy term in the non-degenerate ground vibrational state is $F_o(J) = B_o J(J + 1)$ with the selection rule $\Delta J = 0, \pm 1$. The "vibrational" selection rules allow fundamentals in which the upper state is triply degenerate only. Coriolis interaction is possible between the three degenerate components of each vibration, causing splitting of the rotational levels into three sub-levels. At medium resolution the Coriolis splitting will usually not be resolved and the band will have simple P, Q and R branch structures.

1.1.7.4 Asymmetrical Top Molecules:

The most complex molecules are classed as asymmetrical tops, with three different moments of inertia, $I_a \neq I_b \neq I_c$. Due to the complexity of this situation there would be little merit in discussing it in any detail here. For the fundamentals in which $I_a < I_b < I_c$, the observed bands may be divided into three distinct types, A, B and C, depending on whether the dipole moment change occurs along the axis of least, intermediate or greatest moment of inertia, respectively. In general it is found that the greater the difference in the three moments of inertia the more complex are the bands. Only for the most simple molecules, e.g. water has anything like a complete analysis been achieved thus far.

1.2 MOLECULAR SYMMETRY.

The symmetry of a molecule is discussed in terms of the symmetry elements that a molecule has in its equilibrium configuration. These may best be explained in terms of symmetry operations that may be performed on the molecule which will produce a configuration of the nuclei, indistinguishable from the original. From these operations the point group to which the molecule belongs may be determined — a point group being a combination of symmetry elements that can occur.

A molecule such as H_2O belongs to the point group C_{2v}. The symmetry elements of the point group C_{2v} are the identity symmetry element, a twofold rotational axis of symmetry and two vertical planes of reflection (some other molecules may also have a centre of symmetry). The four symmetry operations are rotation by 2π, rotation about the molecular axis twice by $2\pi/2$ and reflection through two different planes respectively.

Application of the symmetry operations to the molecule result in displacement of the atoms such as occur in a translation or rotation of the molecule, or a normal vibration of the atoms of the molecule. In a polyatomic molecule a normal mode or normal vibration may be defined as a vibrational state in which each atom carried out a simple harmonic motion about its equilibrium position with each atom having the same frequency of oscillation and, in general, moving in phase. Any other motion of the system can be represented as the superposition of a number of these normal vibrations. (A few of these have zero frequency and actually represent translational motion of the atom).

In the vibrating molecule the mode does not necessarily lead the molecule to self-coincidence, and the various normal vibrations may thus be either symmetric or antisymmetric with respect to the principal axis of symmetry of the molecule. In this manner the normal vibrations are assigned to a symmetry species. It is customary to denote A for symmetrical and B for the antisymmetrical fundamental vibrations, E for doubly degenerate vibrations and F (or T) for triply degenerate vibrations. Subscripts g and u specify whether the representation is even (gerade) or odd (undgerade) with respect to inversion (centre of symmetry); whereas subscripts 1 and 2 indicate symmetry or antisymmetry with respect to a rotation-reflection axis, other than the principal axis.

With the help of group theory it is therefore possible to determine the number and activity of normal vibrations in a particular symmetry species.

35/.. .. .. ..

Not all vibrational species are necessarily infra-red active. The symmetry of the molecule and the normal vibrations will determine whether the transition moment for a particular symmetry species is zero or not.

It is not only possible to determine the number of infra-red active vibrations from the symmetry of the molecule but, conversely, it is also possible to determine the geometry and symmetry from the number of infra-red absorption bands that are observed. In general, the more symmetrical the molecule, the fewer are the distinct vibrational modes. The symmetry selection rules hold rigorously for gases at low pressures.

1.3 SPECTROSCOPICAL ANALYSIS.

1.3.1 Qualitative Analysis:

In paragraphs 1.2 and 1.1.4 it was mentioned that a normal coordinate treatment of the observed absorption bands, can in principle help to determine the geometry and symmetry of a molecule. As the complexity of the molecule increases, so does the number and complexity of the possible vibrational modes. Although it is in principle possible (given suitable data on masses and force constants, etc.) to calculate the frequencies and determine the modes for any molecule, this is not always possible due to formidable mathematical and computing difficulties. The interpretation of the spectra of complex molecules is, therefore, done by essentially empirical methods based on rather gross approximations referring to the theoretical results for simpler cases.

In infra-red spectroscopy the fraction of infra-red radiation selectively absorbed by the substance is determined as a function of the wave length or wave number. The spectrum consists of narrow bands; each one corresponding to a particular vibration of the molecular structure. The vibration frequency is determined by the masses of the atoms, the strengths of the binding forces, the configuration of the compound and the state of dispersion. For this reason no two compounds will display the same infra-red spectrum (apart from optical enantiomorphs). This property is used for the identification of compounds, called "fingerprinting".

Although each observed band is due to the vibration of the molecule as a whole, the bands may be regarded, in general, as falling into either of two classes:

(a) Bands due to vibrations largely localized in a particular bond or group-type, when the movement of the atoms directly concerned is large in comparison with the movement of the remainder of the molecule. Thus certain absorption bands are characteristic of the relative vibration of two adjacent parts of a molecule, such as —O——H, =C=O, ——C——C—, ⋗C—H, ⋗N—H, etc. The presence of such a band in the spectrum of an unknown compound is evidence of the presence of the corresponding group or bond in the molecule. The modes of vibration can generally be

classified as those along a bond, called stretching vibrations; and those perpendicular to the bond, called bending or deformation vibrations. The frequency associated with a particular bond or group in a molecule can be modified by factors such as local electronic influences of neighbouring groups, conjugation, ring strain or the formation of hydrogen bridges, etc.

(b) Bands due to overall or skeletal vibrations. These depend specifically upon the geometry, constituent atoms, and valence forces of the molecule. They furnish a unique pattern or "fingerprint" for each molecule species.

1.3.2 Quantitative Analysis:

When light (monochromatic or continuous) falls upon a homogeneous medium, a portion of the incident light may be reflected or scattered, some may be absorbed within the medium and the remainder transmitted. The reflected light is usually compensated for by using some form of "control" and, consequently, provided no appreciable fraction of the radiation is scattered:

$$I_o = I_a + I_t$$

where I_o = the intensity of the incident radiation

I_a = the fraction of radiation absorbed by the matter

and I_t = the fraction of radiation transmitted.

I_a and I_t may be expressed as percentages of I_o.

1.3.2.1 The Beer-Lambert Law:

Lambert's law states that when monochromatic radiation passes through a homogeneous absorbing medium, equal thickness of the medium will absorb the same fractions of radiation. The law may thus be expressed mathematically, using logarithms to the base 10, as:

$$I_x = I_o\, 10^{-kx} \qquad 1.41.$$

where k = the extinction coefficient, a constant characteristic of the medium

and x = the thickness of the absorbing medium.

Beer's law for solutions states that the intensity of a beam of monochromatic light decreases exponentially as the concentration of the absorbing substance increases arithmetically. Thus

$$I_t = I_o\, 10^{-k'c} \qquad 1.42.$$

where k' = constant characteristic of the absorbing solute

c = the concentration.

By combining 1.41 and 1.42 we have

$$I_t = I_o\, 10^{-\varepsilon cx}$$

or $$\text{Log}_{10}\, I_o/I_t = \varepsilon cx \qquad 1.43.$$

where ε is called the extinction coefficient. Equation 1.43 states the Beer-Lambert law. The numerical value of ε will depend upon the units of length and concentration employed. If c is expressed in gram mols per litre and x in centimetres, then ε is the molar extinction coefficient. From the Beer-Lambert law the optical density, D, of a solution is defined as:

$$D = \text{Log}_{10} \frac{I_o}{I_t} = \varepsilon cx = -\log T \qquad 1.44.$$

where the transmission, T, is defined as the ratio of the intensity of transmitted to that of the incident light, i.e. $T = I_t/I_o$.

1.3.2.2 Deviations from Beer-Lambert's Law:

Beer's law may generally hold over a wide range of concentration. However, deviations (real or apparent) are often found. Apparent exceptions to the law have been attributed to chemical changes, such as complex formation, when the composition of the solution may depend upon the concentration. There are three other cases in which there are real or apparent exceptions to Beer's or Lambert's laws. These result from

(1) the use of finite wave band widths rather than monochromatic radiation for the measurements,

(2) pressure broadening of absorption bands in the case of gases, and

(3) the diffusion of radiation by the absorbing medium.

The effects of the first two of these factors are most commonly encountered in practice.

.3.2.2.1 Effects of Finite Slit Widths:

An infra-red adsorption band may be defined most precisely in terms of a plot of the molar extinction coefficient, ε, against λ. In practice, however, a plot of optical density, D, against ν (in wave numbers) may be preferred. The optical density, at the absorption maximum, provides a measure of the band intensity.

Beer's and Lambert's laws apply to strictly monochromatic radiation, but in practice a single wave length is an unattainable ideal. The energy which passes through the exit slit of a monochromator always contains a range of wave numbers on either side of the centre. Thus a relatively wide finite wave band is obtained, when a more accurate measure of the intensity of the band is given by the integrated absorption intensity; i.e. the area under the absorption curve. This type of intensity measurement is, however, often impractical due to overlap with neighbouring bands.

It is possible to come closer to the ideal finite wave band by computing a spectral slit width, based on the geometry of the monochromator, and by analysis of the shapes and intensities of interference bands. (The spectral slit width is defined as the separation in wave number units of two monochromatic lines such that they just fail to be resolved). It is in general found that, as the computed spectral slit width is increased, the bands become wider and the peak height smaller; the integrated absorption intensity also diminishes.

These effects are less pronounced for the infra-red having fairly wide absorption bands. Somewhat narrower bands may occur in solids, while in gases very much narrower rotational lines are common.

Another source of error, particularly at the longer wave length region, is due to the scattering of intense short wave length radiation in the monochromator. This results in a false zero signal at the detector, which may be measured by inserting a filter which cuts out the long wave lengths. Thus appropriate corrections may be applied.

1.3.2.2.2 Pressure Broadening Effects:

It is found that the bands of a number of gases at low pressures show deviations from Beer's law, i.e. the optical density of a given band at a particular wave length will depend upon the partial pressure, but not be directly proportional to it. Further, for these gases the optical density will depend upon the total pressure.

In the classical theory the molecule is regarded as absorbing electromagnetic frequencies that are identical with their own vibrational frequencies. The intensity of absorption will depend upon the number of effective collisions between molecules, i.e. the number of collisions which are effective in interrupting the process of radiation absorption. The frequency of effective collisions between the molecules of the absorbing gas, or of the absorbing gas and other molecules, is in turn governed by the optical collision diameters of the molecules.

40/.. .. .. ..

Consequently, the presence of a foreign gas in the gas cell increases the number of collisions, and thus the optical collision diameter of the absorbing gas phase; which results is an increase in the absorbing intensity observed.

It is found in practice that different foreign gases can have the same pressure broadening effect on an infra-red active gas. In this instance it is possible to construct a single empirical calibration curve which will serve for correlating optical density with concentration for the infra-red active gas in the presence of any one, or a combination of the infra-red inactive gases present. Naturally, when the inactive species differ in their "broadening powers" the problem can become far more complicated.

REFERENCES:

(a) Standard Text-books:

G. Herzberg, Infrared and Raman Spectra of Polyatomic Molecules, Van Nostrand, Princeton, N.J., 1945.

J.C.D. Brand and J.C. Speakman, Molecular Structure, Edward Arnold Publishers, Ltd., London, 1960.

J.W. Linnett, Wave Mechanics and Valency, Wiley and Sons, Inc., New York, 1960.

G.M. Barrow, Introduction to Molecular Spectroscopy, McGraw-Hill, New York, 1962.

E.B. Wilson, J.C. Decius, and P.C. Cross, Molecular Vibrations, McGraw-Hill, New York, 1955.

W. West, Chemical Applications of Spectroscopy in Technique of Organic Chemistry, Vol. IX by A. Weissberger, Interscience Publishers, New York, 1956.

M. Davis, Infrared Spectroscopy and Molecular Structure, Elsevier Publishing Company, Amsterdam, 1963.

R.E. Dodd, Chemical Spectroscopy, Elsevier Publishing Company, Amsterdam, 1962.

A.I. Vogel, Quantitative Inorganic Analysis, Longmans, London, 1961.

41/.. .. .. ..

(b) Reference Papers:

P.C. Cross and F. Daniels, J. Chem. Phys., 2, 6 (1934).

N.D. Coggeshall and E.L. Saier, ibid., 15, 65 (1947).

N.D. Coggeshall and E.L. Saier, J. Appl. Phys., 17, 450 (1946)

N.D. Coggeshall, Anal. Chem., 22, 381 (1950).

CHAPTER 2.

THE INFRA-RED SPECTRA OF ADSORBED MOLECULES (CO IN PARTICULAR) ON METALS.

2.1 INTRODUCTION:

During the last fifteen years a number of new tools and new uses of old tools have been developed to examine the phenomenon of the adsorption of gases on metal surfaces. Infra-red spectroscopy has proven to be one of the most powerful tools for the determination of structure.

In the infra-red technique a large area metal surface and of a sufficiently small particle size is prepared such that a sample will transmit infra-red radiation. On subjecting the sample to synthesis gases the reaction intermediates can in principle be identified according to the way in which they interact with the infra-red radiation. The following is designed to make this point clear.

Consider a gas molecule consisting of two unlike atoms, e.g. carbon monoxide. On subjecting such a polar molecule to the alternating electric field of infra-red radiation, the two atomic nuclei will tend to vibrate and the interaction between the radiation and the molecule will be intense at the natural frequency of vibration of the molecule. Radiation will be absorbed at this frequency (e.g. carbon monoxide has an intense infra-red band at 2143 cm^{-1}.) Conversely the frequency of absorption of radiation will characterise the molecule. Furthermore, the extinction coefficient of the absorption band will indicate how polar the molecule is; intensity increasing with polarity. The same will apply to more complex molecules which will give a variety of infra-red bands.

The power of the infra-red technique lies in the fact that sorbed molecules still give infra-red bands and a study of the sprectra gives information on the structure of the species.

2.2 A LITERATURE REVIEW:

Eischens and co-workers[5] were the first to demonstrate the feasibility of applying infra-red techniques to the study of many types of adsorbed species on metals. The infra-red spectra of carbon monoxide chemisorbed on a variety of metals have been reported[6-10]. Spectra have also been obtained of simple hydrocarbons and carbon dioxide adsorbed on nickel; hydrogen, carbon dioxide, oxygen and water on silica supported iron[3,10]; ammonia, water and other gases on activated iron (III) oxide[11]; carbon monoxide on iron evaporated from

a tungsten filament[12]; carbon monoxide on high area metal films[13]; nitrogen oxide adsorbed on nickel and iron[14]; nitrogen dioxide on oil- and silica-supported nickel and iron[15]; some C_xH_yO compounds adsorbed on oil-supported iron[16], nickel[17], and cobalt[18]; acetylene and ethylene on silica-supported palladium, copper and nickel[57]; acetone and acetaldehyde on silica and silica-supported nickel[58].

In many of the investigations evidence has been found for the existence of several different species resulting from the chemisorption of a single gas on a single solid.

It is known from fundamental catalyst studies that a decrease in the heat of chemisorption is generally observed as the surface coverage increases. Attempts have been made to explain this phenomenon on the basis of surface heterogeneity, repulsive interactions between adsorbed species and changes in the work function of the adsorbent surface induced by the adsorbed gas[19].

The infra-red spectra of chemisorbed carbon monoxide provides a new approach to the general problem. Spectra obtained at a single pressure do not reveal the relative strength of bonding for the chemisorbed carbon monoxide contributing to each band, or the effect of interaction on the band positions. An increase in the number of bands with increasing surface coverage can indicate the existence of surface heterogeneity of the samples.

The question of the nature and importance of catalyst acidity with respect to catalytic reactions has been under intensive study for many years by a large number of workers[20]. One of the early questions which arose is whether the acidity is of the Brönsted (protonic) or Lewis (eletron acceptor) type. While this question remains unsolved, the data seem to favour the predominance of Lewis acidity.

In the next few paragraphs only those spectra most relevant to this work, are briefly discussed. For a more comprehensive discussion the reader is referred to two recently published textbooks[21,22].

2.3 SPECTRA OF CHEMISORBED CARBON MONOXIDE ON SUPPORTED NICKEL:

Bands attributed to carbon monoxide bonded to single metal atoms were observed by Eischens et. al.[5] at 2041 and 1908 cm^{-1} in the case of silica-supported nickel. The admission of hydrogen to a sample with chemisorbed carbon monoxide, shifts the bands toward smaller wave numbers by about 21 cm^{-1}, and broadens the bands. It was also found that the absorption peak at 1908 cm^{-1} is much more intense than the

44/.. .. .. ..

band at 2041 cm^{-1}. This is assumed to be correlated with two types of bond to single metal atoms when carbon monoxide is chemisorbed on nickel.

Later, Eischens, et. al.[19] came to the conclusion that, in analogy to the carbonyls of iron[23,24], nickel, cobalt, manganese, and rhodium[19], the spectra divide themselves into two parts with the region near 2000 cm^{-1} serving as the dividing line, i.e. bands below 2000 cm^{-1} are assigned to bridging carbonyl groups and those above 2000 cm^{-1} to terminal carbonyl groups. This would mean that the band at 2041 cm^{-1} should be assigned to the linear structure, Ni —C≡O.

In the case of iron nonacarbonyl[24] and iron tetracarbonyl[23], bands are found in the 1833 to 1818 cm^{-1} region and are assigned to CO bridged between two metal atoms. Thus it is reasonable to assign this region to bridged CO species. No previous work could be found by which to interpret the bands in the 2000 to 1833 cm^{-1} region, but the pattern of change produced by increasing surface coverage on palladium[19], suggests that these bands should be assigned to bridged CO structures rather than to those involving CO bonded to single metal atoms[5]. This interpretation implies that the band at 1908 cm^{-1} should be assigned to carbon monoxide in the bridged structure, $\begin{matrix}Ni\\Ni\end{matrix}\!>\!C{=}O$.

The fact that the spectrum of carbon monoxide, chemisorbed on nickel, has more than one band makes it possible to study surface heterogeneity based on the effect of increasing surface coverage, θ, on the rate of growth of the bands. Under equilibrium conditions, if all of the bands increase at the same relative rate as θ increases, it would be known that the position of the band was very unlikely to be a function of the bonding strength and that the factors which produce a multiple band spectrum are not related to surface heterogeneity. A difference in the growth rate would indicate that the surface was heterogeneous and that the first bands to appear must be associated (since the system is at equilibrium) with the most strongly bonded CO. A third possibility is that an increase in θ would produce new bands, coupled with the disappearance of bands formed at low coverages. In this instance the structure of the chemisorbed CO would be a function of θ.

For the above reasons Eischens, et. al.[19] studied the effect of the diminution of θ on the spectrum of carbon monoxide chemisorbed on nickel. Two bands at shorter wave lengths were found at 2075 and 2040 cm^{-1}. The possibility that the band at 2040 cm^{-1} should be assigned

45/.. .. .. ..

to single CO ligands linked to single nickel atoms was considered, as was the relation of the 2075 cm^{-1} band to more than one ligand per nickel site. No firm conclusion to the hypothesis was warranted.

It was found that the lower wave number bridged CO assigned to the 1924 cm^{-1} band is the most strongly held on decreasing the surface coverage. At the same time the number of bands decreased and was assumed to indicate surface heterogeneity.

Eischens, et. al.[19] also concluded from their work on carbon monoxide on nickel, and on palladium, that the positions of the bands assigned to bridged CO ligands are sensitive to bond strength, i.e. the lower the wave number of the band, the more tenaciously the species are held upon desorption. On the other hand, the species contributing to a band at 2070 cm^{-1} for carbon monoxide chemisorbed on palladium or nickel is weakly held for the band disappears immediately on reducing the pressure to 10^{-4} mm. Hg. On the other hand the species contributing to a band at 2070 cm^{-1} for carbon monoxide on platinum was found to be strongly held. This shows that the band position for linear O—C—M, on different metals, is not a measure of the bond strength.

O'Neill and Yates[9] studied the effect of the support on the infrared spectra of carbon monoxide on nickel. The nature of the support was found to have drastic effects, but the bands again fell in one of two classes; viz.: bands above and below 2000 cm^{-1}. In the case of silica-supported nickel the bands above 2000 cm^{-1} were observed at 2050 cm^{-1} (attributed to strongly held linear CO) and at 2075 cm^{-1} (due to weakly held linear CO). Two explanations for these conclusions were offered, namely:

(1) The band at 2075 cm^{-1} is assigned to more than one ligand CO per Ni atom.

(2) A change in lateral interaction between adsorbed molecules is expected to displace the band at 2050 cm^{-1} to higher wave numbers at higher coverages.

The effects of the metal concentration on the infra-red spectra of carbon monoxide adsorbed on nickel were investigated by Yates and Garland[8]. The variety of the bands obtained were attributed to different crystalline, semicrystalline, and amorphous sites. Thus, a band located at 2082 cm^{-1} was ascribed to a weakly held linear CO species bonded to amorphous Ni sites. Bands occuring at 2058 and 2025 cm^{-1} were attributed to linear groups on semicrystalline and crystalline sites, respectively.

46/.. .. .. ..

A band at 1925 cm^{-1} was assigned to a bridged species on a semicrystalline site and a band at 1880 cm^{-1} to a bridged species on a crystalline site.

Blyholder and Neff[25] reported that exposure of a supported nickel surface to methanol gives infra-red bands for surface species at 2040 and 1900 cm^{-1}. The bands were attributed to chemisorbed CO species. When hydrogen and carbon monoxide were admitted to the cell at 20°C, the only infra-red bands observed were the same two at 2060 and 1900 cm^{-1} for chemisorbed CO with the exception of a band at 2180 cm^{-1} which was ascribed to gas phase CO. Upon evacuation, only the 2060 and 1900 cm^{-1} bands remained, but when the system was heated to 240°C all the bands disappeared. These workers were unable to say whether the carbon monoxide (while chemisorbed in the structures that produce the bands at 2060 and 1900 cm^{-1}) would react with hydrogen. They also found that the bands at 2060 and 1900 cm^{-1} showed no change in intensity over a period of several weeks when the pressure was reduced to 10^{-5} torr at room temperature. This demonstrated that great stability with respect to desorption of the chemisorbed CO at 20°C.

Thus far the spectra of adsorbed CO on silica-supported nickel indicates several types of adsorption, rather inadequately understood. In view of this, it was felt by Peri[26] that too little attention had been paid to possible changes in the spectrum of silica caused by the presence of the nickel. He investigated bands mainly in the region of 2200 cm^{-1}. A band near 2200 cm^{-1} was ascribed by Eischens and Pliskin[9] to an active intermediate in the catalytic oxidation of carbon monoxide, having the probable structure Ni.....O=C=O. A similar band on reduced Ni—SiO_2 was attributed by O'Neill and Yates[27] to CO loosely attached to oxide ions on the surface, but similar bands have been reported[26] for CO adsorbed on several oxides which do not contain Ni. Gardner and Petrucci[28] proposed that a relationship exists between the vibration frequencies of gaseous molecules and ions and their number of valence electrons. They attributed bands near 2200 cm^{-1} to CO ions ranging up to CO^{2+} (presumably generated by metal ions on the surface). Other workers[26] believe they are due to weak σ complexes with metal ions on the surface.

Peri argued that, in the hydrated form of nickel-silica, the nickel ions are undoubtedly shielded through coordination with H_2O and -OH groups. When H_2O is removed by drying at high temperatures, nickel ions are apparently exposed on the surface near silanol groups as shown in Fig. 1(a). When carbon monoxide is adsorbed, bands were found near

47/.. .. .. ..

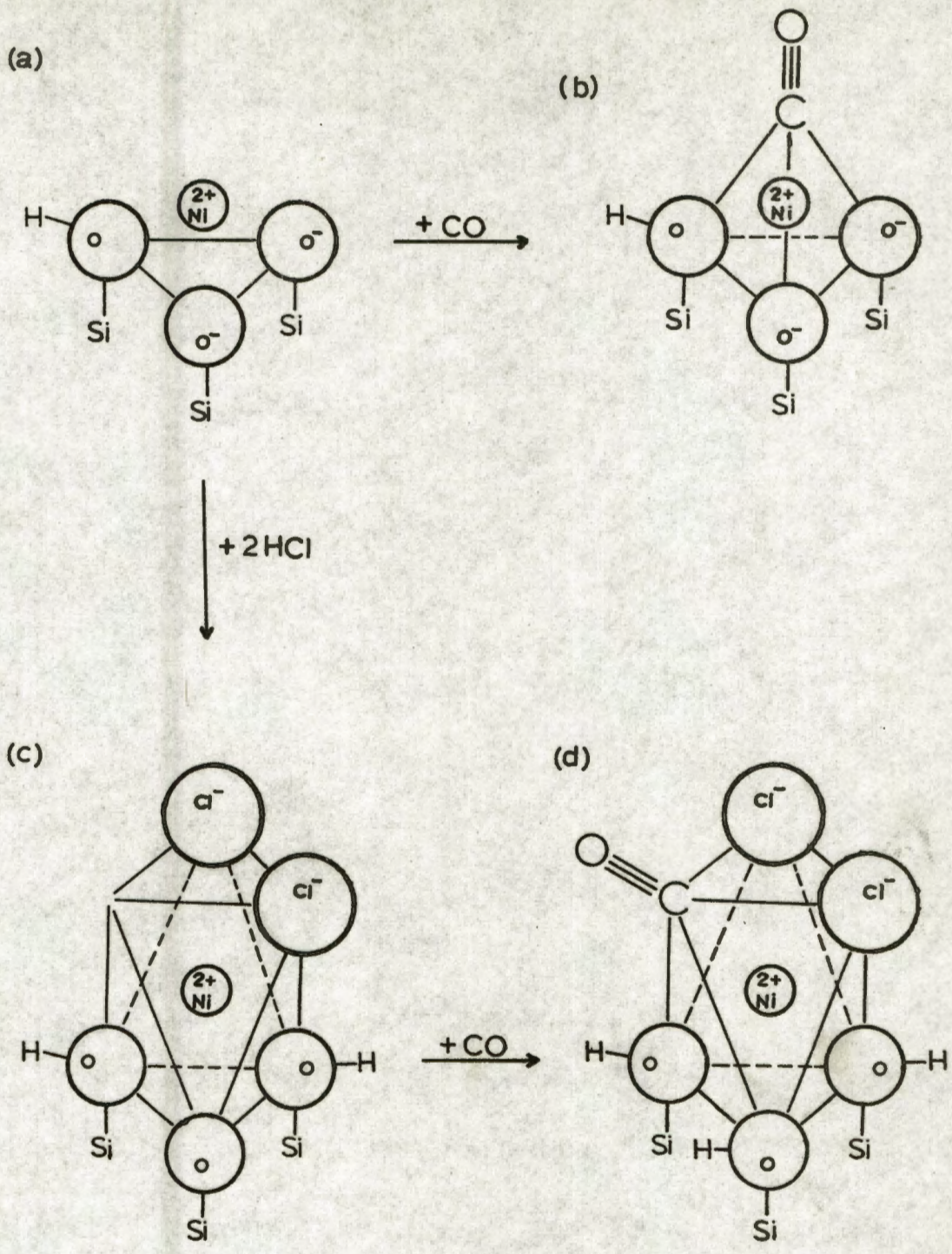

Fig. 1. Peri's view of CO and HCl adsorption on Ni—SiO_2.

2200 cm^{-1} which were attributed to CO species held as shown in Fig. 1(b); where the Ni^{2+} ion is tetrahedrally coordinated through a weak σ bond.

The existence of two bands near 2200 cm^{-1} (at 2198 and 2210 cm^{-1}) was ascribed to CO attached respectively to two kinds of Ni^{2+} ions that differ slightly in their local environments[26].

Chemisorbed carbon monoxide also gives a band near 2140 cm^{-1}, while chemisorbed hydrochloric acid gives rise to a band at 2135 cm^{-1}. It was found by Peri[26] that adsorption of hydrochloric acid, prior to adsorption of carbon monoxide, could change the sites, responsible for the band at about 2200 cm^{-1}, to sites that displayed the 2140 cm^{-1} band only. It was suggested that the chemisorbed hydrochloric acid probably modifies the tetrahedral coordination of Ni^{2+} ions to octahedral coordination, as shown in Fig. 1(c); and thus changes the way in which CO ligands are subsequently held. This is possibly as shown in Fig. 1(d).

2.4 SPECTRA OF CHEMISORBED CARBON MONOXIDE ON UNSUPPORTED NICKEL:

The first spectra for carbon monoxide chemisorbed on nickel films were obtained by Pickering and Eckström[29], who observed infra-red absorption bands at 2170, 2122, and 2058 cm^{-1}. These bands all disappeared upon evacuation. Gardner and Petrucci[4] also found bands at 2174, 2115 and 2060 cm^{-1}, whose intensities were proportional to the carbon monoxide pressure. The 2060 cm^{-1} band was the most intense of the three. Upon evacuation all three bands vanished. Blyholder[30] found strong bands at 1940 and 2080 cm^{-1}, and one of medium intensity at 435 cm^{-1}. It was found that either of the former two bands can be the most intense one; interpreted in terms of two independent structures for chemisorbed CO. Blyholder considered both the symmetric and antisymmetric stretching frequencies expected for the bridged structure of chemisorbed CO species. The calculations indicated the 435 cm^{-1} band to be the result of an asymmetric stretching mode if the most unlikely force constant of less than 1 millidyne/Å for the Ni—C bond can be accepted. It was therefore proposed that both the bands at 1940 and 2080 cm^{-1} arise from linear structures for chemisorbed CO. This conclusion conflicts with the original proposal by Eischens, *et. al.*[5], i.e. that the band at 1940 cm^{-1} for chemisorbed CO is due to a bridged structure.

Similarly, if by analogy to the spectrum of nickel tetracarbonyl the band at 435 cm^{-1} is assumed to be the Ni—C stretching frequency for CO chemisorbed in a linear structure, the Ni—C force constant was calculated to have the more probable value of 2 md/Å.

Sardisco[13] reported a doublet at 2020 and 1980 cm^{-1} for CO adsorbed on Ni films. The transmission spectra of CO adsorbed on Ni films evaporated in a carbon monoxide atmosphere were obtained by Garland, Lord and Troiano[13]. The transmission properties of the film depend upon the carbon monoxide pressure at which the films were prepared. Also, Ni films prepared in 12 mm of carbon monoxide were relatively more stable than the films prepared at a pressure of 2 mm. Furthermore, the Ni films prepared in 2 and 12 mm of carbon monoxide exhibit reproducibly different spectra. Electron micrographs showed that the particle size of a 2 mm (pressure) Ni film is about 65Å whereas that of the 12 mm (pressure) Ni film is approximately 200Å.

The spectrum of carbon monoxide chemisorbed on the 2 mm (pressure) Ni film showed a prominent band at 2083 cm^{-1}, with a shoulder at 2058 cm^{-1}, both associated with linearly adsorbed CO species[6]. In the region ascribed to bridged CO species[6], bands were observed at 1950, 1925, 1880, as well as a prominent band at 1620 cm^{-1}. The exact position of the latter was found to be very sensitive to sample preparation.

In the case of the 12 mm (pressure) Ni films, strong bands were observed at 2058, 1880 and 1620 cm^{-1} and a weak band at 2025 cm^{-1}.

The assignment of Yates and Garland[8] were followed by Garland, et. al.[13] for the classification of the spectra, viz.: bands were associated with amorphous, semicrystalline and crystalline Ni sites.

On the question of the band at 1620 cm^{-1} there was much speculation as to whether it was due to film contamination (for example water or carbon monoxide on nickel oxide) or the result of an increase in the Ni—Ni spacing; since the carbonyl stretching frequency is a function of the angle between carbon-metal bonds[41]. However, Garland, et. al.[13] rejected the above ideas in favour of what was thought to be a more reasonable explanation, viz. that a carbonyl species exhibiting a band at this low frequency must possess considerable single bond character. This might arise through the weakening of the carbonyl bond via association of the oxygen atom with another Ni atom, like

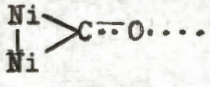

where all of the Ni atoms are to be considered part of the same complex. The authors[13] thought that this explanation is in reasonable agreement with the frequencies observed for metal chelated di-ketones such as nickel acetylacetonate which has a carbonyl band at 1598 cm^{-1}.

49/.. .. .. ..

2.5 SPECTRA OF CHEMISORBED CARBON MONOXIDE ON COBALT:

Three absorption bands were observed by Gardner and Petrucci[4] upon admission of carbon monoxide to Cabosil supported reduced cobalt oxide; namely at 2179, 2160 and 2091 cm^{-1}. These wave numbers were used in correlations, i.e.:

(a) A relationship was postulated between the vibration frequency of the carbon monoxide unit and the number of valence electrons associated with that unit.

(b) The various carbon monoxide species resulting from the chemisorption of carbon monoxide on a single adsorbent differ from each other by having different integral numbers of valence eletrons.

These correlations were found to hold under the experimental conditions practiced.

The only other spectra to be found for carbon monoxide chemisorbed on cobalt, were obtained by Russian workers and are reported by Basila[47]. Bands were found at 2179 - 2140 (strong) and 2091 - 2070 cm^{-1}, and in some experiments, at 1950 and 1820 cm^{-1}. It is not known what structure assignments (if any) were given to the species.

2.6 SPECTRA OF CHEMISORBED CARBON MONOXIDE ON IRON:

Spectra of carbon monoxide chemisorbed on iron were reported by Eischens and Pliskin[6]. At a carbon monoxide pressure of 10^{-3} torr a band at 1960 cm^{-1} attributed to CO species in the linear structure, Fe—C≡O, was found. At a pressure of 1 torr a second band at 2020 cm^{-1} was observed, i.e. the number of bands increases with pressure. This probably indicates that the iron surface is heterogeneous. It was also found that the iron/carbon monoxide system is extremely sensitive to small traces of oxygen. Normally the band at 1960 cm^{-1} disappeared and was replaced by one at 2128 cm^{-1}.

Blyholder[12] found a band at 1960 cm^{-1} for carbon monoxide chemisorbed on oil-supported iron and assigned this band (in general agreement with Eischens *et. al.*[5]) to CO species chemisorbed in a linear structure, Fe=C=O. Further, Blyholder[10] also found bands at 2020, 1980 and 1887 cm^{-1} for silica-supported iron. The two bands at 2020 and 1980 cm^{-1} were regarded as arising from basically a linear structure, Fe=C=O, on two different surface sites. The relative intensities of these two bands were different from those found earlier by Eischens, *et. al.*[6]. This difference was ascribed to different reduction procedures which in turn might influence the relative development of crystal faces.

The band at 1887 cm^{-1} can be assigned to the bridged structure $Fe_{Fe}>C=O$, after Eischens, et. al.[5]. However, the possibility of CO species chemisorbing by forming a π complex was considered by Blyholder.

2.7 CONCLUSIONS:

The above survey of the literature on the subject reveals that, in spite of the valuable and informative data obtained, there still remains much uncertainty as to the assignment of infra-red bands in different regions of the spectra. For instance, bands found (for carbon monoxide chemisorbed on metals) above 2000 cm^{-1} were usually assigned to CO species held in a linear fashion[5] on edges and on planes, as illustrated in Figs. 12(c) and (d); whereas bands found below 2000 cm^{-1} were attributed to CO species held in a bridged fashion[19], Figs. 12(a) and (b).

Blyholder[10] has rejected the idea of bridged species in favour of a π complex mechanism, which permits all the bands to be assigned to terminal carbonyls. This molecular orbital view will be discussed later.

Also, there was still the question of the possibility of more than one CO molecule adsorbed per single Ni atom[19].

In addition to various unsolved problems, mentioned above, very little work has been done on the effects of temperature and of the presence of hydrogen. This is of interest as the industrial synthesis (Fischer-Tropsch or Fischer-Pichler) occurs at higher temperatures and in the presence of carbon monoxide and hydrogen. The effect of the presence of a chemical promoter (such as potassium carbonate), which under certain conditions, is of vital importance to the synthesis process, has not been touched on at all. Furthermore, the work on iron and cobalt was sparse and poorly investigated.

REFERENCES:

See Chapter 4.

CHAPTER 3.

THE INFRA-RED SPECTRA OF CARBON MONOXIDE ADSORBED ON NICKEL, COBALT, IRON AND NICKEL, COBALT AND IRON OXIDE SUPPORTED ON COLLOIDAL SILICA - EXPERIMENTAL.

3.1 INTRODUCTION:

As we had no previous experience in this field, it was necessary to first set up the infra-red technique before it could be applied to hydrocarbon synthesis reactions. In order to establish a foothold in this field, it was necessary to design apparatus in which infra-red spectra could be obtained while the samples were subjected to a wide range of temperatures and pressures. Further, the sample preparation is also a critical step in obtaining spectra of chemisorbed CO species[21,22]. Because of the need to obtain suitably intense spectra, high area samples, and which will transmit a usable amount of infra-red radiation, are needed. Metals absorb strongly in the infra-red region. Therefore the samples are usually in the form of finely divided powders to increase the available surface for adsorption of gases and to decrease the particle size below the wave length of the infra-red radiation, so as to minimize the scattering losses. Furthermore, in order to prepare clean metal surfaces it is essential to purify all gases.

These objectives, mentioned above, will now be discussed in more detail in the next few paragraphs.

3.2 APPARATUS:

3.2.1 The Infra-red Spectrometer:

An Unicam SP100 infra-red spectrometer was used for these investigations. This is a double-beam prism/grating double monochromator instrument, and can be operated "single beam".

The standard gratings are:
one of 1500 lines per inch, for the frequency range 650 to 2150 cm^{-1}, blazed at 900 cm^{-1} in the first order;
and one of 3000 lines per inch, for the frequency range 2150 to 3650 cm^{-1}, blazed at 3000 cm^{-1} in the second order. This is the most suitable angle for satisfactory resolution over the whole of this range.

A 60° NaCl prism is used in conjunction with either of the gratings.

The 2000 cm^{-1} region is of particular interest when the spectra of carbon monoxide on metals is studied. The grating with blaze at 900 cm^{-1} is severly energy limited, with a loss in resolution in the 1600 to 2150 cm^{-1} region. Consequently, this grating was replaced with one of 1500

lines per inch and blazed at 1650 cm^{-1}, which improved the resolving power considerably in the region of interest.

The resolving power of a grating is given by the Rayleigh criterion[31] as:

$$\frac{\lambda}{\Delta\lambda} = Nm \qquad (a)$$

where λ = the average wave length of the lines

$\Delta\lambda$ = their separation in wave length

N = total number of rulings

m = the order used.

From equation (a), the resolving power for a grating blazed at 1650 cm^{-1}, is calculated to be 0.57 cm^{-1} at 2000 cm^{-1}.

The Unicam SP100 infra-red spectrometer can be operated with the optics in nitrogen at atmospheric pressure, partially evacuated, or completely evacuated. A change of the gas pressure in the optical path of the monochromator causes a change in the calibration due to the difference in the refractive index of the environment of the prism and grating. This difference can be as much as 60 cm^{-1} at 2150 cm^{-1}. Therefore, it is very important to keep the pressure in the monochromator constant, once it has been calibrated for a specific environment.

3.2.2 Miscellaneous Equipment:

An all glass high vacuum line was constructed for the gas adsorption studies. It is comprised of an oil rotary pump, mercury diffusion pump, McLeod gauge, manometer, traps, gas storage bulbs and two purification trains. The one train is used for purifying carbon monoxide and the other for purifying hydrogen and helium. The following further accessories were also constructed:

(1) A furnace with a wide mouth, capable of attaining temperatures up to 500°C;

(2) A gas flow meter, calibrated for flows up to 500 ml/min.;

(3) A die, for pressing the silica-supported samples into discs; and

(4) An all glass infra-red cell.

Items (3) and (4) are described in more detail in the next few paragraphs.

3.2.3 The Die:

Normally a non-evacuable KBr die consists of a cylinder, plunger, and backing plate (Fig. 2). The backing plate has a small protuberance

53/.. .. .. ..

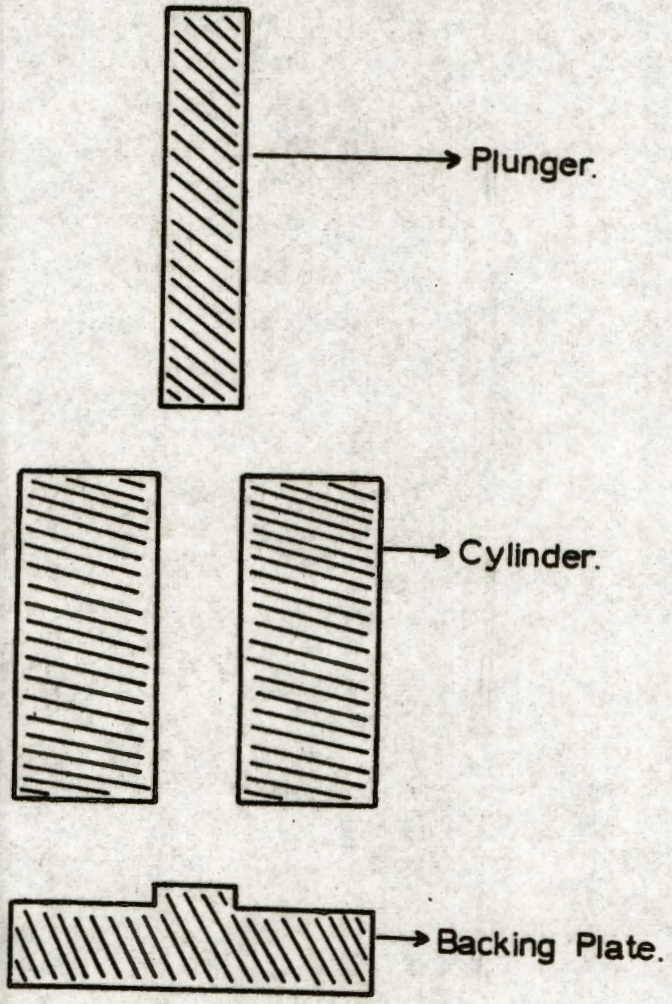

Fig. 2. Basic components of a standard die for pressing alkali halide discs.

so that the actual die face fits into the bore of the cylinder. When pressing discs of supported metal samples, it was found that under load the plunger expands and so causes a widening of the bore diameter. The disc is thus pressed in an opening slightly wider than normal. When the pressure is released, the plunger contracts and so does the bore, which results in too little room for the disc. It therefore buckles in a dome shape and eventually cracks.

Accordingly, the design of a new die was considered. From a Norelco Reporter[32] it was learned that the design as shown in Fig. 3 was suitable for making pellets for X-ray studies. This design was accepted. The main differences evident in the second pattern lie in the bevelled mouth at the bottom of the cylinder, the flat backing plate and the great strength of the apparatus. This allows the sample to be pressed in a "free" space, less affected by the expansion/contraction of the bore.

The success of the KBr die for making KBr pellets, can perhaps be ascribed to the fact that these pellets are usually much thicker than the silica-supported metal discs, allowed for infra-red transmission studies; the greater thickness allows more strength to the pellet. Another possible explanation is the following: The melting point of KBr is 730°C, whereas the melting point of amorphous SiO_2 is >1600°C. Under pressure the KBr will flow more readily than SiO_2. For this reason, during the pressure releasing stage, the KBr pellet will follow the bore diameter of the die more closely than the silica-supported metal disc. While a complete explanation might prove difficult the important fact is that great success is being obtained with this die.

3.2.4 <u>An All Glass High Temperature Infra-red Cell:</u>

The main objective of having a special infra-red cell is to hold the silica-supported metal discs in a fixed position and at a constant temperature in the infra-red beam. The cell must enable the samples to be reduced <u>in situ</u> (to avoid contamination by air) and to be heated at the same time that the infra-red spectrum is recorded. Further, it must be designed in such a way that the beam path cannot be obstructed by glass or other materials which are not transparent to infra-red radiation. The windows (CaF_2 or other salts) which pass infra-red radiation must be secured to the body of the cell by a suitable wax or resin. Ideally, this seal should be able to withstand temperatures up to 400°C (for reduction and to bake out the entire cell in order to remove residual gases). However, at high temperatures the salt windows crack[19] due to the differences in thermal expansion of the materials.

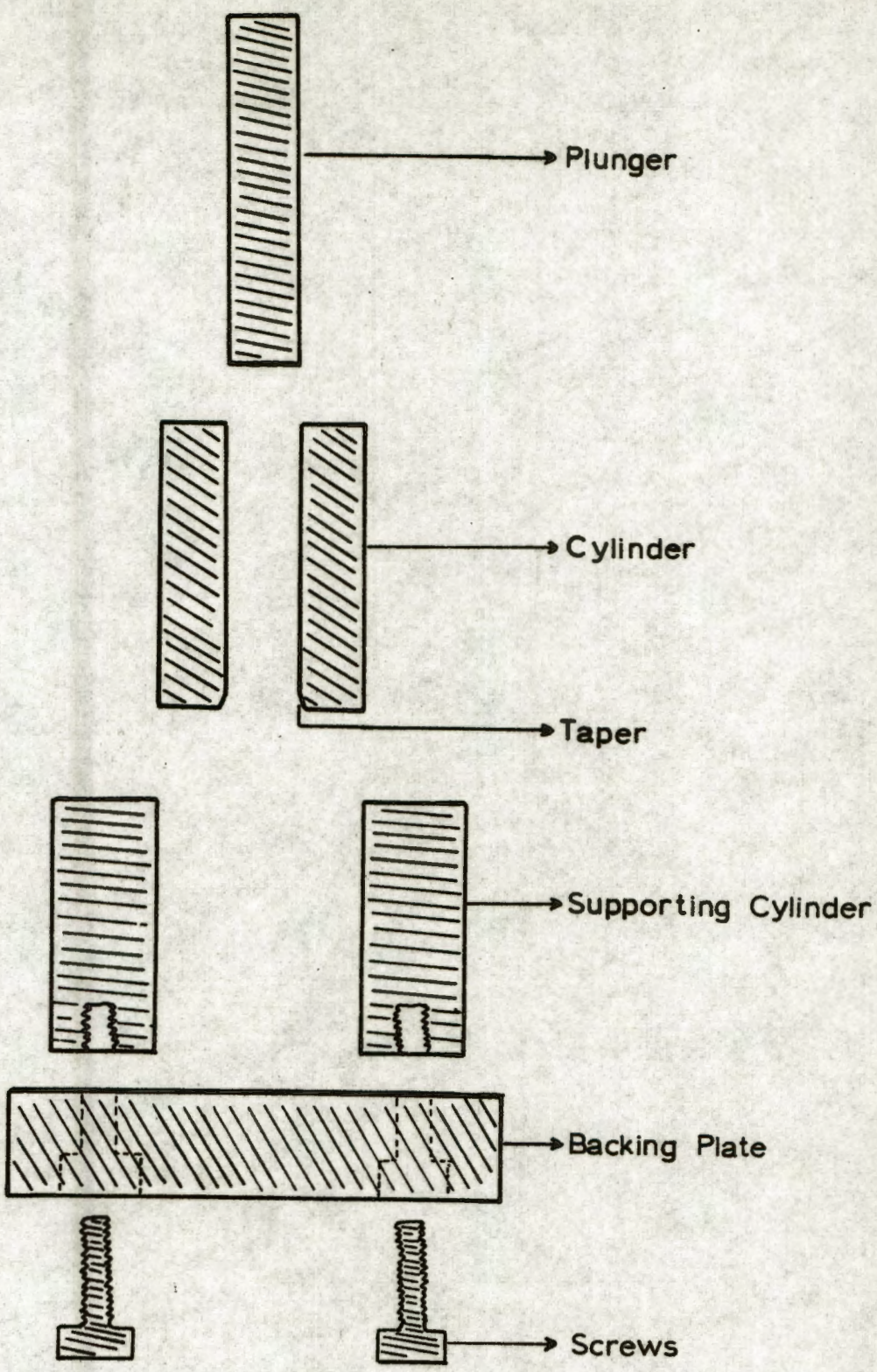

Fig. 3. Basic components of the re-designed die for pressing silica discs.

Therefore, the cell must be designed to keep the salt/glass seal cool while the sample is heated. The construction of this type of infra-red cell is crafty because an *in situ* furnace, a cooling system for the windows, and thermocouple and vacuum connections all have to be designed to fit into a cell compartment of 11 cm long.

Various *in situ* high temperature infra-red absorption cells were designed and constructed. Difficulties were encountered with the question of the cooling of the greased joints, and, in part, with furnace design. The copper tube cooling coils used at first, were found inefficient for certain joints; whereas a furnace consisting of a glass enclosed heating spiral, one on each side of the sample, merely overheated the edges of the sample.

The best cell design found was that shown in Fig. 4. The heating element (30 gauge 80:20 nichrome wire) is wound round the middle part of an 85 mm long Pyrex tube, 26 mm in diameter. In this way the furnace is long enough to achieve good heat distribution across the whole sample. The temperature of the sample disc is measured close to its centre by means of a thermocouple situated in a well in the cell body. The sample is held in position between two small Pyrex rings which just fit the inside of the outer glass furnace tube. Loading is performed by removing one of the cell windows.

The calcium fluoride windows are secured to the cell body with Apiezon T grease thickened by mixing in about 25% of colloidal silica. A thickened silicone grease was tried, but was found to give rise to leaks over long periods. This is probably because silicone grease is less tacky than Apiezon T grease.

The ends of the cell are equipped with water jackets in order to ensure efficient cooling. This prevents the grease from flowing onto the windows. The cell is also equipped with two side arms, fitted with stopcocks, for gas introduction, circulation or evacuation purposes.

This cell functions quite satisfactorily. It can be used continuously at temperatures up to 400°C and for shorter periods up to 500°C. A vacuum of $< 10^{-5}$ mm Hg can be obtained easily.

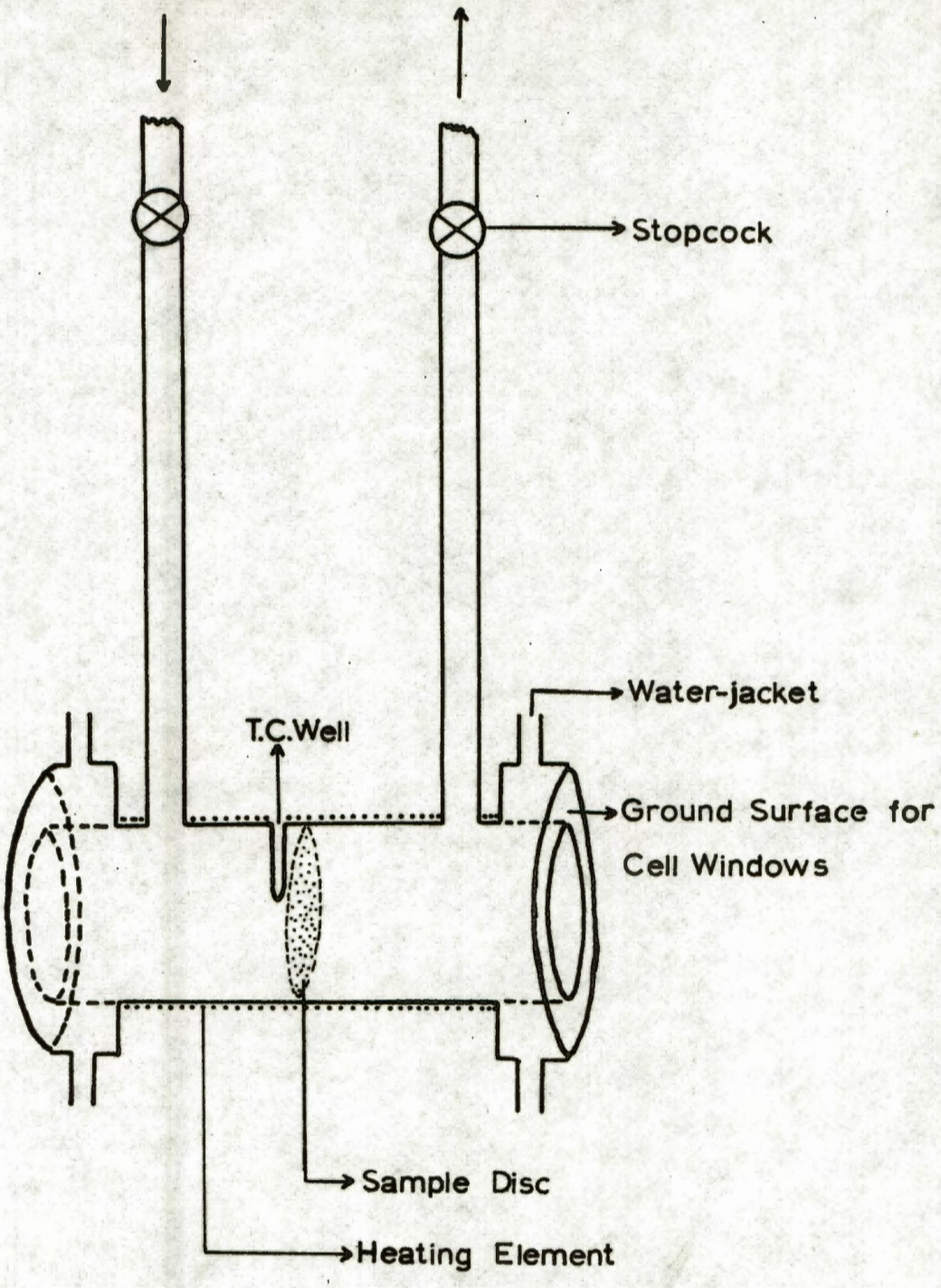

Fig. 4. The <u>in situ</u> infra-red cell.

3.3 GAS PREPARATION:

3.3.1 Purification of Hydrogen and Helium:

Gas from a cylinder was purified[10,48] by passing it over copper turnings at 360°C. This removed the oxygen. The gas was then dried by passing it through a trap cooled with liquid nitrogen, followed by an activated charcoal trap, also cooled with liquid nitrogen. This ensures removal of any other impurities present in the gas.

3.3.2 Purification of Carbon Monoxide:

Iron carbonyl and other impurities were removed[10] from carbon monoxide by passing the gas through a trap cooled with oxygen enriched liquid nitrogen (boiling point about -193°C), and then through an activated charcoal trap at near liquid nitrogen temperatures to remove any other impurities.

3.3.3 General:

The gases used for the experimental studies were stored, after purification, in glass bulbs previously evacuated to about 10^{-6} mm Hg.

The charcoal was re-activated before using it by evacuation at 300°C. It was then cooled down *in vacuo* before use.

3.4 ADSORBENT PREPARATION:

Different types of silica-supported metal samples were prepared. Those used in the spectroscopy contained 5% metal by weight. These are now described.

3.4.1 Silica-Supported Nickel Catalysts:

3.4.1.1 Type I:

Samples containing varying amounts of nickel were prepared by dissolving reagent grade nickel nitrate in de-ionized water. The amount of water was just sufficient to produce a thin slurry with the required amount of Cabosil M5 silica. The slurry was dried at 100 to 115°C and crushed and ground to a fine powder. About 100 mg of the mixture was pressed into a disc, 25 mm in diameter and about 0.2 mm thick using a pressure of 8,000 lb/in^2. The self-supporting discs were used as infrared samples. However, they were first placed in a special furnace and the nitrate decomposed at temperatures ranging from 250 to 370°C in a stream of nitrogen. (Later it was found that decomposition under vacuum *in situ*, yielded a more "active" metal surface — see Appendix 1).

Brown vapours indicated the evolution of nitrogen dioxide. The colour of the discs were brown-black at lower temperatures to black at the higher temperatures of decomposition. The discs were brought into position in the in situ infra-red cell which was then evacuated. Reduction was carried out at temperatures between 250 and 400°C for periods of 2 to 16 hours using hydrogen flow rates of 40 to 400 ml/min.

Purified hydrogen was used. A cold trap at —197°C was placed between the mercury manometers and the sample in order to prevent mercury poisoning of the metal surface. At the exit of the infra-red cell a mercury check valve was placed to prevent back diffusion of air onto the sample. With this valve a positive pressure of about ten millimeters above atmospheric pressure was maintained inside the cell at all times during the reduction. It was considered that there was no risk of poisoning from the check valve since the hydrogen flow would sweep mercury vapour away from the cell.

The reduced sample was either cooled down under vacuum or in a hydrogen atmosphere; the cell being finally evacuated to $<10^{-5}$ mm Hg.

Type I reduced discs were black and remained black on exposure to air.

It was found that a disc containing 5% nickel by weight gave discs of convenient transparency. This is equivalent to about 1 mg nickel per cm^2 of surface.

An X-ray analysis of the reduced supported nickel catalyst proved that the sample was better than 99.5% reduced as no diffraction lines ascribed to nickel oxide were found. Quite sharp X-ray diffraction lines were obtained for both the reduced and unreduced silica-supported nickel oxide.

3.4.1.2 Type II:

It is known[20] that some adsorption sites on silica have an acidic nature. Aqueous solutions of the metal nitrates are also slightly acidic and as a result of this one might expect an uneven distribution of the metal nitrate on the surface of the silica when these two are mixed. When ammonium ions are added to the silica the number of Lewis and Brönsted acid sites are both decreased. For this reason the Type II catalyst was prepared by neutralizing the nickel nitrate solution by adding ammonia until the solution turned blue, prior to mixing with the Cabosil. By doing this it was hoped to get a better distribution of the metal on the surface of the silica (see Appendix 2).

When a disc prepared in this way was decomposed at temperatures from 230 to 330°C, a white deposit was found on the cooler parts of the glass furnace. This white material was most probably ammonium nitrate. At this stage the discs remained a very light-green colour, regardless of the temperature of decomposition, and possibly contained nickel oxide, NiO, which is green; whereas Ni_2O_3 is black [60]. Both oxides show the same X-ray diffraction pattern so that it was not possible to distinguish between the two by this method.

On reduction the discs again turned black, but in general it was found that it was more difficult to reduce Type II catalysts as compared with the Type I. This observation insinuates that the nickel was more evenly distributed for the following further reason: It is generally accepted[1] that the bulk of an aggregate may be readily reduced, but that it is difficult to remove the last traces of oxygen. If the oxide is evenly distributed and therefore, on reduction, it will reach the "difficult stage" earlier. This in effect implies that the Type I catalyst is more crystalline than the Type II. X-ray line broadening studies gave further support to the above.

On one occasion a Type I black nickel oxide disc was left in a hydrogen atmosphere for 1 hour at about 200°C. The disc turned light green but on further reduction it again changed to black without any difficulty. From this observation it is concluded that the reduction of black Ni_2O_3 might proceed <u>via</u> the green NiO phase. The difficulty experienced with the Type II catalysts on reduction possibly cannot therefore be ascribed to the difference in the nickel oxide phase, but rather to the difference in the thickness of the nickel oxide layer and the way it is packed between the silica spheres.

The black reduced Type II discs when exposed to air at room temperature again changed to the pale green colour they had before reduction, whereas, the Type I discs stayed black. X-ray diffraction experiments showed that the bulk of the nickel of the Type I discs remained as nickel metal. Due to the better distribution of the nickel metal for Type II discs, the bulk of the nickel was easily re-oxidized.

The Type II reduced discs were in general also more active to carbon monoxide chemisorption than the Type I reduced samples as shown by their infra-red spectra.

The greater activity of Type II material, relative to Type I, has been explained on the hypothesis that the introduction of ammonia, in

58/.. .. .. ..

the preparative stage, leads to a more uniform silica surface. Alternatively it might be thought that a more finely distributed metal would result by the decomposition of metal ammine complexes, were these to be formed. However, even if there is a strong ammine complex process, the first product formed on heating is the oxide as, prior to reduction and on the introduction of carbon monoxide, band F (CO adsorbed on the oxide lattice) only was observed.

3.4.1.3 Type III:

During preliminary studies on a supported cobalt catalyst it was found that the amount of water used, in preparing the metal nitrate/silica slurry, had a pronounced effect on the rate of reduction of the cobalt oxide. In general it was found that the more water used, the more difficult it was to reduce the oxide to the metal. Other workers[49] have reported that supported nickel and cobalt oxides reduce with greater difficulty than the unsupported oxides. This was ascribed to compound formation between the carrier and the metal oxide. From our experience it appeared that this effect is enhanced by increasing the amount of water at the slurry stage. This could possibly be explained by the longer time of drying of the slurry, i.e. a greater "reaction time". It was thought that a similar effect might be in operation in the case of nickel, but that it would not be observed due to the ease of reduction of nickel compounds as compared with cobalt compounds[49].

Nevertheless, it was decided to prepare a silica-supported nickel sample under anhydrous conditions. In order to achieve this nickel nitrate was dried at 60°C so as to eliminate most of the water of crystallisation. The dried nickel nitrate was dissolved in reagent grade acetone and slurried with Cabosil, dried at 60°C and treated further in the usual manner.

It was found upon reduction that these Type III samples have better transmission properties than either Type I or Type II discs. Also, the method appeared to yield a more active metal surface as measured in terms of the intensities of the infra-red bands. The general pattern of the bands however, was no different from that previously obtained, so that no new information was forthcoming. Nevertheless, it was felt that a more active metal would be more useful in the study of the mechanism of the reaction of chemisorbed carbon monoxide and hydrogen. According to these expectations, small changes in the spectrum would be more easily observed. However, that may be, in practice it was found that samples prepared according to the above procedure have very little (if any)

advantage above those prepared in the "conventional" manner, since the activity of the Type I could be markedly improved (see Appendix 1).

3.4.1.4 Potassium Promoted Silica-Supported Nickel Samples:

A series of potassium promoted samples was prepared. Quantities were calculated in advance in order to yield 5% Ni and a K:Ni ratio of up to 20:100, w/w, in the final product. Two different potassium salts were used, namely

(a) potassium nitrate
and (b) potassium carbonate.

(a) Nickel nitrate and potassium nitrate were dissolved in water. The amount of water was just sufficient to produce a thin paste with the required amount of Cabosil M5 silica. The samples were dried and treated in the usual manner.

(b) Nickel nitrate was dissolved in water and a thick paste prepared with the required amount of silica. An aqueous solution of potassium carbonate was then added in order to yield the required proportions. The samples were dried at 100°C and further treated as above.

(The method described in (a) cannot be used in this case because of the precipitation reaction[59],

$$Ni(NO_3)_2 + K_2CO_3 + H_2O \longrightarrow K_2CO_3.NiCO_3.4H_2O\downarrow$$

which may disturb the distribution of the metal salts).

3.4.2 Silica-Supported Cobalt Catalysts:

Two different types of silica-supported cobalt samples were prepared, both containing 5% Co by weight.

3.4.2.1 Type I:

The Type I cobalt samples were prepared in an analogous manner to Type I nickel samples (see 3.4.1.1) except that in this case a minimum amount of water was used.

3.4.2.2 Type III:

It was found (see 3.4.1.3) that the activity of the cobalt catalyst Type I was very much dependent on the amount of water used in its preparation. An attempt was therefore made to prepare a cobalt catalyst analogous to Type III nickel catalyst. Unfortunately, cobalt nitrate as such does not dissolve completely in acetone. In order to overcome this snag, the cobalt nitrate was first dissolved in a few drops of water,

60/.. .. .. ..

after which acetone was added. This solution was then mixed with the required amount of Cabosil M5 silica. The samples were further treated in the usual manner.

3.4.2.3 Potassium Promoted Silica-Supported Cobalt Samples:

A series of potassium promoted cobalt samples was prepared. Quantities were calculated in advance in order to yield 5% cobalt and a K:Co ratio of up to 20:100, w/w, in the final product. Potassium carbonate was used. The samples were prepared using the standard method as described in paragraph 3.4.1.4.

3.4.3 Silica-Supported Iron Catalysts:

Type I, II and III silica-supported iron samples were prepared as above (see 3.4.1 and 3.4.2), containing 5% Fe by weight. These samples were reduced under identical experimental conditions as used for nickel and cobalt, and subjected to carbon monoxide chemisorption. The transmittance of the discs varied between 20 and 80%. However, no chemisorbed bands were found.

Therefore, other factors, aimed at producing active surface sites were explored, such as: different temperatures and times of reduction; different metal to silica ratios; using iron pentacarbonyl and other iron compounds (e.g. iron oxalate, iron hydroxide and iron carbonate) as starting material instead of iron nitrate. All the above experiments, however, failed to give positive results.

Two possible reasons for our failure in the case of iron are:

(a) Compound formation between the silica (used as a support) and the iron compounds or metal. These metal silicate compounds are more difficult to reduce than the pure metal oxides[1].

(b) If the thermodynamics of reactions of iron, cobalt, and nickel are considered, it is found that the ease of reducibility of oxides increases in the order iron, cobalt and nickel[1]. In order to reduce iron oxide at 350°C the ratio P_{H_2O}/P_{H_2} must be below 0.08, as compared to 80 for cobalt oxide and 550 for nickel oxide[1].

3.5 THE SPECTRA:

3.5.1 Recording the Spectra:

After reduction of the discs and evacuation of the cell the background spectra of the discs were recorded (double beam, with the reference beam evacuated) from 1500 to 2700 cm^{-1}. Experience showed that

61/.. .. .. ..

beyond these limits nothing of interest was to be found in the spectra. The transmittance of the blank samples over this region varied between about 30 and 80%. Immediately after this a few torr carbon monoxide were admitted to the cell and the spectra recorded (superimposed on the background spectra). Usually the spectra were recorded first at increasing carbon monoxide pressures and then at decreasing pressures, especially over the regions where bands were observed. The final spectra, as represented in the figures, were obtained by plotting the differences between the "compound" and "blank" spectra, either as percentage transmission, or as optical density; the latter in order to bring the relationship between band intensities and concentration onto a linear basis. In some cases it also showed the inflection points more clearly.

In the cases where chemisorption was studied at elevated temperatures it was found necessary to record the background spectra at the same temperature and before the gas was brought in contact with the samples. The recording of spectra at elevated temperatures were time consuming, and in order to save time, fixed temperatures were decided upon, usually 390, 300, 200, 100°C and room temperature (i.e. the temperature of the thermostatted spectrometer, viz., 30°C).

Carbon monoxide in contact with metallic nickel forms nickel tetracarbonyl quite readily[34] at about 40°C (see Appendix 4). Therefore the recording of the spectra was done on the same day and as soon as possible after admitting carbon monoxide.

In an attempt to improve the resolution of very intense bands, single beam operation was tried; however, no new information was gained.

3.5.2 Classifying the Spectra:

"Idealized" spectra for carbon monoxide chemisorbed on nickel and cobalt metal and nickel and cobalt oxide supported on colloidal silica are presented in Fig. 5. (For the detail description of the experiments see Appendixes 5 and 10 (nickel), and 14 and 15 (cobalt). It was found that the peak positions of the bands, ascribed to different chemisorbed species do not remain stationary at one particular frequency, but can be displaced. These shifts were found to be influenced mainly by carbon monoxide pressure, but also by small differences in surface such as crystallinity, etc. Therefore, instead of describing the bands with reference to where they were originally found, it was decided to define them as follows:

62/.. .. .. ..

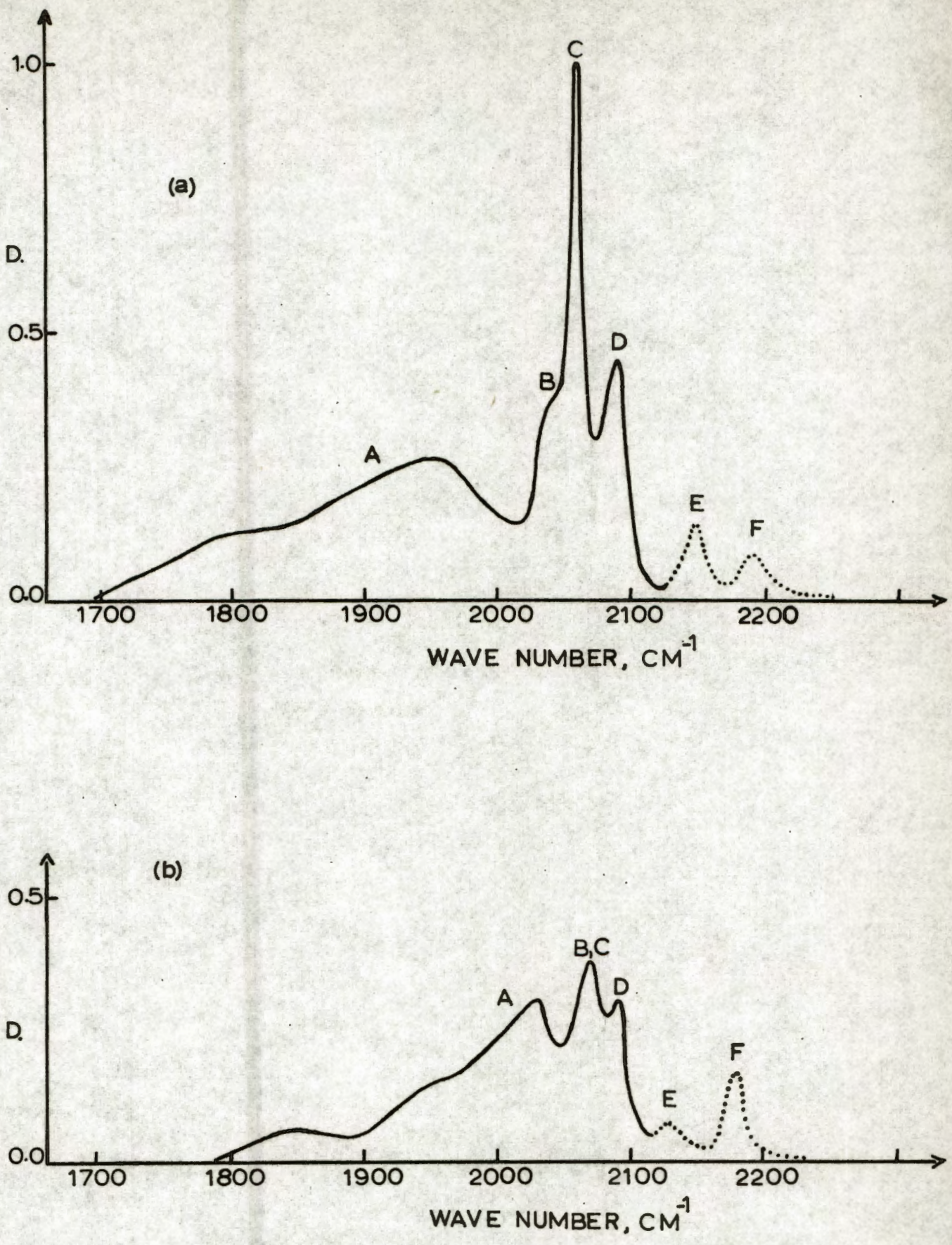

Fig. 5. Typical infra-red spectra for carbon monoxide chemisorbed on (a) nickel and (b) cobalt; supported on colloidal silica.

3.5.2.1 Nickel:

Band A: A broad band found at 1700 to 2000 cm^{-1}. It occasionally has more than one inflection point and can perhaps be subdivided into band A1, A2, etc. The main inflection points are at about 1950 and 1820 cm^{-1}.

Band B: Found at 2035 to 2050 cm^{-1}, but more often at about 2040 cm^{-1}.

Band C: Always found at 2058 $\pm$ 2 cm^{-1}.

Band D: Found between 2060 and 2090 cm^{-1}.

Band E: Found at 2100 to 2130 cm^{-1}.

Band F: Found at 2165 to 2195 cm^{-1}, but more often at about 2190 cm^{-1}.

3.5.2.2 Cobalt:

Band A: A broad triplet occupying the region 1800 to 2040 cm^{-1}; the main inflection point is found between 2015 and 2033 cm^{-1} but more often at 2030 cm^{-1}. Minor inflection points are at about 1960 and 1850 cm^{-1}.

Band B: Found between 2060 and 2073 cm^{-1}.

Band C: Found at about 2070 cm^{-1}, on top of band B.

Band D: Found between 2090 and 2100 cm^{-1}.

Band E: Found at about 2130 cm^{-1}.

Band F: Found at about 2180 cm^{-1}.

3.5.3 The Effects, on the Spectra, of the Method of Preparing the Discs:

3.5.3.1 Nickel:

Type I discs prepared as above (see 3.4.1) and containing 5% of nickel, w/w, showed bands A, B, C and D (Fig. 5(a)) on adsorbing carbon monoxide at pressures up to about 100 torr. It being known[20] that silica is inhomogeneous in that its surface has acid sites, it was argued that the nickel would be more evenly distributed if these were neutralised. Accordingly an ammoniacal nickel nitrate solution was used in preparing Type II discs, since ammonia should neutralise both Lewis and Brönsted sites. Type II discs gave more intense spectra, indicative of better distribution of the metal and a smaller particle size. Subsequently it was found[48] that Type II material chemisorbed relatively more carbon monoxide.

63/.. .. .. ..

Type II material was relatively more difficult to reduce in that the hydrogenation took longer and the presence of bands E and F (Fig. 5(a)), attributed to oxide (see later), were persistently retained relative to more drastic reduction; as might well be expected for more finely divided material. While the facts appear clear, the explanation is possibly obscure. Hofer[49] states that nickel and cobalt hydrosilicates are more difficult to reduce than the oxides (e.g. nickel oxide reduces at 275°C while the hydrosilicates require 500°C).

In the case of cobalt (see 3.4.2.) solutions of the nitrate in acetone were used in the preparation of a Type III material. As an incidental matter, therefore, Type III nickel catalyst was prepared, but found not to differ significantly from Type I, except that it was more active (as shown by more intense bands); however, oxide bands E and F were absent.

For approximately equivalent carbon monoxide pressures the effect of method of preparation of the discs may be summarised in the following way on going from Type I to Type II:

(a) Increase in band intensities.

(b) Broadening and lowering of wave number of band A.

(c) Loss of resolution of band D and better resolution of band B.

(d) Appearance of bands E and F.

When Type II material was reduced at higher temperatures, the following changes in the spectra were obtained:

(a) Increasingly better resolution of bands B and D.

(b) Increasingly larger shifts of bands A, B and D and toward the positions occupied in the case of Type I material i.e. to greater wave numbers.

(c) Lower intensities of bands E and F, ending in their disappearance after prolonged reduction at higher temperatures.

3.5.3.2 Cobalt:

Type I cobalt discs, prepared in an analogous manner to Type I nickel discs (see 3.4.2.), and containing 5% of cobalt, w/w, showed bands A,B, C,D,E, and F (Fig. 5(b)) on adsorbing carbon monoxide at pressures up to about 100 torr. The reduction of Type I cobalt samples took longer

64/.. .. .. ..

relative to Type I nickel. Also, bands E and F (Fig. 5(b)), attributed to oxide (see later), were persistently retained relative to nickel. Even when higher reduction temperatures were used the bands persisted. In general it was found that the intensities of these bands were less than the equivalent nickel bands. Furthermore, the amount of water used in making the slurry was found to have a pronounced effect on the rate of reduction of the oxide; the more water the greater the difficulty of reduction.

It is well established that long times of reduction lead to sintering and thus reduction of surface area and loss of activity. For this reason, and because of the above observations, it was decided to devise a technique for preparing discs in the absence of water in order to promote rapid reduction and higher activity. Accordingly, in preparing Type III discs, water was replaced by acetone. These discs were found to be more active. However, during decomposition of the nitrate a white material was deposited on the windows of the infra-red cell, an obvious disadvantage.

Despite the above, Type I samples proved to be superior in the end provided that (a) a very small amount of water was used in making the slurry, and (b) the nitrate was decomposed slowly and under vacuum prior to reduction.

3.5.4 The Effects, on the Spectra, of Carbon Monoxide Pressure,

A: On the Intensities of the Bands:

3.5.4.A1 Nickel:

A rough average assessment of the effect of carbon monoxide pressure on the intensities of the bands is shown in Fig. 6. Bands A and B appeared first at low pressure, followed by D. With increasing pressure C, E and F appeared in this order.

At the same time, with increasing pressure, A increased at first, reached maximum intensity, then decreased. Upon evacuation A at first increased, but after prolonged evacuation decreased. A is however persistently retained.

The intensity of B was found to vary in proportion to pressure. On evacuation this band was also persistently retained.

The intensity of C was found to be very sensitive to pressure. At high pressure it was the most intense band, but readily disappeared on evacuation.

65/

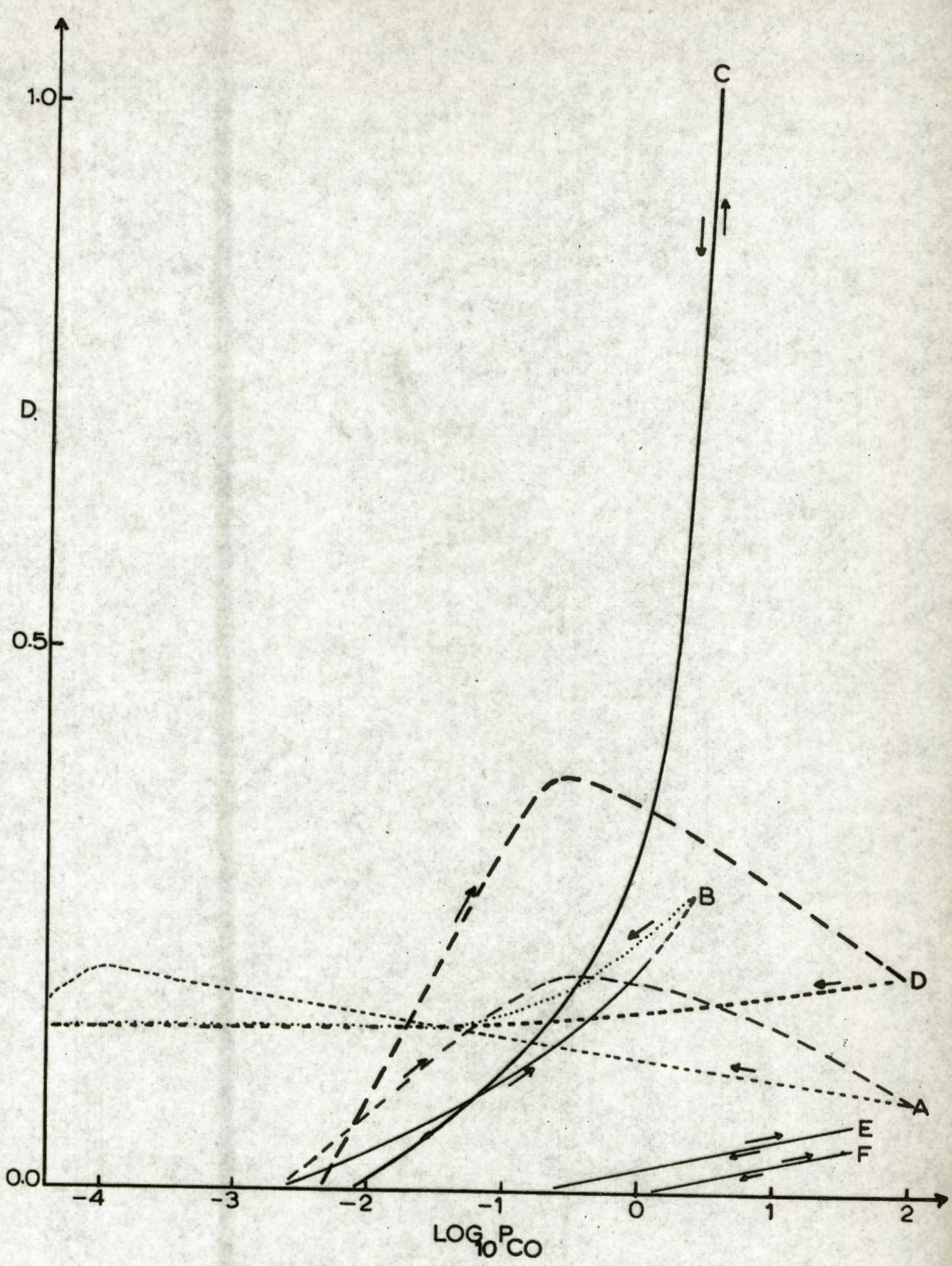

Fig. 6. A rough average assessment of the optical density of the bands, found for nickel, as a function of the carbon monoxide pressure. ⟶ denotes increasing pressure, ⟵ denotes decreasing pressure.

The intensity of D increased rapidly with increasing pressure, reaching a maximum, then decreased. On evacuation it decreased further, although it was persistently retained.

The intensities of E and F, found only at relatively high pressures, were directly proportional to pressure. On evacuation these bands disappear.

3.5.4.A2 Cobalt:

The effect of carbon monoxide pressure on the intensities of the bands is shown in Fig. 7. Cobalt discs were found to be far less active than nickel discs. Consequently, the technique was too insensitive for the recording of the low pressure data found for nickel on increasing the coverage with rising pressure. However, on decreasing the pressure the coverage remained in the detectable range.

In the case of nickel the bands appeared in the order A + B, D, C, E, F. For cobalt, because of the relative insensitivity, this order could not be established, A, B, D, E and F appearing more or less simultaneously, followed by C. From Fig. 7 it can be seen that the bands follow the same pattern as for nickel samples (see Fig. 6). However, band A appears to be more persistently retained than is the case for the nickel samples.

B: On the Wave Numbers of the Band Maxima:

3.5.4.B1 Nickel:

The peak positions of bands A, C, E and F were not affected by pressure. However, B and D underwent displacements towards larger wave numbers with increasing carbon monoxide coverage, and conversely, shifted to smaller wave numbers, with decreasing pressure. Also with increasing pressure, D was displaced to smaller wave numbers after the maximum intensity had been attained.

After evacuation, the peak positions of B and D were at higher wave numbers (after the application of high carbon monoxide pressure) relative to those at which the bands were first observed at low pressures.

3.5.4.B2 Cobalt:

The peak positions of bands C, E and F remained unchanged with carbon monoxide pressure variation. Bands B and D were either unaffected or shifted towards higher wave numbers, (about 5 cm^{-1}-, with increasing pressure. The peak position of band A could also be regarded as unaffected, although cases were found upon evacuation where its maximum

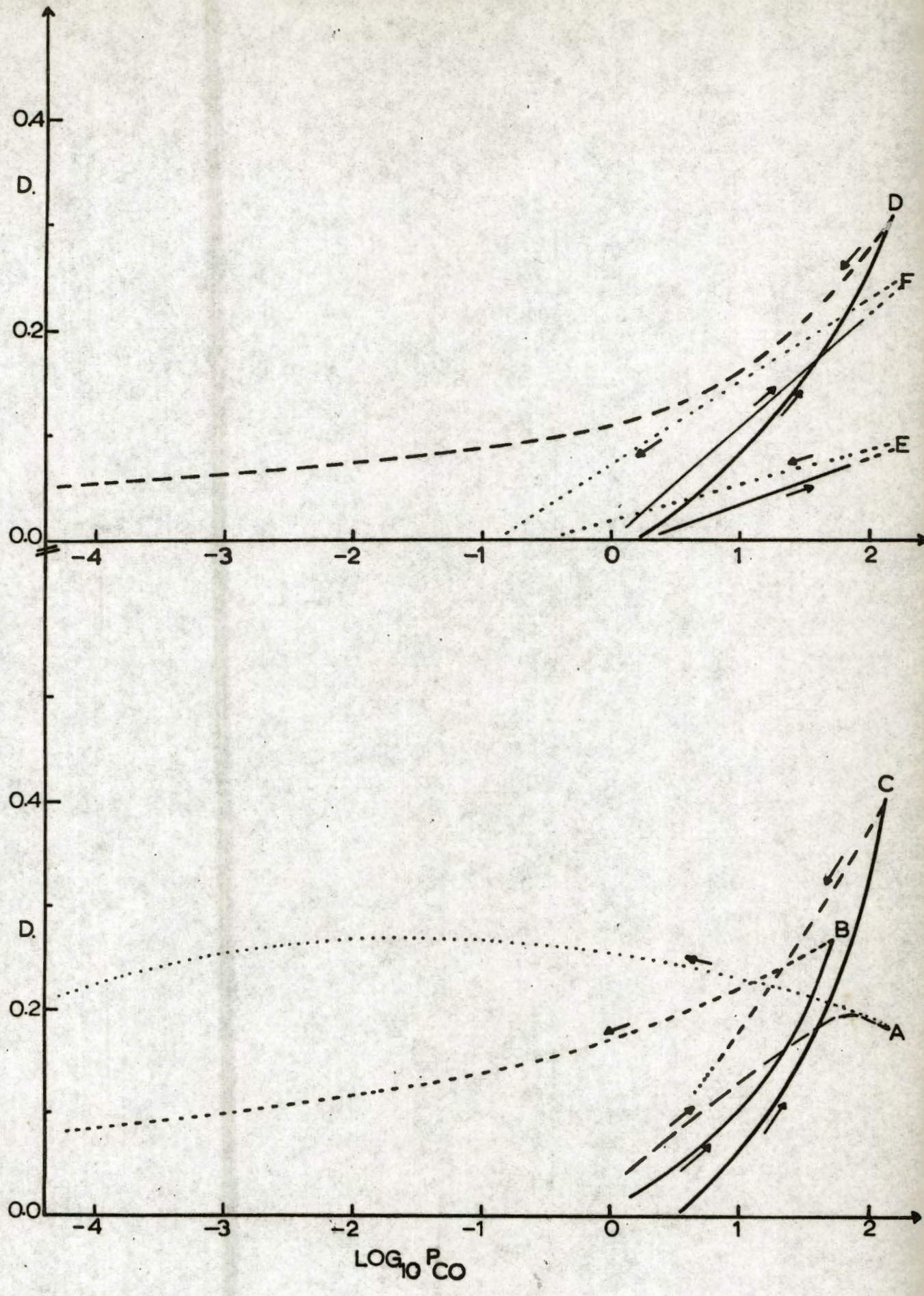

Fig. 7. A rough average assessment of the optical density of the bands, found for cobalt, as a function of the carbon monoxide pressure. ⟶ denotes increasing pressure, ⟵ denotes decreasing pressure.

shifted to lower wave numbers.

3.5.5 The Effects, on the Spectra, of Temperature:

3.5.5.1 Nickel:

Unpromoted Samples:

The effect of temperature was analogous to that of desorption on evacuation; at higher temperatures the bands were simply less intense and bands B and D were displaced to lower wave numbers. At 300°C (about the temperature of Fischer-Pichler synthesis) bands A, B and D were still present (see Appendix 8).

3.5.5.2 Nickel:

Promoted Samples:

Samples promoted with potassium (used as an "industrial synthesis" promoter) showed effects similar to the above. Both the peak position and the intensity of band D were very much dependent upon the temperature — the band was shifted to a lower wave number and decreased in intensity with increasing temperature (see Appendix 12). In the case of band A, it was mainly the high wave number side of the band that was affected in the same way.

3.5.6 The Effects, on the Spectra, of the Presence of Potassium in the Discs:

3.5.6.1 Nickel:

The presence of potassium (used as an "industrial synthesis" promoter) in the reduced discs caused a displacement towards lower wave numbers of bands A, B and D (see Fig. 8). The shifts were found to be related to the concentration of potassium up to a certain limit, whereafter the peak maxima remained constant. For the potassium promoted samples band B was found at relatively high carbon monoxide presure only (see Appendix 11). The positions of the absorption maxima of bands C and E were unaffected by the presence of potassium. Band F (for the unreduced discs) showed a very slight lowering in wave number at high potassium concentrations. Also, at high potassium concentrations the optical densities of all the bands decreased, except that the integrated intensity of band A increased in the presence of potassium, due to the general increase in the optical density of the low wave number side of this band. From Table I it can be seen that, at almost constant carbon monoxide pressure, the intensity of band D (relative to A) decreased with increasing potassium concentration.

67/.. .. .. ..

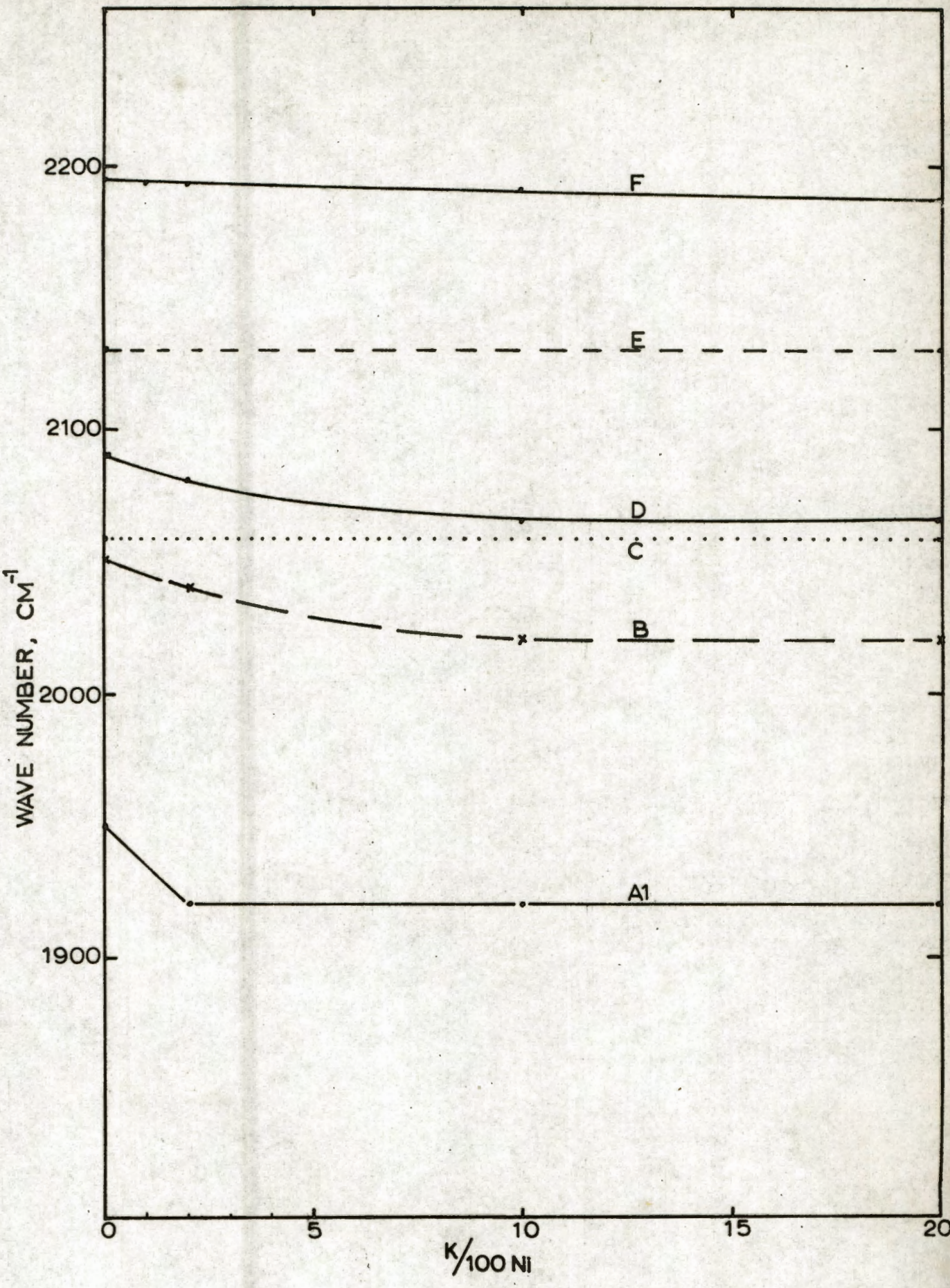

Fig. 8. The effect of potassium on the wave number of the bands found for carbon monoxide chemisorbed on nickel.

Note: At these low carbon monoxide pressures, bands D and A were the only two found for the potassium promoted samples.

TABLE I

K/100 Ni	P_{CO} x 10^{-2} torr	Optical Density*		
		Band D	Band A	D/A
2	3.5	0.35	0.12	3.0
10	3.5	0.21	0.17	1.2
20	4.0	0.21	0.16	1.2
20	3.0	0.17	0.18	0.95

* Optical density as measured by height.

Further, band F behaved differently in that at low potassium concentrations it first increased in intensity, reached a maximum, and then decreased. This effect is illustrated in Fig. 9. (Carbon monoxide chemisorption on treated Type I nickel oxide gave bands F and F2 — see Appendix 10. The effect of potassium on both bands F and F2 was similar as can be seen from Fig. 9).

At high temperatures A, B and D were usually still present but in the presence of potassium, shifted to wave numbers below those at which the bands were initially observed at room temperature and at low carbon monoxide coverage.

3.5.6.2 Cobalt:

The effect of the presence of potassium in the discs, on the wave numbers of the maxima of the bands, are shown in Fig. 10. All the bands, perhaps with the exception of band C, were displaced to lower wave numbers. The bands became broader and consequently it was more difficult due to their overlap, to determine the maxima accurately (see Appendix 16). Furthermore, just as was the case for nickel, bands B and D were found only at relatively high carbon monoxide pressure.

In the case of the unpromoted cobalt oxide catalyst, only one band F (at about 2180 cm^{-1}) was found. With increasing potassium concentration the intensity of this band decreased (see Fig. 11), while simultaneously, a new band F2 (at about 2160 cm^{-1}) appeared (Fig. 11). At high potassium concentration F2 was the most intense band, although much less intense than F for the unpromoted samples.

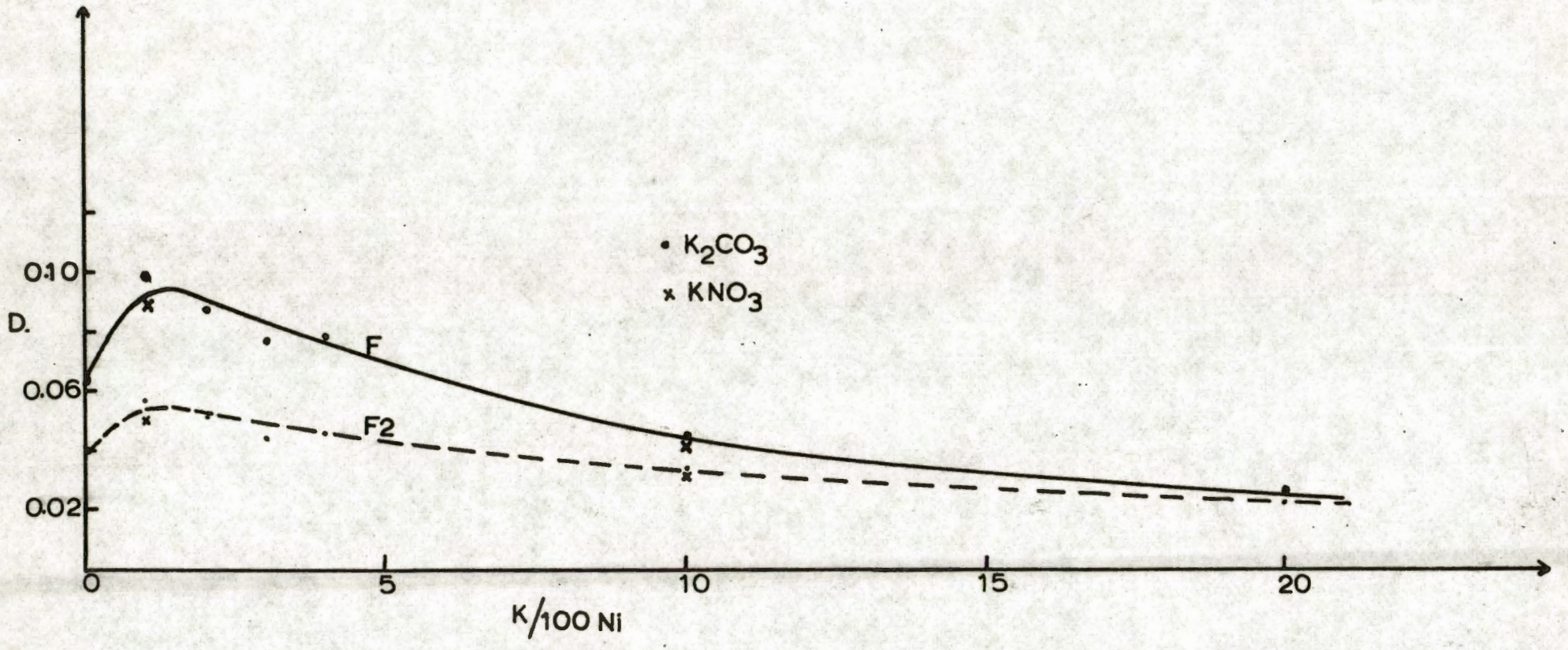

Fig. 9. The effect of potassium on the intensities of bands F and F2 found for carbon monoxide chemisorbed on nickel oxide, at 20 torr pressure.

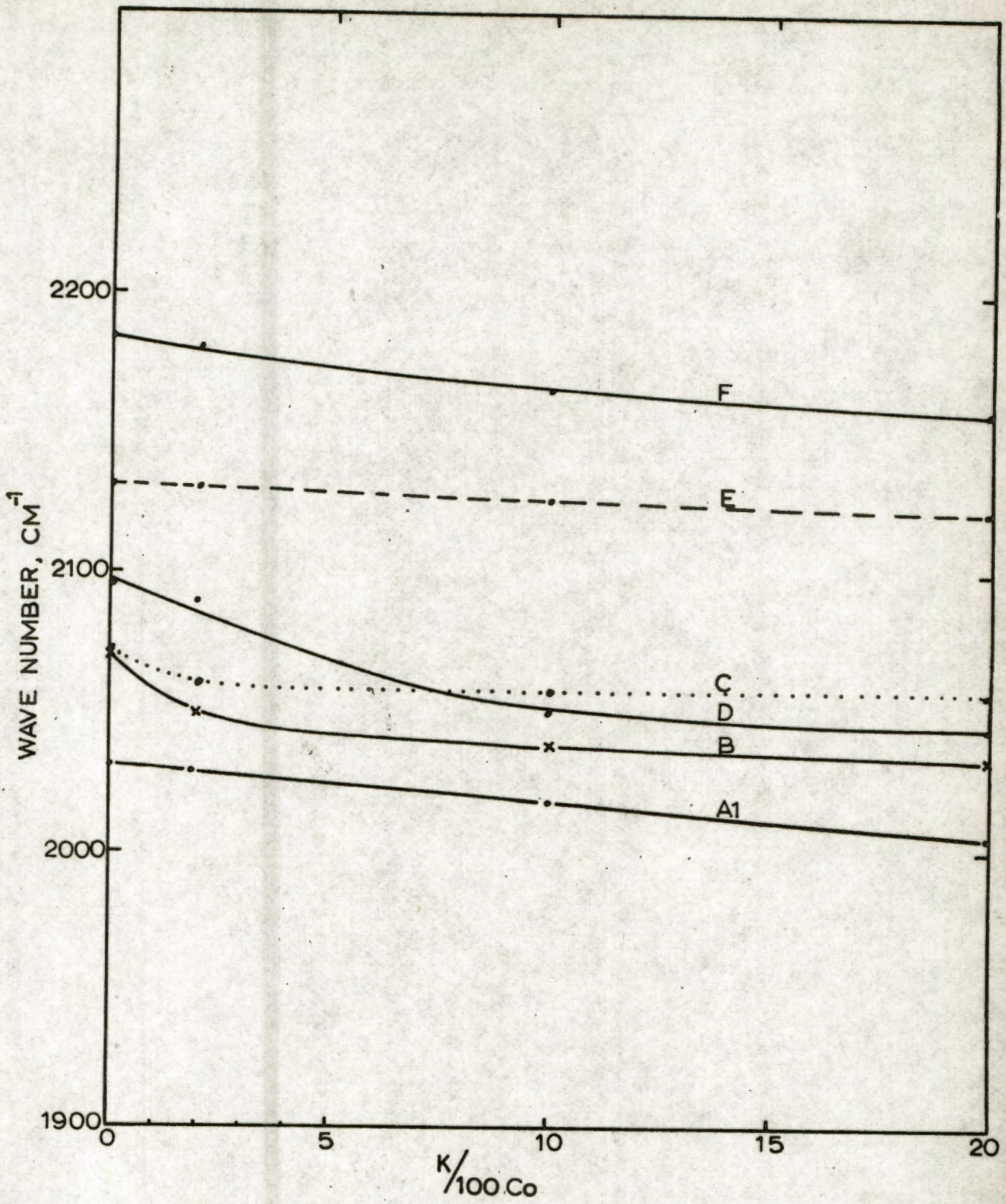

Fig. 10. The effect of potassium on the wave number of the bands found for carbon monoxide chemisorbed on cobalt.

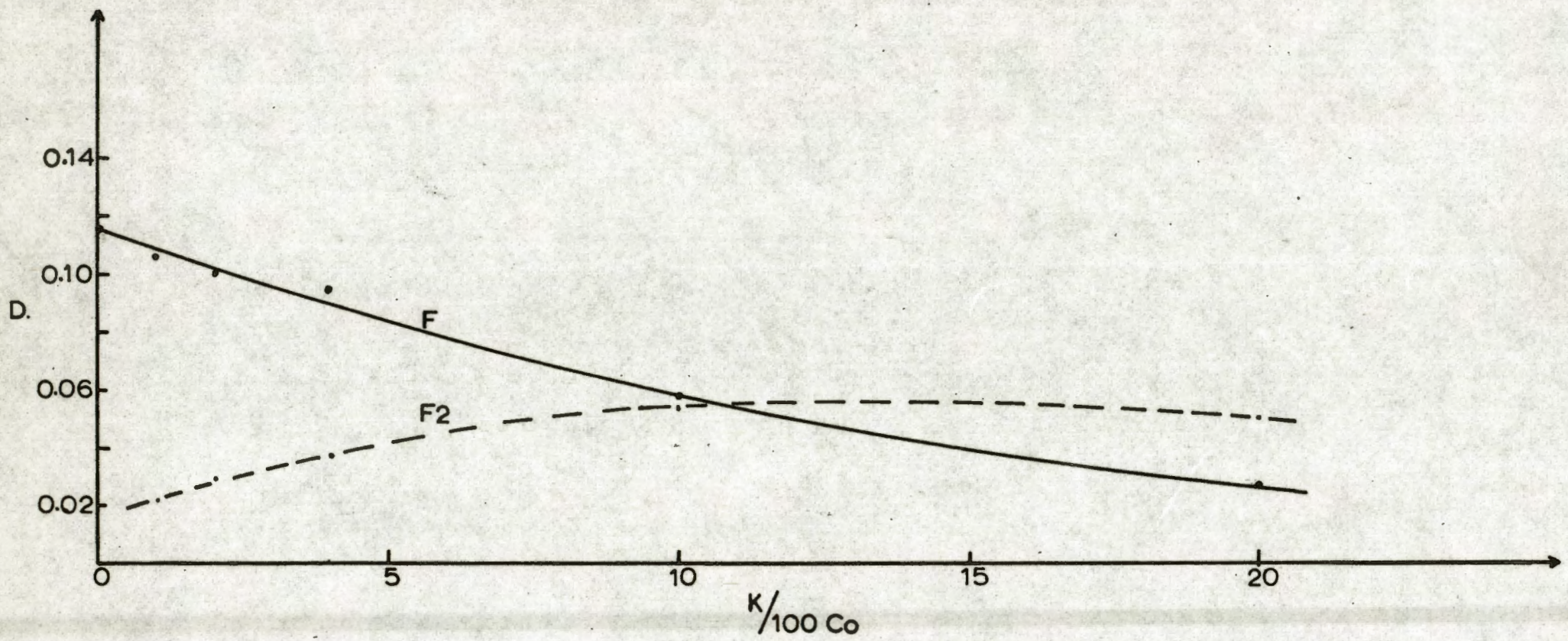

Fig. 11. The effect of potassium on the intensities of bands F and F2 found for carbon monoxide chemisorbed on cobalt oxide (at 3 torr pressure).

3.5.7 The Effects, on the Spectra, of adding Hydrogen:

3.5.7.1 Nickel:

Unpromoted Samples:

The following observations were made at room temperature. When hydrogen was admitted to the cell (containing nickel samples upon which carbon monoxide had been adsorbed), the initial effect on the spectrum was that band B decreased or disappeared, while D increased in intensity and simultaneously shifted to higher wave numbers. After a few hours the intensity of A usually increased. The remainder of the spectrum remained essentially unaffected.

Further interaction took place (see Appendix 9) when the temperature was raised, A and D decreased in intensity (the latter at a faster rate) and these bands finally disappeared. However, during rapid heating and cooling, A decreased in intensity with temperature more rapidly than D, relative to observations made when the temperature was constant. At the same time methane was detected in terms of a band observed at 3016 cm^{-1}, both at low and high hydrogen pressures, and irrespective of the rate of heating to the reaction temperature.

3.5.7.2 Nickel:

Promoted Samples:

When hydrogen was introduced to a potassium promoted nickel surface containing adsorbed carbon monoxide it was found that(in the course of time) band A increased in intensity. This effect was more pronounced with increasing potassium concentration (see Appendix 13). Also, as potassium concentration increased, higher reaction temperatures (or else longer reaction times) were necessary to hydrogenate the chemisorbed CO species. This is illustrated in Table II.

TABLE II.

K/100 Ni	Reaction Temp. (oC)	Reaction Time (Min)	O.D. of A *	
			Before hydrogenation	After hydrogenation
0	220	5	0.22	0.12
10	220	10	0.17	0.13
20	200	30	0.115	0.13

* Optical density as measured by height.

69/

At low hydrogen concentrations methane was not detected. For larger amounts of hydrogen, and on heating, methane was not detected until after the A band diminished. Furthermore, at low H_2:CO mole ratios not only was the formation of methane inhibited, but carbon dioxide was formed. With high ratios the converse was found. This is illustrated in Table III.

TABLE III

K/100 Ni	P_{H_2} (torr)	P_{CO} (torr)	H_2:CO ✱	Reaction		Optical Density ✱ ✱	
				Temp. (°C)	Time (mins.)	CH_4	CO_2
0	10.5	1.0×10^{-3}	high	100	(3 days)	0.03	-
	10.0	2.5×10^{-3}	high	200	30	0.04	-
	26.0	5.5×10^{-3}	high	200	30	0.06	-
2	0.1	3.5×10^{-2}	low	200	5	-	0.01
	20.0	3.5×10^{-2}	high	200	5	0.02	0.02
10	0.1	3.5×10^{-2}	low	200	10	-	0.02
	0.1	3.5×10^{-2}	low	200	30	-	0.05
	11.0	3.5×10^{-2}	high	200	5	0.02	0.04
	11.0	3.5×10^{-2}	high	200	10	0.03	0.02
	0.7	1.3	low	200	45	-	0.07
	20.0	1.3	high	220	10	0.03	0.03
20	1.0	2.8	low	300	30	0.02	0.03
	21.0	2.8	high	300	30	0.07	0.01

✱ Note: High means the mole ratio is above 7; low means below 3.

✱ ✱ Optical density as measured by height.

REFERENCES:

See Chapter 4.

CHAPTER 4.

DISCUSSION OF THE SPECTRA.

4.1 INTRODUCTION AND THEORY:

The vibrational interaction of gaseous carbon monoxide molecules, with electromagnetic radiation, generates an infra-red band centred at 2,143 cm^{-1}. In the metallic carbonyls the same stretching mode gives bands at about 2,000 cm^{-1} for terminal groups and from 1,750 to 1,875 cm^{-1} for bridging groups. There is a preponderance of evidence[38] showing that, in both cases, the molecule is linked to metals from the carbon atom. The facts (infra-red and Raman studies, magnetic properties, calorimetry, etc.) are probably best summarised in terms of molecular orbital models.

4.1.1 Terminal Ligands:

In the mononuclear carbonyls carbon monoxide ligands are symmetrically arranged about central metal atoms. The carbon atoms exist in a state of sp hybridisation and the ligands are attached via their carbon atoms. Similar terminal ligands exist in the multinuclear carbonyls which also contain bridging carbonyl groups in which the carbon atoms are in a state of sp^2 hybridisation analogous to the carbonyl groups of ketones.

According to the molecular orbital theory ten electrons of the carbon monoxide molecule occupy the molecular orbitals: $\sigma 2s$, $\sigma^* 2s$, $\sigma 2p$, $\pi_y 2p$ and $\pi_z 2p$ ($z\sigma^2$, $y\sigma^2$, $x\sigma^2$, $w\pi 4$ by the Mulliken notation). The molecule has a low dipole moment (about 0.1 Debye) because the negative charge of the four bonding orbitals, associated more with the oxygen nucleus, is more or less neutralised by: (a) the larger positive charge of the oxygen nucleus relative to the carbon and (b) the stronger association of the filled antibonding orbital with the carbon. Thus the $\sigma^* 2s$ orbital forms a "lone pair", with its charge directed along the axis of the molecule, away from the carbon atom.

Carbon monoxide must be a very weak Lewis base as its complexes (for example with the halides of boron), if they exist at all, are very unstable[21]. Its bonding with transition metal atoms in the carbonyls, and on chemisorption, may thus be explained according to the following theory: Were a σ bond to be formed only by overlap between the $\sigma^* 2s$ lone pair orbital of carbon monoxide and an empty σ metal or lattice orbital, the ligand would be very weakly attached

71/.. .. .. ..

because the bonding would be neutralised by electrostatic repulsion arising out of the transfer of negative charge to the metal. In order to explain the relatively strong bonds existing between the carbon of the ligand and the metal, further bond formation and charge transfer are postulated; namely so-called "π back bonding", formed by overlap between occupied metal d orbitals and unfilled π^* orbitals of the ligand and yielding charge transfer in the opposite direction. Thus the electronic charge transferred from the ligand to the metal is more or less neutralised by that transferred from the metal to ligand by π back bonding, and both the new σ and the π contributions are able to combine their weights, as it were, in attaching the ligand to the metal, in the absence of electrostatic repulsion.

Blyholder[39] makes the point that, according to calculation, π back bonding gives the electrons involved a state of lower energy (relative to the energy levels in the lattice); furthermore the orbitals involved are of compatible symmetry, i.e. bonding for the metal-carbon bond but anti-bonding for the carbon oxygen bond. Orgel[50] points out a synergism in that the π back bonding assists σ bonding, in the matter of avoidance of electronic repulsion, and vice versa. (Dipole moment studies[38] indicate that the moment of a metal-carbon bond is only very low, about 0.5 Debye, suggesting a close approach to electron neutrality). In the case of metallic carbonyls there is evidence[38] for a bond order of ligand attachment, greater than unity. (In particular, although donation from the metal to the empty ligand orbital is the predominant π interaction, there is also mixing of the bonding and non-bonding π orbitals of CO under the influence of the metal[50]. This leads to an increase of the double-bond character of the metal carbon bond).

On the above basis, σ bonding between metal and ligand, will withdraw anti-bonding within the carbonyl group, and therefore tend to raise the infra-red frequency. Conversely, and for the converse argument, π back bonding will lower the frequency. Thus the infra-red spectrum will, as it were, indicate the resultant of the two effects.

4.1.2 Bridged Ligands:

Bridged carbonyl ligands are well known in the binuclear metal carbonyls. The carbon atom of this ligand is sp^2 hybridised and forms σ bonds with both metal atoms and with the oxygen.

72/.. .. .. ..

There is also a π bond to the oxygen formed by overlap of the carbon p_z orbital.

In binary metal carbonyls the bridging carbonyl groups contribute one electron to each of the metal atoms in order to form σ bonds. π back bonding from the metal in this case is more complicated and it appears to be more extensive than, or of a different form to, that in terminal carbonyl groups[51]. The carbon-oxygen stretching frequencies are observed around 1,850 cm^{-1}, much lower than those for the terminal carbonyls.

In most cases bridging carbonyl groups are symmetrically bound to the two metal atoms, but cases were found in which it was believed[51] that the bridging groups were asymmetrically disposed between the two metal atoms. The vibration frequencies of such groups would be observed part-way between a purely terminal carbonyl group and a purely bridging carbonyl group.

In the case of saturated aldehydes and ketones the carbon atom in the carbonyl chromophore is in a state of sp^2 hybridization. In ketones the bonding in the carbonyl group is similar to that of binary metal carbonyls in that the carbonyl contributes one electron to each of the adjacent carbon atoms in order to form covalent σ bonds. In the aldehydes one σ bond is formed with the hydrogen atom.

If the carbonyl group is bound to unsaturated atoms (as in conjugated aldehydes or ketones) the electrons of the carbonyl and of the adjacent radicals must be considered[64] as a single system of delocalized electrons. This allows a maximum π electron delocalization and a maximum stability of the molecule in the absence of other steric factors.

Pure organic compounds containing a bridging carbonyl group show[64] a strong band in the region 1,650 to 1,850 cm^{-1}. However, an analysis[64,65] of the carbonyl stretching frequencies of various types of carbonyl compounds, suggests that the observed band position results from the interplay of both chemical and physical effects; among which the physical state of the compound, the inductive effect, the electronic and mass effects of neighbouring substituents, bond angle effects, hydrogen bonding, etc., are important. For example, groups with a strong electron-repelling inductive effect increase the negative charge on the oxygen and the vibration frequency decreases relative to that of the normal ketones. In the case of unconjugated aliphatic ketones[41] the carbonyl stretching frequencies lie within the narrow range from 1705 to 1720 cm^{-1}.

73/.. .. .. ..

4.1.3 Chemisorption and Infra-red Frequencies:

It seems[3,6,8,10,30] that carbon monoxide is chemisorbed to transition metal (iron, nickel, platinum, rhodium, palladium, etc.) surfaces in a manner analogous to its bonding in the metallic carbonyls, i.e. terminally and bridged. As has been seen in the literature survey (Chapter 2), various carbonyl stretching infra-red bands were observed and assignments made. It seems that in going from the free carbon monoxide molecule to consideration of the terminal ligand, the carbon to metal π bond must strongly influence the chromophore (relative to the σ bond) since there is a pronounced shift to lower wave numbers from 2,143 to about 2,000 cm^{-1}. This conclusion is supported by Blyholder's[39] theoretical work. Bridged structures show an even more pronounced shift to lower wave numbers as expected since the carbonyl bond order has changed from three to two.

Eishens, et. al.[52] attributed absorption bands at about 2,190 cm^{-1} to adsorption of carbon monoxide onto oxygen sites of oxide lattices. This is in agreement with the above theory since oxygen cannot supply d electrons for π back bonding and only the σ effect leading to higher wave numbers, relative to carbon monoxide, can operate.

Various of the above workers[8,21,22] found sharp bands near 2,050 cm^{-1}, ascribed to terminal ligands. Multiplicity of the structure of this band was ascribed to variations, say in crystallinity, of the adsorbent.

π back bonding will occur from an adsorbent which contains dπ bonding electrons, e.g. a transition metal ion in its crystal lattice. Once again, the shift in frequency will be determined by the amount of π back bonding overlap. In order to promote bonding, overlapping orbitals must be of compatible symmetry and of comparable energies. Apart from this, the extent of back bonding will be determined by (a) the availability of metal d π bonding electron density and (b) the number of ligands attached to the central metal ion and sharing the electron density. The greater the number of metal dπ bonding electrons, the greater the shift in frequency will be. On the other hand, an increase in the number of ligands (attached to the central metal ion), the greater the competition for dπ electrons, and the lower the frequency shift will be. Therefore a terminal CO ligand bonded to a metal ion has a frequency lower than that of the free carbon monoxide molecule. If more than one absorption band is observed it quite possibly means that it is due to different terminal ligands in varying environments. Furthermore, Blyholder[39] suggested that, in order to explain the multiplicity of the structure of the spectrum at about 2,000 cm^{-1}, the metal

atoms surrounding the metal atom to which carbon monoxide is adsorbed, are all considered as ligands. As such they will be all involved in π bonding with partly filled metal d orbitals. The carbon monoxide will thus be in competition for d electrons of the central metal atom. For the metal carbonyls it was found[53] that substituents which do not engage in π bonding with the metal atom, permit stronger π bonding between the metal atom and carbon monoxide. As the π character of the metal - carbon bond increases, the bond order of the carbon - oxygen bond decreases which results in a lowering of the carbon-oxygen stretching frequency. It must be concluded, therefore, that carbon monoxide chemisorption on sites rich in d electron density, i.e. edge, corner or defect sites or sites in crystallographic planes of low coordination number, would form a stronger metal-carbon bond, than on sites of high coordination number.

All the above workers[6,8,10] found broad bands spread over the approximate region 1,850 to 2,000 cm^{-1}. It was generally agreed that this must be assigned to bridged chemisorbed species, in analogy to the carbonyls of manganese, iron, cobalt and rhodium[19]. In contract to the above assignment, Blyholder[39] explains the low frequency in terms of exceptionally strong π back bonding operating on terminal ligands chemisorbed on very dispersed metal sites. However, this view was sternly criticised by Yates in the "discussion" of Blyholder's paper[39]. Furthermore following Blyholder's view, it is surprising that different ways of sample preparation and different supports yielded almost identical spectra[9], i.e. the same inhomogeneity is reproduced with every independent preparation.

4.2 THE ASSIGNMENT OF THE INFRA-RED BANDS OBSERVED FOR CARBON MONOXIDE CHEMISORBED ON SILICA-SUPPORTED NICKEL AND COBALT.

As shown under "experimental" a number of well characterised bands were observed in the region of 2,000 cm^{-1} for carbon monoxide species chemisorbed on silica discs containing metallic nickel (Fig. 5(a)) and cobalt (Fig. 5(b)). The spectra are essentially similar; their main differences being: A different distribution of intensity ratios and a significant shift to higher wave numbers from nickel to cobalt. This shift will be explained later. Incidentally, metallic nickel and cobalt have the same crystallographic structures (face centered cubic) and this may well be the reason for the similarities in the spectra. An assignment of the bands to hypothetical structures in the case of nickel follows.

75/.. .. .. ..

4.2.1 Nickel Spectra:

4.2.1.1 Bridged Ligands

From Fig. 5 it can be seen that band A is broad and occurs at low frequency. In the case of nickel it is a doublet occupying the region 1700 to 2,000 cm^{-1}. Although it is a band of medium optical density only, it is very broad, and must therefore be representative of a large fraction of the total population. We are in agreement with Eischens, et. al.[6] (and in disagreement with Blyholder[39]) that band A must be assigned to carbonyl ligands attached to two metal sites analogous to the bridging groups that occur in the metallic carbonyls. The correctness of the latter assignments have been well established by vibrational mode analysis (for example the work of Sheline and Pitzer[54] on iron enneacarbonyl).

Our evidence for the assignment of band A, as suggested in Fig. 12 (a), is as follows:-

(a) Band A appeared first (Fig. 6.) at very low pressures and persists most tenaciously on evacuation of the cell. It must therefore be attributed to species involving the most active sites and the case of low surface coverage. These conditions are optimum for the sharing of metal sites by one ligand without competition from other ligands.

(b) While the broadness of band A may be attributed to ranges of variation in the bonding character due to surface heterogeneity, it seems very likely that a bidentate ligand might well respond more sensitively than a terminal group. In fact A has the character of a doublet in the case of nickel and this might be assigned to diagonal versus "in line with lattice" adsorption or with adsorption on two different crystallographic planes. Similarly the A triplet for cobalt might be indicative of three crystal planes (e.g. 110, 100 and 111; the three main planes for face centered cubic structures).

In contract to the above is Blyholder's[39] molecular orbital "view", suggesting that all the bands could be assigned to terminal carbonyls. He explains the low wave numbers in terms of particularly strong chemisorption involving the formation of virtual double bond character for the link joining the carbon to the lattice.

76/.. .. .. ..

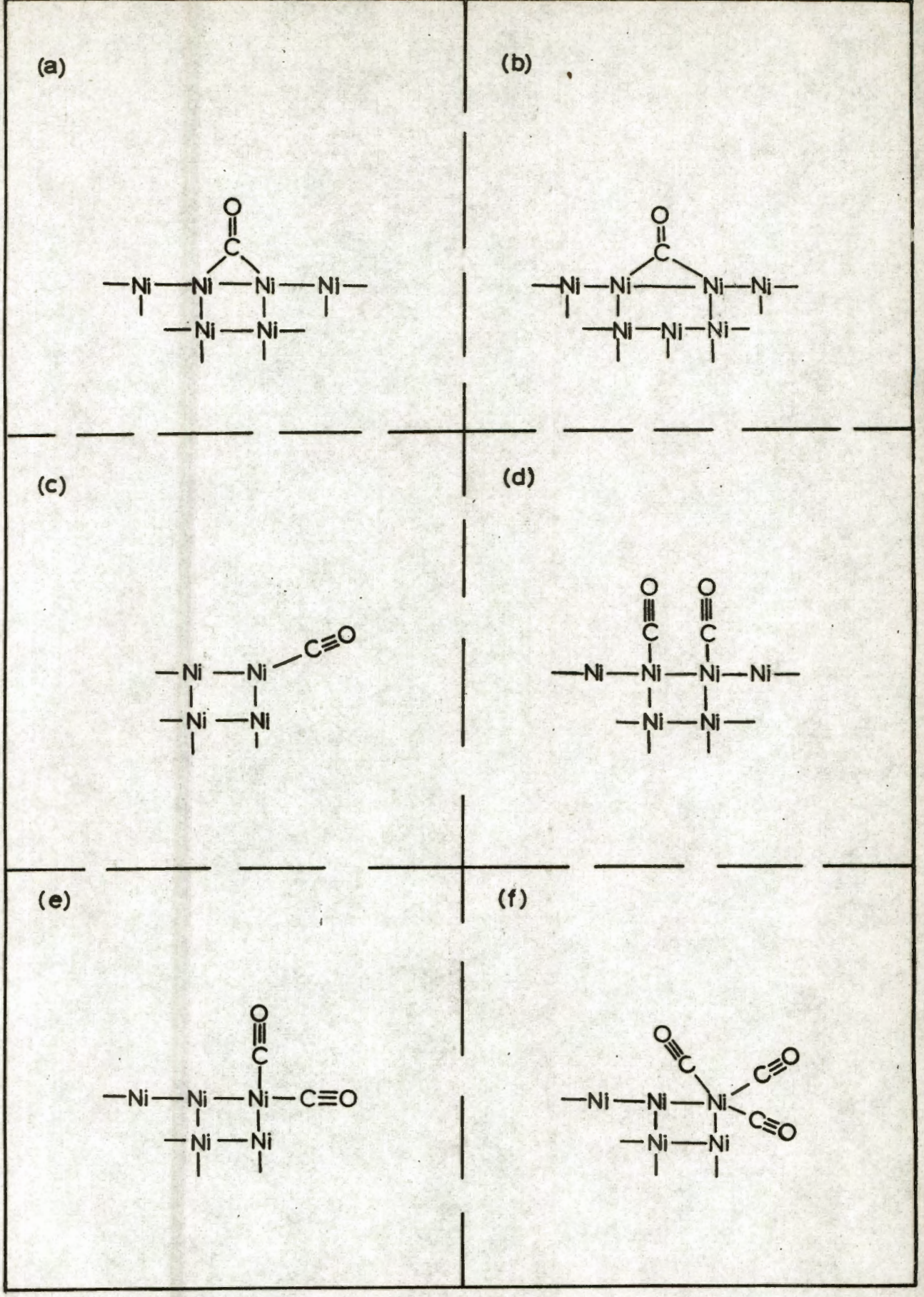

Fig. 12. Possible structures for carbon monoxide chemisorbed onto nickel atoms.

In these cirumstances, the carbon-oxygen bond order would be expected to be lowered to such an extent as to include band A. He explains the broadness of such bands in terms of low coordination number sites with large degrees of freedom.

There is further reason for adopting the Eischens hypothesis rather than Blyholder's view, because band B (see later) is well explained in terms of assignment to the very sites suggested by Blyholder. (Incidentally Blyholder observed but two bands and was unable therefore, to see this more complete picture).

(c) As the carbon monoxide pressure is increased to about 0.5 torr, the intensity of A diminishes with pressure, indicating that "bidentate" ligands are being displaced by "terminal" ligands. On evacuation the reaction reverses; so adding to the weight of the explanation.

(d) Type II discs yielded a more active surface which resisted reduction (relative to Type I discs) and the material was shown[48] to have a greater capacity for adsorbing carbon monoxide. The carbonyl spectra were more intense. X-ray work showed the nickel to be less crystalline and hence more dispersed.

On changing from Type I to Type II discs there is a shift of the maximum of band A from about 1955 to 1920 cm^{-1}. Accepting that Type II nickel is the more dispersed, this is consistent with the concept of larger M-C-M bond angles for the corresponding bridge structure. In confirmation, Halford[41] has shown, empirically, for unconjugated ketones, that increasing bond angles give shifts to lower wave numbers (Fig. 12(b)).

(e) When Type II discs were further reduced at higher temperatures, it was considered to improve the crystallinity by sintering. Band A was shifted to higher wave numbers from 1920 to 1945 cm^{-1}, which is interpreted as the reverse of (d), above. This is in agreement with the expected smaller bond angles.

Thus Blyholder's[39] suggestion, that low frequency bands be assigned to strongly held terminal ligands must surely fall away.

4.2.1.2 Terminal Ligands.

(1) One Ligand per Site:

Bands B and D must be assigned to terminal carbonyls chemisorbed onto single nickel atoms in agreement with the conclusions of earlier

workers[6,8,39] and with the spectra of the metallic carbonyls.

Band B (with A) appeared first when carbon monoxide is introduced at low pressure, and persists tenaciously on evacuation. B is a shoulder of medium intensity, on the low wave number side of band C, resolved at low pressures. It lies between 2,030 and 2,050 cm^{-1} depending on the sample and on the carbon monoxide pressure. Its intensity and its wave number increases with pressure as shown in Fig. 6. On increasing the surface coverage band B shifts in the direction of band C and B is obscured, so that it is not possible to follow the fate of B at the higher coverage.

Band D represents also (like A and B) a species held strongly to the metal surface. It appears shortly after B (and A) and is also very persistent upon lowering of the surface coverage on reducing the pressure and/or on increasing the temperature. D is a band of medium intensity and occurs between 2,060 and 2,090 cm^{-1}, depending upon the sample and on the carbon monoxide pressure. In the present experiments it was found (Fig. 6) that the intensity of D increases with pressure up to optical densities of about 0.4; corresponding to pressures of the order of 0.15 torr. Thereafter the intensities generally dropped, indicating diminution of species concentration. This diminution is very plausibly explained by supposing the adsorption of one or more further carbonyls on the same sites, thus diminishing the D species concentration. While the intensity of D increases with pressure so does its wave number increase from 2,060 to 2,090 cm^{-1}. D often ends up as a shoulder on the high wave number slope of C, because of the rapid increase in the intensity and broadness of C with increasing pressure.

Eischens, et. al.[19], and later O'Neill and Yates[9], considered the probability that band D might be due to more than one carbonyl group chemisorbed onto a single nickel atom as they observed this band only at the higher coverages, but no firm conclusion could be warranted.

On the other hand, Yates and Garland[8] ascribed band D to terminal ligands on dispersed nickel sites and band B to terminal carbonyl groups on crystalline sites. This conflicts with Blyholder's[39] molecular orbital theory for carbon monoxide chemisorption on metal surfaces. According to this view (see 4.1.3) the converse assignment should be made, i.e. band B represents carbon monoxide species adsorbed on metal sites on edges, corners or defect sites, or sites in crystallographic

planes of low coordination number, such as the 110 plane (Fig. 14). Band D should perhaps thus be assigned to ligands chemisorbed on sites of high coordination number, such as the 100 crystallographic plane (Fig. 14.) (For steric hindrance reasons the 111 plane is not chosen for band D). Hypothetical structures for B and D are suggested in Fig.'s 12(c) and (d), respectively.

We must therefore agree with Blyholder's view and for the following reasons:

(a) Band D, as compared to band B, was in general better resolved for Type I samples, which are expected to be the more crystalline. On the other hand, band B was found to be better resolved on the more dispersed Type II samples. This is in accordance with the assignments of the two bands.

(b) Band B was found to be better resolved on the samples reduced at lower temperatures. The lower the temperature of reduction the less the probability of sintering and hence the greater the number of dispersed sites.

(c) Conversely to (b), the resolution of band D improved with increasing temperature of reduction, i.e. considered to improve the crystallinity by sintering (see Appendix 5 (b)).

(d) In further support of the above ideas, the shifts to higher wave numbers shown by B and D, with increasing coverage, are in agreement with two theoretical concepts:

(i) When relatively isolated Ni—C—O species are compared with the case in which ligands exist side-by-side, as it were, there will be increasing competition for lattice d electron density. The resulting diminution in π bonding will lead to less transfer of charge from the carbon-oxygen bonds to oxygen, and hence to increasing wave numbers.

(ii) An increasing dipole-dipole interaction between adjacent ligands in the highly crowded state is expected. Herzberg[35] discusses the form of the perturbing potential energy function in such a case. The dipoles, being of similar signs, will of course repel one another and Herzberg points out that the potential energy of interaction may be expressed in the form of a polynomial of the type:

$$-ar^{-3}+br^{-4}+ \ldots\ldots\ldots$$ where a,b, ...

79/.. .. .. ..

are constants and r is the distance of separation. The first term in the expression represents the dipole-dipole interaction. Eischens, et. al. discuss this factor in one of their first papers[19]. Later they show[40], on the basis of a mathematical treatment, that the dipole interaction would be expected not only to increase the vibration frequency, but also the intensity of the band. The latter would of course be obscured by the concurrent increase in species concentration.

(e) Beyond a certain, critical, coverage the wave number of D (band B is by now obscured by C) was observed to diminish slightly, and in the end D was assimilated by C (see Appendix 5). It can therefore be supposed that singly held ligand species (i.e. one ligand per site) are being replaced by $Ni(CO)_x$ ($2 \leq x \leq 4$) species, leading to a reduction of the dipole-dipole repulsion and hence to a lower carbonyl vibration frequency.

(2) More Than One Ligand per Site:

Band C was always found at the higher coverages after bands A, B and D had appeared. It was of high optical density and sharp, and its intensity was sensitively dependent upon carbon monoxide pressure. Its wave number is virtually constant (2058 ± 2 cm^{-1}), and it coincides with that of nickel tetracarbonyl. However, the P and R branches at about 2053 and 2061 cm^{-1} respectively being absent, it can be concluded that band C cannot be ascribed to nickel carbonyl. It seems most plausible, therefore, even if perhaps a little naive, that this band must be assigned to sites in which two, three or four ligands are chemisorbed on single metal atoms, as suggested in Fig's. 12(e) and (f).

In some experiments part of the intensity of band C could be ascribed to the presence of nickel tetracarbonyl since the P and R branches appeared and the nickel carbonyl bands at 2,480 and 2,550 cm^{-1} were observed. The presence of this substance in the contents from the liquid nitrogen cooled trap was confirmed by its spectrum.

Evidence, confirming the above assignment of band C, is as follows:

(a) Band C increased in intensity, at the expense of D, as the carbon monoxide pressure was increased.

(b) Band C did not suffer pressure broadening when helium was admitted to the cell, relative to a similar experiment conducted on nickel carbonyl.

80/.. .. .. ..

(c) In certain experiments, on evacuating the cell via a cold trap after observing intense C bands, no nickel carbonyl could be found on re-introducing the contents of the trap to an infra-red cell (see Appendix 6).

(d) The P and R branches of nickel tetracarbonyl is about 8 cm^{-1} far apart whereas the separation between bands B and D is about 30 cm^{-1} so that these latter bands cannot be ascribed to the P and R branches of gaseous nickel tetracarbonyl.

(3) Ligands Attached to Oxide Lattices:

Band E is a weak band which occurs at the intermediate frequency range of 2,100 to 2,130 cm^{-1}. Band F is also a weak band which lies between 2,165 and 2,195 cm^{-1}. Both bands (E and F) were observed at high coverages; their intensities increased with pressure. They represent species held weakly to the surface as they readily disappeared upon degassing.

Band E is assigned to carbon monoxide ligands adsorbed on the nickel ions of nickel oxide lattices (Fig. 13(a)), whereas band F (after Eischens, et. al.[52]) is attributed to the asymmetric stretching vibration of carbonyls adsorbed onto the oxygen ions of nickel oxide (Fig. 13(b)).

Evidence for the assignment of E is as follows:-

(a) E was not found on unreduced nickel oxide.

(b) It was observed only in those instances when it was known that the original sample was poorly reduced. This was confirmed by the disappearance of the band on further reduction.

(c) Band E appeared when the discs had suffered partial oxidation on heating with carbon monxide.

In agreement with the above, O'Neill and Yates[27] described a band at 2,125 cm^{-1} as "probably due to a CO molecule weakly held to a nickel site, ... only found with a band at 2,060 cm^{-1} when the nickel oxide has been reduced by CO". Also in agreement, Yang and Garland[7] found a band at 2127 cm^{-1} for carbon monoxide chemisorbed on alumina-supported rhodium; which they ascribed to the species $^{O}C\diagdown\diagup O$ —Rh— , being the oxidation product of $^{O}C\diagdown\diagup C^{O}$ —Rh— .

81/.. .. .. ..

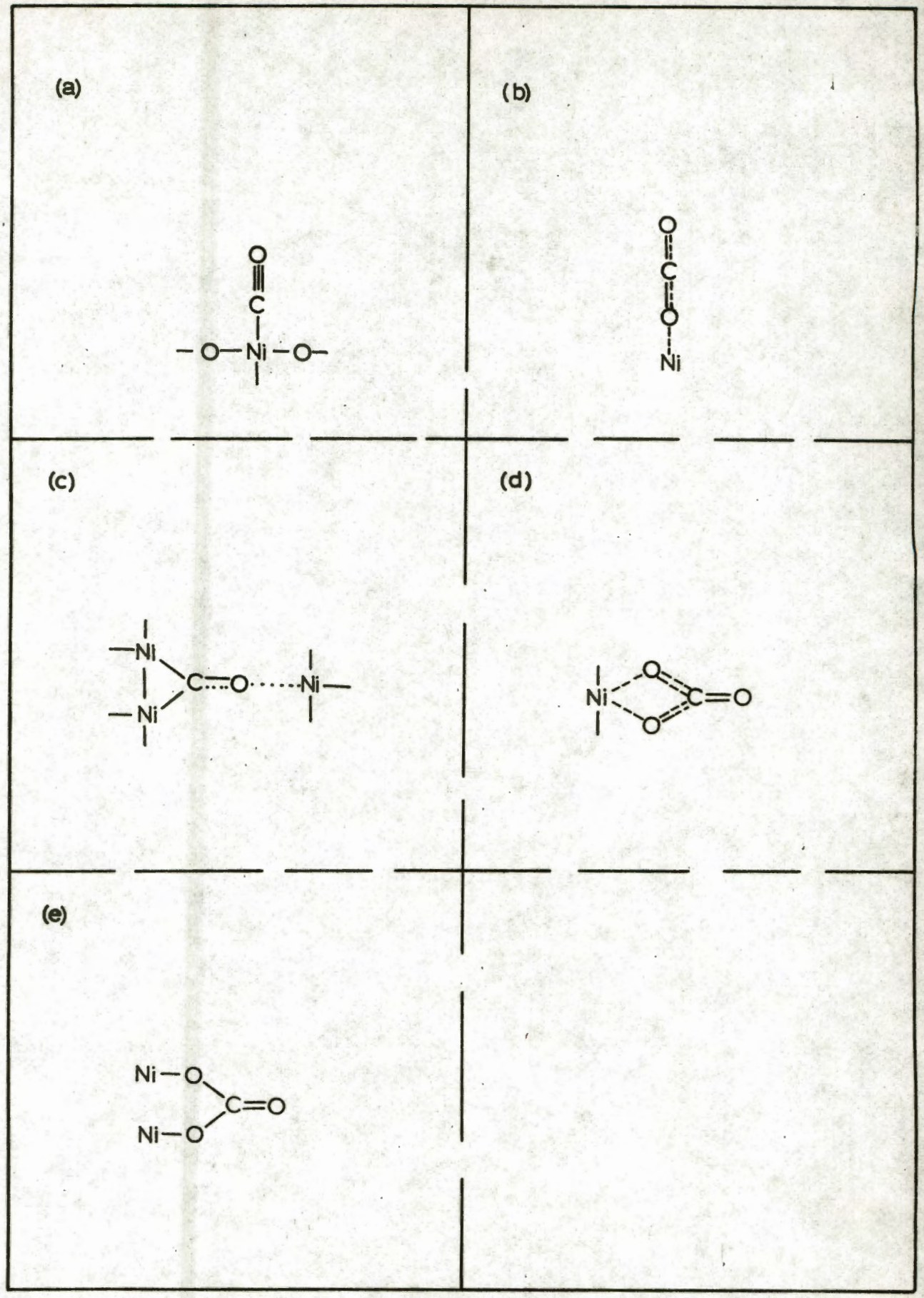

Fig. 13. Possible structures for carbon monoxide chemisorbed onto (a) partly reduced nickel oxide, (b) nickel oxide, (c) two nickel atoms and associated with a third nickel atom; (d) and (e), carbon dioxide chemisorbed onto nickel oxide.

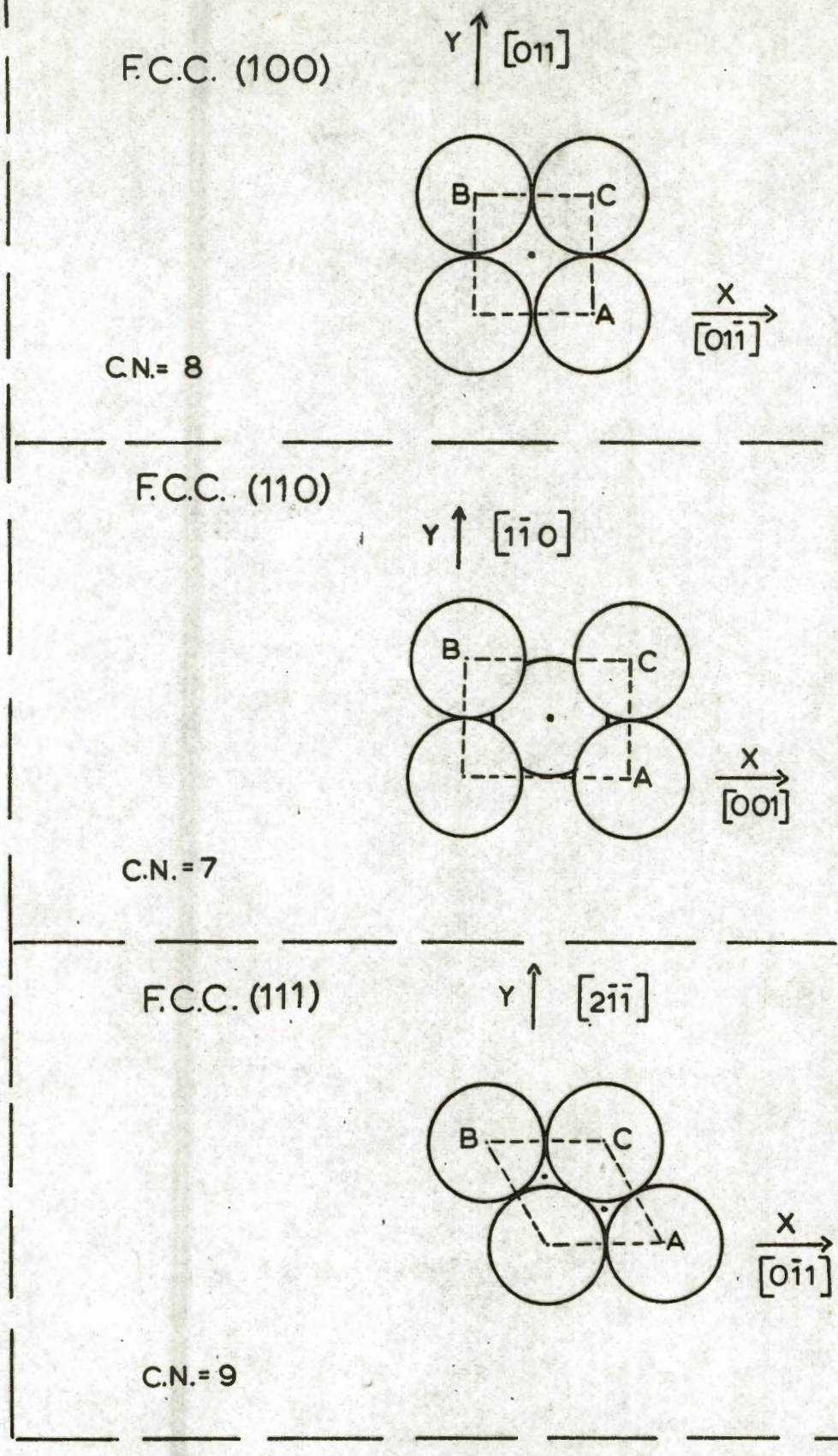

Fig. 14. Atom positions in the 100, 110 and 111 planes of a face centered cubic structure.

Parkyns[42] found a band at 2,075 cm^{-1} on decomposing nickel carbonyl on silica which he interpreted as above. It seems more likely that he was observing carbon monoxide adsorbed on metallic nickel.

Evidence for the assignment of F is as follows:

(a) Band F was found on the unreduced nickel oxide.

(b) It was observed when incomplete reduction of the sample was suspected.

(c) It appeared when the discs had suffered partial re-oxidation.

(d) The observation of band F goes hand in hand with the formation of carbon dioxide, detected in terms of the doublet observed at 2,345 cm^{-1}. It was found both in the cell and in the liquid nitrogen trap.

The assignment of F is in agreement with O'Neill and Yates[27] who described the band as due to "the stretching vibration of a carbon monoxide molecule loosely attached to an oxygen atom unlikely to be part of the support". However these workers[27] and others[43,52] failed to detect the formation of carbon dioxide.

Blyholder's[39] theoretical work is also in agreement with the above assignments. In the metal oxides part of the d electrons are used in the formation and bonding of the oxide species and are therefore not so readily available for π bonding with a carbon monoxide ligand. Carbon monoxide molecules bound to nickel ions in oxide lattices will therefore be bound more loosely than in the case of metal lattices; π back bonding will be less and the C—O bond will be stronger; hence the wave number (band E) will be expected to be higher than in the case of carbonyls attached to metal lattices. When carbon monoxide is bound to oxygen ions the withdrawal of antibonding density from the C—O moiety actually leads to a higher vibration frequency (band F) than observed for the free CO molecule.

Peri[26] also found band F near 2,200 cm^{-1} on silica-supported nickel oxide. On mild treatment of the sample with hydrogen, band E appeared at about 2,140 cm^{-1}. When the number of hydrogen treatments was increased, band E remained fairly strong while F decreased in intensity. Thus Peri's observations are in agreement with the above assignments. However, in his[26] experiments bands E and F did not completely disappear upon prolonged reduction. This could be due to the static reduction conditions used, instead of a flow method (used in this work) which is much more efficient.

4.2.1.3 The Assignment of a Band at 1,620 cm^{-1}.

In an experiment (see Appendix 9) in which a large amount of carbon dioxide and methane were formed, a fairly intense band at 1,620 cm^{-1} was found. In other experiments in which only methane was formed, no band was found in this region. It was therefore decided that the band must be due to carbon dioxide adsorbed onto either a nickel phase or the silica support itself.

In order to distinguish between these two possibilities, carbon monoxide was admitted to a pure silica disc and heated to about 390°C. A small amount of carbon dioxide was slowly formed (due to disproportionation of carbon monoxide, according to the Boudouard reaction[45]), but no bands other than the gas phase carbon dioxide band was found. From this it was concluded that the band at 1,620 cm^{-1} was due to carbon dioxide adsorbed onto nickel or nickel oxide (this is supported in the literature[22]).

There exists much confusion[21,22] as to what the correct assignment for a band in this region might be. An interesting assignment is shown in Fig. 13(c) as suggested by Garland, et. al.[13]. Another acceptable assignment is that of the bidentate carbonate type structure[21] shown in Fig. 13(d). The band at 1,620 cm^{-1} would be assigned to the stretching vibration of the free ketonic group. However, the most likely assignment[22] for a band at 1,620 cm^{-1}, under these experimental conditions, will be that of the bidentate carbonate structure as suggested in Fig. 13(e) for the reason that the structure of Figs. 13 (e) and (d) are expected to show pairs of bands[22] respectively at 1,630 and 1,220 cm^{-1} and at 1,570 and 1,330 cm^{-1} respectively. We were unable to observe the low frequency bands in the present work as our samples were opaque in these regions of the spectrum.

4.2.2 Cobalt Spectra:

Cobalt, having one less 3d electron than nickel is expected to form weaker $d\pi$ back bonds. The σ bond will not be strengthened to the same extent as in nickel and the carbon - oxygen bond strength should be greater; resulting in a shift to higher wave numbers of bands A, B, C and D relative to nickel. Thus the cobalt spectra are well explained, qualitatively, by these considerations.

4.2.2.1 Bridged Ligands:

For the cobalt discs band A is a triplet occupying the region 1,800 to 2,040 cm^{-1}. The pressure of carbon monoxide was found to

83/.. .. .. ..

to have a similar effect on its intensity (Fig. 7), as was the case for nickel, and the interpretations must therefore be the same.

It is of interest to note that the unit cell length of cobalt (a_o = 3.55Å) is slightly greater than that of nickel[62] (a_o = 3.51Å). Due to the relation between X—C—X bond angle and carbonyl frequency[41], one would expect band A for cobalt at lower wave numbers as compared to nickel. The band for nickel was, however, in fact found in the region of 1,700 to 2,000 cm^{-1} which is lower than for cobalt. It appears that the greater $d\pi$ electronic back bonding for nickel dominates the mechanical angle effect; in agreement with the carbonyl frequency shifts in substituted metal carbonyls[63].

The 1,876 cm^{-1} band of dicobalt octacarbonyl gas has been assigned[55] to a bridged carbonyl. Bands attributed to terminal carbonyl frequencies were found in the region of our bands A, B and D. It might be argued, therefore, that the frequency of band A, in the case of cobalt, lies at too high a wave number to be attributed to bridged species. However that may be, we are convinced that our assignments must be correct, despite the anomaly, because not only does the cobalt spectrum closely resemble the nickel one, but the bands show very similar intricate pattern of responses to the various factors studied. In defence of this hypothesis, therefore, we must appeal to the following considerations:

Liquid and gas phase spectra differ considerably and the spectra of ligands sited at a gas-solid interphase can be expected to differ very considerably from those of ligands bound within a gaseous molecule. In our studies the single CO molecule is sited on one or two metal atoms in contact with many others. $d\pi$ back donation to the carbonyl chromophore may well not be as extensive as that from the metal atom in an isolated gaseous compound. Thus, although gas and liquid phase spectra might give an indication of assignments to be considered, such comparisons should not be taken too far. In this connection it seems worth mentioning that the vibration frequencies for terminal carbonyl groups in substituted metal carbonyls have been found as low as 1,723 cm^{-1}, well within the region usually accepted for bridged carbonyls[21]. Thus the reverse might perhaps also be possible; it seems that up till now, no-one has had reason to attribute vibration frequencies in the generally accepted linear region, to bridged carbonyl species. The above is somewhat strengthened by a point made in a review by Abel[51], in which the existence of "partially"

84/.. .. .. ..

bridged CO species with an intermediate vibration frequency has been reported.

4.2.2.2 Terminal Ligands:

Bands B, C, D, E and F were found in the same region as for nickel. Their response to carbon monoxide pressure were similar and, accordingly, they must be assigned in an analogous manner. However, it was observed that for the cobalt discs, the optical density of band C was not as intense relative to the other bands as was the case for nickel. This is explained as follows:-

(a) The nickel surface was more active than that of cobalt.

(b) Nickel tetracarbonyl forms quite readily in contrast to cobalt octacarbonyl which only forms at very high carbon monoxide pressures[1,38,55]. Therefore, the concentration of the species, say $M(CO)_x$ $(x>1)$, responsible for band C and to be considered as an intermediate in the reaction path, will be expected to be much lower for cobalt; resulting in the observed relative intensities.

The above strengthens the general conclusions reached on the interpretation of the spectra for both nickel and cobalt.

4.3 EFFECTS OF POTASSIUM:

A: On the Spectra Attributed to Metal Surfaces:

As discussed earlier (see 4.1), the theory[39] of metal $d\pi$ back donation of electrons to the ligand predicts that enhancement of this property will displace the carbonyl frequency to lower wave numbers. The presence of potassium (used as a synthesis promoter) decreases the wave numbers of bands A, B and D fairly generally, both for nickel (Fig. 8) and for cobalt (Fig. 10).

In explanation one might consider the metal lattice to consist of M^{2+} ions embedded in a "sea" of electron waves, containing the K^+ ions as "defects" in its structure and on the surface. For the moment may neglect the fate of the anoinic entity possibly coming in with the potassium at the preparative stage. The defect sites are expected to be electron repelling because of the smaller formal charge on potassium ions relative to M^{2+}, so increasing the d donorship π back bonding potential of the metal lattice. Low energy electron diffraction studies[56] show that the arrangement of surface atoms could be different from that within the lattice and it is therefore

85/.. .. .. ..

quite likely that the surface will accomodate large foreign ions.

It is noticed that for the potassium promoted nickel the frequency of band C was not affected whereas for the cobalt case, a shift of about 15 cm^{-1} towards lower wave numbers was observed. In explanation it seems possible, in the case of nickel, that the metal ion, which is part of the C band species, is partly removed from the surface. The frequency of the carbonyl chromophore would therefore not be influenced by the improved π back bonding properties. On the other hand, the metal ion, which is part of the C band species for cobalt, is expected to be more closely associated with the lattice, and thus the slight shift to lower wave numbers (see also section 4.2.2.2).

For the potassium promoted samples band B was found at relatively high carbon monoxide pressures only. A three dimensional representation of the 100, 110 and 111 faces of a face centered cubic structure (Fig. 14) shows that the spacings between metal atoms in the 110 plane would certainly readily accomodate large foreign ions. It therefore seems plausible to consider that potassium may be accomodated in these vacancies and would thus inhibit the adsorption of CO ligands. This could thus explain why the presence of potassium diminished the intensity of band B at low pressure. At high pressure the ligands must be very weakly held to the surface because B disappeared more readily than previously upon desorption. This is a rather unexpected result since the low frequency of this band implies strong chemisorption. Incidentally it was observed that the frequency of band B remained unchanged with increasing carbon monoxide pressure. This indicated that the potassium ions (which improve the electron donating properties of the metal), must be associated with the sites responsible for the B band species for the reason that the previous minimum wave number was attained immediately on appearance of the band, and did not change as the pressure increased.

Further consideration of the three dimensional representation of the crystal faces shows that the spacings in the 100 plane may also accomodate large foreign atoms, but being smaller than the 110 spaces, they would be expected to be available only after the holes in the 110 plane had been filled. But the occupation of 100 positions by potassium ions will block the species D ligand sites, an explanation that is in agreement with the observations: From Table I

86/.. .. .. ..

(section 3.5.6.1) it can be seen that at almost constant carbon monoxide pressure, the intensity of band D (relative to A) decreased with increasing potassium concentration.

In the case of the unpromoted silica-supported nickel it was found that both the "linear" and "bridged" CO species desorb to the same extent with increasing temperature (Appendix 8). However, with the potassium promoted nickel (Appendix 12), the bands attributed to linearly held CO species desorb at a faster rate than the bridged species. This phenomenon may be attributed to the presence of potassium which acts as an electron donor to the nickel lattice. In the case of a bridge carbonyl the improved π electron back donation occurs from <u>two</u> Ni atoms. Thus, the metal-carbon bond will be strengthened more than for a linear structure in which back donation comes from only <u>one</u> Ni atom.

B: <u>On the Spectra Attributed to Metal Oxide Surfaces:</u>

4.3.B1 <u>Nickel Oxide:</u>

From Fig. 9 (section 3.5.6) it can be seen that the intensity of band F at first increased with increasing alkali concentration, and thereafter decreased. If we accept the assignment of F (section 4.2), then we can explain the results as follows:

It is known[46] that "stoicheiometric" NiO is an insulator, whereas the "non-stiocheiometric" oxide, which has a proportion of Ni^{3+} ions, has p conductivity. Non-stiocheiometric NiO could be formed[46] when oxygen is taken up by NiO to give a cation deficient semi-conductor. The addition of a neutral oxygen atom to the surface, as an extension of the anion lattice, establishes an adjacent vacancy in the extension of the cation lattice. Electrons are drawn from the valence band of the lattice to produce an O^{2-} ion. The cation vacancies trap positive holes, associated with Ni^{3+} sites, in their fields. The following reactions:

$$O^{2-} \longrightarrow O^{-} + e^{-}$$
$$Ni^{3+} + e^{-} \longrightarrow Ni^{2+}$$

will establish normal doubly charged nickel ions without unbalancing the lattice in any way. Alternatively

$$Ni^{2+} + \text{excess } O \longrightarrow Ni^{3+} + O^{-}$$
$$(\text{or } 2Ni^{2+} + O \longrightarrow 2Ni^{3+} + O^{=})$$

will create positive holes in the lattice.

Adsorption of CO may now occur, followed by desorption, according to:

$$(\text{lattice } Ni^{3+})\ O^{-} \leftarrow C \equiv O \longrightarrow (\text{lattice } Ni^{2+})\ O{=}C{=}O.$$

The ligand so formed would be desorbed as carbon dioxide and the defect destroyed. (The fact that two chemisorption bands (at 2,165 and 2,190 cm^{-1}) were found in some experiments (Appendix 10), can possibly be explained by the supposition of vacant lattice sites in two different environments; say (i) on the surface and (ii) adjacent or in the second layer).

Potassium ions may promote this mechanism as follows:

In order to simplify the "model" consider a NiO lattice containing equal numbers of Ni_2O_3 and K_2O, i.e. in the ratio of 4 cation sites to 4 O^{2-} sites. The lattice is not stoicheiometrically disturbed, but positive holes are introduced as well as singly charged cation sites. Hence the surface can be expected to more actively chemisorb CO according to the hypothesis made. In passing it might be noted that the ionic radius of K^{+} (1.33Å) is so large relative to that of Ni^{2+} (0.78Å) that the phenomenon must surely be restricted to the surface, and increasing concentrations of potassium can be expected to simply mask the surface and so "poison" the activity. This can account for the decline in the intensity of band F beyond the maximum (Fig. 9).

If a NiO particle diameter of 100Å is assumed, and if the K^{+} ions are restricted to the surface, then, according to calculation, 6:100 K:Ni will cover the surface. However, a CO_2 group, associated with every K_2O molecule will take up extra space, i.e. it will help to block the surface. Therefore, there will be some optimum K:Ni ratio at which the creation of defect sites will be in competition with the poisoning of these sites for carbon monoxide chemisorption, as indicated by Fig. 9. By the experiment of Fig. 9 and at the atom ratio of 1.3:100 K:Ni, the poisoning effect begins to predominate.

4.3.B2 Cobalt Oxide:

When silica-supported cobalt nitrate was heated to about 250°C, the nitrate was decomposed to black cobalt oxide, identified[61] by its colour as Co_3O_4. On evacuation at 250°C the oxide turned to a pale green-brown colour, presumably changing to CoO[61]. Chemisorption of carbon monoxide on the latter gave a band at 2180 cm^{-1}, which corresponds with the position of band F obtained for CO on nickel oxide.

In the case of nickel oxide, band F could be explained satisfactorily in terms of CO chemisorbed onto an oxygen in a defect NiO lattice. The band observed at 2180 cm^{-1} for cobalt oxide can therefore be probably interpreted in an analogous manner.

In explanation, we suppose that in the evacuation reaction most of the Co_3O_4 decomposes with evolution of oxygen. However, if some of the oxygen, excess to the CoO structure, is not expelled, it can perhaps react with the lattice according to:

$$Co^{2+} + O \longrightarrow Co^{3+} + O^{-}.$$

Thus a defect lattice, some of whose sites would seem most likely to function as a Lewis acid towards CO, can be hypothesised and so explain the chemisorption species observed as in the case of nickel oxide.

As in the case of nickel oxide, the observed CO_2 doublet, at about 2,345 cm^{-1}, further confirms these explanations since it provides positive proof of the formation of the carbon dioxide species.

When potassium ions are added these may "poison" the sites responsible for band F, resulting in a lowering of its intensity as is observed (Fig. 11). Simultaneously, new defects are created on the surface in an analogous manner to nickel oxide. These actively chemisorb carbon monoxide according to the above hypothesis, and band F2 is shown.

4.4 THE INTERACTION BETWEEN CHEMISORBED CARBON MONOXIDE AND HYDROGEN ON NICKEL SURFACES.

4.4.1 Unpromoted Samples:

Hydrogen and carbon monoxide both in the chemisorbed state, reacted to form methane, detected in terms of a band observed at 3,016 cm^{-1}, both at low and high hydrogen pressure. The hydrogen presumably chemisorbs on the B sites as B disappeared (and D simultaneously increased) in the presence of relatively high hydrogen concentrations. The interaction may proceed *via* either species D or A, or both (C being absent at the reaction temperature).

The intensity of band A increased when hydrogen and carbon monoxide were left in contact with a nickel surface (Appendix 9). It was considered, therefore, that species A may be involved in the reaction path, rather than D. This view was strengthened by the observation that, on rapid heating and cooling, A decreased in intensity with temperature more rapidly than D, relative to observations made

when the temperature was constant.

4.4.2 Promoted Samples:

At low hydrogen concentrations methane was not detected. In explanation it is evident that the promoter retards hydrogen adsorption and it must be concluded that both reactants (hydrogen and carbon monoxide) must be chemisorbed prior to the formation of a product. This is in agreement with the previous observation that potassium retards the formation of B species; and hence inhibits the formation of methane.

Furthermore, the shifts towards lower wave numbers of bands A, B and D imply an increase in the bond strength of the metal-carbon linkage. This concept is supported by the finding that potassium increases the heat of carbon monoxide chemisorption[66]. This in turn may impede desorption of the CO species with the inhibition of methane formation.

It has been mentioned (4.4.1) that band A increased in intensity when carbon monoxide and hydrogen were left in contact with the nickel surface. This effect was more pronounced with increasing potassium concentration (3.5.7.2 Table II). Also, higher reaction temperatures (or, alternatively, longer reaction times) were necessary to hydrogenate the chemisorbed CO species; especially the species responsible for band A. The "promotion" of band A by potassium, can in part be correlated with the improved electron π back donating properties due to the presence of potassium (see also 4.3).

4.4.3 Possible Reaction Mechanisms:

For the unpromoted samples it was found that in the presence of hydrogen, D disappeared first, but this does not necessarily mean that these species are active for methanation. On the potassium promoted nickel, and in the absence of hydrogen, the D band species desorbed first with increasing temperature. It was concluded therefore that A and not D is the methanation species, since A is diminished in the end on introduction of hydrogen, and on heating, and methane was not detected until after the intensity of A diminished; but A is of much greater integrated intensity than D - it could be that D does not form sufficient methane for detection.

From Table III (3.5.7.2) it can be seen that at low H_2:CO mole ratios (i.e. below 3) carbon dioxide was the main reaction product; whereas with high ratios (i.e. above 7) methane was the predominant product.

Thus, on the basis of the above it became possible to postulate a reaction mechanism for the formation of methane. The usually accepted postulates include the formation of adsorbed intermediates such as carbides and oxygenated alcoholic-type compounds[1]. If oxygenated intermediates are formed the reaction scheme may be:

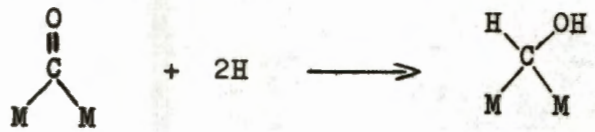

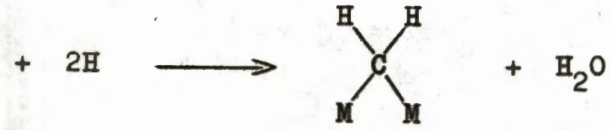

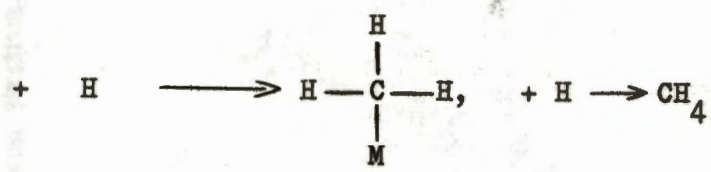

or

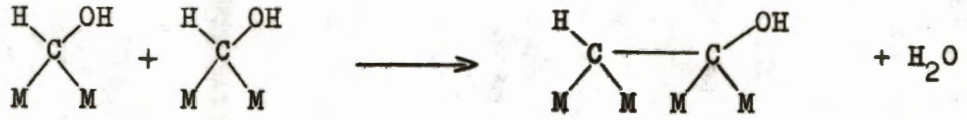

and

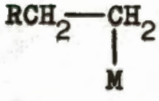

From the above one would expect to observe the -OH stretching at about 3,500 cm^{-1}, a =CH stretching mode at 3,100 cm^{-1} in =CHR or at 3,030 cm^{-1} in $=CH_2$[3,25], and a C—H stretching vibration at 2,940 cm^{-1} for a mixture of $-CH_2-$ and $-CH_3$ groups belonging to saturated carbon atoms[25]. None of these bands were detected except that the very sharp band at about 3,016 cm^{-1}, ascribed to gas phase methane, was found for high H_2:CO ratios.

On the other hand, surface carbides may also be intermediates. If species A is assumed to be involved in the reaction path the mechanism may well be:

91/.. .. .. ..

$$M_2CO + H_2 \longrightarrow M_2C \text{ (surface carbide)} + H_2O \ldots\ldots \text{(a)}$$

followed rapidly by:

$$M_2C + 2H_2 \longrightarrow 2M + CH_4 \ldots\ldots\ldots\ldots\ldots \text{(b)}$$

It must be concluded that the two reactions must proceed almost simultaneously, at the reaction temperature, since band A did not decrease in intensity until after methane was observed.

Surface carbides may also be formed according to:

$$M_2CO + CO \longrightarrow M_2C \text{ (surface carbide)} + CO_2 \ldots\ldots\ldots\ldots \text{(c)}$$

With low H_2:CO ratios the main reaction product was in fact carbon dioxide which pointed to the formation of surface carbide intermediates under the experimental conditions employed. This does not exclude the possibility of oxygenated intermediates present in trace amounts.

From the absence of rotational features in the shape of the carbon dioxide band, it can be concluded that the molecule is not free to rotate and that it is therefore physically or weakly chemisorbed on the carbide, such as in:

$$M_2 \equiv C \cdots O=C=O \qquad \ldots\ldots\ldots\ldots \qquad \text{(d)}$$

In addition to the probability that surface carbides do form (as intermediates) there is also another reason for higher carbon dioxide production at low H_2:CO ratios:

It is generally assumed that the basic reaction in Fischer-Tropsch is:

$$CO + H_2 \longrightarrow (CH_2) + H_2O \qquad \ldots\ldots\ldots\ldots \qquad \text{(e)}$$

This can be followed (if the temperature is high enough, and it probably is for nickel at 200°C) by the water gas shift reaction:

$$CO + H_2O \rightleftharpoons CO_2 + H_2 \qquad \ldots\ldots\ldots\ldots \qquad \text{(f)}$$

Now, on lowering the H_2:CO ratio the reaction (f) above will be driven forwards and more carbon dioxide will be formed.

Carbon dioxide can oxidise the catalyst according to:

$$M + CO_2 \longrightarrow MO + CO \qquad \ldots\ldots\ldots\ldots \qquad \text{(g)}$$

The chemisorption of carbon monoxide on corresponding sites would account for band E (see 4.2.1.2.). On the admission of excess hydrogen to the cell, at the reaction temperature, both the chemisorbed CO and CO_2 would be removed as shown by the disappearance of A, E and the carbon dioxide band.

92/.. .. .. ..

The surface carbide would seem to be reactive to hydrogen at the reaction temperature only. In one experiment the optical density of A dropped to about 0.18 and it was assumed that surface carbides were present because carbon dioxide was formed, but no methane was detected. When the hydrogen pressure was increased the intensity of band A remained unchanged in spite of the formation of methane. In order to be sure of this, it was confirmed in a second experiment. These observations suggested the existence of surface carbides, ready to react according to equation (b) above, at the reaction temperature.

Water is formed according to reactions (a) and/or (e). However, it was not definitely detected by I.R. for the following possible reasons:

(1) The silica support will adsorb water very strongly to form hydroxyl groups on its surface which are removed only at high temperatures ($>400^{o}C$).

(2) Water would readily oxidise Ni metal sites at 200°C (if the hydrogen pressure drops too low) to form additional nickel oxide sites (see equation (g)).

(3) If the water gas shift reaction (equation (f)) is active, then at 200°C the ratio $P_{CO_2}:P_{H_2O} > 100$ (assuming $P_{H_2} \approx P_{CO}$), i.e. the concentration of water formed will be much smaller than that of carbon dioxide and therefore more difficult to detect by I.R.

REFERENCES:

1. P.H. Emmett, Catalysis, Vol. IV, Reinhold Publishing Corp., New York, 1956.

2. O.G. Malan, J.D. Louw and L.C. Ferreira, Brennstoff-Chemie, No. 7, 209 (1961).

3. G. Blyholder and L.D. Neff, J. Phys. Chem., 66, 1664 (1962).

4. R.A. Gardner and R.H. Petrucci, J. Am. Chem. Soc., 82, 5050 (1960.)

5. R.P. Eischens, W.A. Pliskin and S.A. Francis, J. Chem. Phys., 22, 1786 (1954).

6. R.P. Eischens and W.A. Pliskin, Advances in Catalysis, Vol. X, Academic Press, Inc., New York, 1958.

7. A.C. Yang and C.W. Garland, J. Phys. Chem., 61, 1504 (1957).

8. J.T. Yates, Jr., and C.W. Garland, ibid., 65, 617 (1961)

9. C.E. O'Neill and D.J.C. Yates, ibid., 65, 901 (1961).

10. G. Blyholder and L.D. Neff, ibid., 66, 1464 (1962).

11. G. Blyholder and E.A. Richardson, ibid., 66, 2597 (1962).

12. G. Blyholder, J. Chem. Phys., 36, No. 8, 2036 (1962).

13. C.W. Garland, R.C. Lord, and P.F. Troiano, J. Phys. Chem., 69, No. 4, 1188 (1965); ibid., 69, No. 4, 1195 (1965).

14. G. Blyholder and M.C. Allen, ibid., 69, No. 11 3998 (1965).

15. G. Blyholder and M.C. Allen, ibid., 70, No. 2, 352 (1966).

16. G. Blyholder and L.D. Neff, ibid., 70, No. 3, 893 (1966).

17. G. Blyholder and L.D. Neff, ibid., 70, No. 6, 1738 (1966).

18. G. Blyholder and W.V. Wyatt, ibid., 70, No. 6, 1745 (1966).

19. R.P. Eischens, S.A. Francis and W.A. Pliskin, ibid., 60, 194 (1956).

20. M.R. Basila, T.R. Kantner, and K.H. Rhee, ibid., 68, No. 11, 3197 (1964).

21. L.H. Little, Infrared Spectra of Adsorbed Species, Academic Press, London, 1966.

22. M.L. Hair, Infrared Spectroscopy in Surface Chemistry, Marcel Dekker, Inc., New York, 1967.

23. R.K. Sheline, J. Am. Chem. Soc., 73, 1615 (1951).

24. R.K. Sheline and K.S. Pitzer, J. Am. Chem. Soc., 72, 1107 (1950).

25. G. Blyholder and L.D. Neff, J. Catalysis, 2, 138 (1963).

26. J.B. Peri, Discussions Faraday Soc., 41, 121 (1966).

27. C.E. O'Neill and D.J.C. Yates, Spectrochim. Acta, 17, 953 (1961).

28. R.A. Gardner and R.H. Petrucci, J. Phys. Chem., 67, 1376 (1963).

29. H.L. Pickering and H.C. Eckström, ibid., 63, 512 (1959).

30. G. Blyholder, Paper I - 38, Proceeding of the Third International Congress on Catalysis, Amsterdam; North Holland Publication Company, Amsterdam, 1964.

31. G.R. Harrison, R.C. Lord and J.R. Loofbourow, Practical Spectroscopy, Blackie & Sons, Limited, London, 1948.

32. A.K. Baird, Norelco Reporter, Vol. VIII, No. 6, 108 (1961).

33. D.F. Klemperer and F.S. Stone, Proc. Roy. Soc., (London), A243, 375, (1958).

34. W.L. Gilliland and A.A. Blanchard, Inorganic Syntheses, Vol. II, 234, McGraw Hill Book Company, New York, 1946.

35. G. Herzberg, Molecular Spectra and Molecular Structure, Vol. II, D. van Nostrand and Company, London, 1947.

36. L.H. Jones, J. Chem. Phys., 23, 2448 (1955).

37. L.H. Jones, ibid., 28, 1215 (1958).

38. F.A. Cotton and G. Wilkinson, Advanced Inorganic Chemistry, Interscience Publishers, London, 1966.

39. G. Blyholder, J. Phys. Chem., 68., 2772 (1964).

40. R.M. Hammaker, S.A. Francis, and R.P. Eischens, Spectrochimica Acta, 21, 1295 (1965).

41. J.O. Halford, J. Chem. Phys., 24, 830 (1956).

42. N.D. Parkyns, Paper I-59, Proceedings of the Third International Congress on Catalysis, Amsterdam; North-Holland Publication Company, Amsterdam, 1964.

43. Taylor and Amberg, from reference 21 .

44. G. Blyholder and L.D. Neff, J. Phys. Chem., 36, 3503 (1962).

45. N.D. Parkyns, J. Chem. Soc.(A), No. 12, 1910 (1967).

46. A.L.G. Rees, Chemistry of the Defect Solid State, J. Wiley and Sons, Inc., New York, 1954.

47. M.R. Basila, Appl. Spectr. Rev., 1 (2), 289-378 (1968).

48. Private Communication with Dr. M.E. Dry, The South African Coal, Oil and Gas Corporation Limited, Sasolburg, South Africa.

49. L.J.E. Hofer, from ref. 1.

50. L.E. Orgel, An Introduction to Transition-metal Chemistry Ligand-Field Theory, Methuen and Company, Limited, London, 1961.

51. E.W. Abel, Chem. Soc. Quart. Rev., 17, 133 (1963).

52. R.P. Eischens and W.A. Pliskin, Adv. in Cat., Vol. IX, 662, Academic Press Inc., New York, 1957.

53. C.S. Kraihanzel and F.A. Cotton, from ref. 21.

54. R.K. Sheline and K.S. Pitzer, from ref. 21.

55. R.A. Friedel, I Wender, S.L. Shufler and H.W. Sternberg, J. Am. Chem. Soc., 77, 3951 (1955).

56. G.A. Somorja, Ann. Rev. Phys. Chem., 19, 251 (1968).

57. L.H. Little, N. Sheppard, and D.J.C. Yates, Proc. Roy. Soc., (London), 259A, 242 (1960).

95/.. ... .

58. R.P. Young and N. Sheppard, J. Cat., 7, 223 (1967).

59. J.W. Mellor, A Comprehensive Treatise On Inorganic and Theoretical Chemistry, Vol. XV, Longmans, Green and Company, London, 1957.

60. N.A. Lange, Handbook of Chemistry, Handbook Publishers, Inc., Sandusky, Ohio, 1956.

61. R.C. Weast and S.M. Selby, Handbook of Chemistry and Physics, The Chemical Rubber Company, Cleveland, Ohio, 1966.

62. R.W.G. Wyckoff, The Structure of Crystals, The Chemical Catalog Company Inc., New York, 1931.

63. S. Besnainou and P. Labarbe, J. Mol. Structure, 2, 499 (1968).

64. S. Patai, The Chemistry of the Carbonyl Group, Interscience Publishers, London, 1966.

65. L.J. Bellamy, Advances in Infrared Group Frequencies, Richard Clay Ltd., Bungay, Suffolk, Great Brittain, 1968.

66. M.E. Dry, T. Shingles, L.J. Boshoff and G.J. Oosthuizen, J. Cat., 15, 190 (1969).

APPENDIX 1.

Improving the Activity of Silica-Supported Nickel Type I:

Most of the studies on the nickel catalyst, described in this thesis, were performed on Type I samples as it was found in practice that these reduce much more readily, than Type II samples. It was also found that the light green nickel oxide obtained from Type II catalysts was active to carbon monoxide chemisorption whereas the black nickel oxide that originates from Type I samples was inactive. From a paper by Blyholder[10] it was learned that, previous to the reduction of the catalyst, the sample was first evacuated for 6 to 9 hours to assure complete removal of any contaminants. It therefore was decided to evacuate the black nickel oxide at 390°C for about 2 hours and it was found that it changed to light green. Carbon monoxide chemisorption on this nickel oxide showed it to be active. This Type I nickel oxide yielded on reduction a more active active catalyst than the previously prepared Type I nickel oxide as measured by the intensity of a band at 2058 cm^{-1}.

Further, during the initial stages of the reduction a large temperature increase was observed - temperatures up to 420°C were measured. If one takes the position of the thermocouple into account, temperatures much above those measured must have been reached by the catalyst particles. Surface sintering can occur at Tammann temperatures[46] as low as 0.25 T_m, where T_m is the melting point of the metal in degrees Kelvin. (In the case of nickel it can start at about 160°C). Therefore, surface sintering could occur more readily in the above cases; which would result in a catalyst with a lower activity. With the above knowledge now in hand it was decided:

(a) to decompose the nickel nitrate in vacuum to assure immediate removal of the nitrogen dioxide and other possible contaminants, by slowly increasing the temperature from room temperature to 390°C,

(b) to cool the sample down to $\leq$ 250°C before the hydrogen was admitted to the sample, and to use a high initial flow rate ($\sim$400 ml. H_2/min.) to carry away excess heat. The temperature was then gradually increased. Reduction was carried out at 300°C for the first half hour and was then increased to 390°C during the next half hour while the hydrogen flow was gradually decreased to 100 ml./min. These conditions were maintained for 16 hours. At the end the catalyst was evacuated at 390°C for 4 hours, after which it was cooled down to room temperature. This resulted in a very active catalyst - in fact so active that in the presence of 20 torr carbon monoxide, nickel tetracarbonyl gas was

immediately formed. This reaction could be minimised by using lower carbon monoxide pressures.

APPENDIX 2.

On the Distribution of the Metal on the Surface of the Silica:

The specific area of Cabosil M5 is about 200 m^2/gram i.e., a 100 mg sample is equivalent to 20 m^2. If the sample contains 5% Ni there are $5x10^{19}$ atoms Ni per 20 m^2. Further, if the area of a Ni atom in the surface is assumed[33] to be 6.5 $\mathring{A}^2$, then the area for a monolayer covered by $5x10^{19}$ atoms is 3.25 m^2 per 20 m^2 silica area available, i.e. in the ideal case the nickel metal will cover about 1/6 of the silica area available. We do not believe that in any of the samples an ideal distribution was reached but we feel that the Type II samples had a better chance to approach this situation.

APPENDIX 3.

(A) The Preparation of Nickel Tetracarbonyl:

At first a method described in the literature[34] was followed for the preparation of nickel tetracarbonyl. Nickel formate was mixed with a small amount of mercuric oxide and decomposed in a stream of hydrogen at a temperature between 190° and 200°C. The hydrogen was then removed by evacuation and carbon monoxide admitted at room temperature. The $Ni(CO)_4$ formed, was frozen out at —78°C and the excess carbon monoxide pumped away. The $Ni(CO)_4$ was stored in a glass bulb as a gas at room temperature.

It was very soon discovered that the nickel intermediate is not as active as claimed, resulting in poor yields. Silica-supported nickel Type I discs were therefore used and the carbon monoxide was admitted to the cell at one atmosphere pressure. The sample was kept at 35 to 40°C for a day or two and the nickel tetracarbonyl recovered in the usual way.

Nickel tetracarbonyl was found to be very unstable, decomposing to form nickel and carbon monoxide — a black deposit of the metal was deposited on the inside of the storage bulb. This difficulty was overcome when it was realised that Apiezon N is a rubber grease and rubber catalyses the decomposition of $Ni(CO)_4$. A silicone grease was used to overcome this snag.

(B) The Infra-red Spectrum of Nickel Tetracarbonyl:

Nickel tetracarbonyl is a typical example of a spherical top molecule with the Ni atom at the centre and each of the four CO groups situated at a corner of a regular tetrahedron[35]. The CO groups are attached to the nickel atom via the carbon atom.

Part of the infra-red spectrum of nickel tetracarbonyl vapour at 53 torr is presented in Fig. 15. Absorption bands occur at 1990, 2019, 2059, 2121, 2210, 2345, 2427, 2480, 2515, 2551 and 2594 cm^{-1}. The band at 2345 cm^{-1}, with its P- and R- branch maxima at 2340 and 2360 cm^{-1}, respectively, can be ascribed to carbon dioxide formed during the preparation of nickel tetracarbonyl.

The very intense Q-branch (P- and R- branch shoulders are evident too) for the antisymmetric CO stretching vibration in Ni—C≡O is found at 2059 cm^{-1}. A band with a similar shape is found at 2019 cm^{-1}. This band is the $C^{13}O$ stretching mode of the isotopic species $Ni(C^{12}O)_3(C^{13}O)$[36] The symmetrical CO stretching vibration for $Ni(CO)_4$, appears in the Raman spectra at 2128 cm^{-1}, but is not observed here[37]. The antisymmetric CO stretching mode (2059 cm^{-1} in nickel carbonyl) is the only one quoted in the literature in respect of assigning the structure for carbon monoxide chemisorbed on metal lattices in a manner analogous to the structure of nickel carbonyl. The band is observed above 2,000 cm^{-1}, but always below 2,100 cm^{-1}. The rest of the bands are assigned to either combinations or differences and merely serve to identify the presence of nickel tetracarbonyl.

APPENDIX 4.

The Combined Influence of Carbon Monoxide Pressure and Time of Contact on the Spectra of CO Chemisorbed on Silica-Supported Nickel:

When carbon monoxide was adsorbed onto silica-supported nickel, at 100 torr pressure, bands were found at about 1990, 2050 (strong), 2213, 2350 (weak), 2435, 2484, 2515 and 2556 cm^{-1} —see Fig. 16. When the spectra were re-recorded after five days it was found that all the bands grew in intensity as shown in Fig. 17. At the same time it was found that the disc changed from black to an almost clear appearance. On pumping on the system all the bands were removed and it was thought that the carbon monoxide was very weakly chemisorbed on the nickel surface. If Figures 16 and 17 are compared with Fig. 15, it is quite clear that nickel tetracarbonyl was present in the

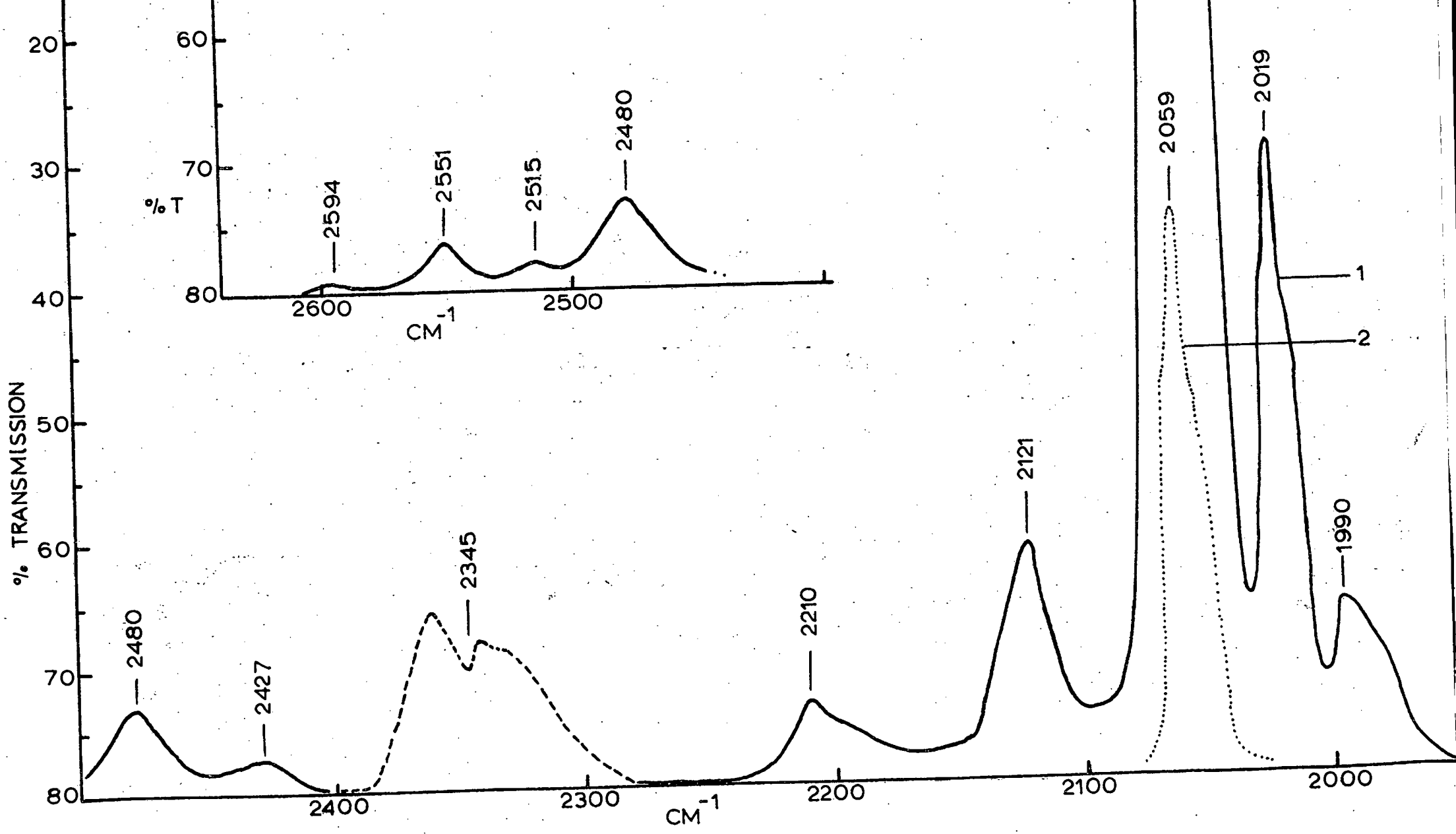

Fig. 15. Nickel tetracarbonyl at 1) 53 torr, 2) 1.7 torr (path length 95 mm.).

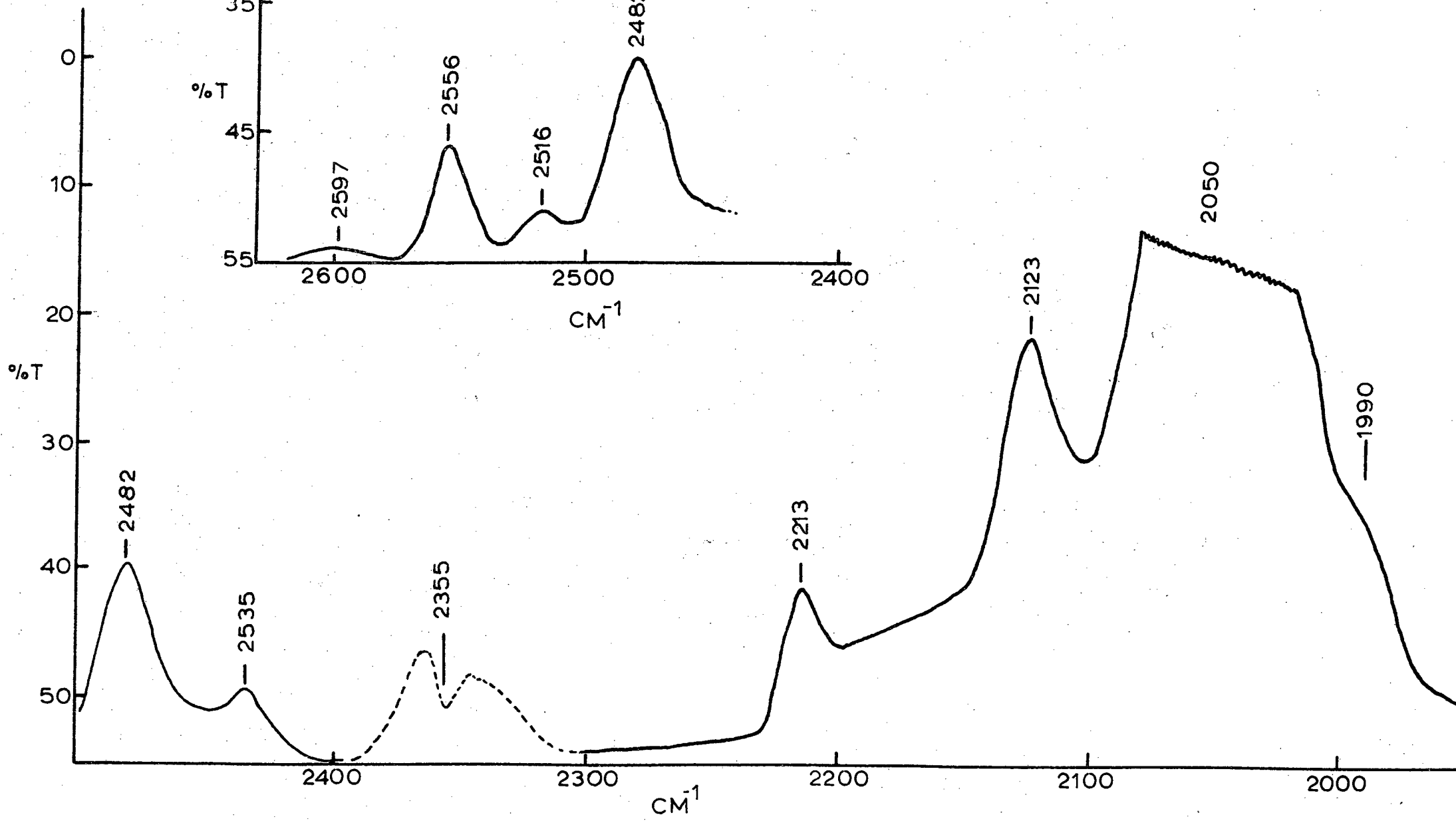

Fig. 17. Carbon monoxide chemisorbed on Type I nickel catalyst after 5 days (100 torr).

infra-red cell. Possible reasons for the formation of nickel tetracarbonyl in this experiment were (a) a too long period between gas admittance and recording of the spectra, and (b) that the sample had not reached room temperature before the gas was admitted.

Furthermore, it was fatal to leave the carbon monoxide in contact with the nickel for a period of five days because most of the chemisorbed CO was converted to $Ni(CO)_4$ during that period. In any event carbon monoxide will slowly attach nickel even at room temperature: For this reason, it was decided to make absolutely sure that the sample had reached room temperature before the carbon monoxide was admitted, and to record the spectrum immediately afterwards.

APPENDIX 5.

(A) Carbon Monoxide Chemisorbed on Silica-Supported Nickel Type I:

In a typical experiment where the disc (prepared without ammonia) had been reduced at 270°C, bands were found at about 1960 (broad), 2058, and 2085 cm^{-1}. The 2058 cm^{-1} band exhibits a shoulder at about 2050 cm^{-1}. The spectra for increasing and decreasing carbon monoxide pressures, starting at 2 torr, are graphically represented in Fig. 18. On increasing the carbon monoxide pressure the intensity of band A (at 1960 cm^{-1}) remained 'constant', but on decreasing the pressure it increased slightly. The intensity of band C (at 2058 cm^{-1}) was very sensitive to carbon monoxide pressure variation. On decreasing the pressure the shoulder at 2050 cm^{-1} (band B) could be more definitely recognised. The peak position of band D shifted from 2085 to 2090 cm^{-1} on increasing and to about 2070 cm^{-1} on decreasing the carbon monoxide pressure. Although this band appears to be the most tightly held above pressures of 1.5×10^{-3} torr, the bands B (at 2050 cm^{-1}) and A (at 1960 cm^{-1}) represent the most strongly held species at lower pressures.

On further reduction at a higher temperature (365°C) and repeating the above spectroscopic study, no new information was obtained except that at very low pressures band C is still present and stronger than D - see Fig. 19. It was again found that the intensity of A decreases as the carbon monoxide pressure increases and vice versa.

The same disc was re-reduced at 400°C (Fig. 20) and the study repeated. In order to ascertain which of the bands appeared first, carbon monoxide was admitted at about 10^{-2} torr. As can be seen from Fig. 20(a), A (at 1960 cm^{-1}, with a shoulder at 1900 cm^{-1}) and B (located at 2040 cm^{-1}), appeared first. At 0.16 torr band A grew to its maximum immediately, while B also grew and at the same time shifted to 2045 cm^{-1}.

100/.. .. .. ..

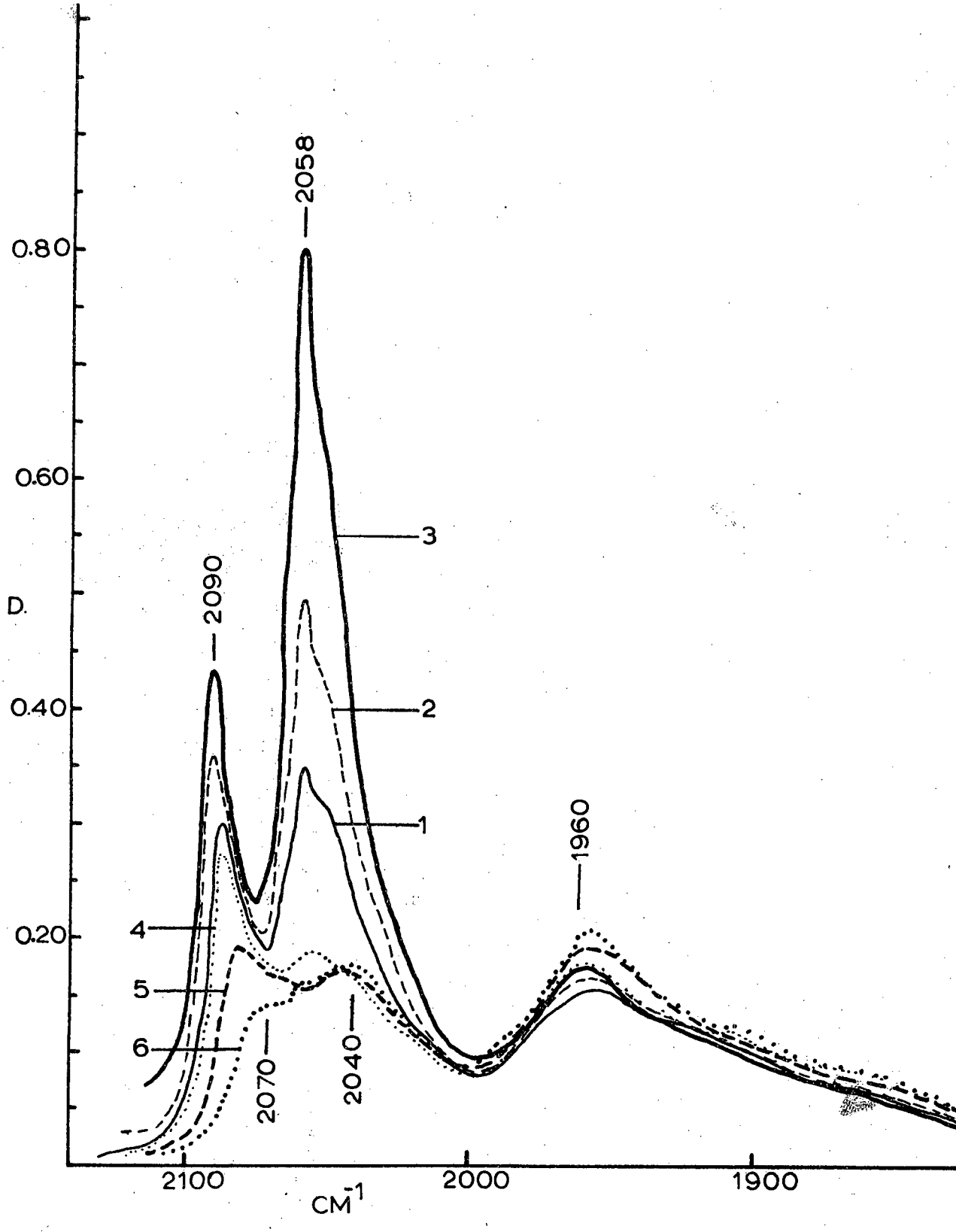

Fig. 18. Type I nickel catalyst reduced at 270°C. Increasing carbon monoxide pressures at 1) 2 torr, 2) 18 torr, 3) 70 torr. Decreasing pressures at 4) 1 torr, 5) 1.3×10^{-2} torr, 6) 1×10^{-5} torr.

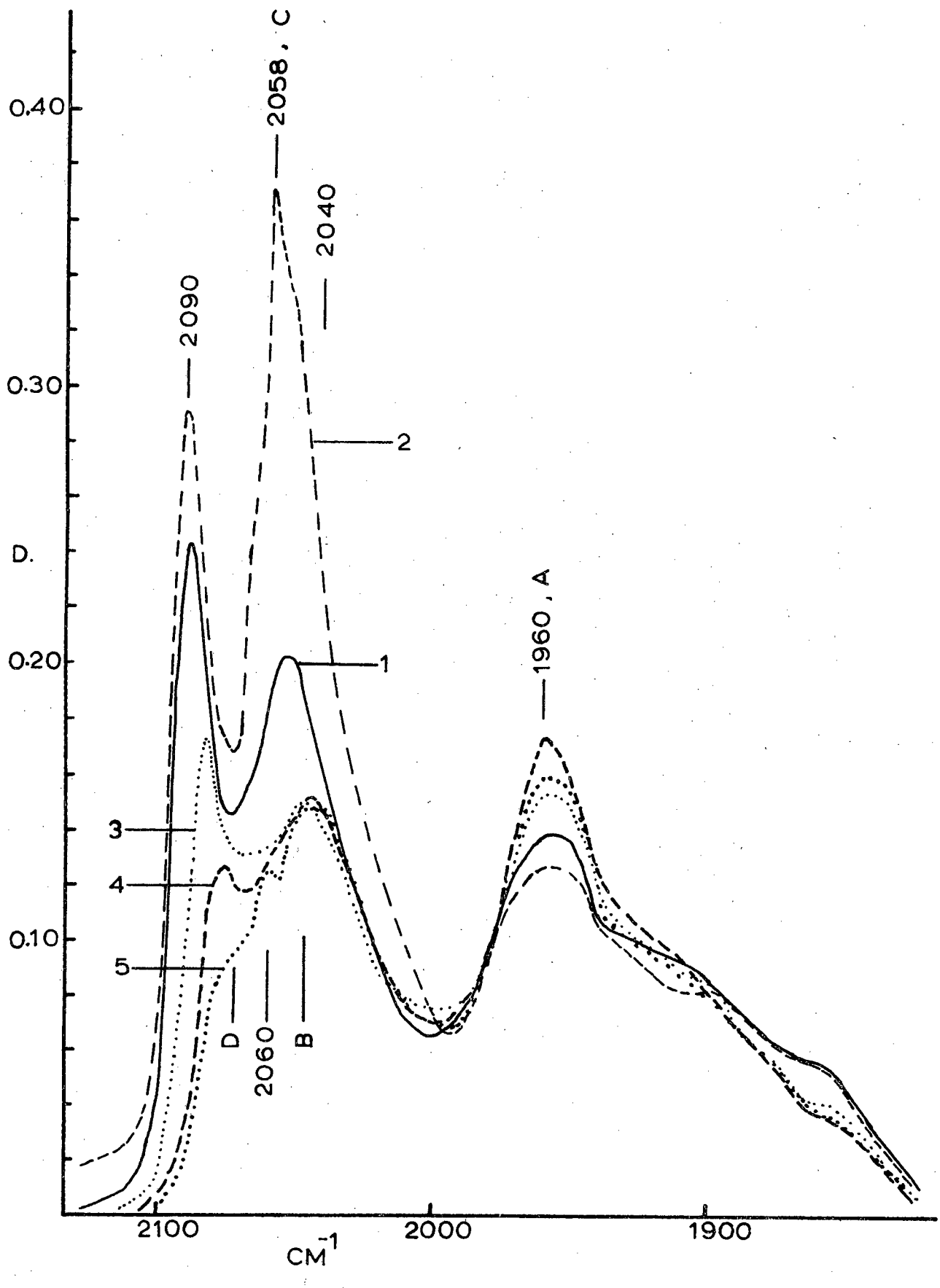

Fig. 19. Type I nickel catalyst re-reduced at 365°C. Increasing carbon monoxide pressures at 1) 2 torr, 2) 18.5 torr. Decreasing pressures at 3) 4.5×10^{-2} torr, 4) 9×10^{-4} torr, 5) 3×10^{-5} torr.

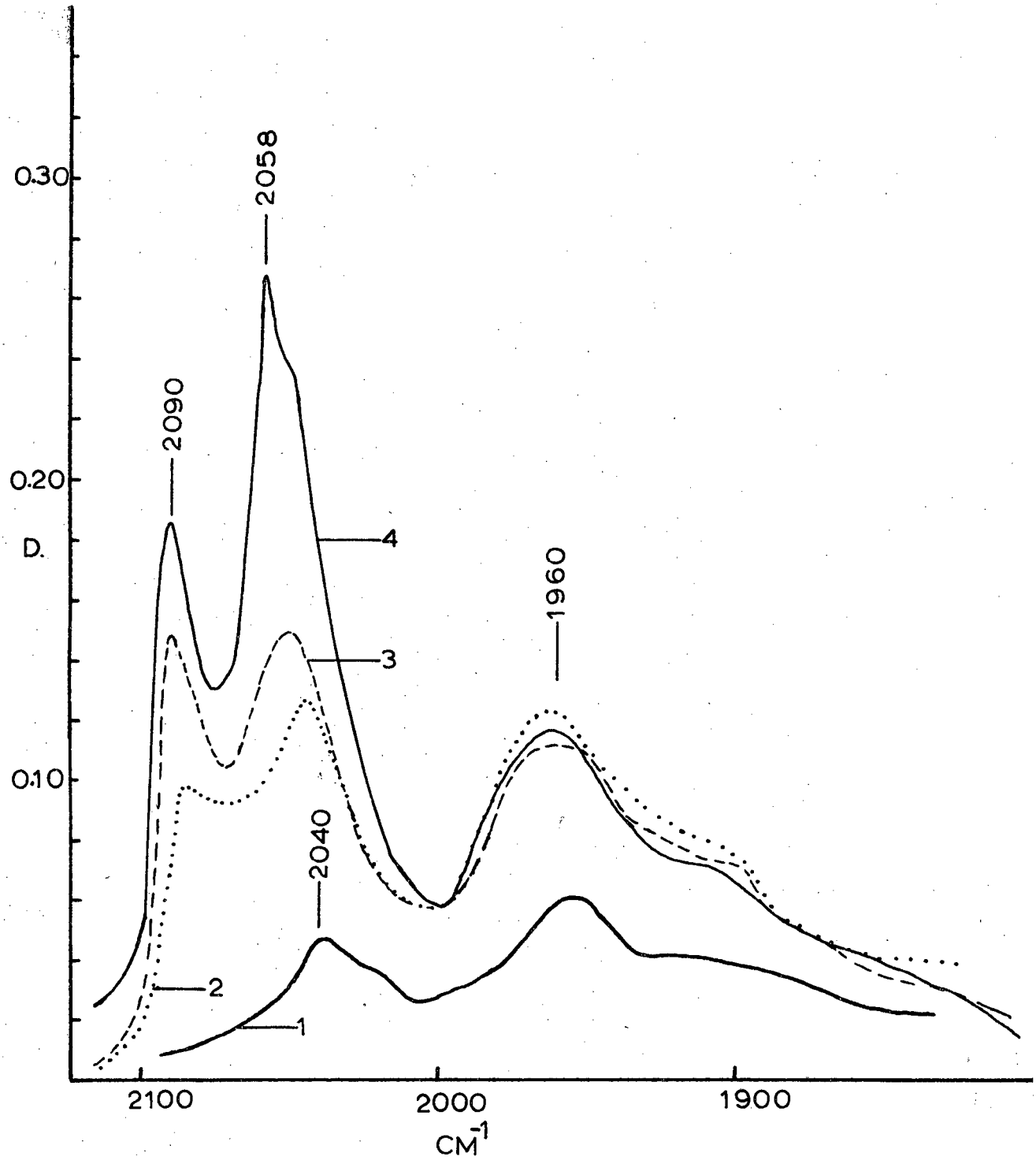

Fig. 20(a). Type I nickel catalyst re-reduced at 400°C. Increasing carbon monoxide pressures at 1) $1x10^{-2}$ torr, 2) 0.16 torr, 3) 3.5 torr, 4) 22.5 torr 5) 105.5 torr (not shown).

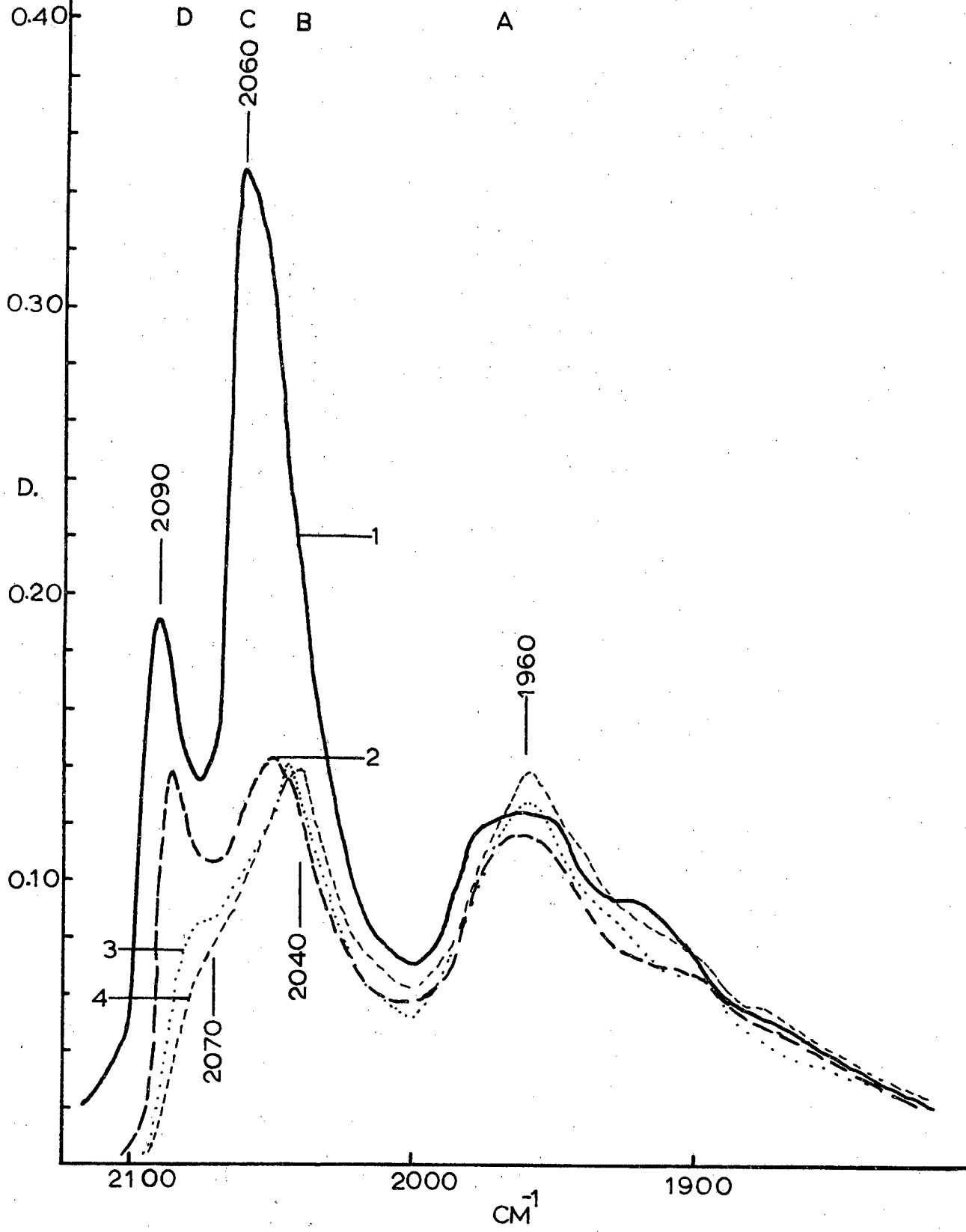

Fig. 20(b). Type I nickel re-reduced at 400°C. Decreasing carbon monoxide pressures at 1) 20 torr, 2) 1 torr, 3) 8×10^{-3} torr, 4) 8×10^{-5} torr (pumped for 6 minutes).

Simultaneously with this, band D appeared. At 3.5 torr carbon monoxide, band A decreased slightly in intensity whereas B and D increased in intensity. They are both shifted towards higher frequencies. At 22.5 torr D reached its maximum at 2090 cm^{-1} while C now appeared at 2058 cm^{-1}. On further increase in pressure only band C increased in intensity and at the same time it revealed a shoulder at 2050 cm^{-1}. The spectra recorded when the pressure was reduced are presented in Fig. 20(b). The pattern was the same as before (see previous paragraph, Fig. 19) except that A at first decreased in intensity (curve 2) after which it again increased in intensity as the carbon monoxide pressure was decreased. Band D now shifts from 2090 to 2075 cm^{-1} instead of to 2070 cm^{-1} as observed previously, and band B shifts from 2050 to 2040 cm^{-1}.

The C band in Figs. 18 to 20 resembles* that given by nickel tetracarbonyl — see Fig. 15. For this reason it was important to find out whether the band was caused by the presence of $Ni(CO)_4$ in the gas phase or whether it belonged to the catalyst phase. If gas phase $Ni(CO)_4$ was present it should have condensed in the liquid nitrogen trap. When this trap was allowed to warm up to room temperature no I.R. evidence for the presence of $Ni(CO)_4$ was however found. Secondly, on introducing 93 torr of helium into the cell, the intensity of band C did not increase as would be expected had $Ni(CO)_4$ been present (later experiments on the pressure broadening of the $Ni(CO)_4$ band confirmed this - see Fig. 21).

*The 2059 cm^{-1} $Ni(CO)_4$ band has a central sharp Q branch maximum with P and R branch shoulders on each side. The bands observed here tend to show similar shoulders. Only a gas molecule could show P—Q—R structure while solid phase molecules would be expected to give simple, "single branch" absorption bands so that shoulders would be attributed to different vibrational species.

(B) Carbon Monoxide Chemisorbed on Silica-Supported Nickel Type II:

In an experiment with a disc reduced at 315°C bands attributed to chemisorbed carbon monoxide species were found at about 1850, 1930, 2058 (strong), 2080, 2127 and 2190 cm^{-1} at an equilibrium pressure of 2.5 torr (Fig. 22). When the pressure was increased to 10.5 torr other bands were found at 2480 and 2550 cm^{-1}. The bands at 1850, 1930 and 2080 cm^{-1} decreased in intensity whereas all the others increased.

101/.. .. .. ..

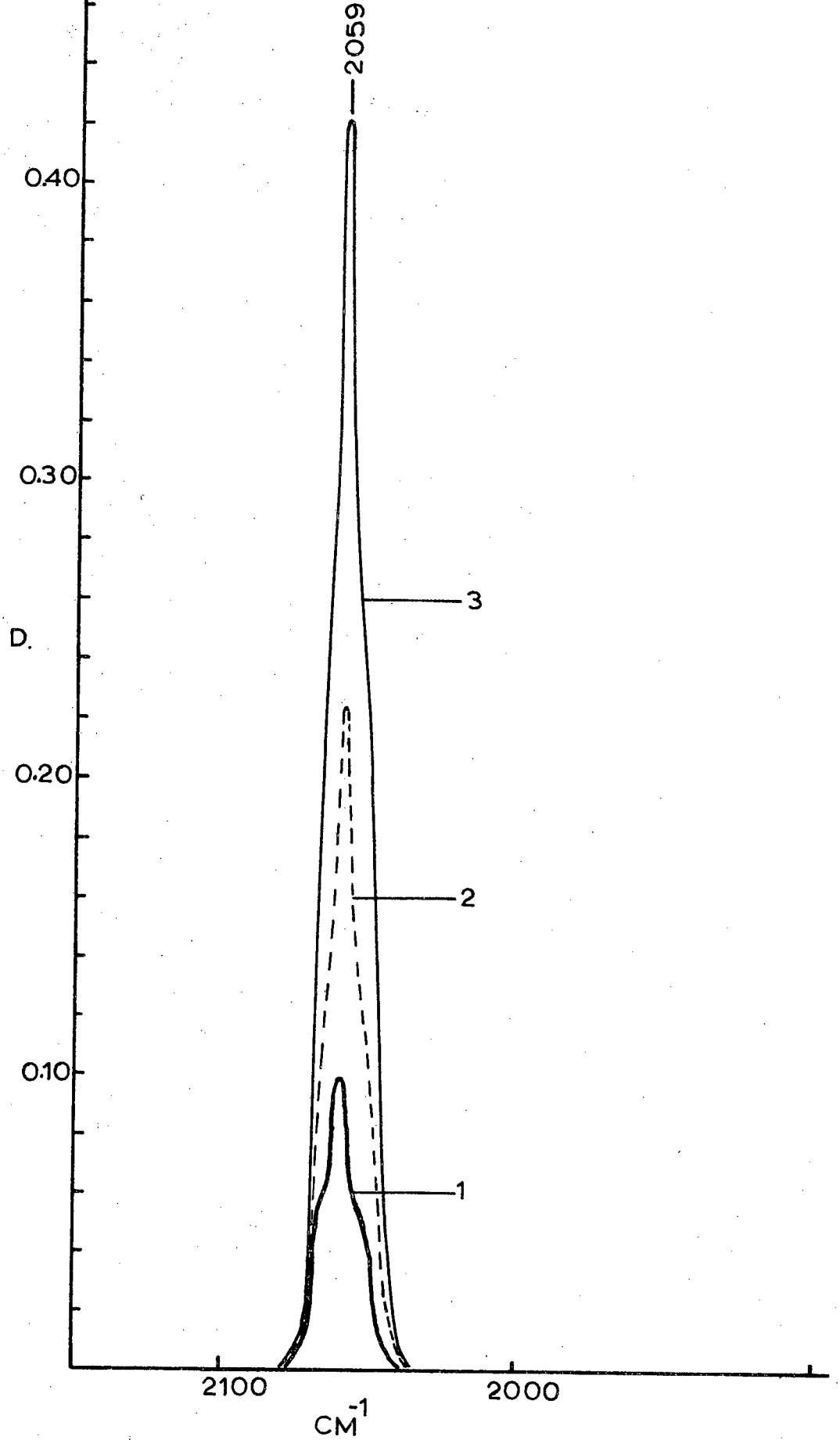

Fig. 21. Pressure broadening of the 2059 cm^{-1} band of nickel tetracarbonyl at 1) 0.28 torr, 2) plus 10 torr helium, 3) plus 15 torr helium.

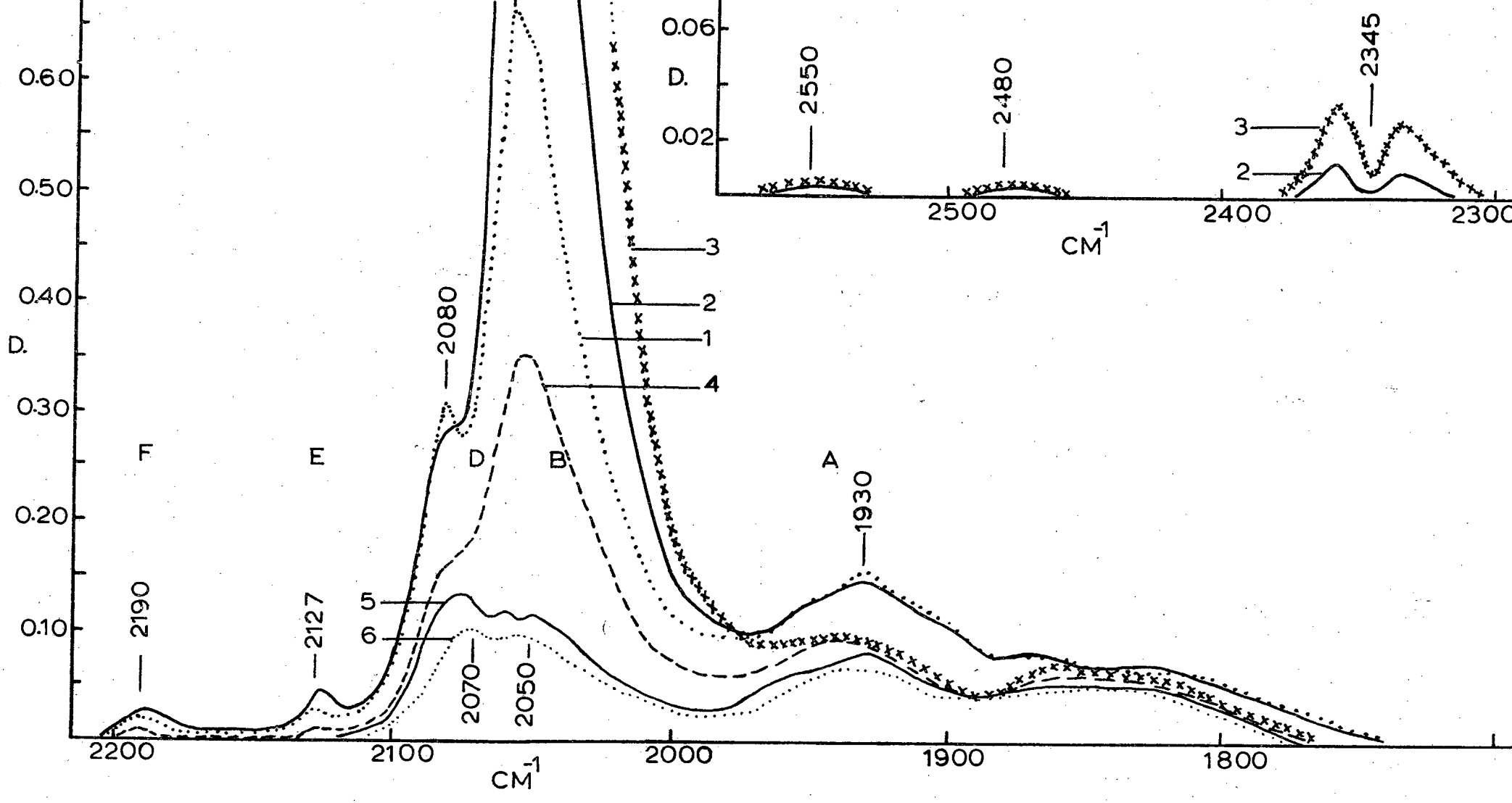

Fig. 22. Type II nickel catalyst reduced at 315°C. Increasing carbon monoxide pressures at 1) 2.5 torr, 2) 10.5 torr, 3) 97 torr. Decreasing pressures at 4) 0.35 torr, 5) 0.15 torr, 6) 1x10-4 torr.

A weak band, ascribed to carbon dioxide, was found at 2345 cm^{-1}. On increasing the pressure to 97 torr, the carbon dioxide band became more intense while the bands at 1850 (A2) and 1930 cm^{-1} (A1) decreased further. Again the largest intensity variation with pressure was found for band C. When the pressure was decreased, all the bands, including A, diminished in intensity. At a pressure of about 10^{-4} torr band D (now at 2075 cm^{-1}) was found to be the most persistent.

When the same disc was further reduced at a higher temperature (365°C) and the experiment repeated, the bands as represented in Fig. 23 were observed. Band D was now better resolved (compare curve 2 in Fig. 23 with curve 2 in Fig. 22) and lay at 2085 cm^{-1} as is the case for the Type I catalyst. Furthermore, band A was now displaced from 1930 to 1940 cm^{-1} which is nearer to that found for Type I catalyst. When the pressure was diminished below 1 torr, band A decreased in intensity but to a lesser extent (Fig. 22).

When the integrated intensity of band A is compared with the total integrated intensities of bands B and D, then it readily can be seen that, in this experiment, band A represents the most strongly held species at 10^{-5} torr (curve 6). The question now arose as to which of these bands appeared first. Moreover, from Fig. 23 it seems as if one can go from the Type II supported nickel catalysts to Type I, simply by increasing the temperature of reduction. An increase in the reduction temperature would be expected to sinter the metal particles, leading to a more crystalline nickel.

Therefore, a new disc of the Type II catalyst was reduced successively at four different temperatures, starting at 275°C. After each reduction the carbon monoxide was adsorbed onto the nickel, initially at very low pressures (of the order of $1x10^{-2}$ torr or less) and then gradually at higher pressures. A set of desorption experiments was carried out in each case. The corresponding spectra are given in Figs. 24 to 27. As can be seen from these, bands A2, A1, B, and D appeared first. On increasing the pressure, band B is very soon camouflaged by D, i.e. the D species surface sites appear to be greater. Bands A2 and A1 reached their maximum intensities first. It was further found that for the low temperature reduced samples (Figs. 24 and 25) these two bands disappeared with further carbon monoxide pressure increments. When the pressure was decreased, these bands did not reappear. On the other hand, the sample reduced at 425°C (Fig. 27) showed band A to be more stable towards carbon monoxide pressure variation. Fig. 26 shows the band to be somewhere inbetween these extremes.

102/.. .. .. ..

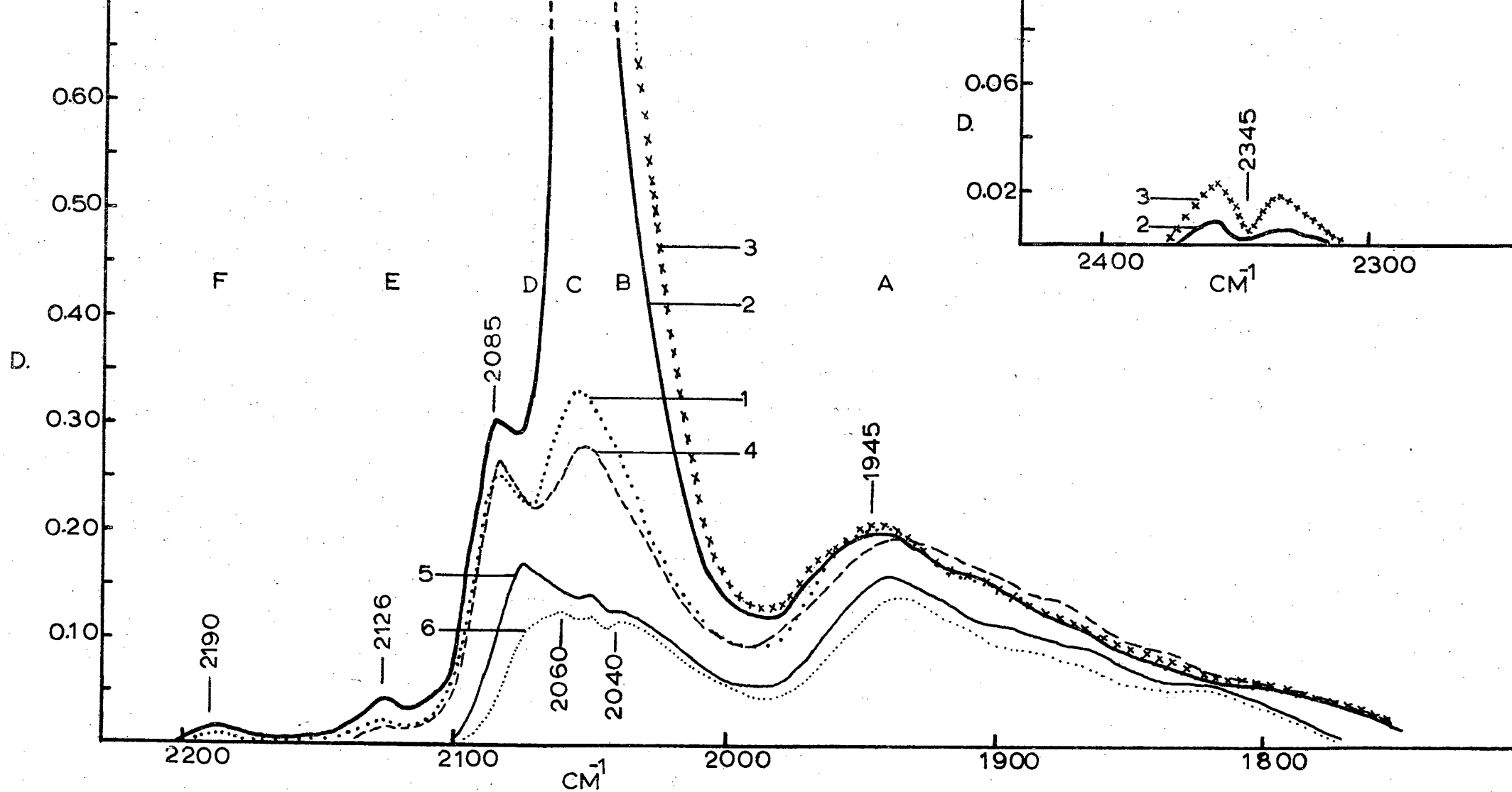

Fig. 23. Type II nickel catalyst re-reduced at 365°C. Increasing carbon monoxide pressures at 1) 2.5 torr, 2) 14 torr, 3) 54 torr. Decreasing pressures at 4) 1 torr, 5) 2.8×10^{-2} torr, 6) 1×10^{-5} torr.

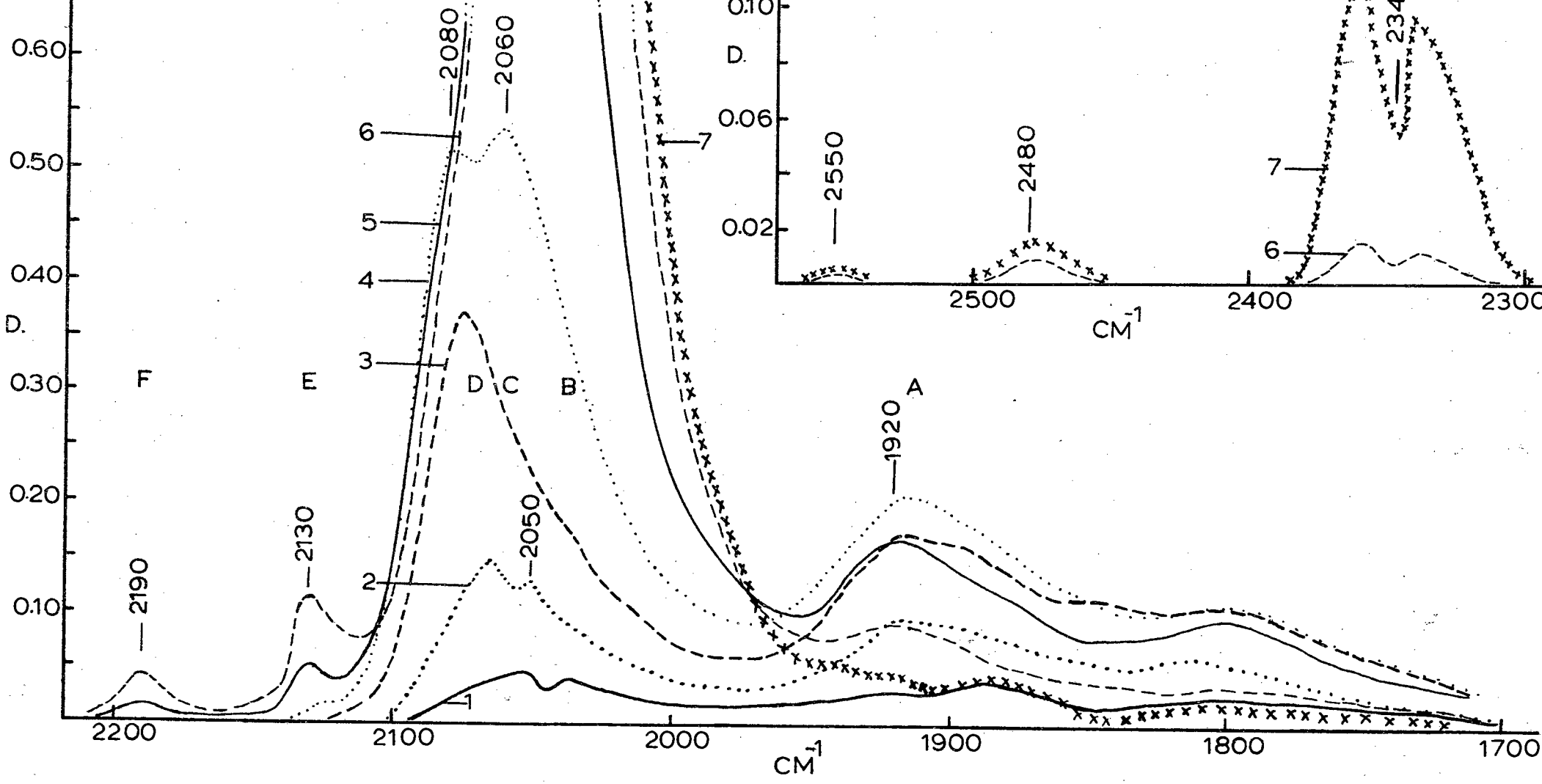

Fig. 24(a). Type II nickel catalyst reduced at 275°C. Increasing carbon monoxide pressures at 1) 9×10^{-3} torr, 2) 4×10^{-2} torr, 3) 6×10^{-2} torr, 4) 0.85 torr, 5) 3.0 torr, 6) 27 torr, 7) 298 torr.

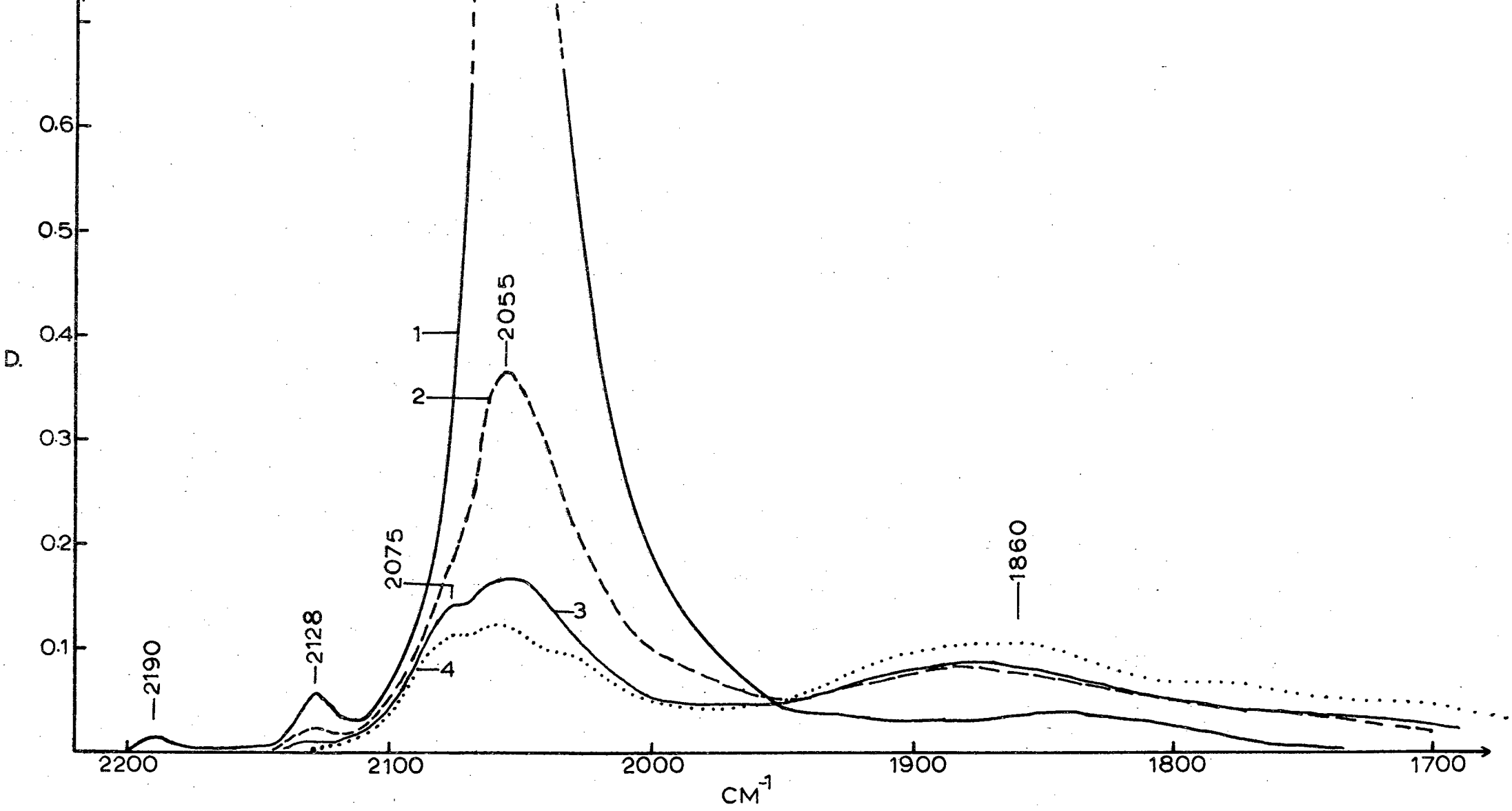

Fig. 24(b). Type II nickel catalyst reduced at 275°C. Decreasing carbon monoxide pressures at 1) 2 torr, 2) 0.5 torr, 3) 8.5×10^{-2} torr, 4) 1.5×10^{-4} torr.

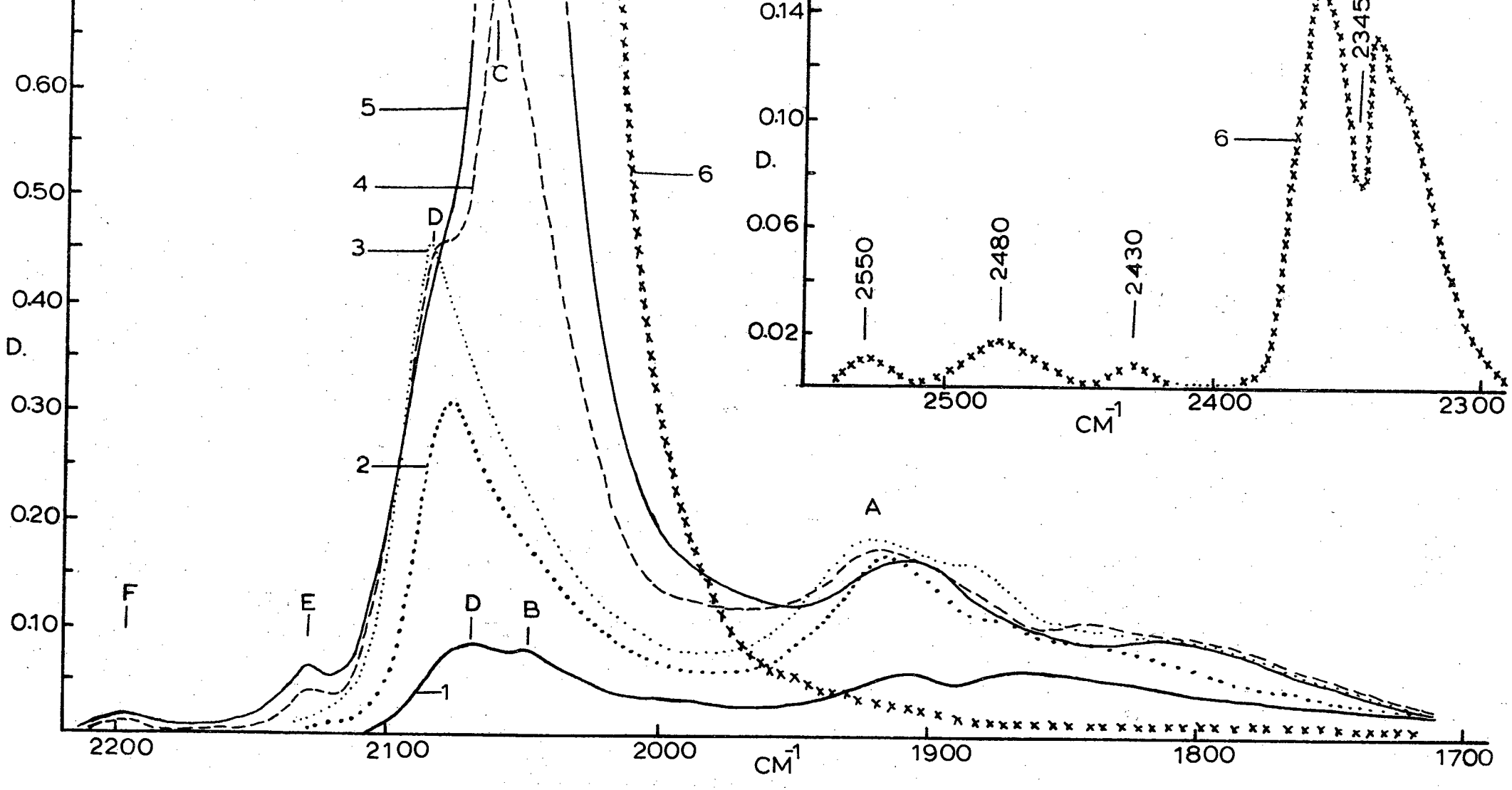

Fig. 25(a). Type II nickel catalyst re-reduced at 325°C. Increasing carbon monoxide pressures at 1) 8×10^{-3} torr, 2) 6.5×10^{-2} torr, 3) 0.11 torr, 4) 0.75 torr, 5) 1.8 torr, 6) 364 torr.

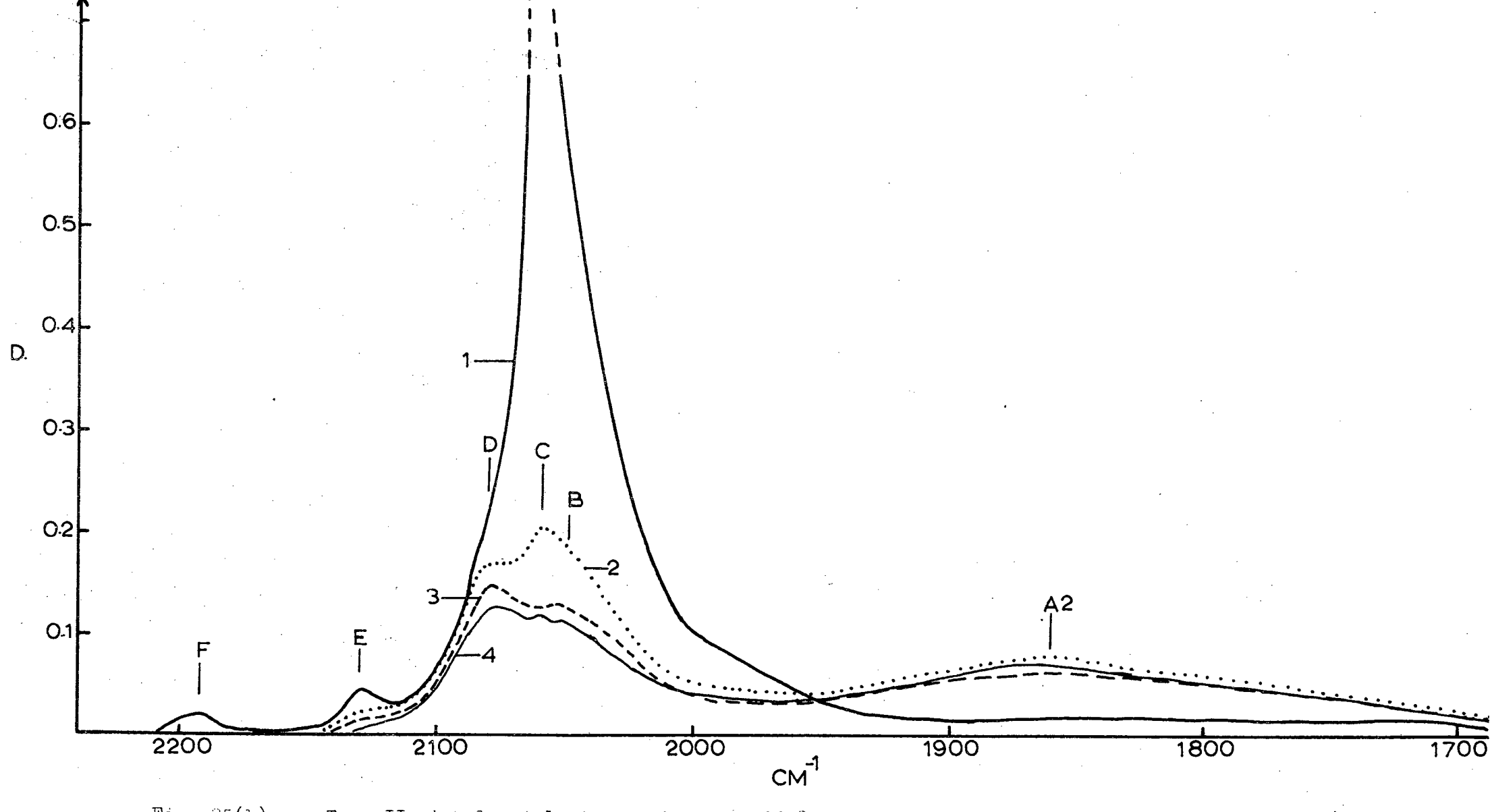

Fig. 25(b). Type II nickel catalyst re-reduced at 325°C. Decreasing carbon monoxide pressures at 1)1.45 torr, 2) 0.13 torr, 3) 3.5×10^{-2} torr, 4) 2×10^{-4} torr.

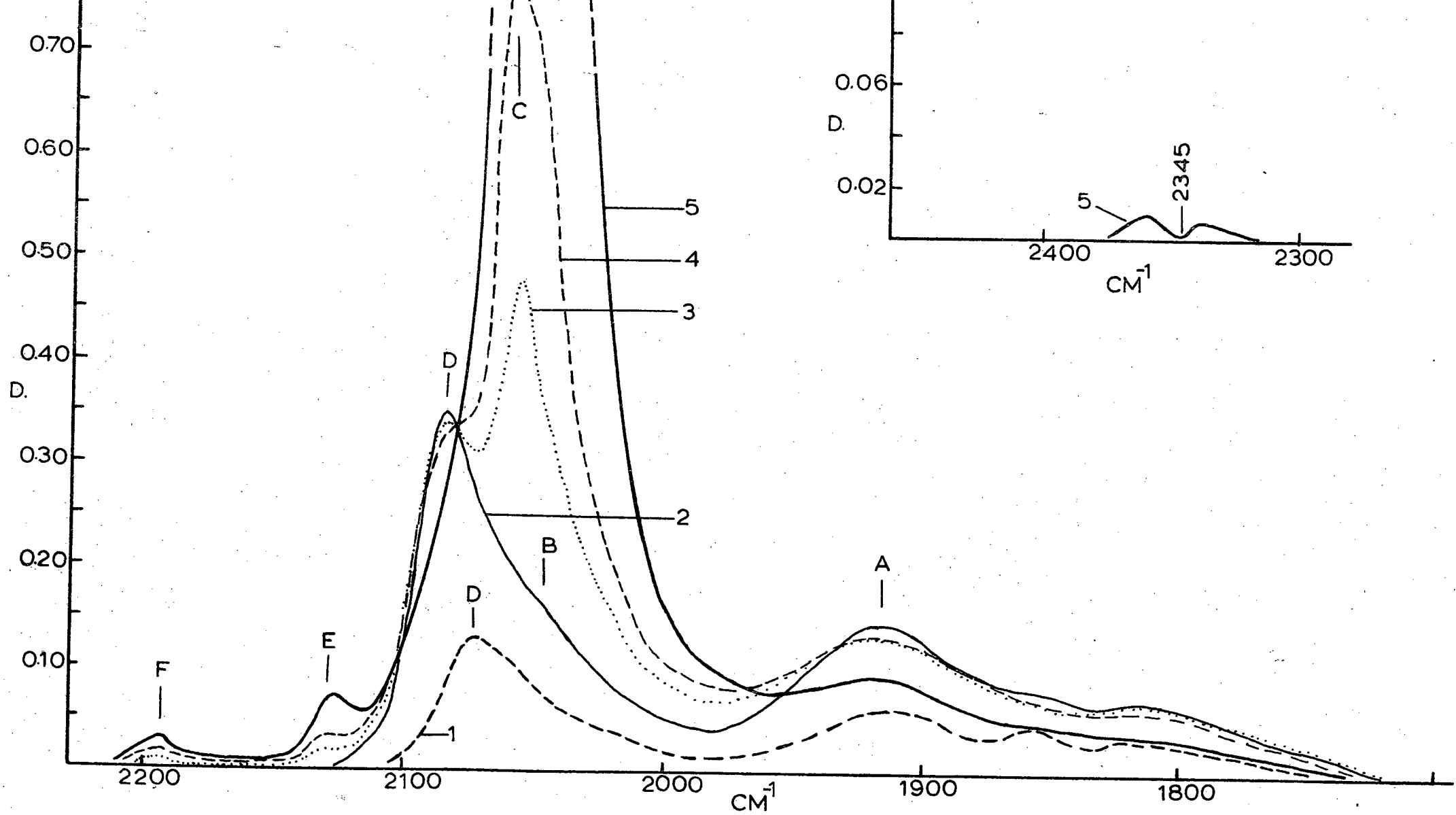

Fig. 26(a) Type II nickel catalyst re-reduced at 385°C. Increasing carbon monoxide pressures at 1) 1.8×10^{-2} torr, 2) 0.15 torr, 3) 0.77 torr, 4) 1.7 torr, 5) 14 torr.

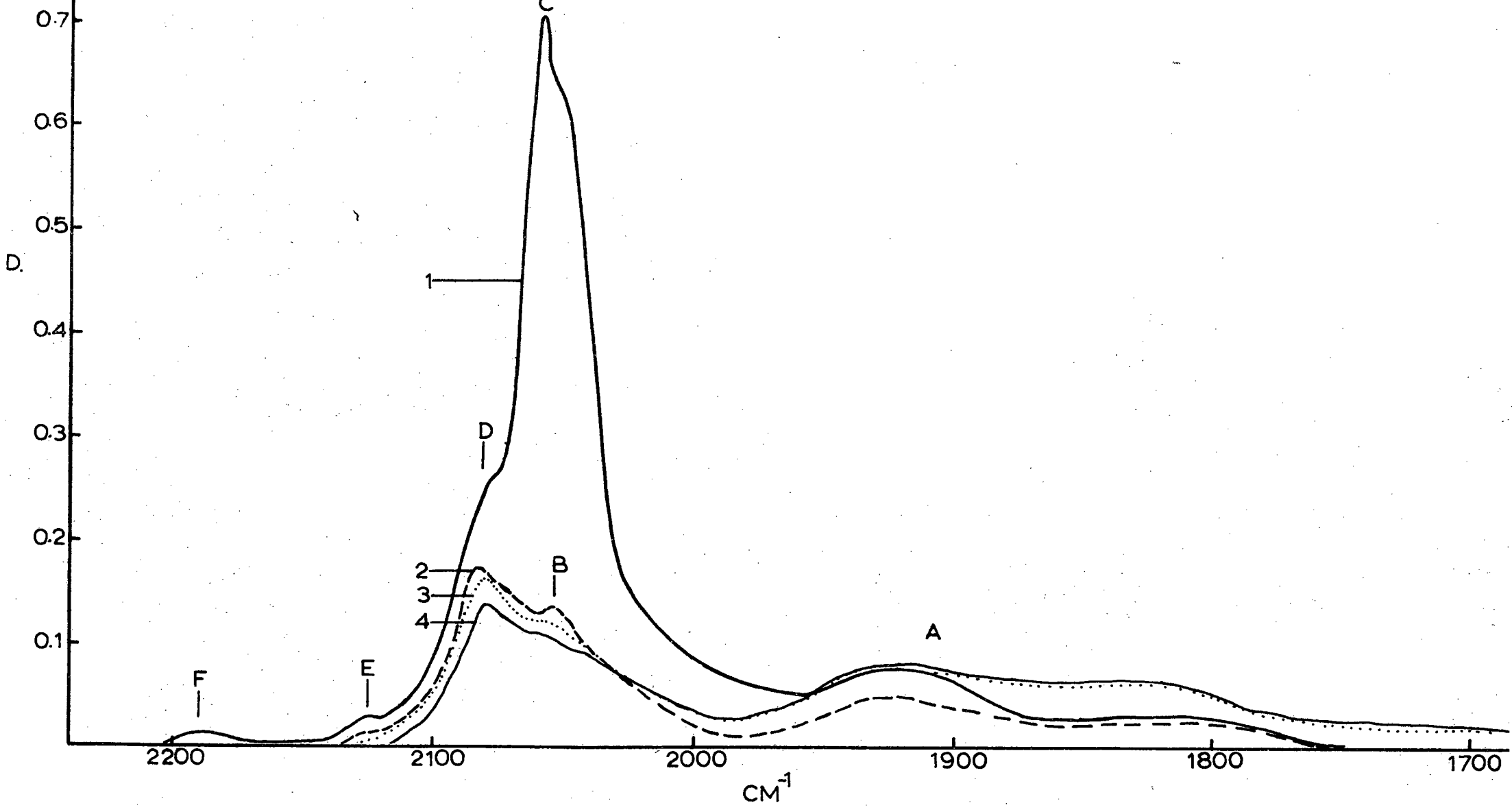

Fig. 26(b). Type II nickel catalyst re-reduced at 385°C. Decreasing carbon monoxide pressures at 1) 0.90 torr, 2) 0.12 torr, 3) 1.6×10^{-2} torr, 4) 2×10^{-4} torr.

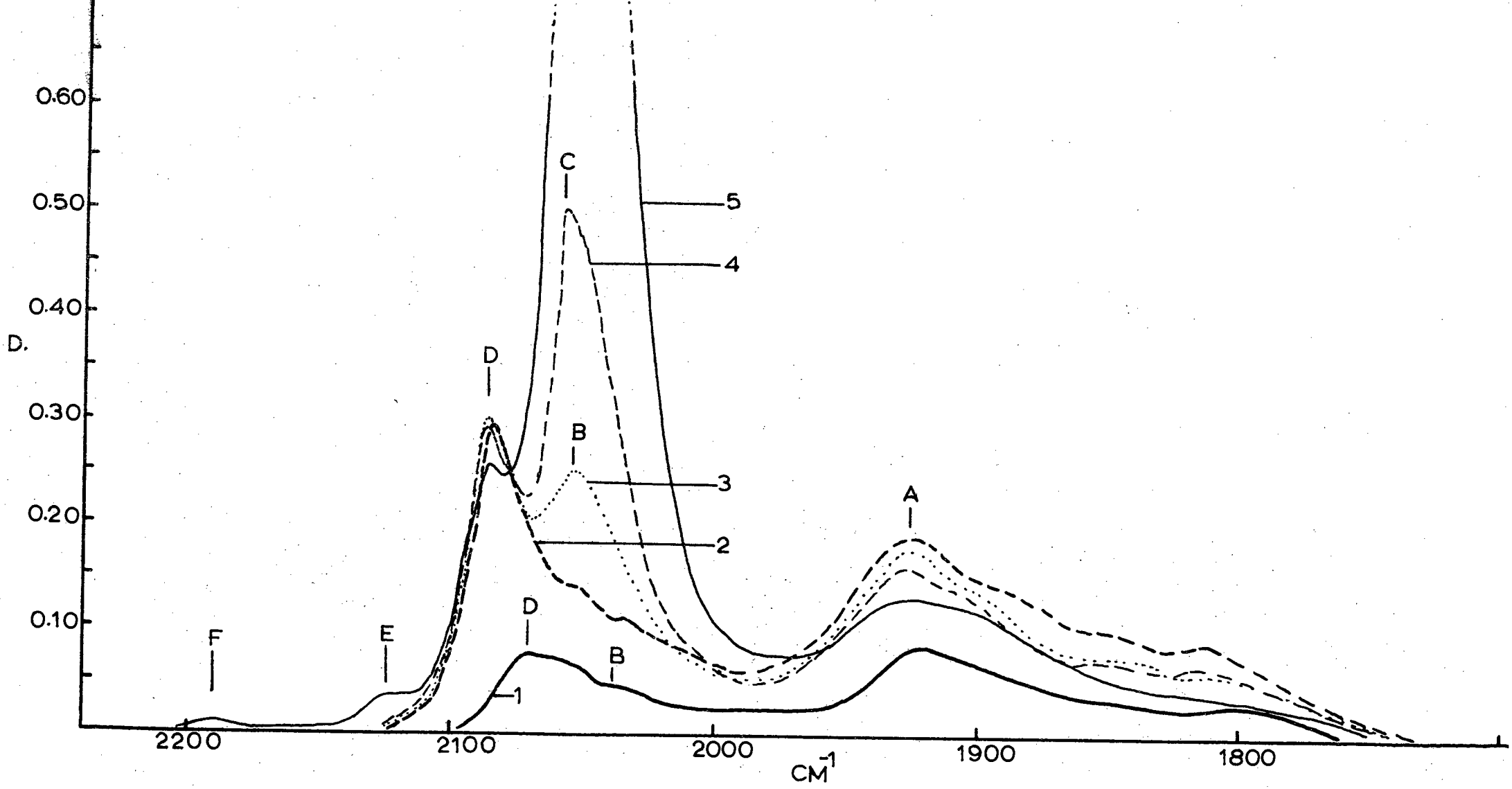

Fig. 27(a). Type II nickel catalyst re-reduced at 425°C. Increasing carbon monoxide pressures at 1) 1.8x10-2 torr, 2) 0.13 torr, 3) 0.77 torr, 4) 2 torr, 5) 15 torr.

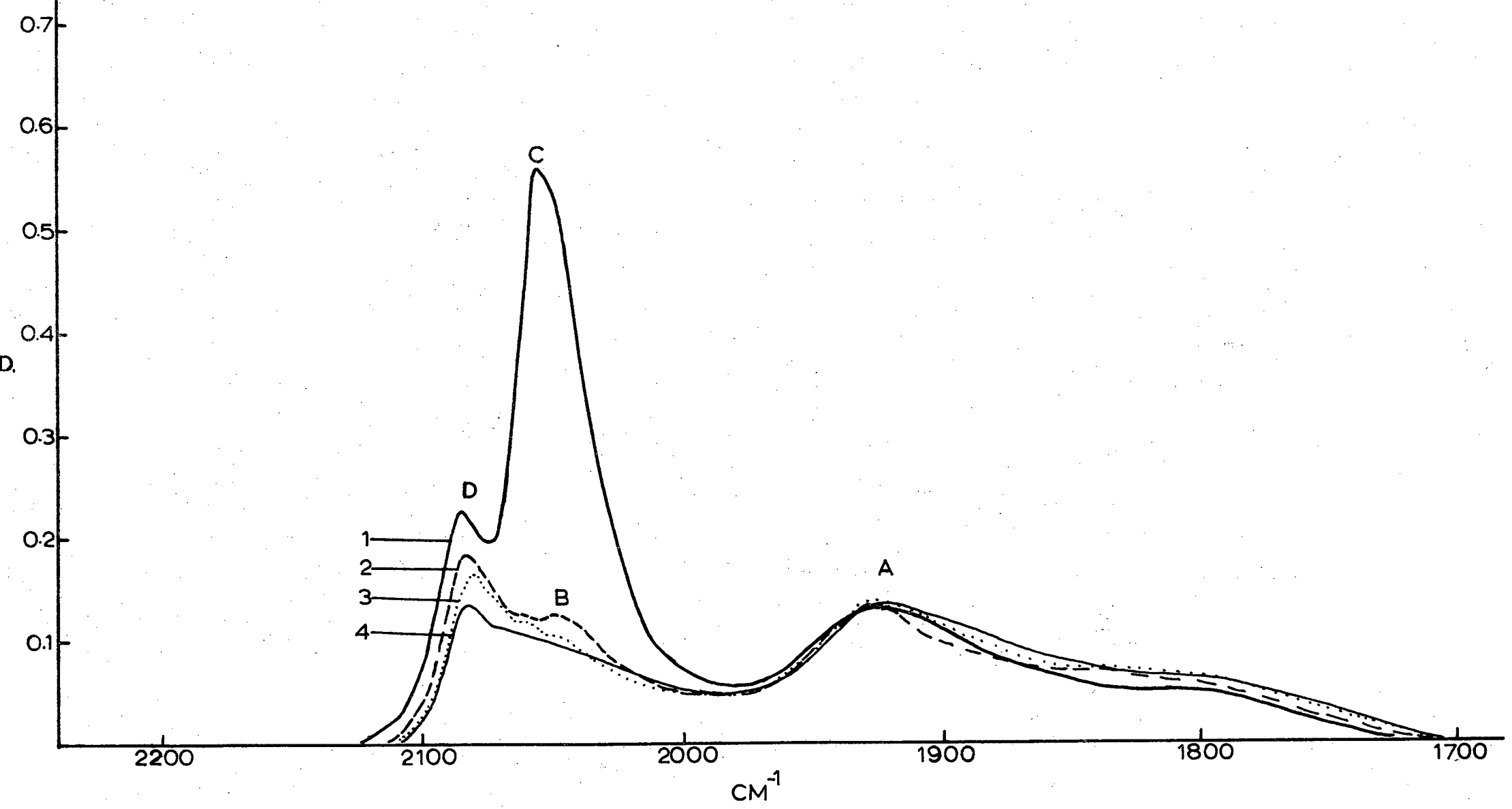

Fig. 27(b). Type II nickel catalyst re-reduced at 425°C. Decreasing carbon monoxide pressures at 1) 1.3 torr, 2) 0.14 torr, 3) 1.6×10^{-2} torr, 4) 6×10^{-5} torr.

Figs. 24 (curve 4) and 25 (curve 4) also reveal that, when the temperature of reduction is increased, band C at 2058 cm^{-1} is formed earlier at a lower carbon monoxide pressure.

It was also found that the lower the temperature of reduction the more intense the 2058 cm^{-1} band for a given "constant" pressure. In order to illustrate this, the spectra shown in Figs. 25(a) curve 5, 26(a) curve 4, and 27(a) curve 4, are shown in Fig. 28.

The presence or absence of the bands at 2480 and 2550 cm^{-1} goes hand in hand with the intensity of band C. Also, the higher the temperature of reduction the better the resolution of the C and D bands. At the same time the bands E (at 2128 cm^{-1}) and F (at 2190 cm^{-1}) decreased in intensity with higher reduction temperature, at constant carbon monoxide pressure (Fig. 28). The formation of carbon dioxide also diminished simultaneously. The desorption experiments show band B better for the low temperature reduced samples (compare Fig. 25(b), curve 4 with Fig. 27(b) curve 4). The desorption experiments also show that in general the band D represents the most strongly held CO species. On desorption the wave number of this band reached its minimum at about 2075 cm^{-1}.

The spectra of the vapour of the condensed phase in the liquid nitrogen trap of two experiments were also recorded and in both cases the same result was found (Fig. 29). (Only the spectra that originates from one experiment are represented in this figure). It is quite clear that nickel tetracarbonyl and carbon dioxide were formed during these experiments.

NOTE:

In most of the above experiments a large number of spectra were recorded over a fairly wide carbon monoxide pressure range. When all the spectra belonging to one particular reduced catalyst are plotted on one graph, the detail is lost due to overlapping of the bands. It was decided, therefore, to plot only the results that will illustrate an effect best.

When carbon monoxide was admitted to the sample at very low pressures it was necessary (in order to control the pressure) to close the stopcock between the gas line and the infra-red cell. The carbon monoxide pressure was then pre-set so that, when this particular stopcock was opened the aimed pressure could be reached. On adding the first few carbon monoxide batches this aim could never be achieved because the pressure-drop was always larger (due to adsorption) than

103/.. .. ..

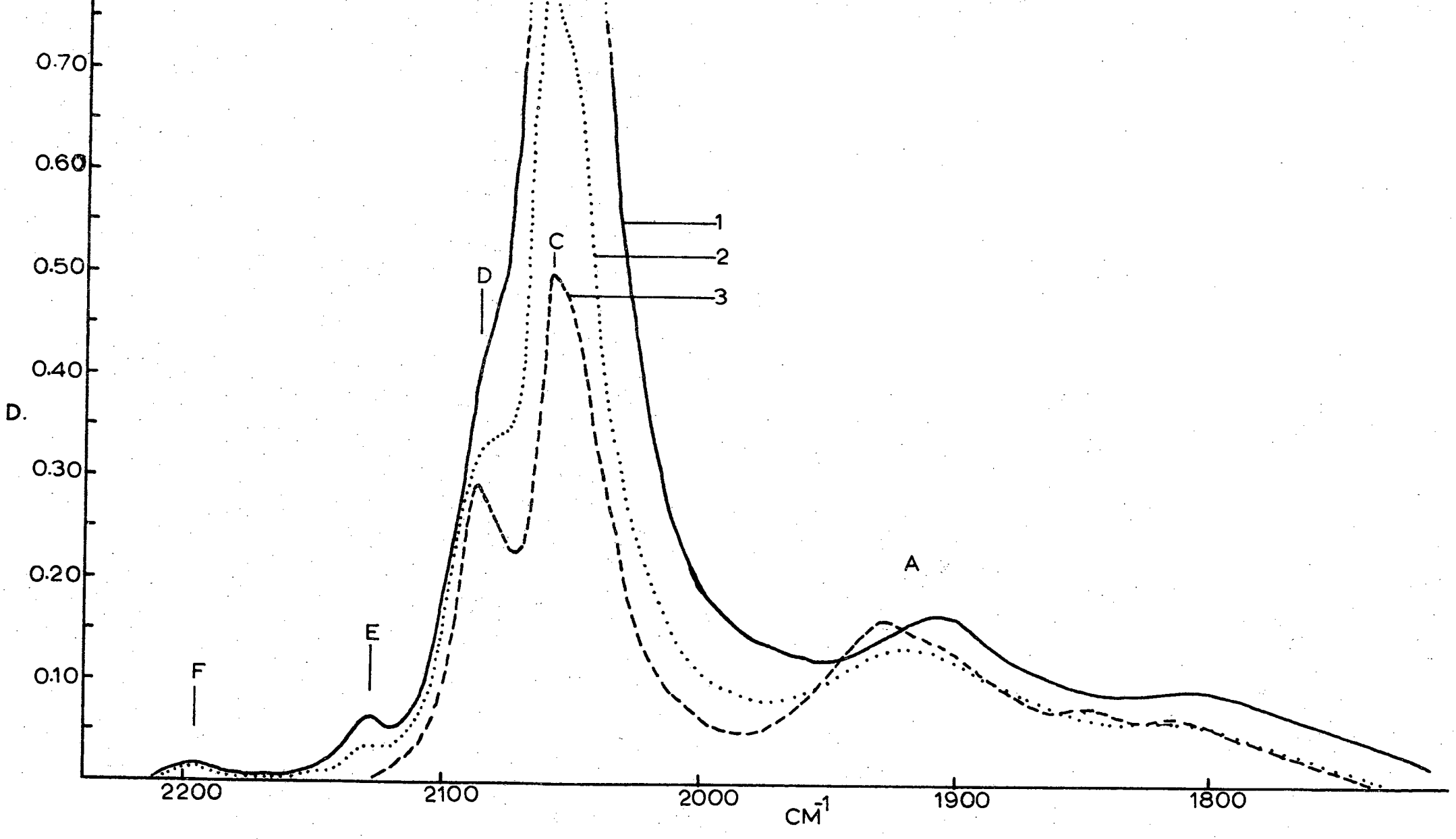

Fig. 28. Type II nickel catalyst 1) reduced at 325°C plus 1.8 torr carbon monoxide, 2) reduced at 385°C plus 1.7 torr carbon monoxide, 3) reduced at 425°C plus 2.0 torr carbon monoxide.

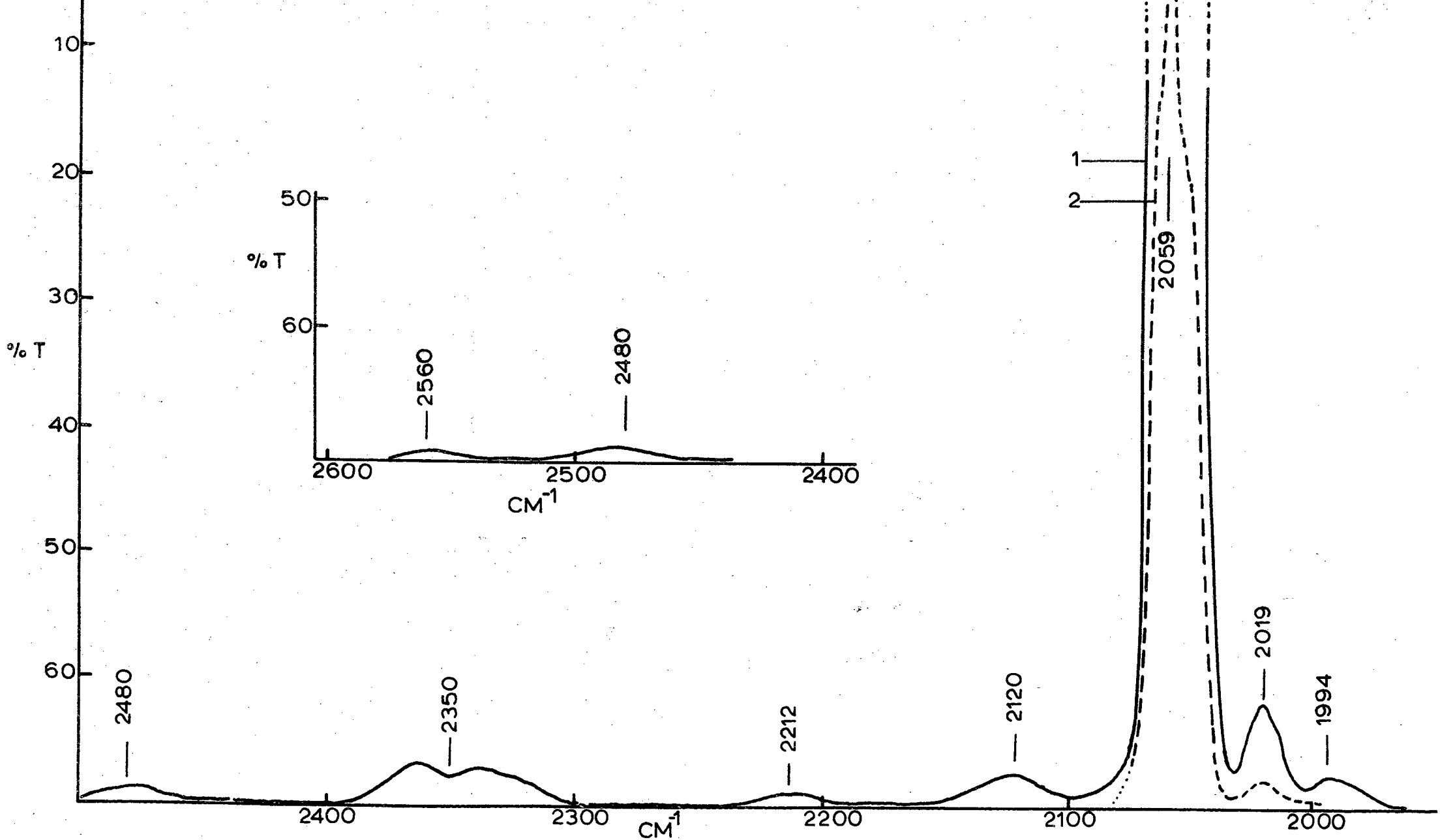

Fig. 29. Vapour of contents of liquid nitrogen trap at about 1) 1 torr, 2) 0.53 torr.

expected from Boyle's law. It was found that large amounts of carbon monoxide can be adsorbed before any infra-red band, are registered. In this connection, it was pointed out by Hair[22] that workers who applied gravimetric techniques to quantitatively estimate the absolute infra-red band intensities, neglect the possibility that there is a contribution to the weight adsorbed from species that are not spectroscopically observed.

APPENDIX 6

The Origin of Band C (Nickel):

(A) Experimental:

From the experiments described in Appendix 5 it was concluded that band C was part of the catalyst phase rather than being part of the vibrational spectrum of $Ni(CO)_4$ in the gas phase. It is also possible that it is due to physical adsorption of $Ni(CO)_4$ onto the catalyst. Further, it was also found that in some cases, especially when lengthy experiments were carried out, $Ni(CO)_4$ was concentrated in the liquid nitrogen cooled trap; whereas for shorter runs nothing was found in spite of a very intense C band. In order to elucidate this anomaly further experiments were conducted.

In a lengthy experiment, when 3 torr carbon monoxide was admitted to the cell, a band of a certain intensity was found (Fig. 30). After 1 hour at room temperature and with the stopcock open to the liquid nitrogen trap, the intensity of this band decreased, whereas the intensities of all the others more or less stayed constant. At the same time the total pressure in the system dropped to slightly below 3 torr. When the carbon monoxide pressure was now increased to 7 torr the original intensity of the band at 3 torr could not be restored. This shows that part of the band in Fig. 30, curve 1, must be due to $Ni(CO)_4$ physically adsorbed onto the surface, which is slowly transferred to the liquid N_2 trap. From the literature[34] it is learned that $Ni(CO)_4$ is very volatile, so that one would expect the $Ni(CO)_4$ gas phase to be frozen out immediately in the liquid N_2 trap. At the end of the run $Ni(CO)_4$ was found in the trap.

In another experiment 50 torr carbon monoxide was admitted to the sample and the region from 1850 to 2150 cm^{-1} was scanned. At the end of the scan the 'CO' was pumped off *via* the trap cooled with liquid nitrogen. When the vapour condensed in this trap was re-admitted to

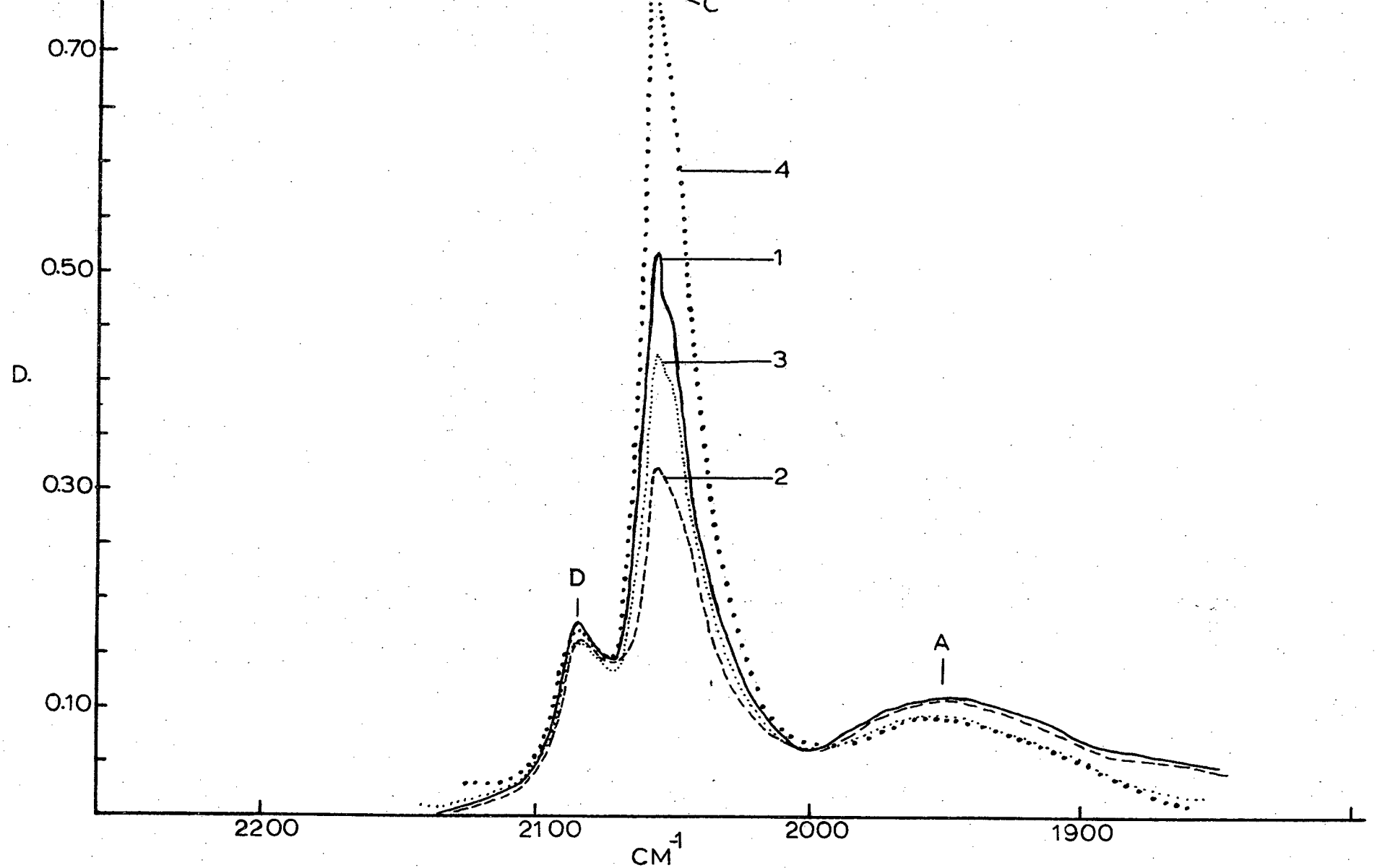

Fig. 30. Supported nickel catalyst reduced at 390°C. Increasing carbon monoxide pressures at 1) 3.0 torr, 2) 3.0 torr after 1 hr. at room temperature, 3) 7.0 torr, 4) 19.0 torr.

the sample an overall increase in absorption in the 2060 cm^{-1} region was observed as shown in Fig. 31. From previous experience we know that the band due to $Ni(CO)_4$ is usually very sharp. It was therefore not certain whether this increase in absorption was due to $Ni(CO)_4$ gas or to carbon monoxide condensed in the liquid N_2 trap now being re-absorbed on the metal surface. Further carbon monoxide adsorptions on this sample also showed that the surface is poisoned by Hg vapour collected in the liquid N_2 trap. Consequently, this experiment was repeated with the following special precautions being taken:

(a) The liquid N_2 trap is replaced by a dry ice trap in order to keep condensation of carbon monoxide to a minimum. At the same time the temperature of the dry ice trap will be low enough to freeze out any $Ni(CO)_4$ gas. (The melting point of $Ni(CO)_4$ is -25^oC).

(b) The trap is cleaned immediately before any carbon monoxide gas is admitted to the sample in order to avoid mercury poisoning.

(c) The carbon monoxide pressure must be high enough so that a fairly intense band at 2058 cm^{-1} can be recorded.

(d) The carbon monoxide was kept in contact with the catalyst for as short a period as possible (5 minutes instead of 10 minutes).

The results are represented in Fig. 32. No band at 2058 cm^{-1} was found when the contents of the dry ice trap was re-admitted to the sample.

(B) Discussion:

From Fig. 30 and Fig. 31 one must conclude that at least part of the band at 2058 cm^{-1} must be due to physically adsorbed $Ni(CO)_4$. The C band tends to show P— and R—branch shoulders on each side of the central sharp (Q-branch) maximum. Normally, solid phase molecules (see Appendix 5) would not be expected to show P—Q—R structure. Blyholder[44] found a P and an R branch for physically adsorbed CO on iron, which indicates that the CO is rotating on the surface. In the light of the above it is quite likely that at least part of the C band must be due to physically adsorbed $Ni(CO)_4$.

On the other hand, from Fig. 32 no evidence could be found for the presence of $Ni(CO)_4$, so that the huge C band in Fig. 32 curve 1, must be assigned to more than one CO molecule attached to single Ni atoms.

105/.. .. .. ..

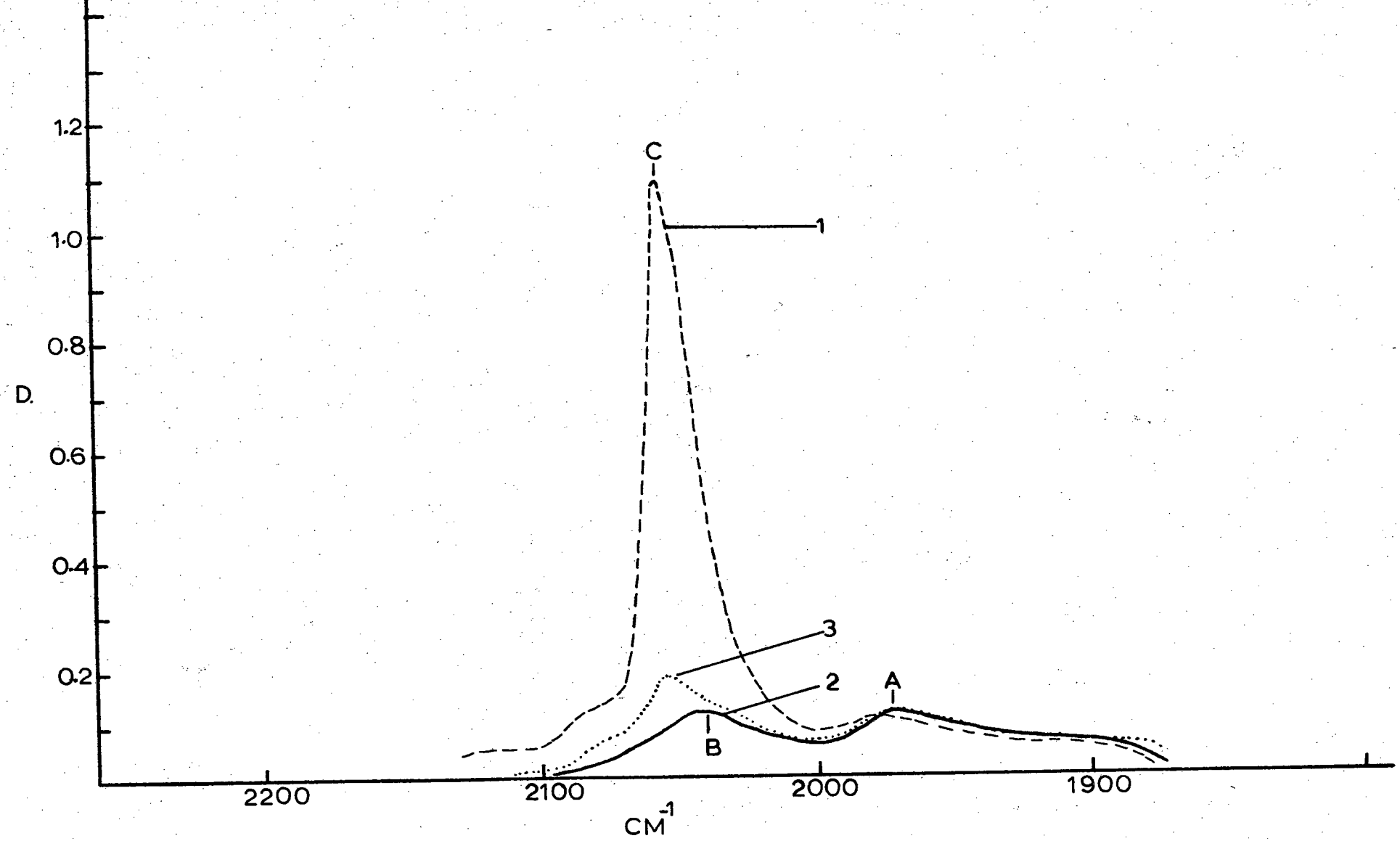

Fig. 31. Carbon monoxide chemisorbed on supported nickel at 1) 50 torr, 2) evacuated to 1×10^{-5} torr, 3) re-adsorbed contents of liquid nitrogen trap.

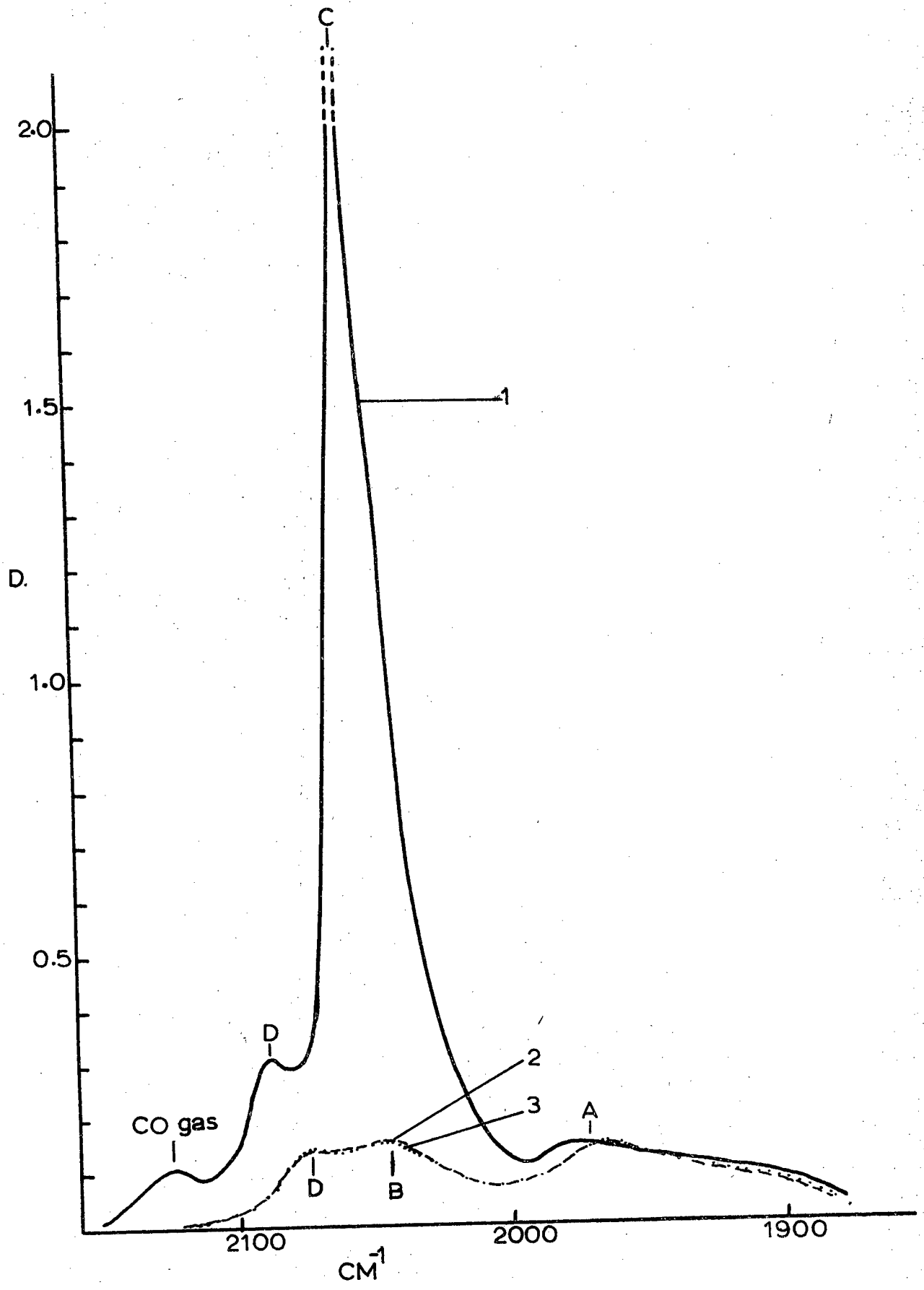

Fig. 32. Carbon monoxide chemisorbed on supported nickel 1) 60 torr, 2) evacuated to 5×10^{-5} torr, 3) re-adsorbed contents of dry ice trap.

This argument is further strengthened by the fact that the C band only appears later at higher carbon monoxide pressures.

It must be mentioned here that some of the other vibrational bands of $Ni(CO)_4$ gas only appear when the intensity of the C band is exceptionally high. Pickering[29] took this absence of other bands as a proof that the band at 2058 cm^{-1} is not part of the vibrational spectrum of $Ni(CO)_4$ gas. The intensity of the C band is so great compared to the intensities of the other bands that, in the light of the present results, such an assumption is not justified.

Furthermore, $Ni(CO)_4$ is formed relatively fast when a nickel catalyst is left in the presence of excess carbon monoxide. The CO molecules responsible for the C band must have chemisorbed; otherwise $Ni(CO)_4$ could not form. On the other hand, upon evacuation or with temperature increase these molecules are the first to desorb. The C band must therefore be in part due to weak chemisorption of CO molecules. This shows that a major chemical reaction might proceed via a weak chemisorption mechanism.

APPENDIX 7.

On Which Band Appears First (Nickel):

In order to ascertain which band appeared first, carbon monoxide was admitted to a clean nickel surface at a pressure of less than $3x10^{-5}$ torr. It was found that the first few increments almost disappeared, pressure-wise, on standing in contact with the catalyst. The pressure readings were therefore somewhat in doubt, especially below 0.1 torr. However, what is important, is the band intensities as related to increasing carbon monoxide pressures; as presented in Fig. 33. Curve 1 shows band A slightly more intense than B, although the bands are not sharply defined. With the next increment of carbon monoxide, both bands increase in intensity as seen from curve 2. (Between 2 and 4 more increments were given prior to recording curve 3). From curve 4, band D can be seen as a shoulder on B. In curve 6 band D is just as intense as A and B which had reached their maxima. At a carbon monoxide pressure of 0.75 torr, D has also reached its maximum, while band C has now appeared. On further increasing the pressure, A starts to decrease in intensity, while at a later stage (Appendix 5), D also decreases. Unfortunately B is camouflaged by band C so that one cannot see what might have happened to it.

106/.. .. .. ..

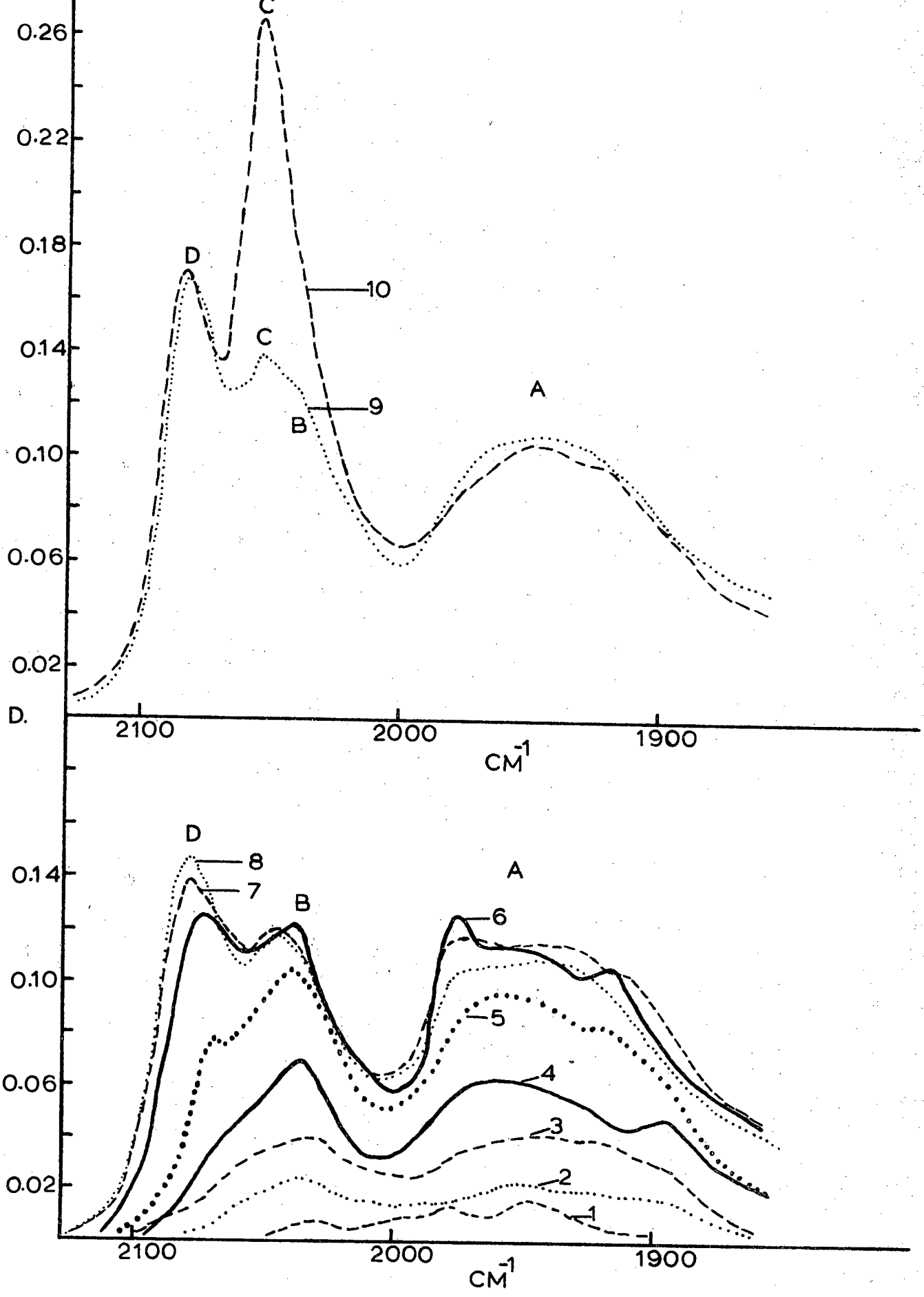

Fig. 33. Carbon monoxide chemisorbed on supported nickel at 1) <3x10-5 torr, 2) <3x10-5 torr, 3) 3x10-5 torr, 4) 5x10-5 torr, 5) 2x10-4 torr, 6) 1.7x10-2 torr, 7) 0.12 torr, 8) 0.25 torr, 9) 0.75 torr, 10) 1.55 torr.

In conclusion it can be said, from the above, that bands A and B are formed simultaneously, followed by band D. From this it follows that the chemisorbed bridged species A is just as firmly bound to the surface as the linear species B. The desorption studies at room temperature confirm this contemplation (e.g. Fig. 32, curve 2). On the other hand when heat is applied to the chemisorbed species (e.g. Fig. 36, curve 4), it was found that band D was the first to disappear, followed by B and lastly A. From this evidence one may conclude that the bridged species A are the most strongly held to the surface.

APPENDIX 8.

The Influence of Temperature on the Bands ascribed to Chemisorbed Species (Nickel):

As the actual Fischer-Tropsch process is carried out at elevated temperatures, it was considered important to see what will happen to the chemisorbed CO species when heat is applied. The spectrum of 19 torr carbon monoxide in contact with a nickel catalyst can be seen in Fig. 34. At 100°C it was found that band C had disappeared while the intensities of the A, B and D bands were slightly less than before. At 240°C the only important observation is that B and D have disappeared to give one broad band inbetween B and D, with its maximum at 2060 cm^{-1}. The integrated intensity is very little different from the sum of the intensities of B and D at 100°C.

When this sample is cooled down to room temperature and then evacuated for 20 minutes to a pressure of about 7×10^{-6} torr, bands A, B, D and E are found as shown in Fig. 35. It is concluded that these bands may be assigned to species strongly held to the metal surface (Band E could result from surface oxidation by carbon dioxide resulting from the Boudouard decomposition reaction[45]

$$2\ CO \longrightarrow C + CO_2$$

which would readily occur at 240°C in the presence of a catalyst[1]).

In order to determine the effect of temperature on the bands without an excess of carbon monoxide gas, a new experiment was devised. In this case 20 torr carbon monoxide was brought in contact with a freshly reduced sample at room temperature and the spectrum recorded. The excess carbon monoxide was then removed by evacuation in steps until band C had disappeared. (It was found in practice that any temperature above about 50°C was sufficient to desorb the adsorbed molecules responsible for band C. This desorption will then increase the number of carbon monoxide molecules in the gas phase).

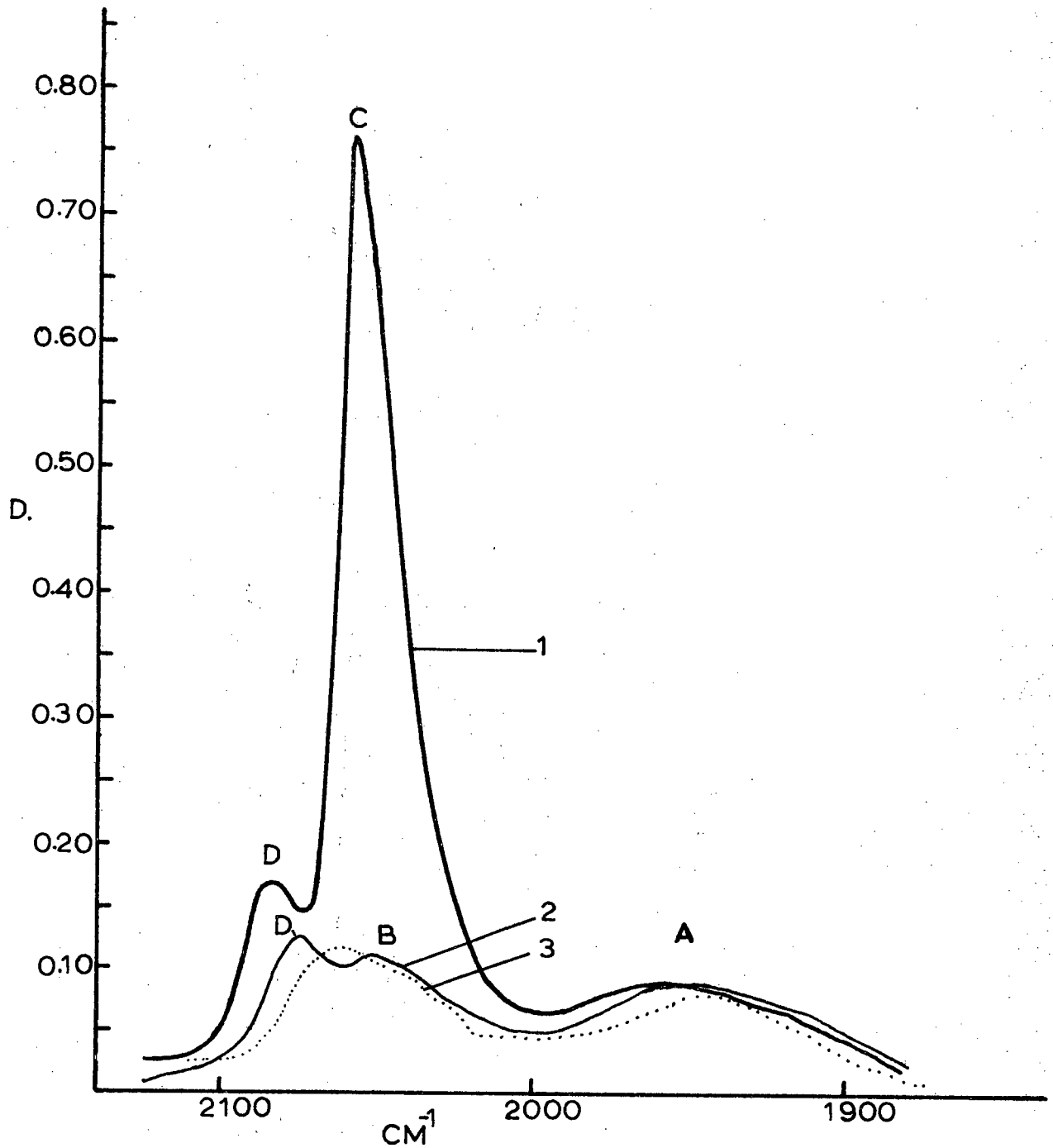

Fig. 34. Carbon monoxide chemisorbed on supported nickel (19 torr pressure) at 1) room temperature, 2) 100°C, 3) 240°C.

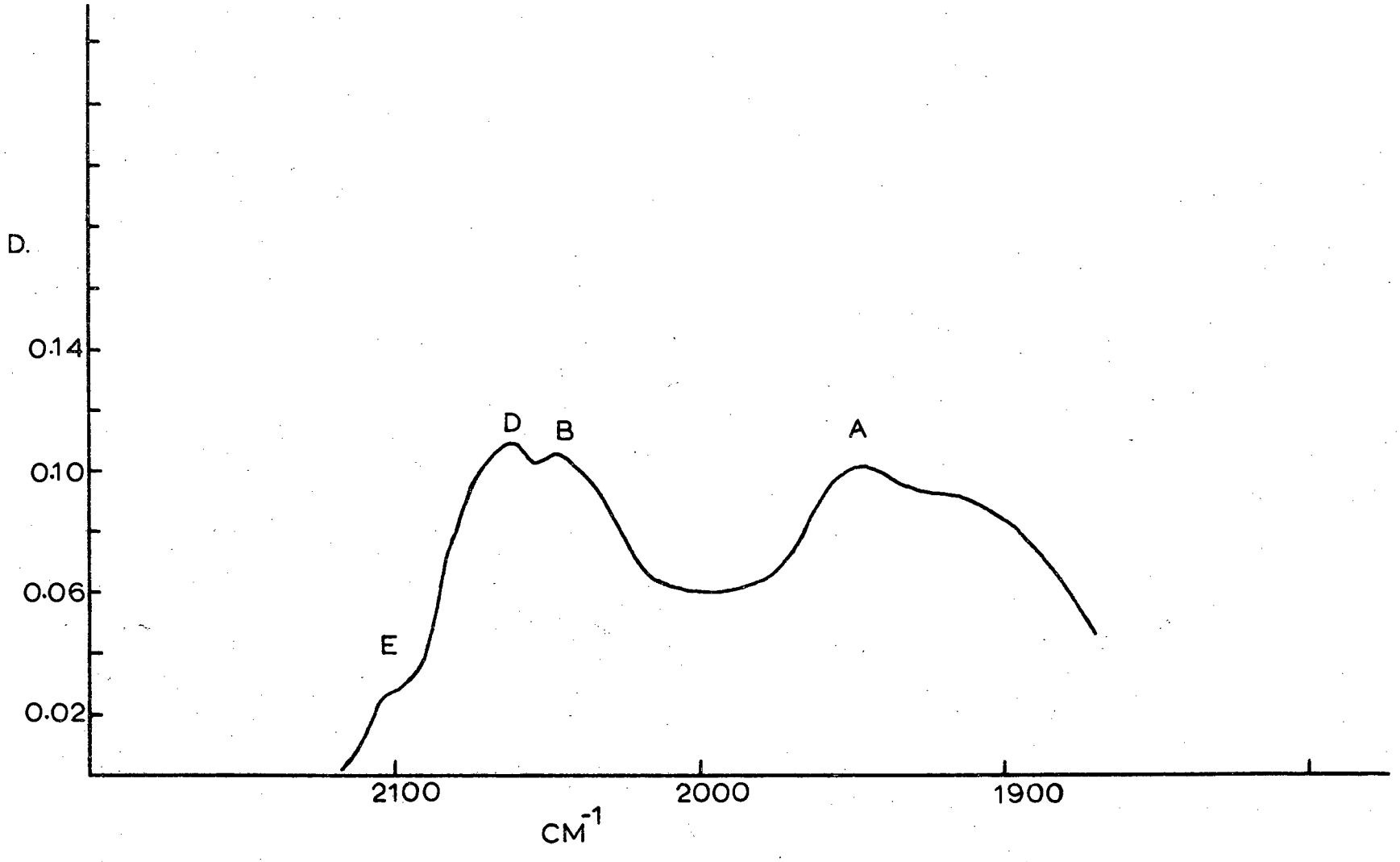

Fig. 35. Carbon monoxide chemisorbed on supported nickel, heated to 240°C followed by evacuation at room temperature for 20 mins. to 7×10^{-6} torr.

At a pressure of 5.5×10^{-3} torr at room temperature, curve 1 in Fig. 36, was obtained. In order to test the stability of the chemisorbed species this sample was kept at room temperature for 66 hours. As can be seen from curve 2 (Fig. 36) the chemisorbed species are very stable. Only a slight decrease of the bands were observed with the appearance of band C. On increasing the temperature it was found that band D is the least stable whereas bands A and B represent, under these experimental conditions, the most strongly held species. When the sample was cooled down to room temperature, only one broad band at 2050 cm^{-1} was found between B and D (e.g. Fig. 34, curve 3).

APPENDIX 9.

The Influence of Temperature and Hydrogen on the Chemisorbed CO Species:

It is well known that nickel is an excellent methanation catalyst[1]. It therefore would be of interest to know which of the adsorbed species is responsible for the methanation reaction.

In one experiment hydrogen at a pressure of 70 torr was admitted to 22 torr carbon monoxide in contact with a nickel catalyst at 390°C. It was found that the carbon dioxide formation increased while a new band ascribed to methane, appeared at 3015 cm^{-1}. The results are represented in Fig. 37. On standing the intensity of the methane band increased. When the sample was cooled to room temperature another band at 1620 cm^{-1} appeared. Upon evacuation all the bands disappeared.

In the above, no reaction intermediates were observed. It was argued that at such a high temperature the reaction rate will be so fast that the concentration of reaction intermediates at any particular moment will be relatively low (due to completion of the reaction) and could thus not be detected. Consequently in the next experiment the sample was first cooled to room temperature before the hydrogen was admitted. Furthermore, the above sample was of the very active type. Special precautions had been taken to obtain a clean metal surface. When high initial carbon monoxide pressures are applied the active centres will react first and will, upon evacuation, be carried away as $Ni(CO)_4$ gas. This will result in a catalyst having less active centres by the time the hydrogen is admitted to the cell. Therefore, in the next attempt 4 torr carbon monoxide only was admitted to the sample, and the spectrum was recorded. This sample was then evacuated in steps to 2.5×10^{-3} torr before 10 torr hydrogen was admitted at room temperature. In order to slow down the reaction rate between the chemisorbed

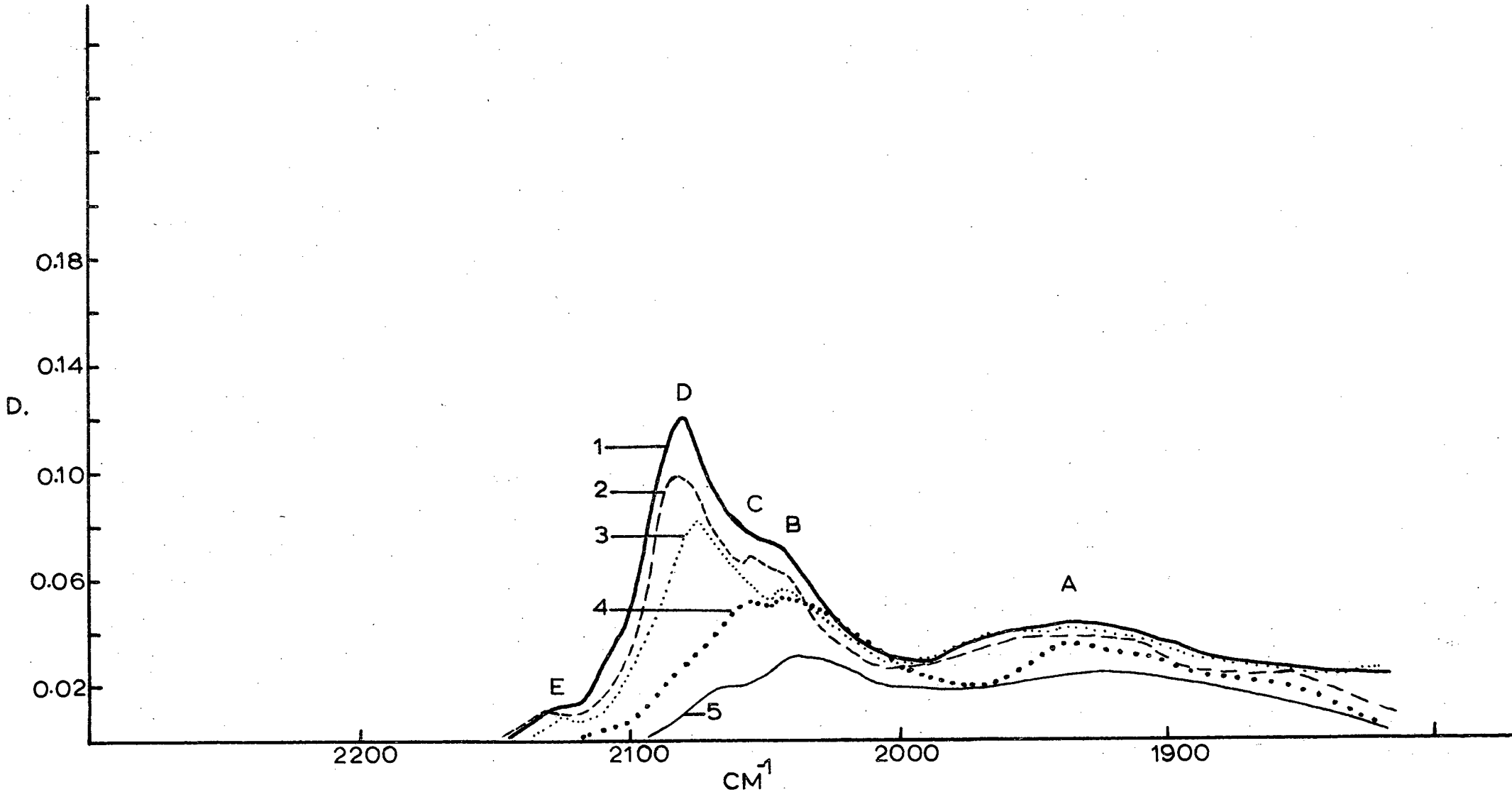

Fig. 36. Carbon monoxide chemisorbed on supported nickel 1) evacuated to 5.5×10^{-3} at room temperature, 2) after 66 hours at room temperature, 3) at 100°C, 4) at 200°C, 5) at 300°C.

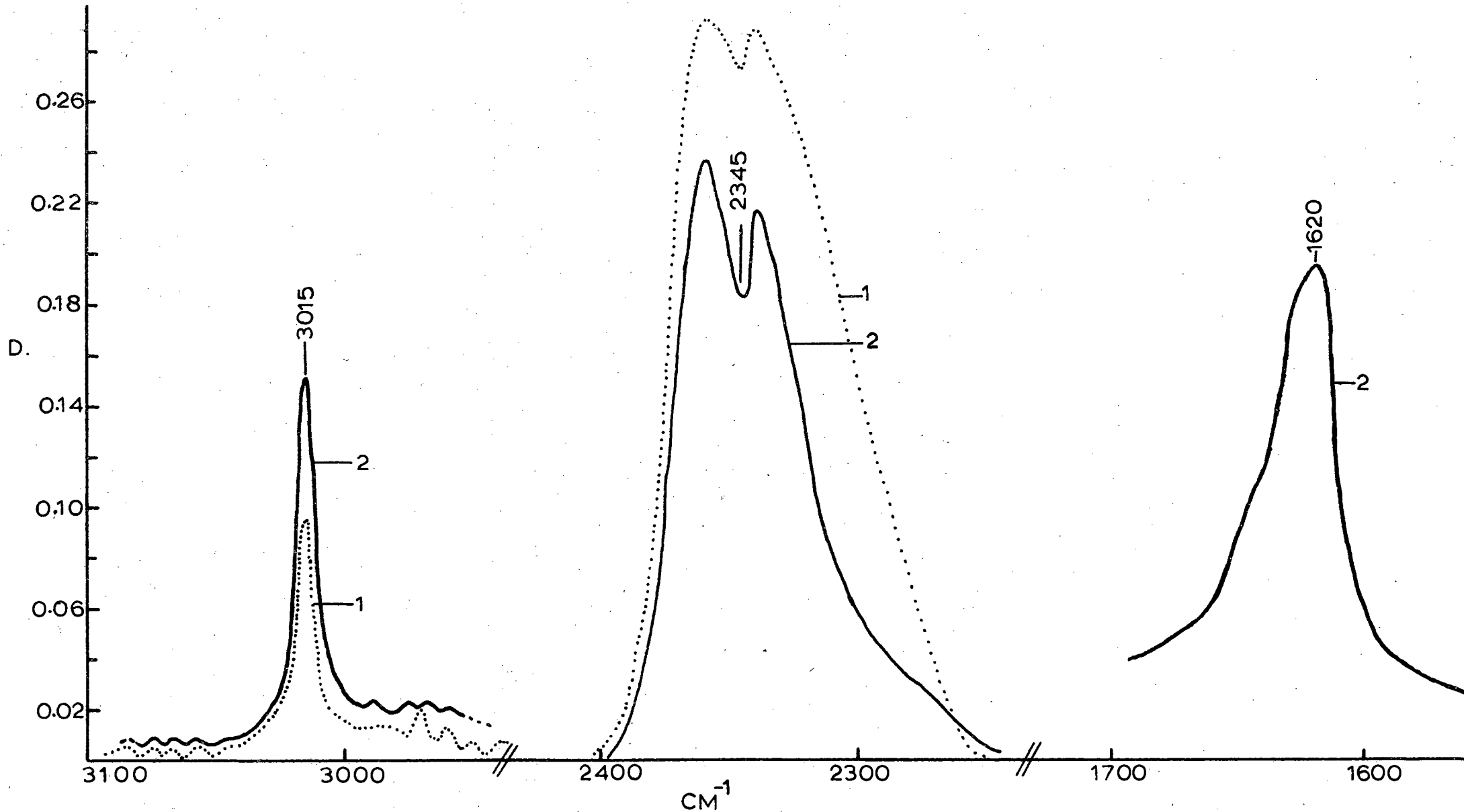

Fig. 37. Supported nickel; 22 torr carbon monoxide plus 70 torr hydrogen at 1) 390°C and 2) room temperature.

CO and hydrogen, the sample was kept for longer periods at low temperatures. The curves can be seen in Fig. 38. It was found that band D immediately increased in intensity when the hydrogen was admitted, while B decreased. On standing for 14 hours at room temperature band A increased while D was now less intense. A small band C was observed, but when the sample was heated to 50°C it disappeared again. After 2 hours at 100°C (curve 6) band B had disappeared with a slight increase in D. In this case traces of methane were found (not shown). At 200°C the formation of methane increased rapidly, and after 1½ hours no chemisorbed CO bands could be detected.

From Fig. 38 it can be seen that when hydrogen is admitted at room temperature band D becomes more intense. Infra-red inactive gases such as hydrogen, helium, nitrogen, etc., could cause a pressure broadening effect when added to an infra-red active gas (see Chapter 1). In this case the hydrogen molecules could collide with CO molecules in the gas phase by which mechanism they will adsorb onto the metal surface and thus add to the D band. It was therefore decided to repeat this experiment by using helium instead of hydrogen. (The pressure broadening effect of helium and hydrogen is the same as carbon monoxide as can be seen in Table IV.

TABLE IV

P_{CO}	P_{H_2}	P_{He}	D
23 torr	-	-	0.023
23 torr	20 torr	-	0.033
23 torr	81 torr	-	0.066
23 torr	-	20 torr	0.033
23 torr	-	81 torr	0.066

D is the optical density of the P-branch of carbon monoxide as measured at 2120 cm^{-1}).

In this work 2 torr carbon monoxide was adsorbed at room temperature and the excess then removed by evacuation to a pressure of 2.5×10^{-3} torr. When 11 torr helium was admitted only a small increase in band D was observed - see Fig. 39. In order to gain confidence the scan was repeated but no change was observed. The helium was then evacuated to 1×10^{-3} torr and the spectrum recorded (curve 3). Thereupon 10.5 torr hydrogen was admitted and a big increase in the intensity of D was observed while B decreased.

109/.. .. .. ..

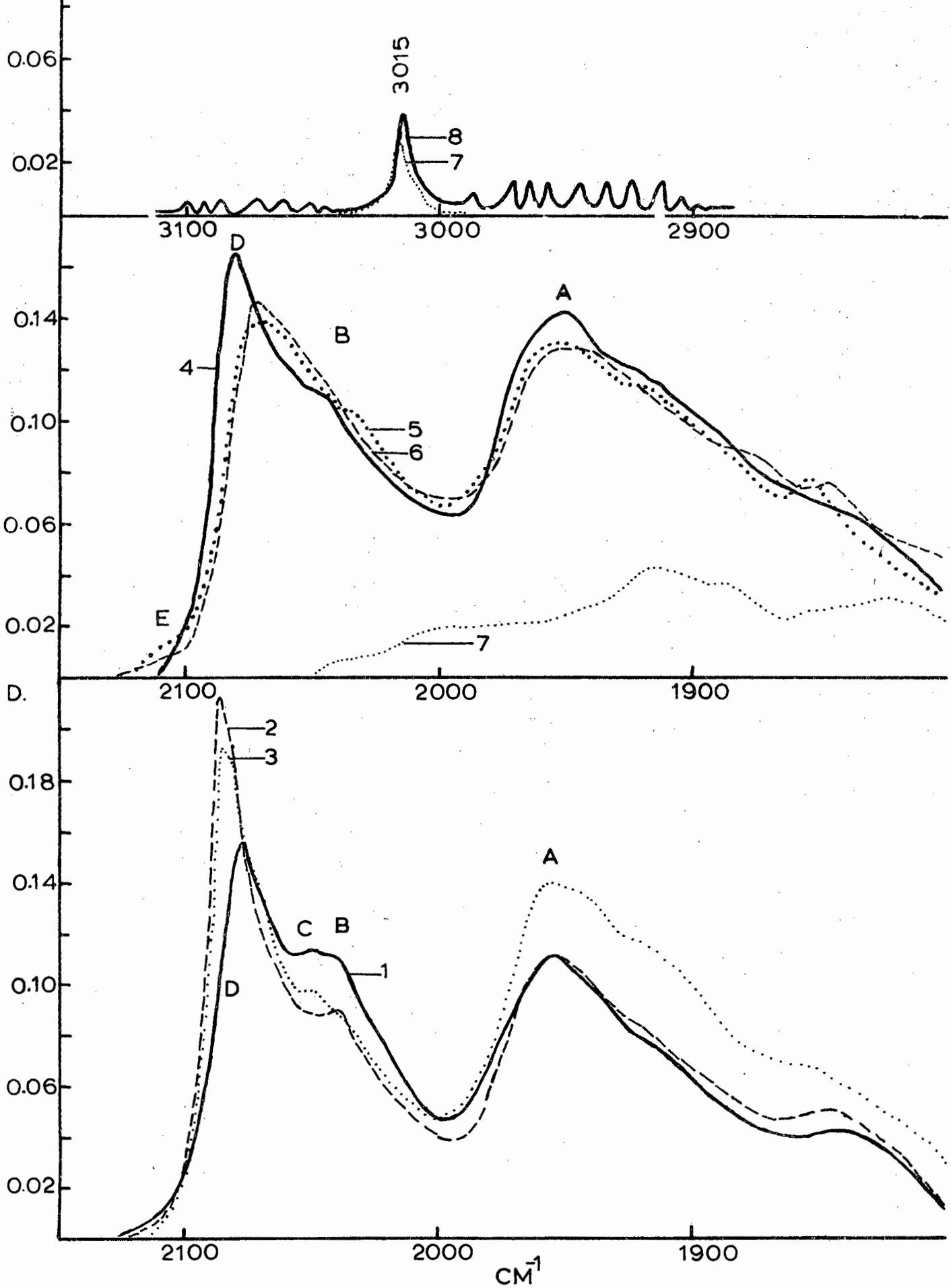

Fig. 38. Carbon monoxide chemisorbed on supported nickel, 1) evacuated to 2.5×10^{-3} torr, 2) plus 10 torr hydrogen at room temperature, 3) after 14 hours at room temperature, 4) at 50°C, 5) at 100°C, 6) 2 hours at 100°C, 7) ½ hour at 200°C, 8) 1½ hours at 200°C.

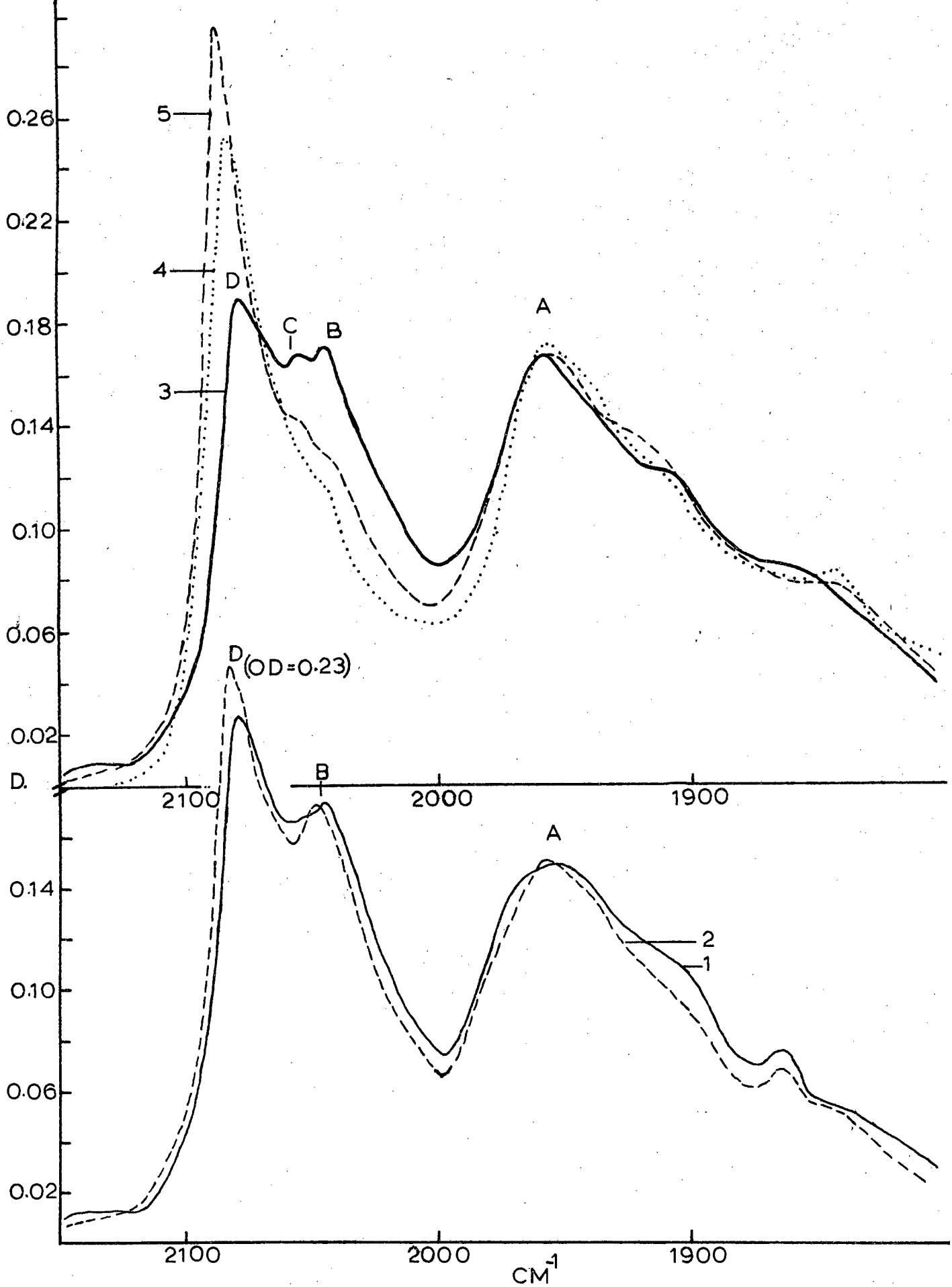

Fig. 39. Carbon monoxide chemisorbed on supported nickel 1) evacuated to 2.5×10^{-3} torr, 2) plus 11 torr helium at room temperature, 3) evacuated to 1×10^{-3} torr, 4) plus 10.5 torr hydrogen, 5) after 24 hours at room temperature.

After 24 hours both bands B and D decreased in intensity but no other bands (not even a methane band) could be found.

This sample was subjected to prolonged heat treatments and the spectra recorded at intervals. The results are shown in Fig. 40. It is seen that the intensity of band D decreased more than that of A. It is also noticed that each band has more than one inflection point (these could hardly be ascribed to resolution of rotational fine structure). During this heat treatment methane was formed. Again no reaction intermediates were found. Also, it was not clear from the change in intensities which of the A and D band species were the most reactive. At low temperatures the most reactive species will be inhibited to a lesser extent, so that these should display the largest intensity change.

Another way of determining which band represents the most reactive species is the following: Increase the temperature rapidly up to the "critical reaction temperature" for a very short period and then decrease the temperature immediately to stop the reaction. By doing this, it was hoped that only the most reactive species would react during that period. The results of such an experiment are shown in Fig. 41. As before, it was again found that band D increased in intensity at the expense of B when hydrogen was admitted at room temperature. After 18 hours at room temperature band A again increased. The sample was then heated to 220°C within 5 minutes, kept at 220°C for 5 minutes and then cooled down to room temperature within the next 5 minutes. After each heating cycle the spectrum was recorded immediately at room temperature. Although no reaction intermediates were observed, the results were very interesting. Bands A and D decreased initially at more or less the same rate but after the second heating cycle it can be seen that band A disappeared at a faster rate. In band A again, the band A1 is the first to disappear, followed by A2, etc.

In a paper by Blyholder[25] it was stated that the authors were unable to say whether the CO, while chemisorbed in structures that produced bands at 1900 and 2060 cm^{-1}, would react with hydrogen. We think that the bands A, B and D represent those structures discussed by them. However, from the above experiments it is quite clear that hydrogen reduces chemisorbed species. Although the D and B bands disappeared first (Figs. 38 and 39), we are hesitant to say that they are reduced first. The reaction mechanism might proceed <u>via</u> the structure represented by A. This can be explained as follows: As species A are reduced and taken away from the surface, more sites become available. The linearly held molecules can now rapidly be reformed into

110/.. .. .. ..

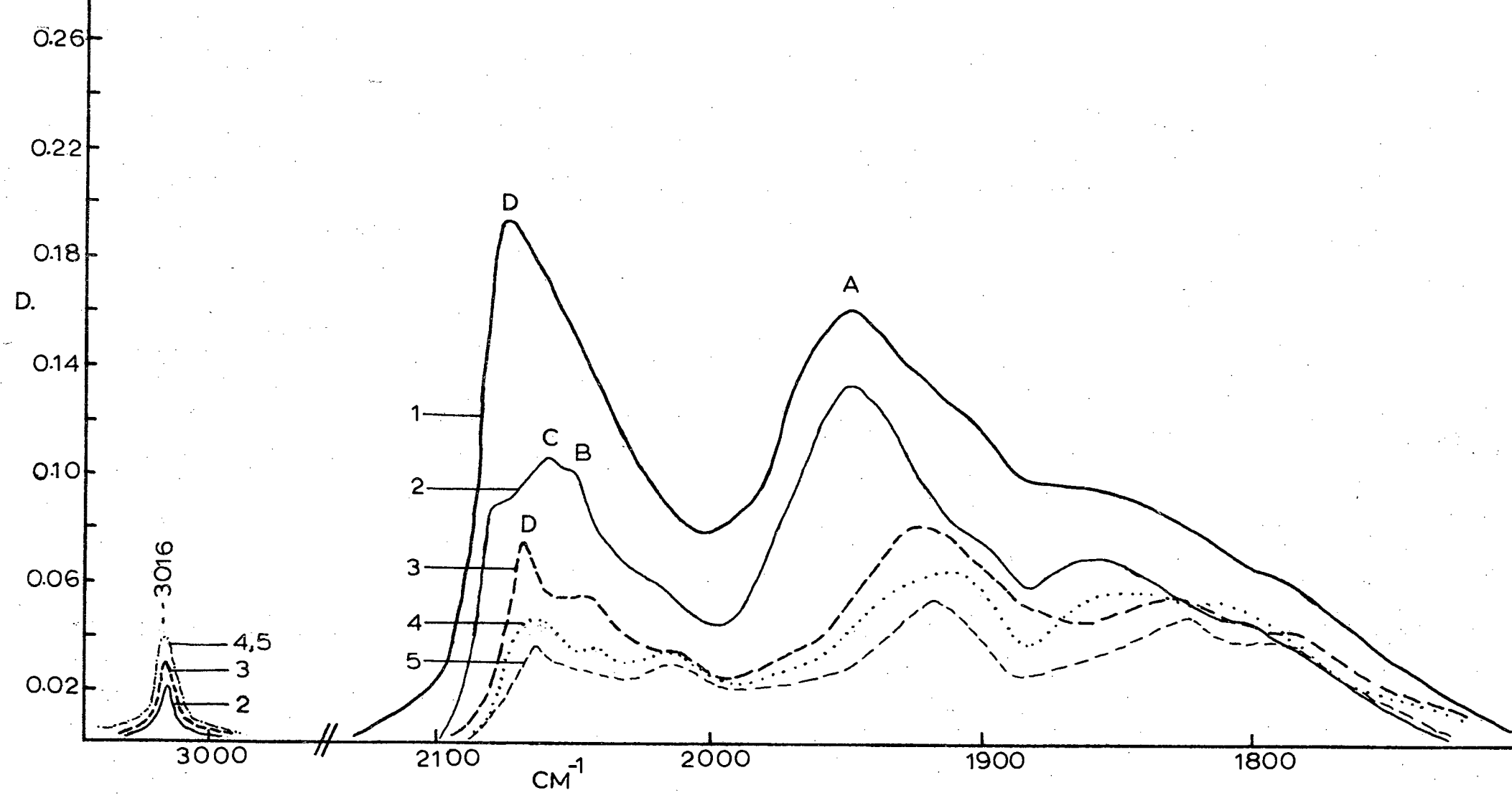

Fig. 40. 1.3×10^{-3} torr carbon monoxide plus 10.5 torr hydrogen over supported nickel, 1) at 100°C for 4 hours, 2) after 3 days at 100°C, 3) plus another 7 days at 90°C, 4) plus a further day at 100°C, 5) plus 20 hours at 105°C.

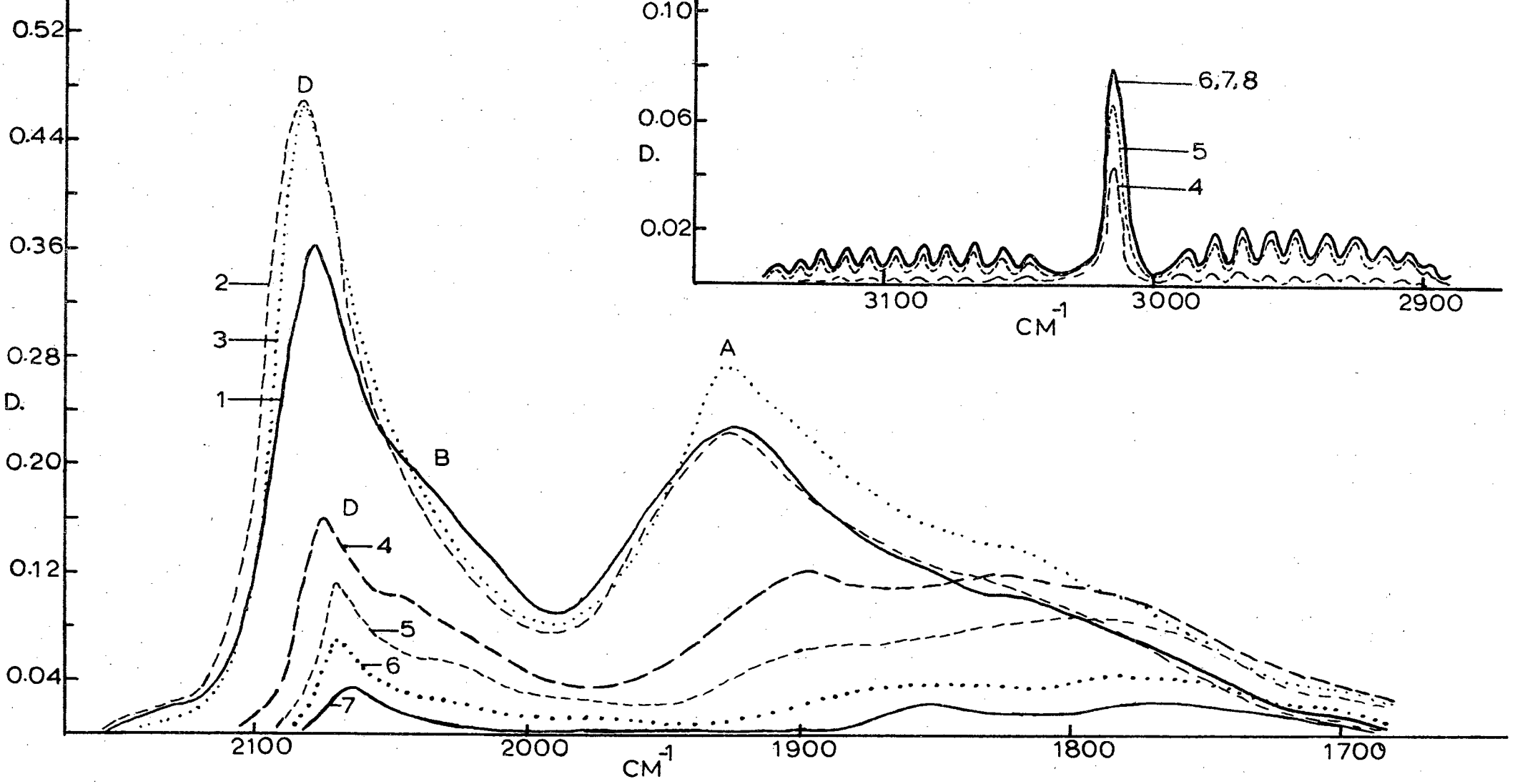

Fig. 41. Carbon monoxide chemisorbed on supported nickel (Type III), 1) evacuated to 8×10^{-4} torr, 2) do, + 30 torr hydrogen at room temperature, 3) after 18 hours at room temperature, 4) room temperature, after first heating to 220°C, 5) room temperature, after second heating to 220°C, 6) room temperature, after third heating to 220°C, 7) room temperature after fourth heating to 220°C, 8) room temperature after fifth heating to 220°C.

bridged molecules. The net effect observed will be a decrease in the intensities of the D and B bands, while the intensity of A will apparently remain constant.

Support for this reaction scheme can be found in Figs. 38 and 41 where A increased in intensity when carbon monoxide and hydrogen are left in contact with the catalyst at room temperature for several hours. This, is further strengthened by the heating curves in Figs. 40 and 41. Especially in Fig. 41, curves 4 to 7, it can be seen that, after each heating/cooling cycle, band A decreased more in intensity than bands D and B. This in effect implies that the reaction path goes <u>via</u> the structure(s) represented by band A.

Another interesting point is the fact that band D increased in intensity at the expense of B when hydrogen was admitted. Although there might be a small pressure broadening effect, it is insignificant and the main phenomenon must be ascribed to a chemical effect. One possibility is that the hydrogen might displace the chemisorbed CO molecules reponsible for band B due to hydrogen chemisorption on these sites. Another possibility is that, due to hydrogen chemisorption on sites elsewhere, the D sites become more active than the B sites and that for this reason the intensity of band D will increase. There might of course be some other explanation. The first possibility is discussed further in the next paragraph.

From the above work one has the impression that the B and D bands are in a way related to one another. Further, when CO only was present on the catalyst (Appendix 8, Fig. 34, curve 3 and others not shown) only one band, located between the B and D bands, was found. Due to the particular experimental conditions, the assumption can be made that the intermediate band is only found at low carbon monoxide coverage. However, the opposite is not true i.e. at low carbon monoxide coverage not only one intermediate band is always found. This would be the case if interactions are in operation between the species responsible for the B and D bands. Blyholder[10] also considered this question of more than one band ascribed to the same type of species. Two possible explanations were offered:

(a) that the two bands are due to interactions of chemisorbed CO molecules with each other, or

(b) are due to surface heterogeneity.

If (a) is responsible, one band would be expected at low coverage and two bands at high coverages.

111/.. .. .. ..

As said above, in this work both one and two bands were found at low carbon monoxide coverage. It was however found that when hydrogen was admitted, the intermediate band immediately splits into the B and D bands. This supports the idea of interaction between the CO species responsible for the B and D bands, although the possibility of two different surface sites cannot be ruled out. These sites can be very closely situated or even directly connected to each other.

Band B is observed at a lower vibration frequency than band D. This means that the carbon-nickel bond of the B band species is stronger than that of the D band species.

On the other hand, the B band species observed at the lower frequency are in an environment of fewer Ni ligands than the D band species (in agreement with the theory of dπ backbonding). For steric hindrance reasons it will be easier for hydrogen molecules, say, to displace B band species than D band species. This can in part explain the initial increase in intensity of D, with the corresponding decrease in the intensity of B, when hydrogen is admitted at room temperature.

In order to determine whether the hydrogen molecules in fact adsorb onto the B sites or just readily attack the CO species represented by band B, a new experiment was devised. In this experiment hydrogen was adsorbed at room temperature prior to the adsorption of carbon monoxide. The results are shown in Fig. 42. From curves 2 and 3 it can be seen that band B was found to be still present. However, when the hydrogen pressure was increased drastically from about 2×10^{-2} to 33 torr (curve 4) the intensity of B decreased and that of D increased. D is simultaneously displaced to higher wave numbers, as was found previously. Upon evacuation (curve 5), part of the D species were reformed back into B species. Therefore, one may conclude that, although at relatively high hydrogen pressures the B band CO species were displaced, at relatively low pressures the B sites hold the CO species more firmly than hydrogen.

APPENDIX 10

Carbon Monoxide Chemisorption on Nickel Oxide:

When carbon monoxide is chemisorbed on Type II green nickel oxide (NiO) a band F was found between 2165 and 2195 cm^{-1} but more often at about 2190 cm^{-1}. Simultaneously a doublet at 2345 cm^{-1} was assigned to carbon dioxide gas.

112/.. .. .. ..

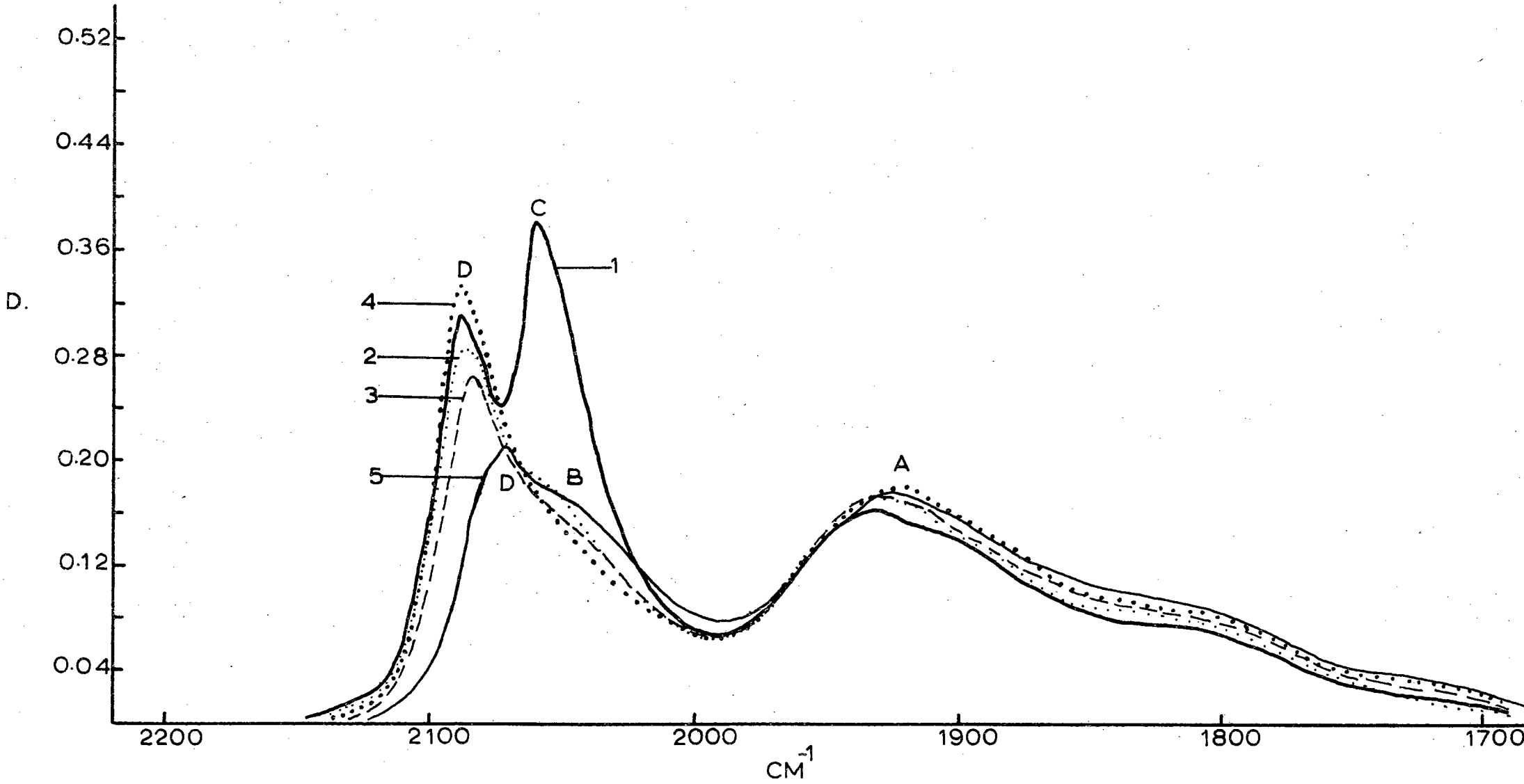

Fig. 42. Supported nickel Type III, 1) plus 0.84 torr hydrogen followed by 0.86 torr carbon monoxide, 2) evacuated to 0.45 torr (carbon monoxide + hydrogen), 3) evacuated to 4.2×10^{-2} torr, 4) do, + 33 torr hydrogen, 5) evacuated for 5 mins. to 1×10^{-4} torr.

This is shown in Fig. 43(a). When carbon monoxide is chemisorbed on Type I black nickel oxide (Ni_2O_3) no band ascribed to chemisorbed species was found. However, when Type I black nickel oxide was heated to about 400°C under vacuum it changed into the light green form. Carbon monoxide chemisorption on this Type I nickel oxide gave bands at 2165, 2195 and 2345 cm^{-1}. This is shown in Fig. 43(b).

Note: In most of the experiments only one band at about 2190 cm^{-1} was found for carbon monoxide chemisorbed onto oxide lattices.

APPENDIX 11

Carbon Monoxide Chemisorbed on Potassium Promoted Nickel:

When carbon monoxide chemisorbed on silica-supported nickel promoted with a K:Ni ratio of 2:100 the spectra as represented in Fig. 44, were found. At 2 torr carbon monoxide, band D appeared as a shoulder at 2080 cm^{-1} on band C, and band B was seemingly absent. The low wave number side of band A was also more intense when compared with spectra obtained in the absence of potassium. In the latter experiments (Type I samples) band A appeared at about 1950 cm^{-1} with a shoulder at about 1800 cm^{-1}. In the present studies, band A appeared as a doublet with band A1 at about 1920 cm^{-1} and band A2 at about 1840 cm^{-1}.

With a K:Ni ratio of 10:100 the spectra shown in Fig. 45 were found. In this experiment, at a carbon monoxide pressure of 2 torr, band D was apparently absent, whereas band B appeared as a shoulder at 2020 cm^{-1} on the low wave number side of C. On decreasing the pressure to 0.15 torr, band D was found at 2065 cm^{-1}, which means that it was camouflaged by C at the higher carbon monoxide pressures. A was still a doublet with A1 at about 1910 cm^{-1}, and A2 at about 1840 cm^{-1}.

In both the above experiments it was found that B disappeared on decreasing the carbon monoxide pressure. This phenomenon was considered as unusual because in all the experiments done on nickel in the absence of potassium, band B was found to be very persistent. At the same time the question arose which of these bands could be assigned to the species most strongly held on potassium promoted nickel surfaces. Therefore, in an experiment with 20:100 K:Ni, carbon monoxide was admitted to the sample at a pressure of about 7×10^{-5} torr. (It was again found, that the first increments almost disappeared, pressurewise, on standing in contact with the catalyst.

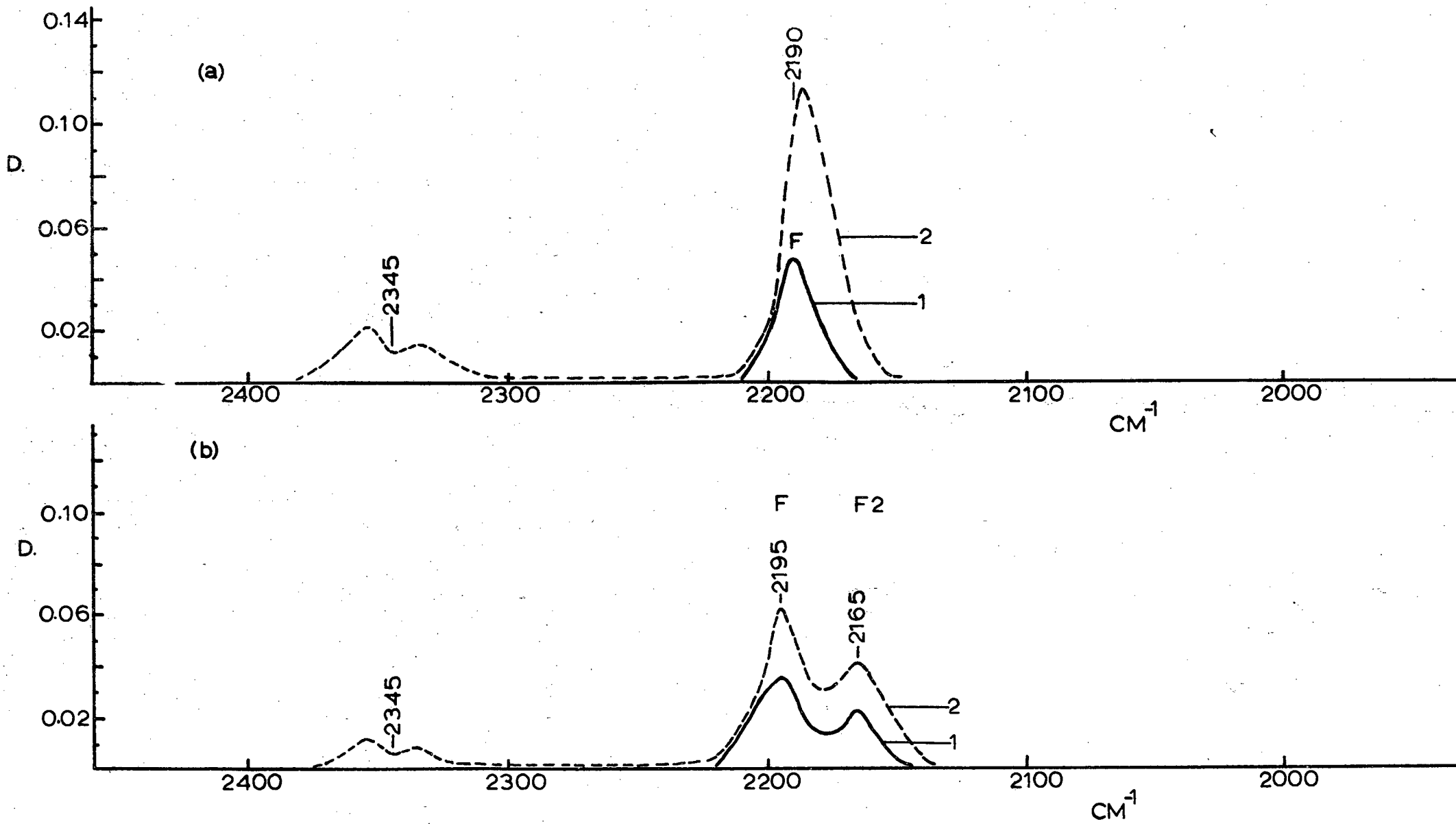

Fig. 43(a) Type II nickel oxide plus carbon monoxide at 1) 2.5 torr and 2) 31.0 torr.

(b) Type I nickel oxide evacuated at 400°C for one hour, followed by carbon monoxide chemisorption at 1) 3.0 torr and 2) 20.0 torr.

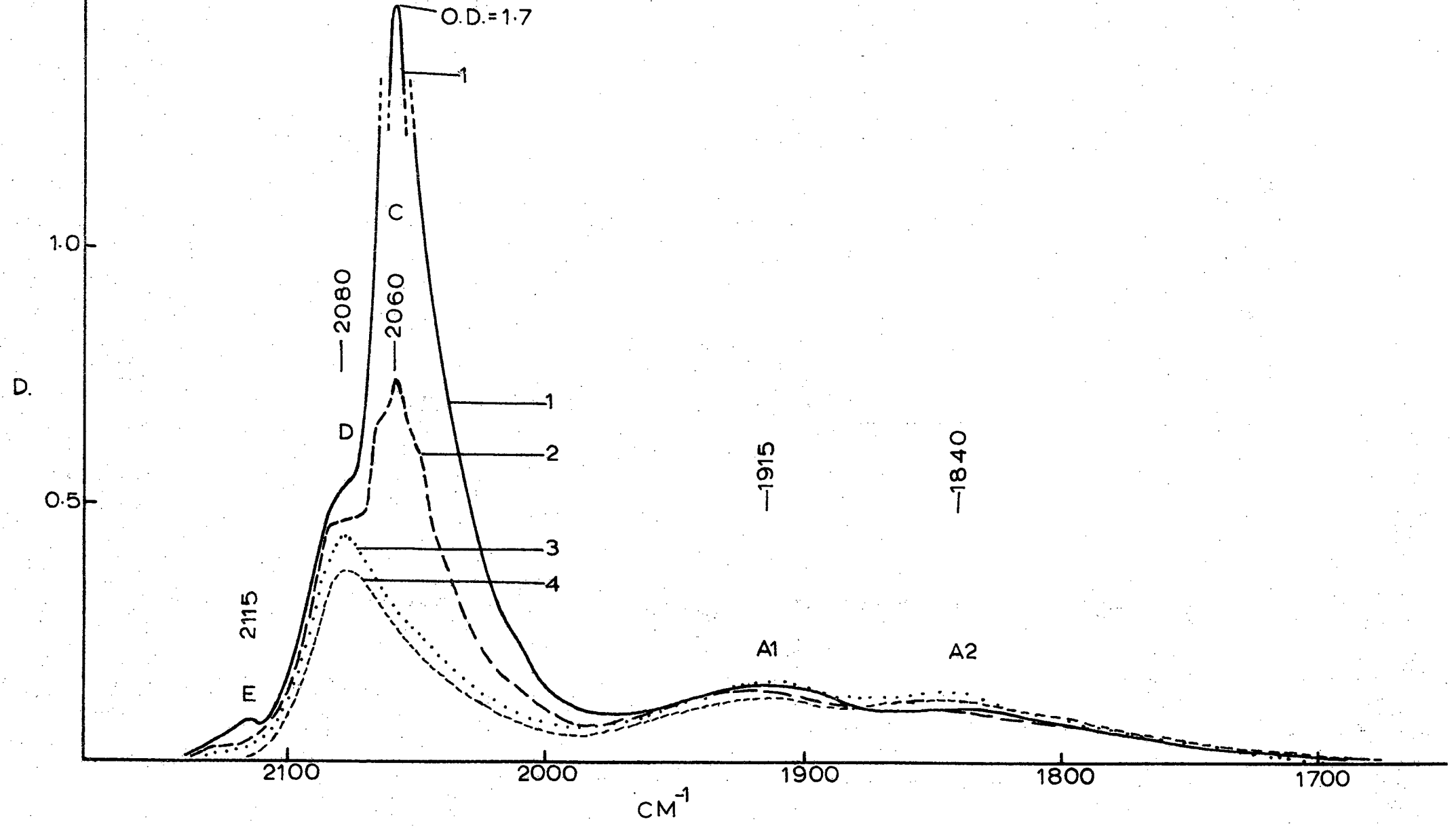

Fig. 44. Carbon monoxide chemisorbed on supported nickel, promoted with 2:100 K:Ni. Decreasing pressures 1) 2 torr, 2) 1 torr, 3) 0.15 torr, 4) 3.5×10^{-2} torr.

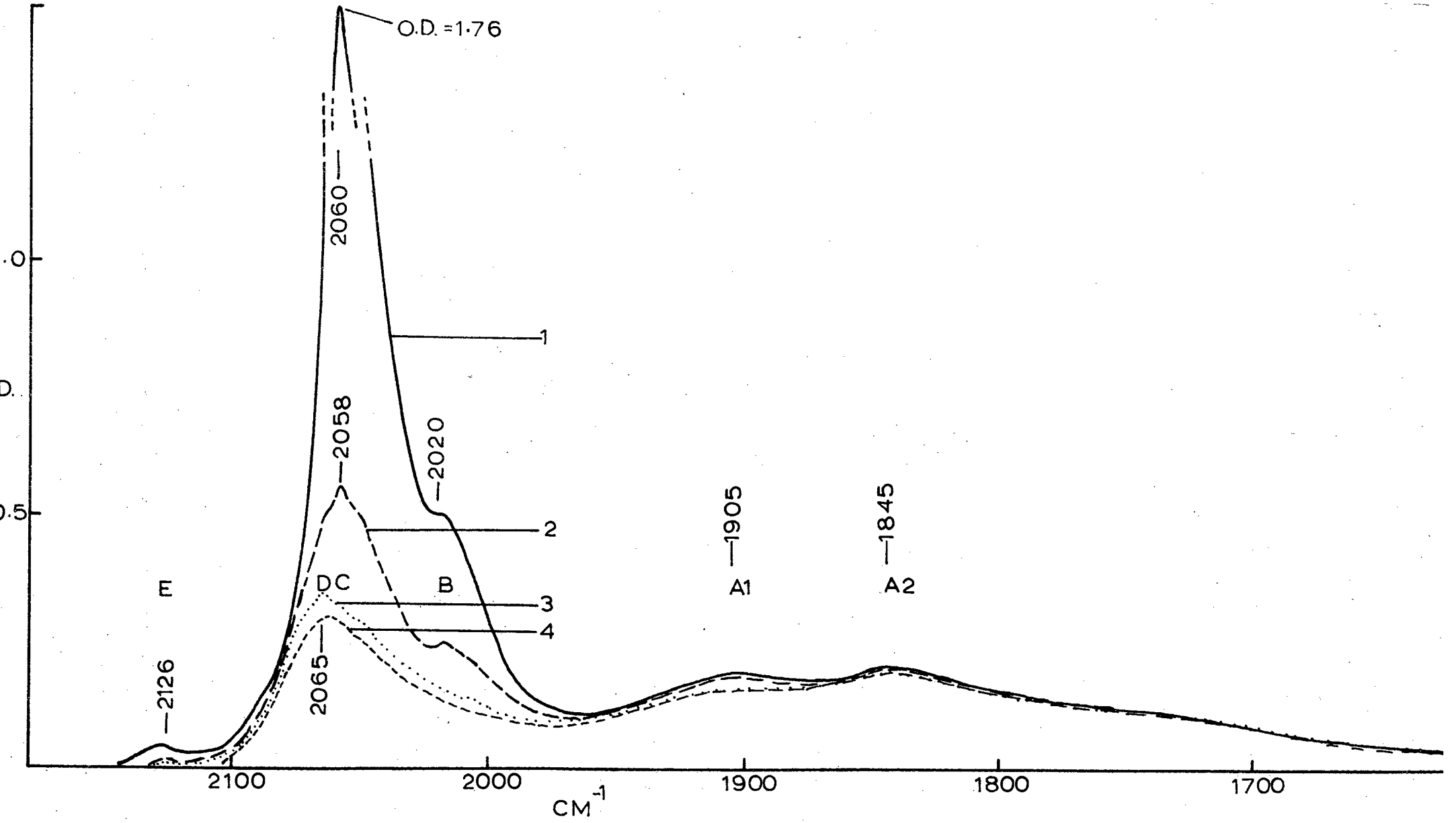

Fig. 45. Carbon monoxide chemisorbed on supported nickel, promoted with 10:100 K:Ni. Decreasing pressures at 1) 2 torr, 2) 0.55 torr, 3) 0.15 torr, 4) 3.5×10^{-2} torr.

The pressure readings were therefore taken at the end of each scan). The results are represented in Figs. 46(a), (b) and (c).

From Fig. 46(a) it can be seen that bands A2, A1 and D all appear simultaneously, although A2 (curve 3) at a pressure of 10^{-4} torr, was slightly more intense. Above this pressure D increased relatively more (i.e. ratiowise) in intensity than A1 and A2. Band B appeared only above 0.81 torr carbon monoxide (curve 6). It lay at 2020 cm^{-1} and its position was fairly constant with increasing pressure. Although band D was found initially at 2040 cm^{-1} its peak position was displaced to 2065 cm^{-1} with increasing carbon monoxide pressures. The peak position of band A1 remained fairly constant at 1920 cm^{-1}, but the maximum of A2 shifted from about 1780 to 1840 cm^{-1} on increasing the CO pressure.

Upon decreasing the pressure, band A1 decreased in intensity and the wave number of the maximum of A2 was lowered to about 1825 cm^{-1} (Fig. 46(c), curve 3). At the same time B disappeared, whereas D was shifted from 2065 to 2060 cm^{-1}.

APPENDIX 12.

The Effect of Temperature on Chemisorbed CO on Potassium Promoted Nickel:

In these experiments the excess carbon monoxide was pumped off in order to study the effect of temperature on the chemisorbed species only. The results obtained when CO, chemisorbed at 3.5×10^{-2} torr on a 10:100 K:Ni sample, was heated to different temperatures, is shown in Fig. 47. It can be seen that both the peak position and intensity of band D were very much dependent upon the temperature - the band was shifted towards lower wave numbers and its intensity decreased with increasing temperature. In the case of band A, it was mainly the high wave number side of the band that was affected in the same way.

This experiment was repeated with a 20:100 K:Ni sample. The results are represented in Fig. 48. Once again it was found that the high wave number bands were affected most upon heating. Thus the observations made, were confirmed with confidence.

APPENDIX 13.

The Interaction of Hydrogen and Carbon Monoxide on Potassium Promoted Silica-Supported Nickel:

It is known from studies of the Fischer-Tropsch process[1] that potassium, when present in the catalyst, acts as a chemical promoter, i.e. its inclusion ha

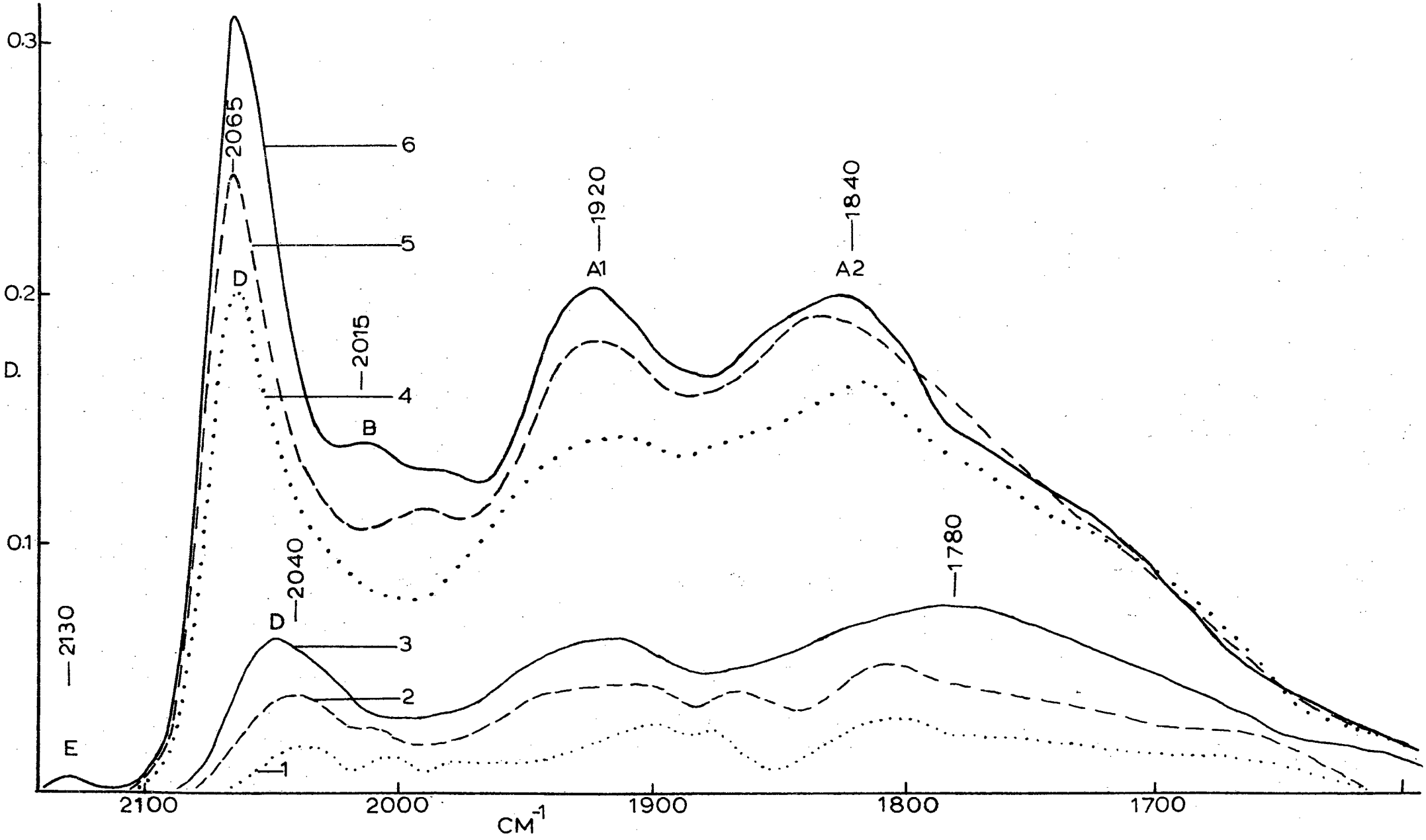

Fig. 46(a) Carbon monoxide chemisorbed on supported nickel, promoted with 20:100 K:Ni. Increasing pressures at 1) ~ 7×10^{-5} torr, 2) < 1×10^{-4} torr, 3) 1×10^{-4} torr, 4) 4×10^{-2} torr, 5) 0.35 torr, 6) 0.81 torr.

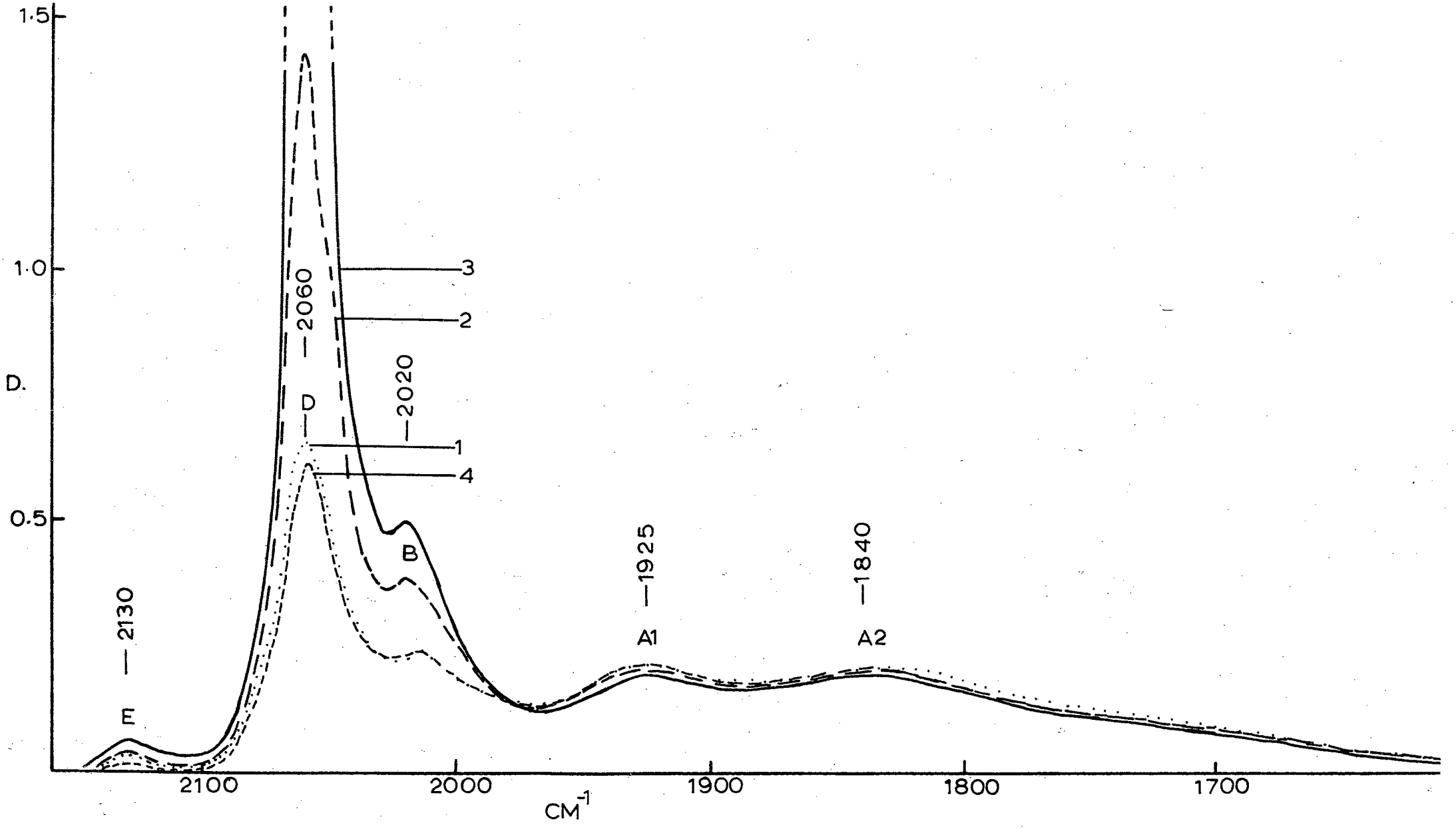

Fig. 46(b). Carbon monoxide chemisorbed on supported nickel, promoted with 20:100 K:Ni. Increasing pressures at 1) 2 torr, 2) 11 torr, 3) 40 torr. Decreasing pressures at 4) 2 torr.

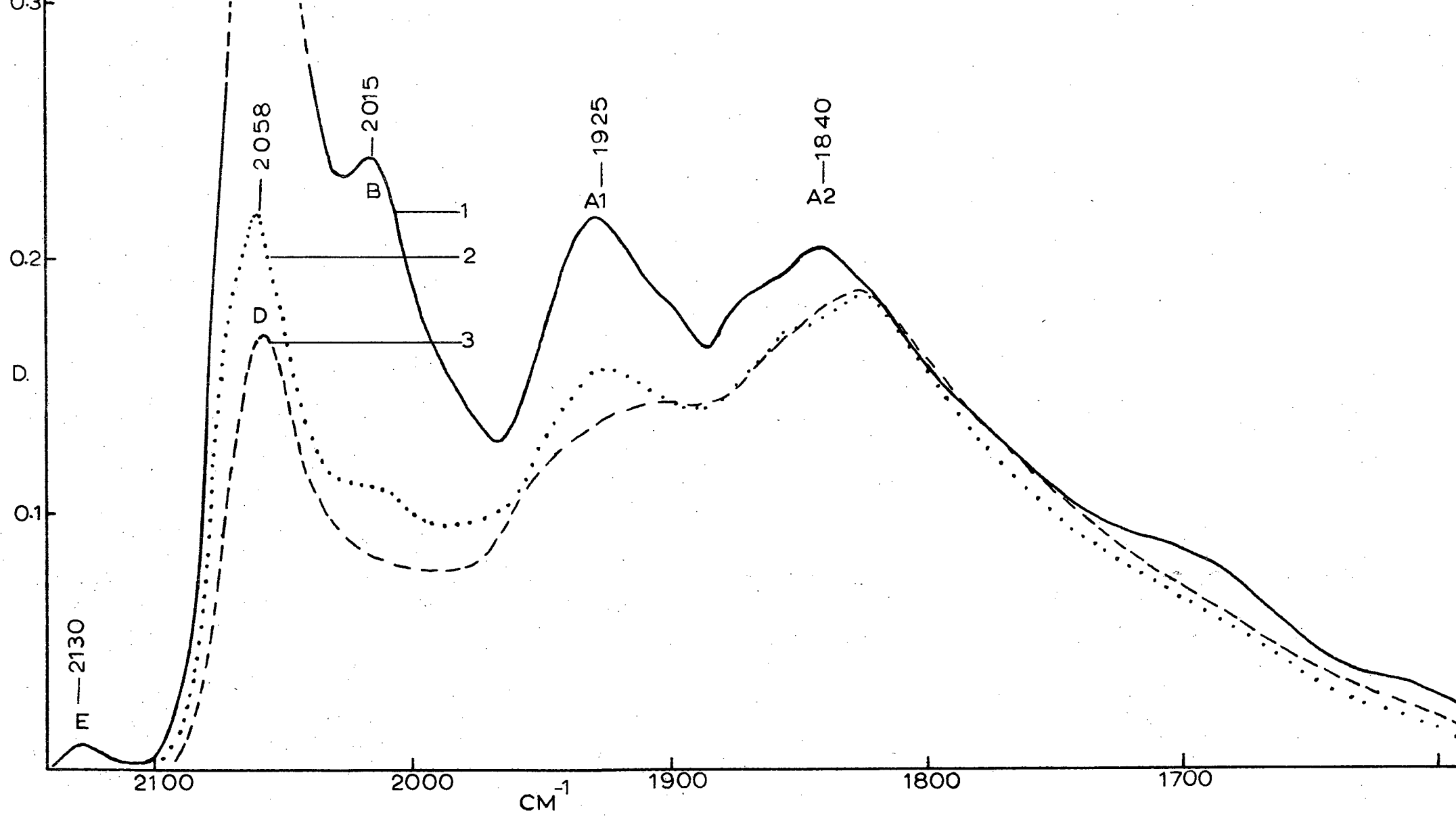

Fig. 46(c). Carbon monoxide chemisorbed on supported nickel, promoted with 20:100 K:Ni. Decreasing pressures at 1) 2 torr, 2) 0.7 torr, 3) 3×10^{-2} torr.

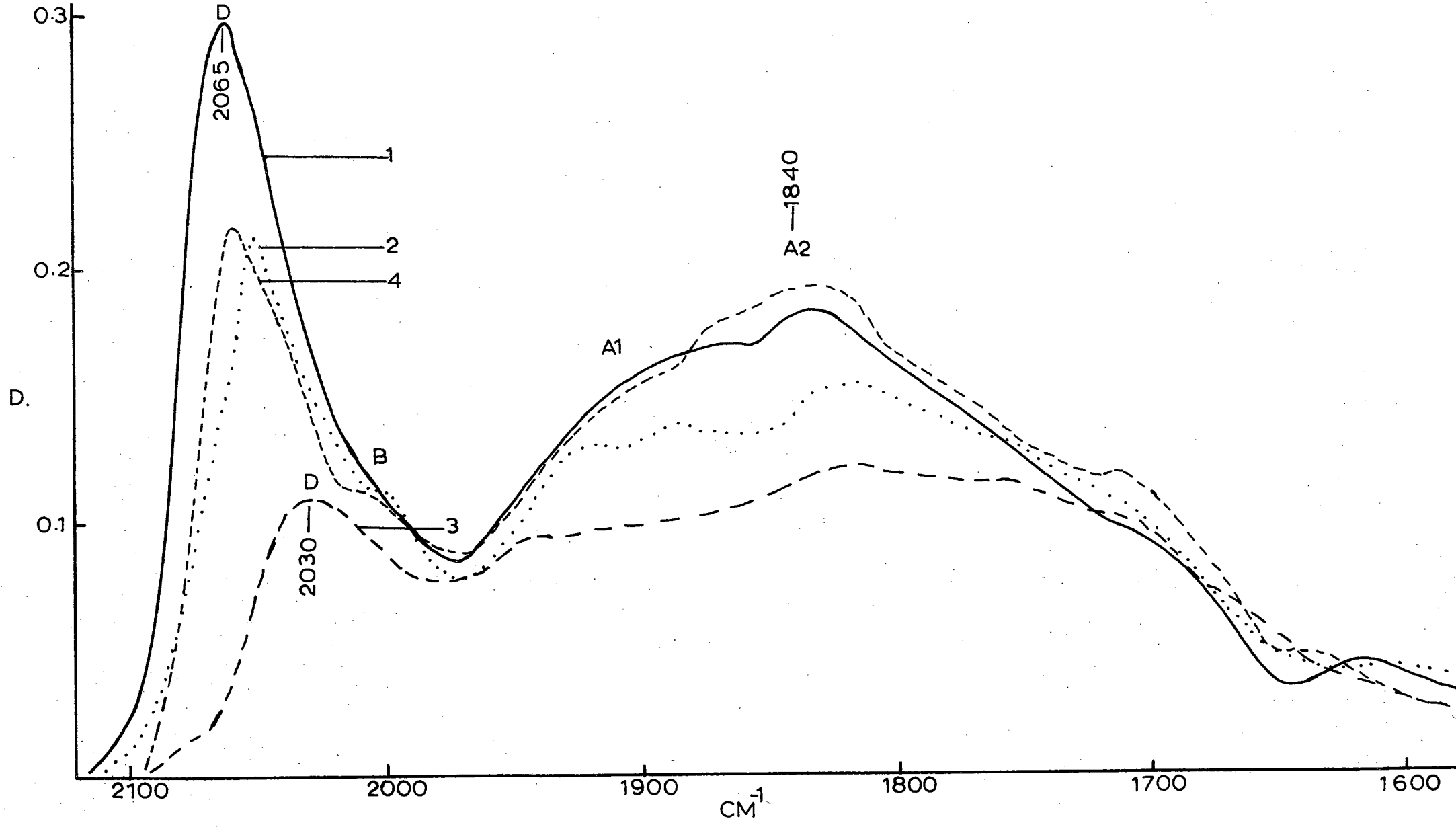

Fig. 47. Supported nickel, promoted with 10:100 K:Ni, plus 3.5×10^{-2} torr carbon monoxide at 1) room temperature, 2) 100°C, 3) 200°C, 4) back at room temperature.

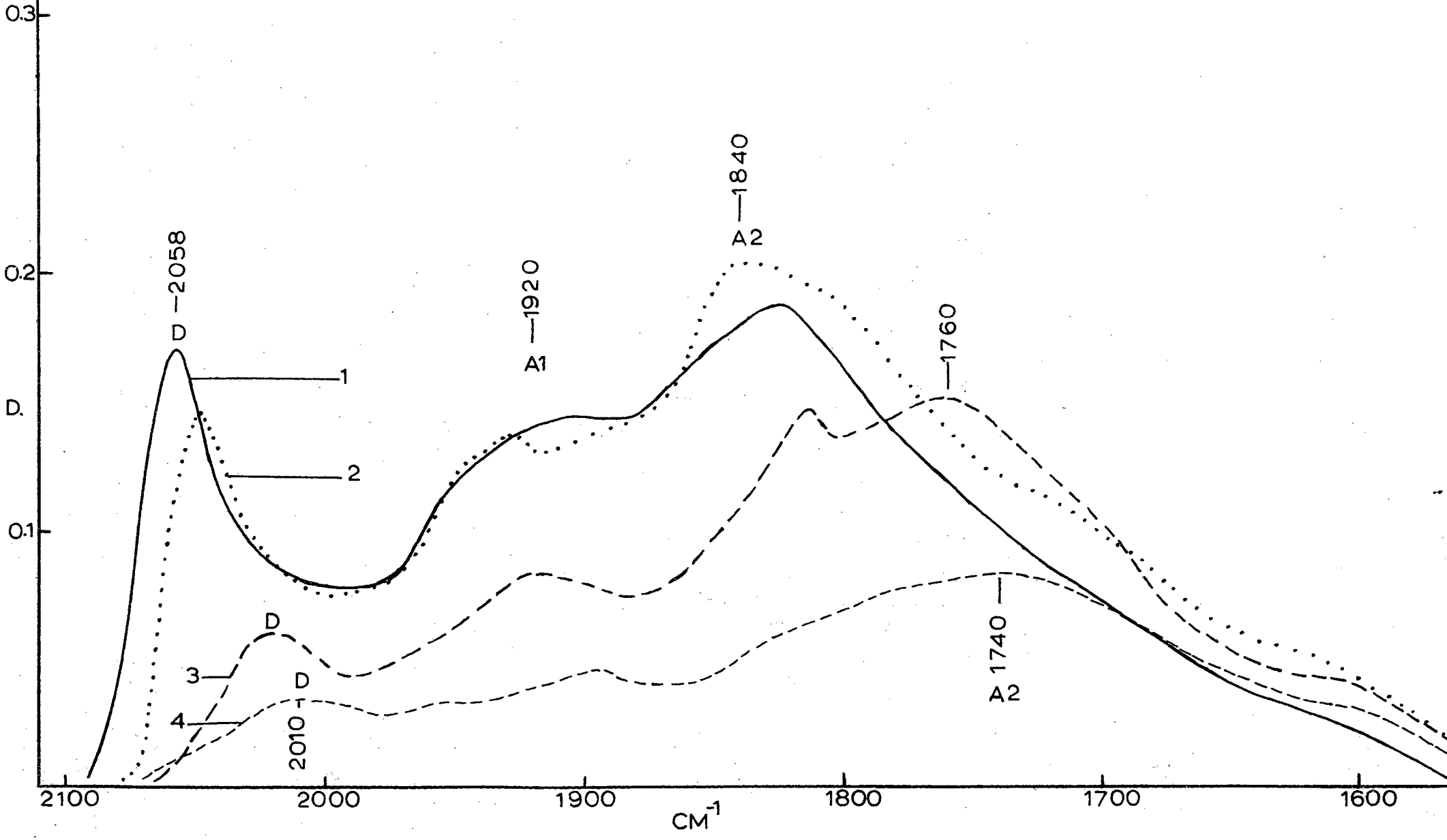

Fig. 48. Supported nickel, promoted with 20:100 K:Ni, plus 3.5×10^{-2} torr carbon monoxide at 1) room temperature, 2) 100°C, 3) 200°C, 4) 300°C.

a marked influence on the spectrum of hydrocarbon products. Usually, an increase in the potassium concentration causes a decrease in the short chain hydrocarbons produced; or, putting it the other way, an increase in the production of long chain hydrocarbons. Thus one might specifically conclude that potassium inhibits methane formation.This in turn leads one to the idea that this phenomenon might be exploited in elucidating aspects of problems aimed at discovering the mechanisms of reactions.

One of the reasons why previous attempts (in this project) to detect reaction intermediates on unpromoted nickel failed, was thought to be the fastness with which the methanation reaction is completed. Thus it was expected that the addition of potassium might give the intermediates a longer life-time, possibly making them more readily detectable.

The results obtained with a 2:100 K:Ni sample are shown in Figs. 49(a) and (b). This experiment was started with a 'low' H_2:CO mole ratio in the hope that this would also favour the formation of a high concentration of intermediates. However, no intermediates were detected spectroscopically. When the hydrogen pressure was increased drastically from 0.1 to 20 torr, methane and carbon dioxide were formed as can be seen from the spectra.

The above experiment was repeated with a 10:100 K:Ni ratio. The results are represented in Figs. 50(a) - (e). In Fig. 50(a) it can be seen that 3.5×10^{-2} torr carbon monoxide plus 0.1 torr hydrogen produced no intermediates and no methane. After the second heating cycle to 200°C (curve 3), a small amount of carbon dioxide was formed and its concentration increased gradually with the number of heating cycles. The amount after the fifth heating cycle can be deduced from the spectrum of Fig. 50(b), curve 1. The hydrogen pressure was now increased to 1 torr and the heating procedure repeated (Fig. 50(b), curve 3). It was found that this increase in the hydrogen pressure had no effect on the bands. Consequently, the hydrogen pressure was increased further to 11 torr (Fig. 50(c)). The heating procedure immediately yielded methane. It is also noticed that the amount of carbon dioxide now decreased with the number of heating cycles.

It should be noted that, up to now, the studies on the interaction between hydrogen and carbon monoxide was mainly done under conditions of very low carbon monoxide pressures. This could also be a reason why no intermediates were detected. Thus in an attempt to detect intermediates it was decided to increase the carbon monoxide pressure and employ a H_2:CO ratio unfavourable to the production of methane; i.e. in terms of the reaction

$$3\ H_2 + CO \longrightarrow CH_4 + H_2O.$$

115/

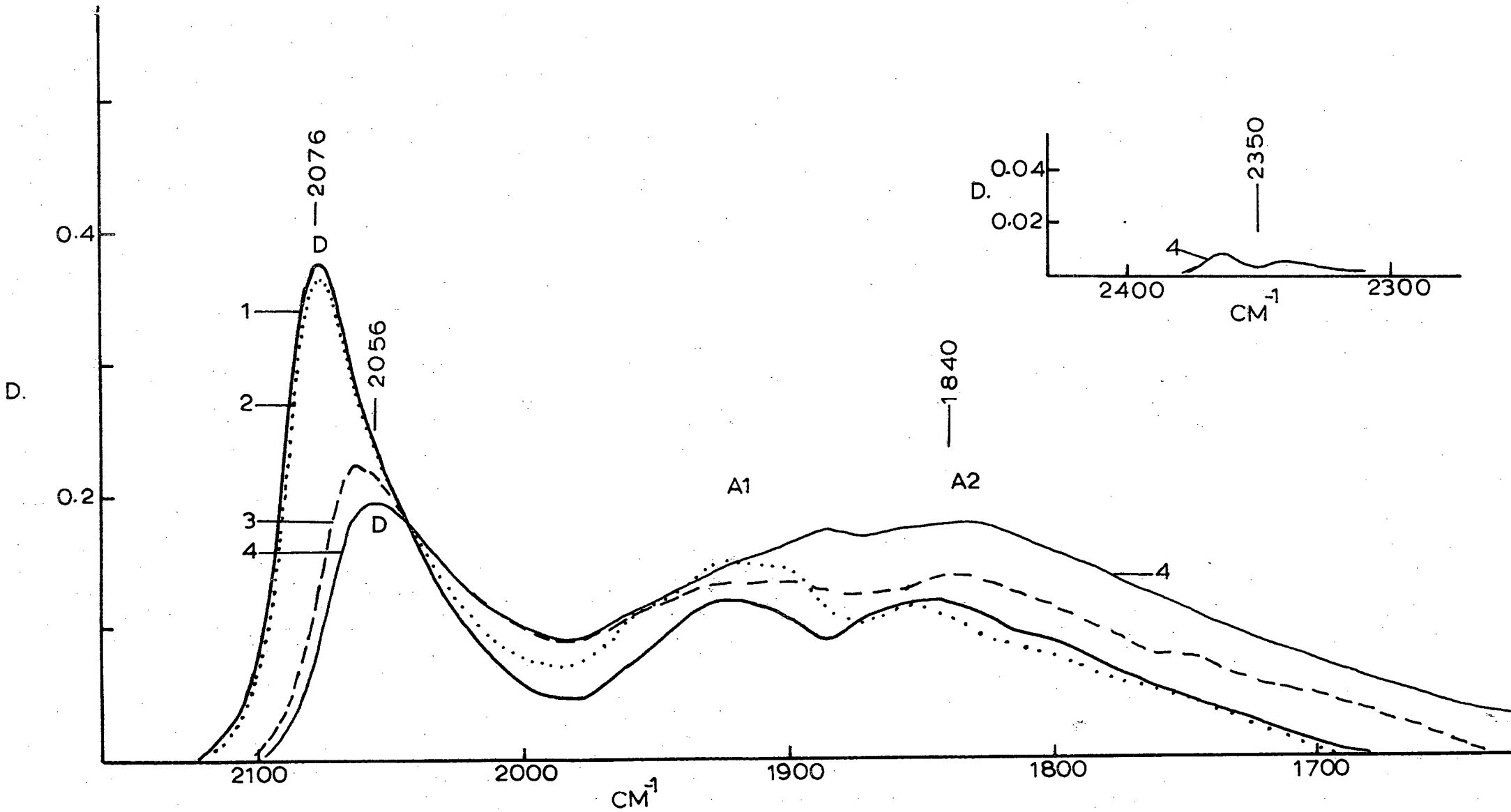

Fig. 49(a). Supported nickel, promoted with 2:100 K:Ni, plus 3.5×10^{-2} torr carbon monoxide 1) at room temperature, 2) plus 0.1 torr hydrogen at room temperature, 3) do, at 100°C, 4) plus 20 torr hydrogen at 100°C.

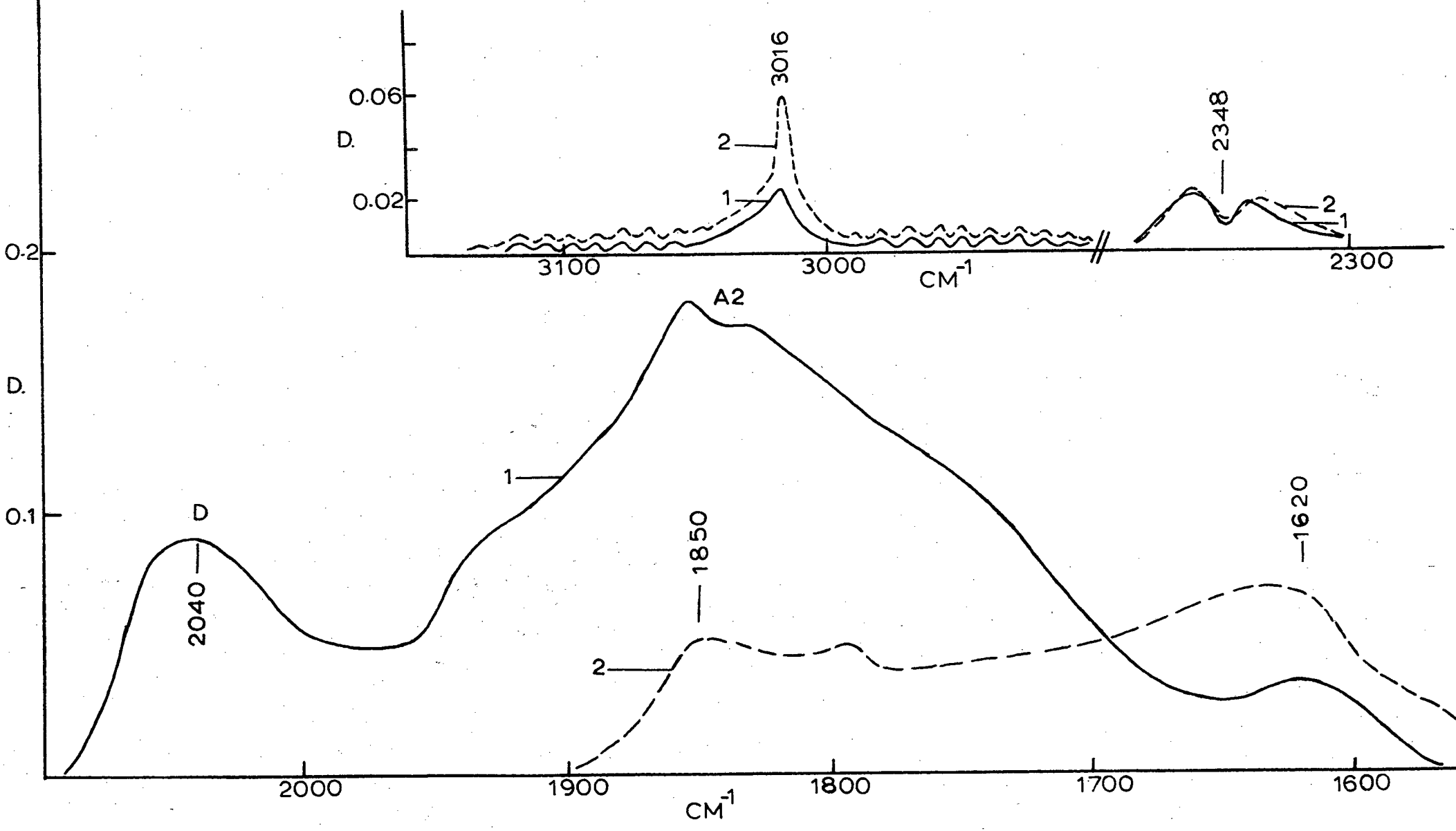

Fig. 49(b). Supported nickel, promoted with 2:100 K:Ni, plus 3.5×10^{-2} torr carbon monoxide and 20 torr hydrogen 1) at room temperature after heating to 200°C for 5 mins., 2) at room temperature, after heating to 300°C for 5 mins.

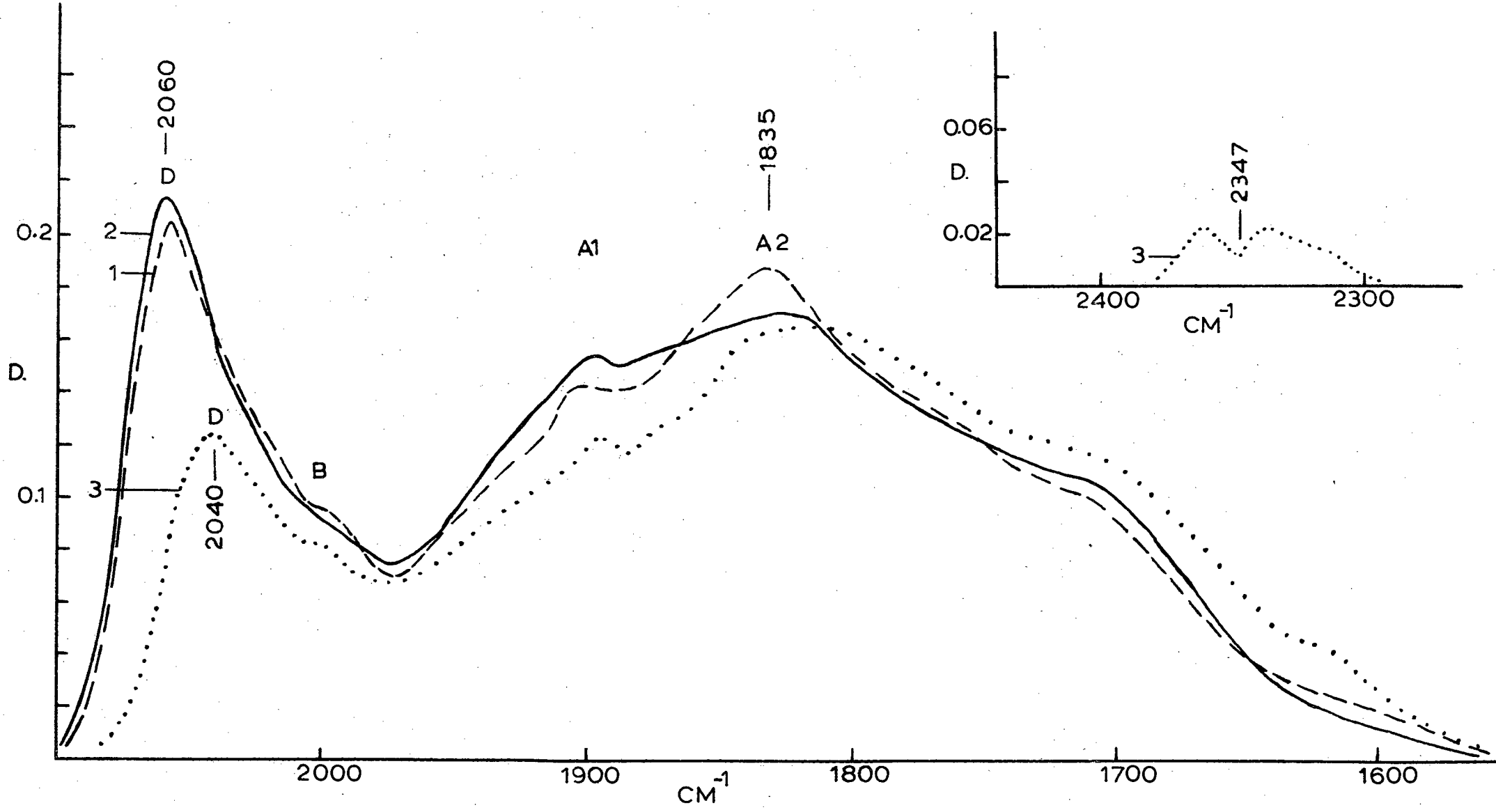

Fig. 50(a). Supported nickel, promoted with 10:100 K:Ni, plus 3.5×10^{-2} torr carbon monoxide, 1) at room temperature, 2) plus 0.1 torr hydrogen at room temperature, 3) at room temperature after heating (10 mins. at 200°C).

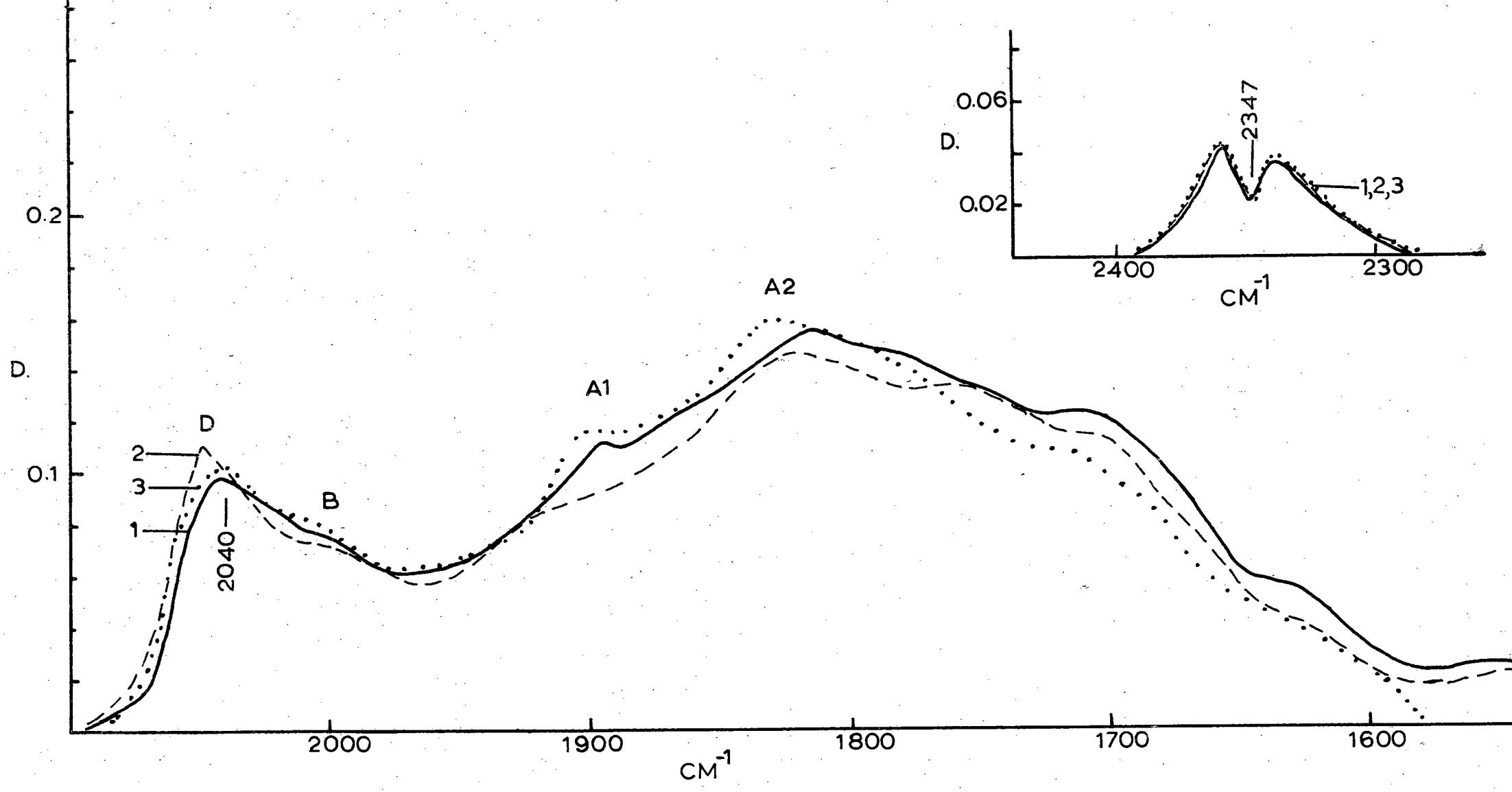

Fig. 50(b). Supported nickel, promoted with 10:100 K:Ni, plus 3.5×10^{-2} torr carbon monoxide and 0.1 torr hydrogen 1) at room temperature, after five heating/cooling cycles (i.e. heating to 200°C + cooling to room temperature), (total period at 200°C = 30 mins.), 2) plus 1 torr hydrogen at room temperature, 3) at room temperature, after another heating to 200°C for 10 mins.

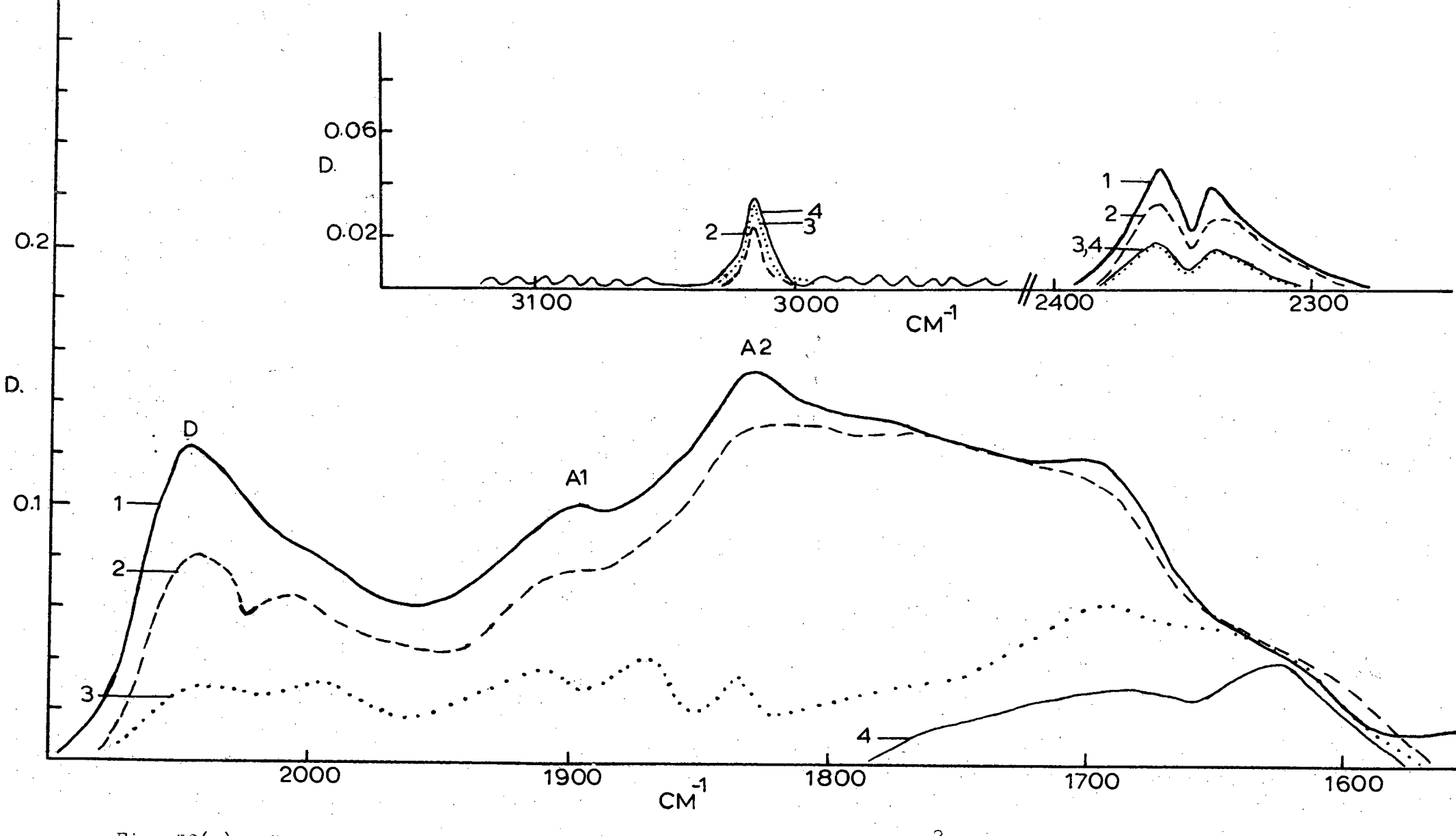

Fig. 50(c). Supported nickel, promoted with 10:100 K:Ni, plus 3.5×10^{-2} torr carbon monoxide and 11 torr hydrogen, 1) at room temperature, 2) at room temperature, after heating to 200°C for 5 mins., 3) at room temperature, after heating to 250°C for 5 mins., 4) room temperature, after second heating to 250°C for 5 mins.

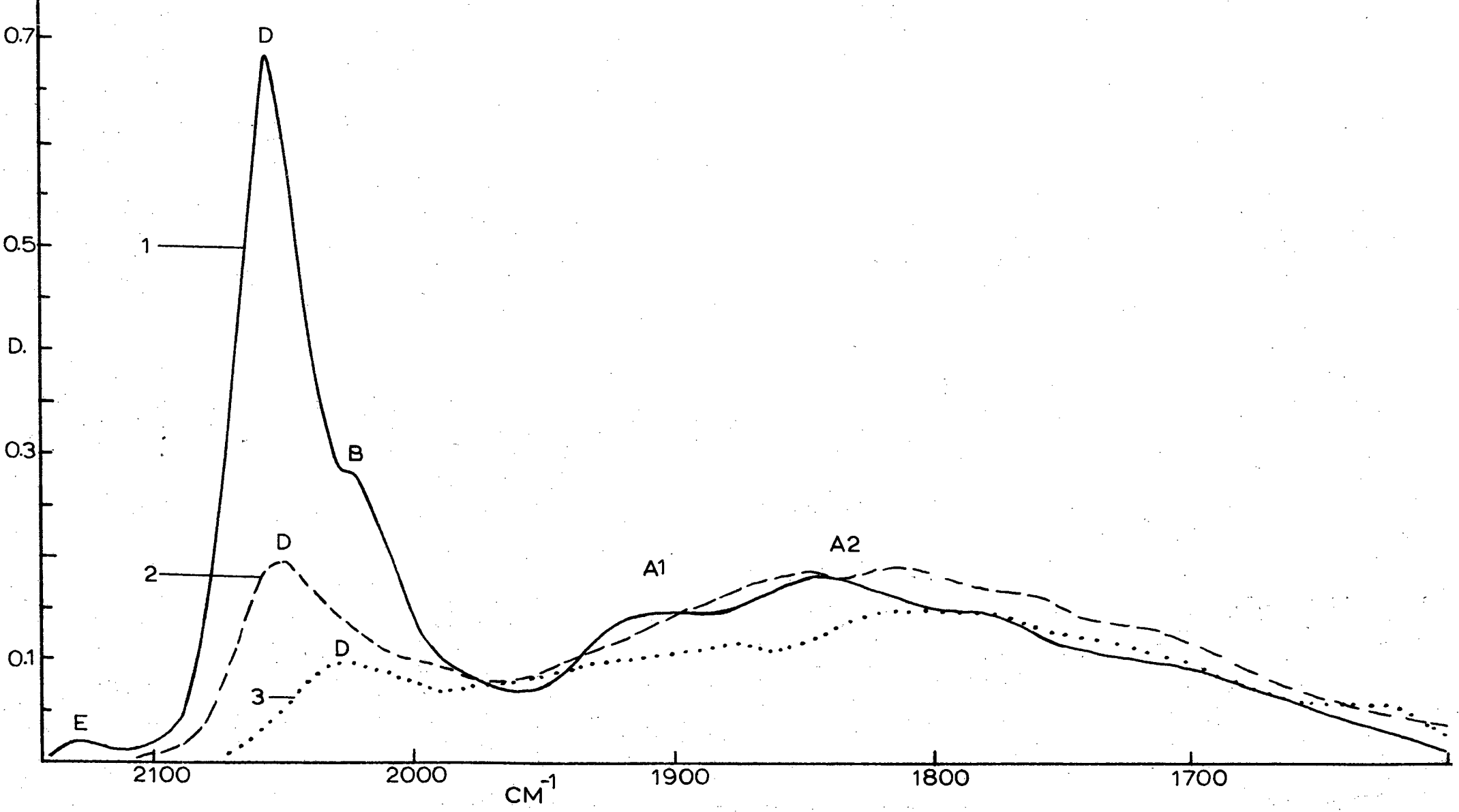

Fig. 50(d). Supported nickel, promoted with 10:100 K:Ni, plus 0.7 torr hydrogen followed by 1.3 torr carbon monoxide, 1) at room temperature, 2) at 100°C for 50 mins., 3) at 200°C for 45 mins.

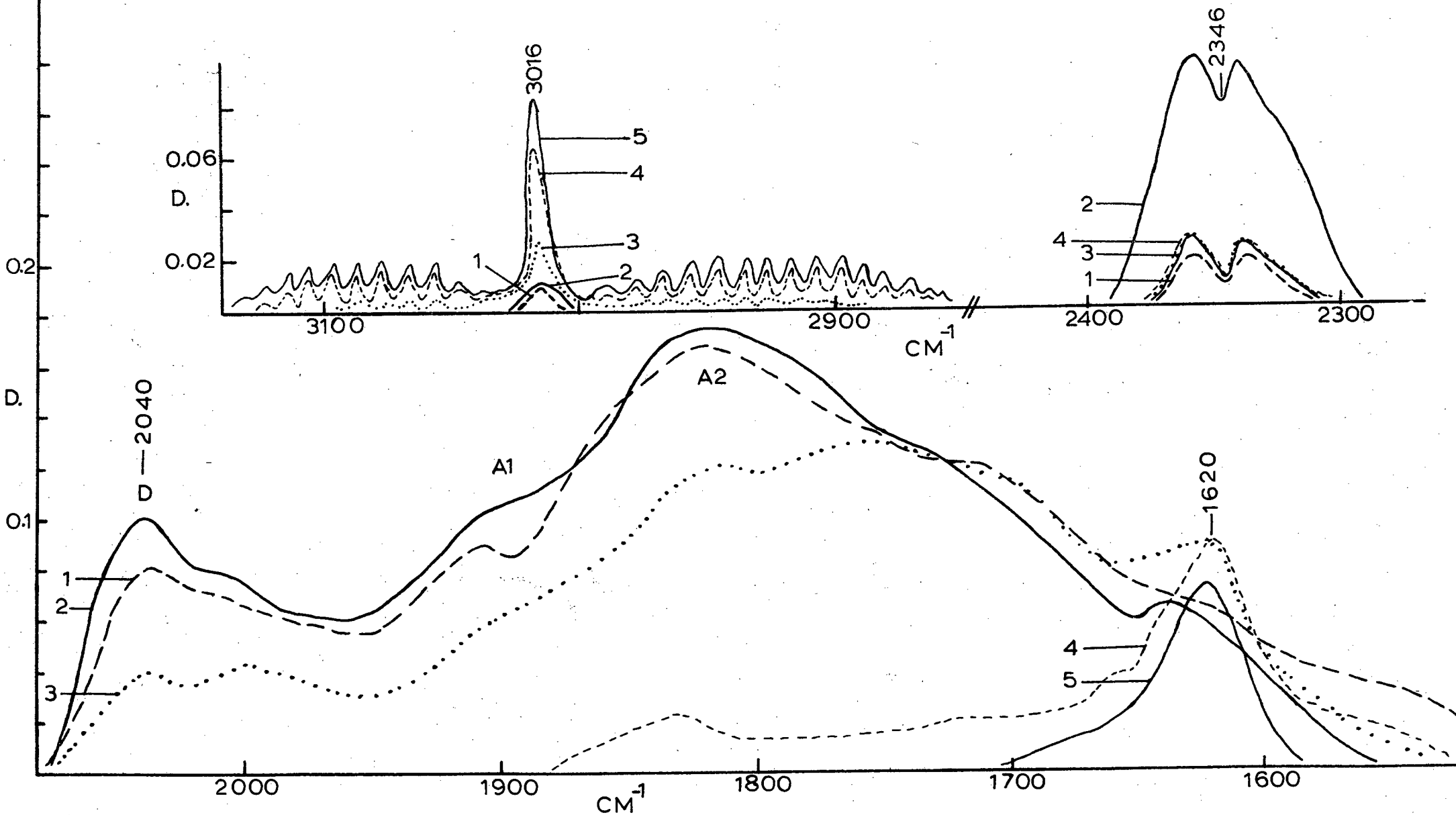

Fig. 50(e). Supported nickel, promoted with 10:100 K:Ni, plus 0.7 torr hydrogen and 1.3 torr carbon monoxide, 1) at room temperature, after heating to 250°C for 5 mins., 2) plus 20 torr hydrogen at room temperature, 3) room temperature after second heating to 220°C for 10 mins., 4) room temperature, after 6 heatings (of 10 mins. each) to 220°C; then P_{H_2} increased to 45 torr, followed by heating to 250°C for 10 mins., 5) room temperature, after heating to 300°C for 15 mins.

The cell was first evacuated to 6×10^{-6} torr and then 0.7 torr H_2 followed by 1.3 torr CO, admitted. From Fig. 50(d) it can be seen that even after 45 minutes at 200°C no detectable methane was formed. When the sample was heated to 250°C and cooled down to room temperature (Fig. 50(e), curve 1), small amounts of methane and carbon dioxide were formed. The hydrogen pressure was then increased to 20 torr. This had a marked pressure broadening effect on the carbon dioxide band (Fig. 50(e), curve 2). However, the next heating cycle to 220°C (curve 3), decreased the carbon dioxide concentration. On going through several heating cycles, the methane concentration increased while the bands due to carbon dioxide and chemisorbed CO gradually disappeared. In the end only a band at 1625 cm^{-1}, apart from those of carbon dioxide and methane, remained. Upon evacuation all the bands disappeared.

As a last effort in the search for intermediates on silica-supported nickel, the experiments were repeated on a 20:100 K:Ni sample. The spectra of 3×10^{-2} torr CO plus 9.5 torr H_2, recorded at different temperatures, are shown in Fig. 51(a). The results followed the same pattern as before.

After evacuation a mixture of hydrogen and carbon monoxide, at a pressure of 3.8 torr, was admitted to the cell. A H_2:CO ratio of 1:4.5 was used. The spectra, recorded at different temperatures, are presented in Fig. 51(b). It can be seen that the carbon dioxide concentration again increased with increasing temperature when a H_2:CO ratio, unfavourable to methane formation, was used. However, in the presence of excess hydrogen (curve 5), the carbon dioxide concentration immediately decreased, and a sharp increase in the methane concentration was observed.

Another interesting observation resulting from these experiments is that band A shifted towards lower wave numbers and increased in intensity with increasing temperatures (curves 2 and 3). These phenomena were observed previously (e.g. Figs. 49(a) and 50(a)) but the effects were not as pronounced as in this case.

APPENDIX 14

Carbon Monoxide Chemisorption on Cobalt Oxide:

Unpromoted Samples:

The adsorbent was prepared by evacuation of silica-supported cobalt oxide Type I at 250°C for 2½ hours, and then cooled down to room temperature in vacuo. When 23 torr carbon monoxide was adsorbed onto this sample,

116/.. .. .. ..

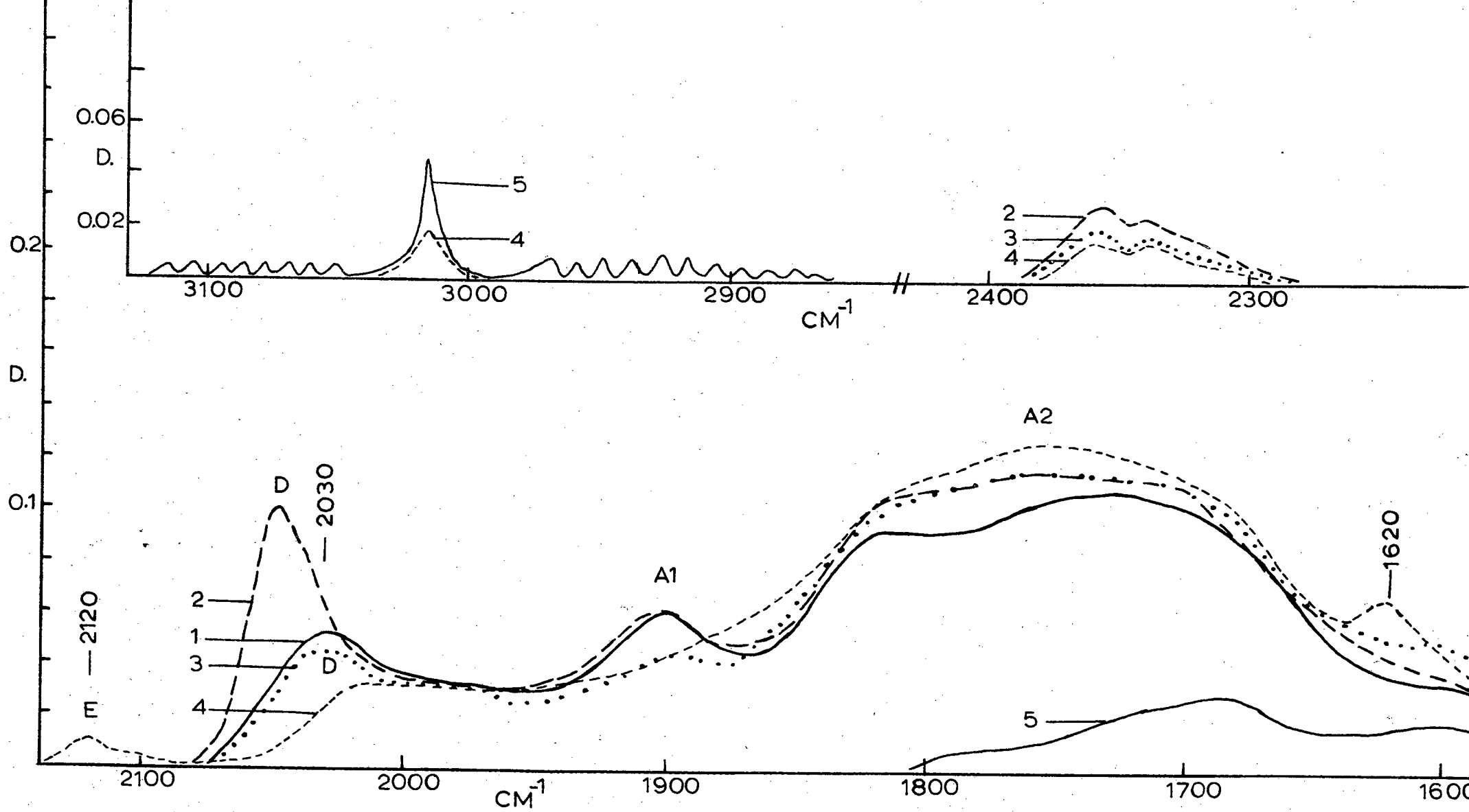

Fig. 51(a). Supported nickel, promoted with 20:100 K:Ni, plus 3.5×10^{-2} torr carbon monoxide, 1) at room temperature, 2) plus 9.5 torr hydrogen at room temperature, 3) at 100°C, 4) at 200°C, 5) at 300°C.

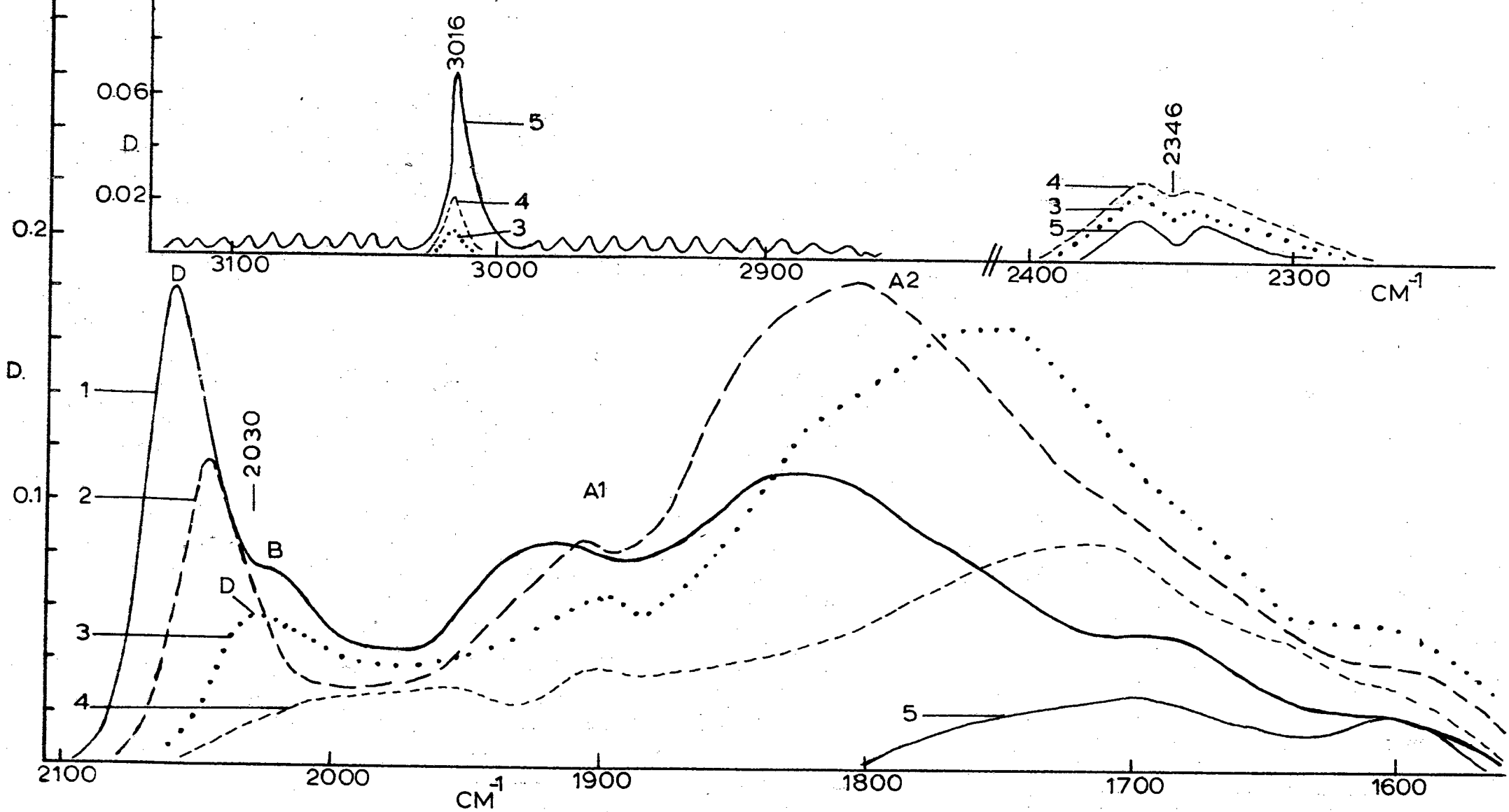

Fig. 51(b). Supported nickel, promoted with 20:100 K:Ni, plus 3.8 torr (hydrogen + carbon monoxide) mixture gas ($CO:H_2 = 1.45$), at 1) room temperature, 2) 100°C, 3) 200°C, 4) 300°C, 5) plus 20 torr hydrogen at 300°C.

the spectrum, as presented in Fig. 52(a), was obtained. Apart from the carbon dioxide doublet, only one band at about 2180 cm^{-1}, ascribed to chemisorbed CO, was found.

Promoted Samples:

The spectrum for carbon monoxide on cobalt oxide promoted with 10:100 K:Co are presented in Fig. 52(b). Bands ascribed to chemisorbed species were found at 2155 and 2170 cm^{-1}.

APPENDIX 15.

(A) Carbon Monoxide Chemisorbed on Silica-Supported Cobalt Type I:

In general it is more difficult to reduce silica-supported cobalt oxide than to reduce silica-supported nickel oxide. In order to overcome this difficulty, different reduction procedures were investigated. These involved varying the times, temperatures and hydrogen flow rates during reduction. In some cases fairly clean metal surfaces were obtained as measured by diminution of the intensity of the band at 2180 cm^{-1}. Unfortunately, when the reduction procedure was repeated on a new sample, the results could not always be reproduced for some or other obscure reason. However, that may be, the samples were active. Only the most interesting of the spectra will be discussed in the next few paragraphs.

When carbon monoxide was admitted to an active sample the spectra as represented in Figs. 53(a) and (b) were recorded. Bands were found at about 2025, 2070, 2095, 2130 and 2180 cm^{-1}. After 1 hour at room temperature (Fig. 53(a) curve 3) the band at 2180 cm^{-1} decreased in intensity, whereas all the others increased. Band B (at 2070 cm^{-1}) showed the biggest increase in intensity with increasing carbon monoxide pressure. (One may therefore conclude that a band C is formed almost on the same position as B). When the carbon monoxide pressure was decreased band A (at 2025 cm^{-1}) increased further while B (+C) at 2070 cm^{-1} and D (at 2095 cm^{-1}) decreased. Upon decreasing the carbon monoxide pressure, band A was found to be the most persistent, followed by bands B and D in that order. Bands E (at 2130 cm^{-1}) and F (at 2180 cm^{-1}) completely disappeared upon evacuation. It was also noticed that band A displayed shoulders at about 1970 and 1850 cm^{-1}.

Note: In general it was found for many samples that band B (and perhaps D and E) was absent or ill-defined initially on admittance of carbon monoxide. On leaving the carbon monoxide in contact with the catalyst surface for several hours

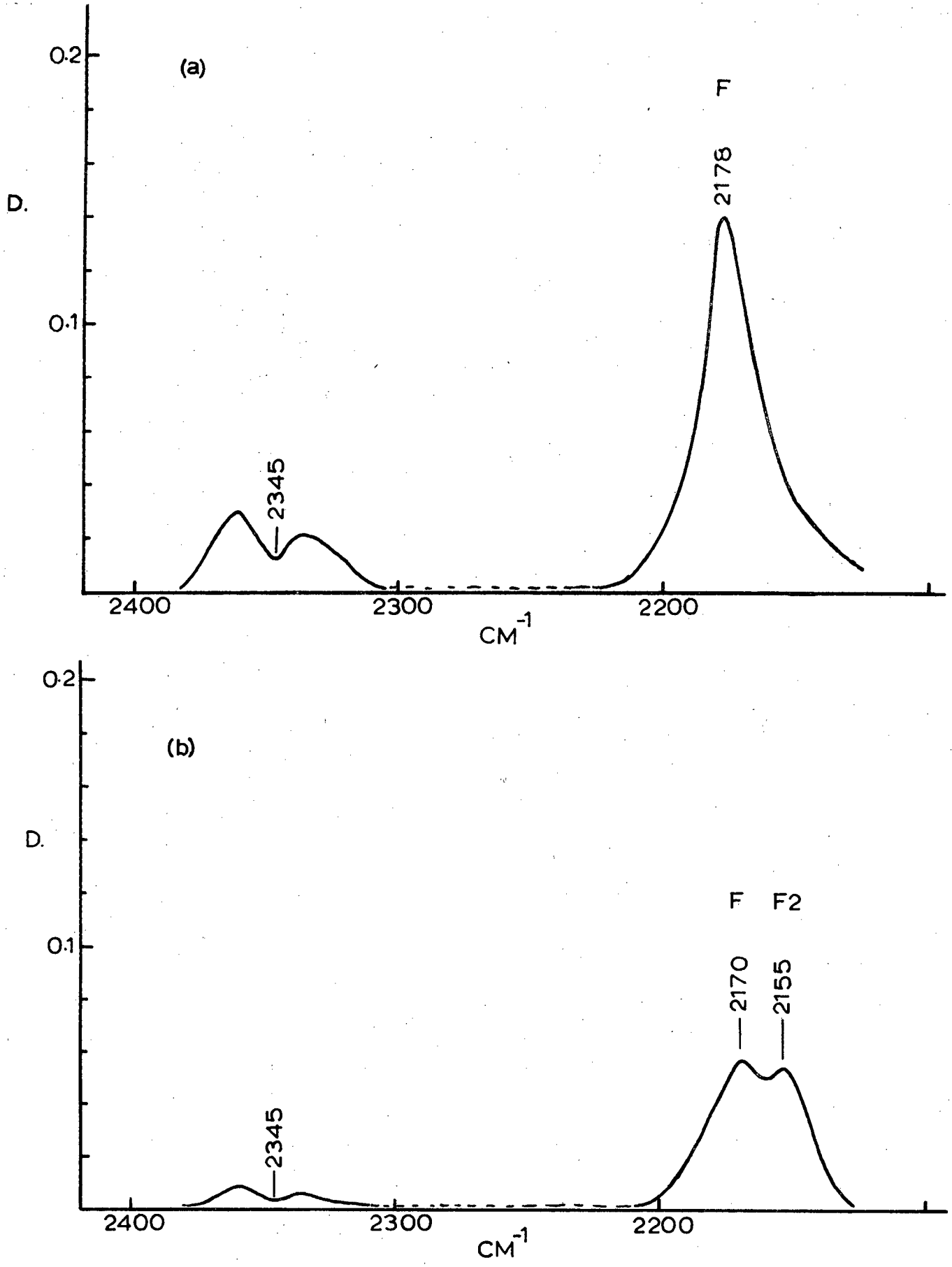

Fig. 52. (a) Supported cobalt oxide (evacuated at 250°C for $2\frac{1}{2}$ hours), plus 23 torr carbon monoxide.

(b) Supported cobalt oxide, promoted with 10:100 K:Co, plus 3 torr carbon monoxide.

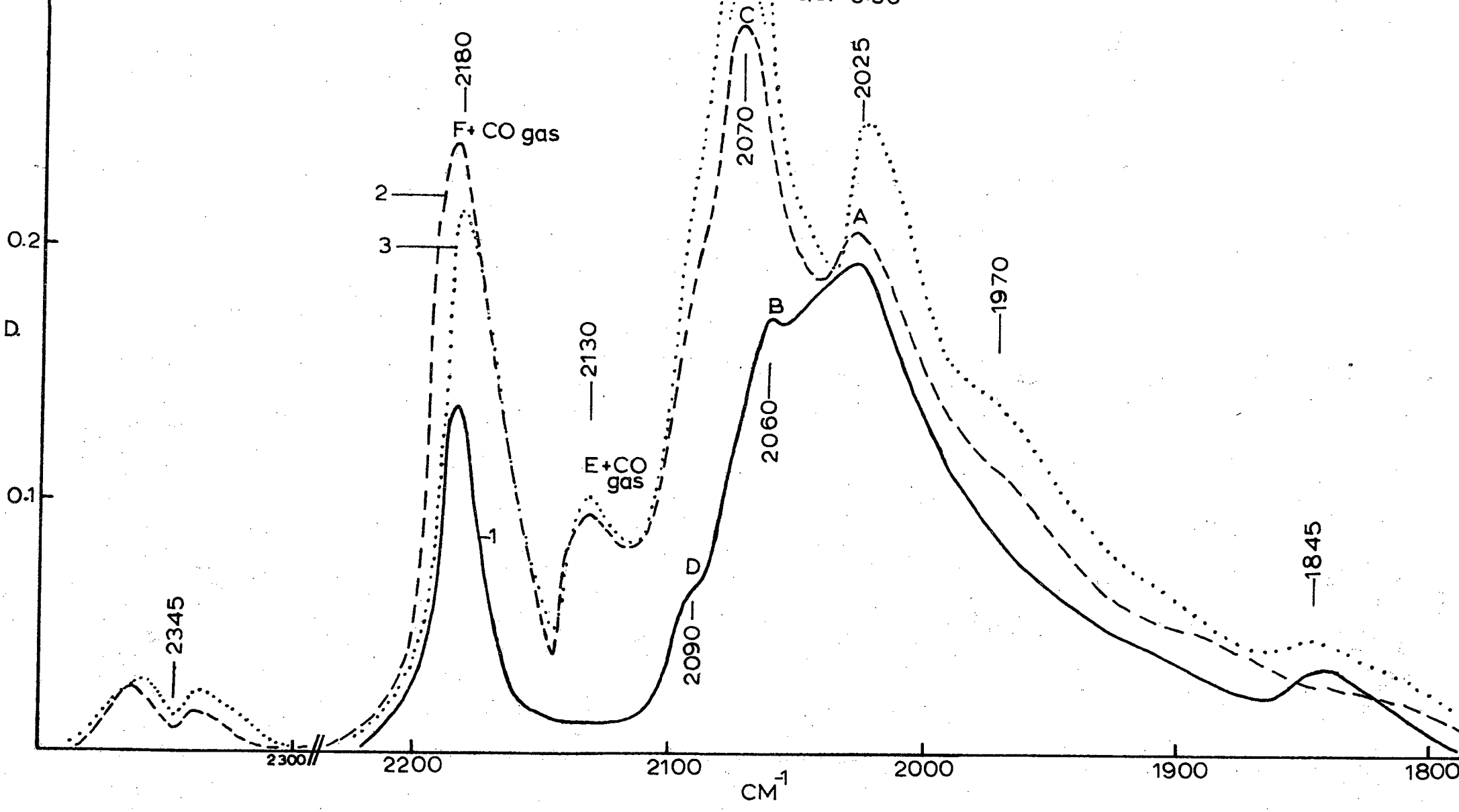

Fig. 53(a). Carbon monoxide chemisorbed on supported cobalt Type I. Increasing pressures at 1) 3 torr, 2) 79 torr, 3) 79 torr after 1 hour.

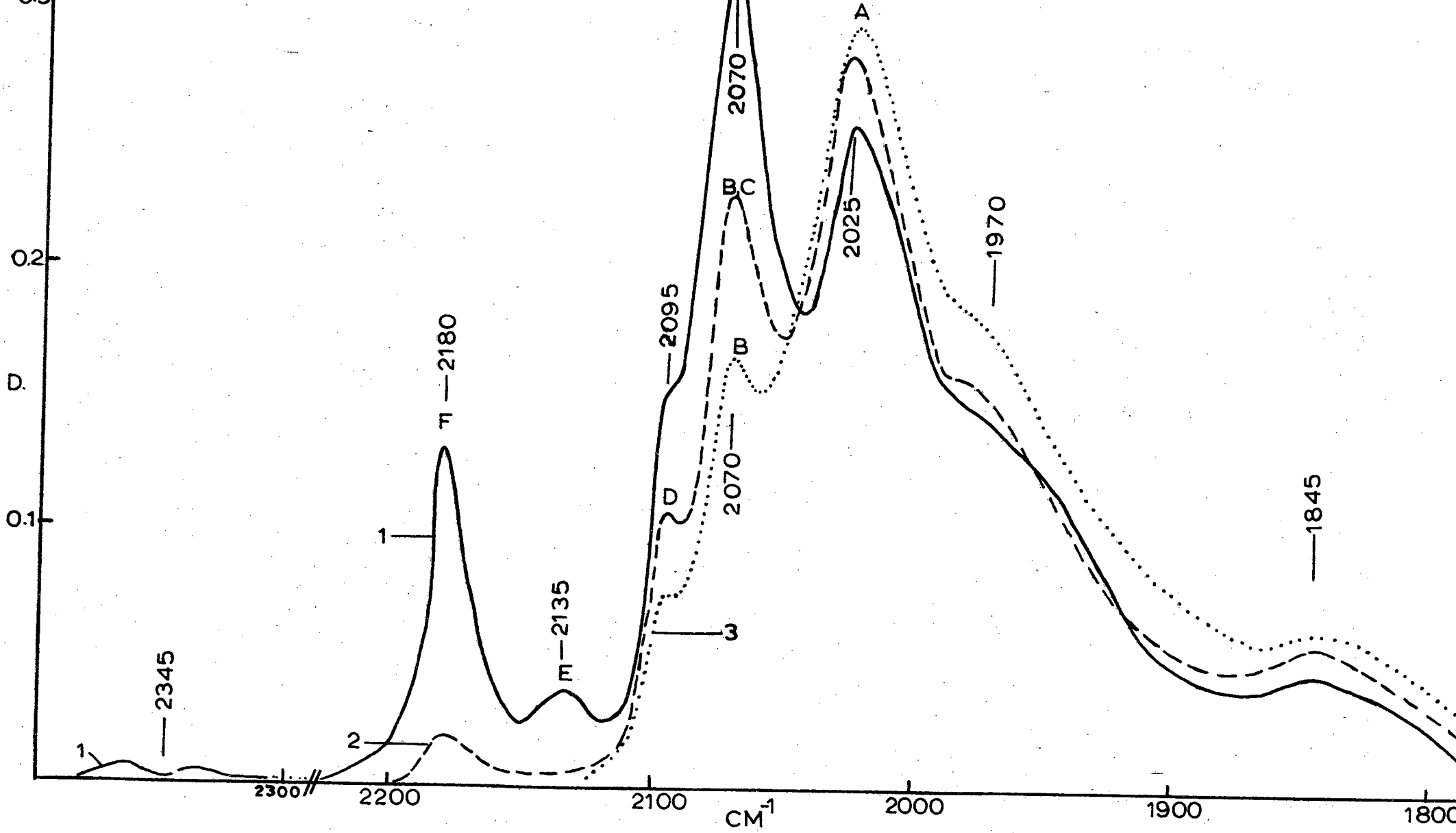

Fig. 53(b). Carbon monoxide chemisorbed on supported cobalt Type I. Decreasing pressures at 1) 15 torr, 2) 1.7×10^{-2} torr, 3) 2×10^{-5} torr.

the intensities of all the bands usually improved. It seems therefore that the treatment with carbon monoxide has a more beneficial effect, as it were, regarding the activity of the sites (especially the B sites), than has the hydrogen reduction.

(B) Carbon Monoxide Chemisorbed on Silica-Supported Cobalt Type III:

With precautions taken to minimise compound formation between the cobalt salt and the silica carrier, this sample was expected to be comparatively active. However, as can be seen from Figs. 54(a), (b) and (c), there was no significant change in the results, as compared with those obtained with Type I samples.

From Fig. 54(a) it can be seen that bands A, B and D were ill-defined and remained so with increasing carbon monoxide pressure. Band E is not plotted at the high pressures because of its superposition on the P-branch of the gas phase carbon monoxide. The position and intensity of band F were also disturbed by the R-branch of the gas phase carbon monoxide, but to a lesser extent. With decreasing pressures all the bands were better resolved (Fig. 54(b)). Band A again displayed shoulders at about 1970 and 1850 cm^{-1}. Upon prolonged evacuation, E and F disappeared. From Fig. 54(c) it can be seen that the intensities of B and D were directly related to the carbon monoxide pressure; the intensity of B being the most sensitive. The intensity of band A was again found to be inversely proportional to a function (not determined) of the carbon monoxide pressure.

APPENDIX 16.

Carbon Monoxide Chemisorbed on Potassium Promoted Cobalt:

When carbon monoxide chemisorbed on silica-supported cobalt promoted with a K:Co ratio of 2:100, the spectra as represented in Fig. 55(a) and (b) were found. Band A (at about 2030 cm^{-1}) was again found to be the most persistent at low pressures. Bands B (at about 2050 cm^{-1}), C (at 2060 cm^{-1}), and D (at about 2095 cm^{-1}), were found at slightly lower wave numbers as compared to samples prepared without potassium. When carbon monoxide was chemisorbed on a sample promoted with a K:Co ratio of 10:100 all the bands were further shifted to lower frequencies. The results are presented in Fig. 56(a) and (b).

The chemisorption of carbon monoxide was repeated on a 20:100 K:Co sample and it was found that the increased potassium concentration further shifted the bands towards lower wave numbers. The results are shown in Fig. 57(a) and (b).

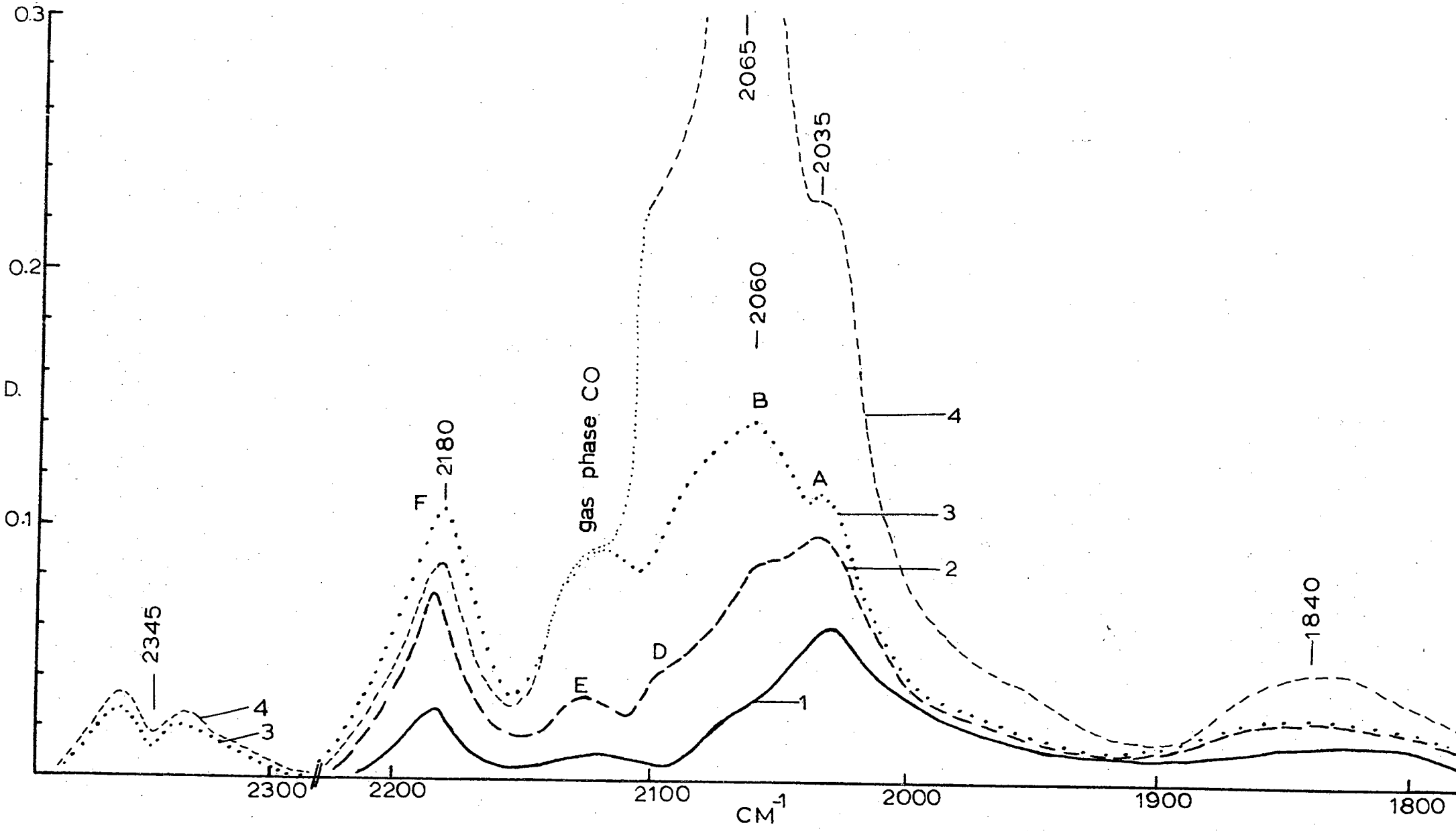

Fig. 54(a). Carbon monoxide chemisorbed on supported cobalt Type III. Increasing pressures at 1) 2 torr, 2) 27 torr, 3) 82 torr, 4) 82 torr after 3 hours.

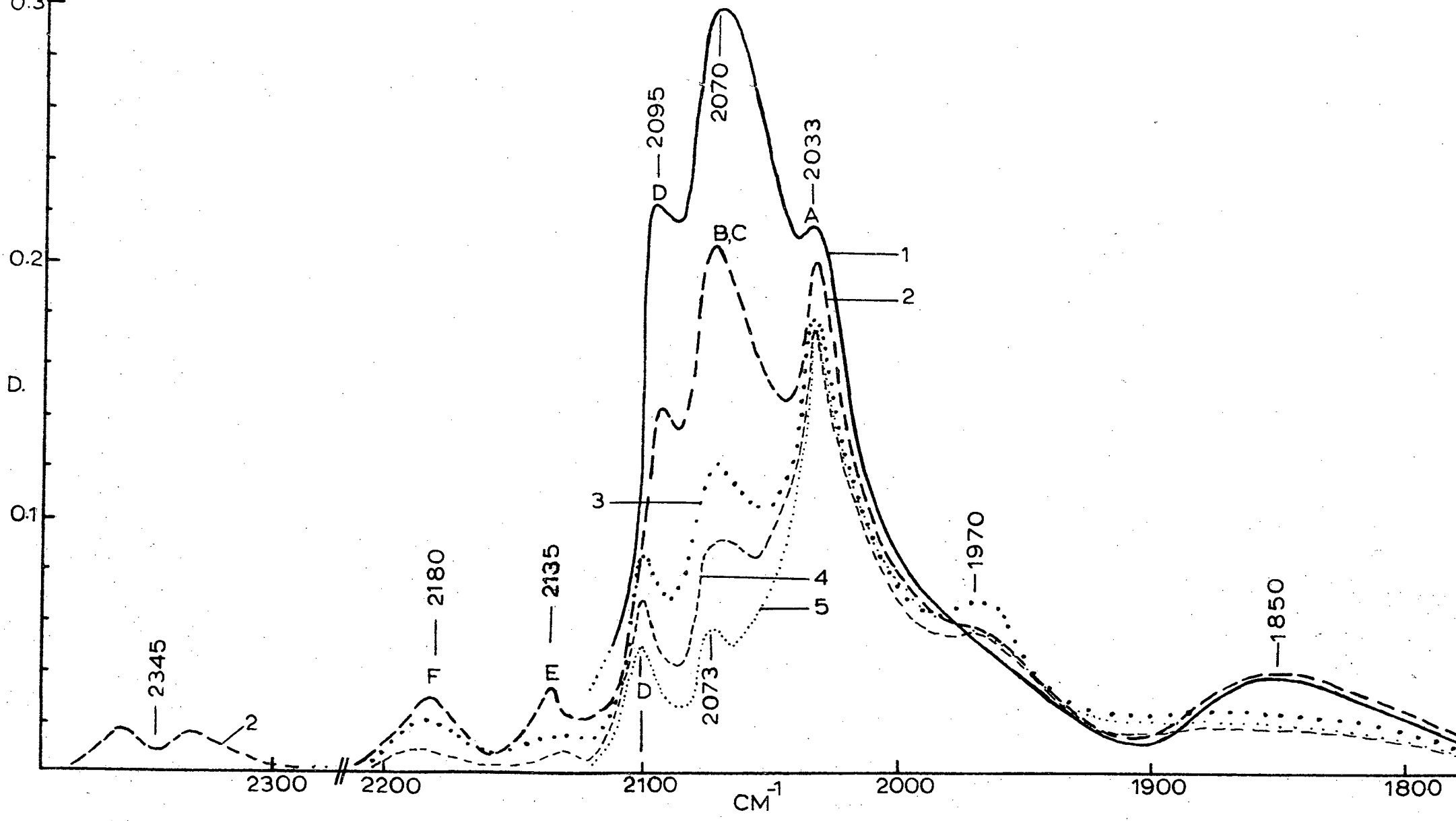

Fig. 54(b). Carbon monoxide chemisorbed on supported cobalt Type III. Decreasing pressures at 1) 35 torr, 2) 11 torr, 3) 1 torr, 4) 0.1 torr, 5) 2×10^{-4} torr.

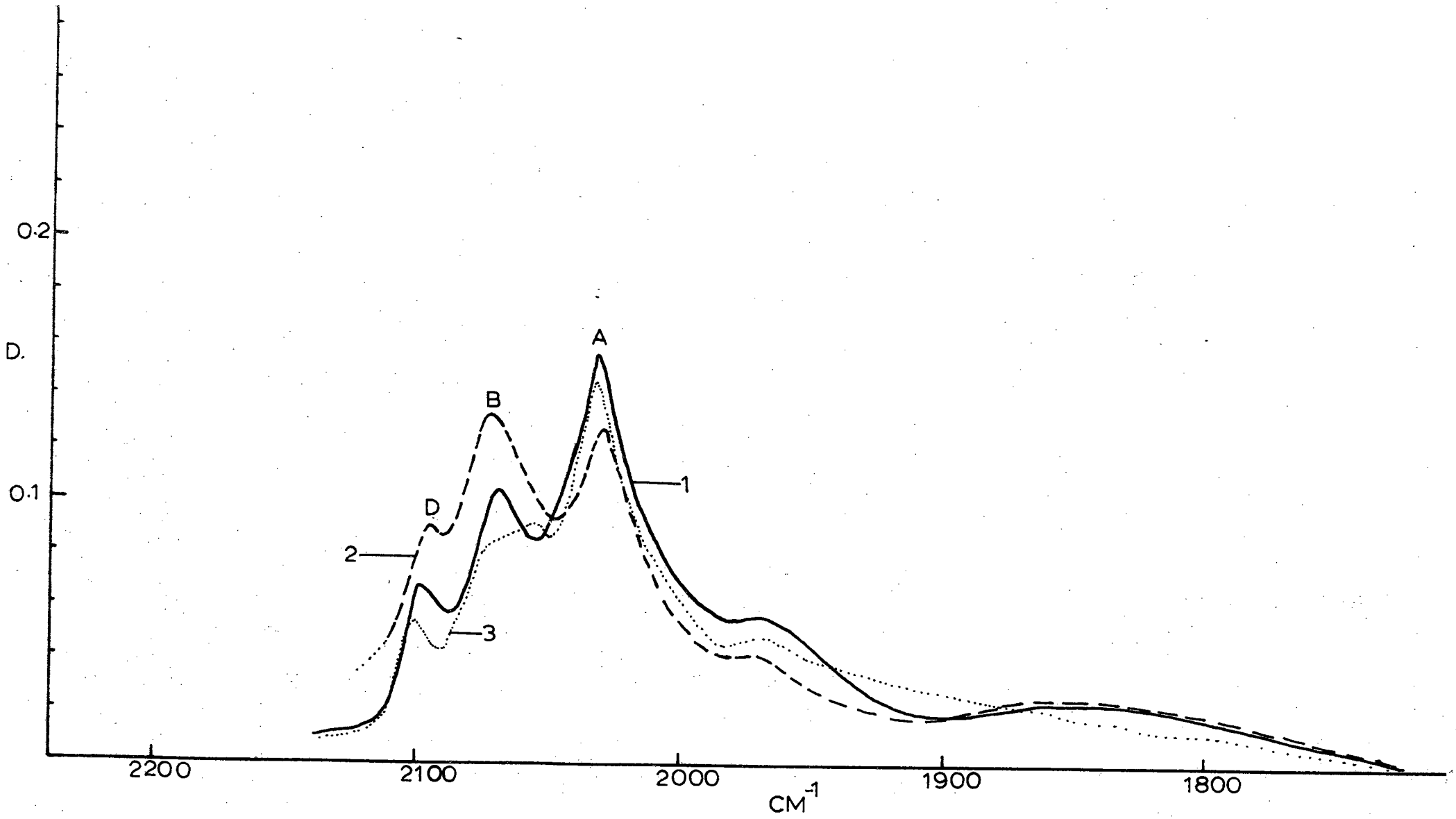

Fig. 54(c). Carbon monoxide chemisorbed on supported cobalt Type III. Increasing pressures at 1) 2 torr, 2) 41 torr. Decreasing pressures at 3) 1 torr.

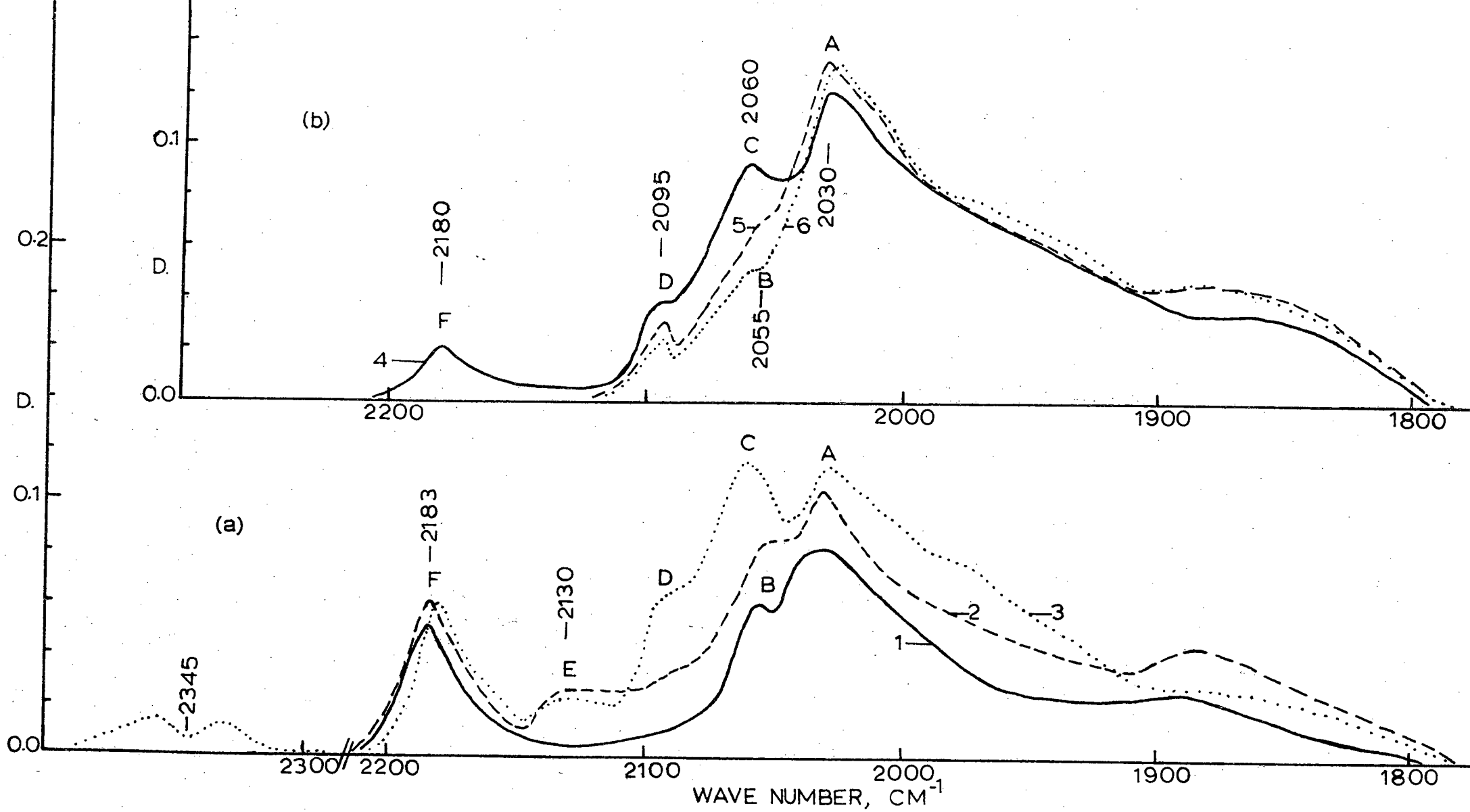

Fig. 55. Carbon monoxide chemisorbed on supported cobalt, promoted with 2:100 K:Co. (a) Increasing pressures at 1) 3 torr, 2) 15 torr, 3) 15 torr after 3 days.
(b) Decreasing pressures at 4) 1 torr, 5) 6×10^{-3} torr, 6) 1×10^{-4} torr.

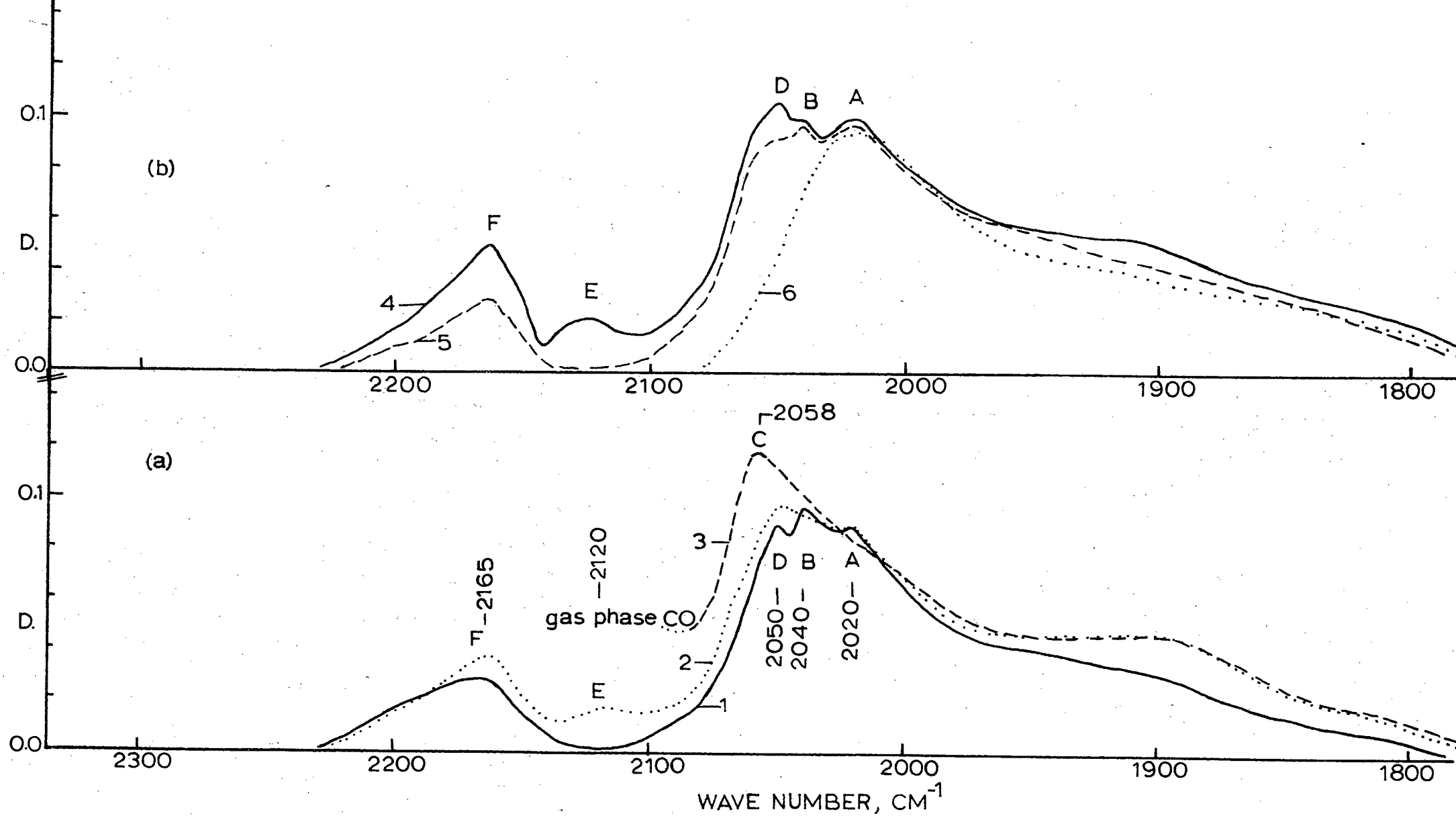

Fig. 56. Carbon monoxide chemisorbed on supported cobalt, promoted with 10:100 K:Co.
(a) Increasing pressures at 1) 3 torr, 2) 15 torr, 3) 80 torr.
(b) Decreasing pressures at 4) 15 torr, 5) 3 torr, 6) 5×10^{-5} torr.

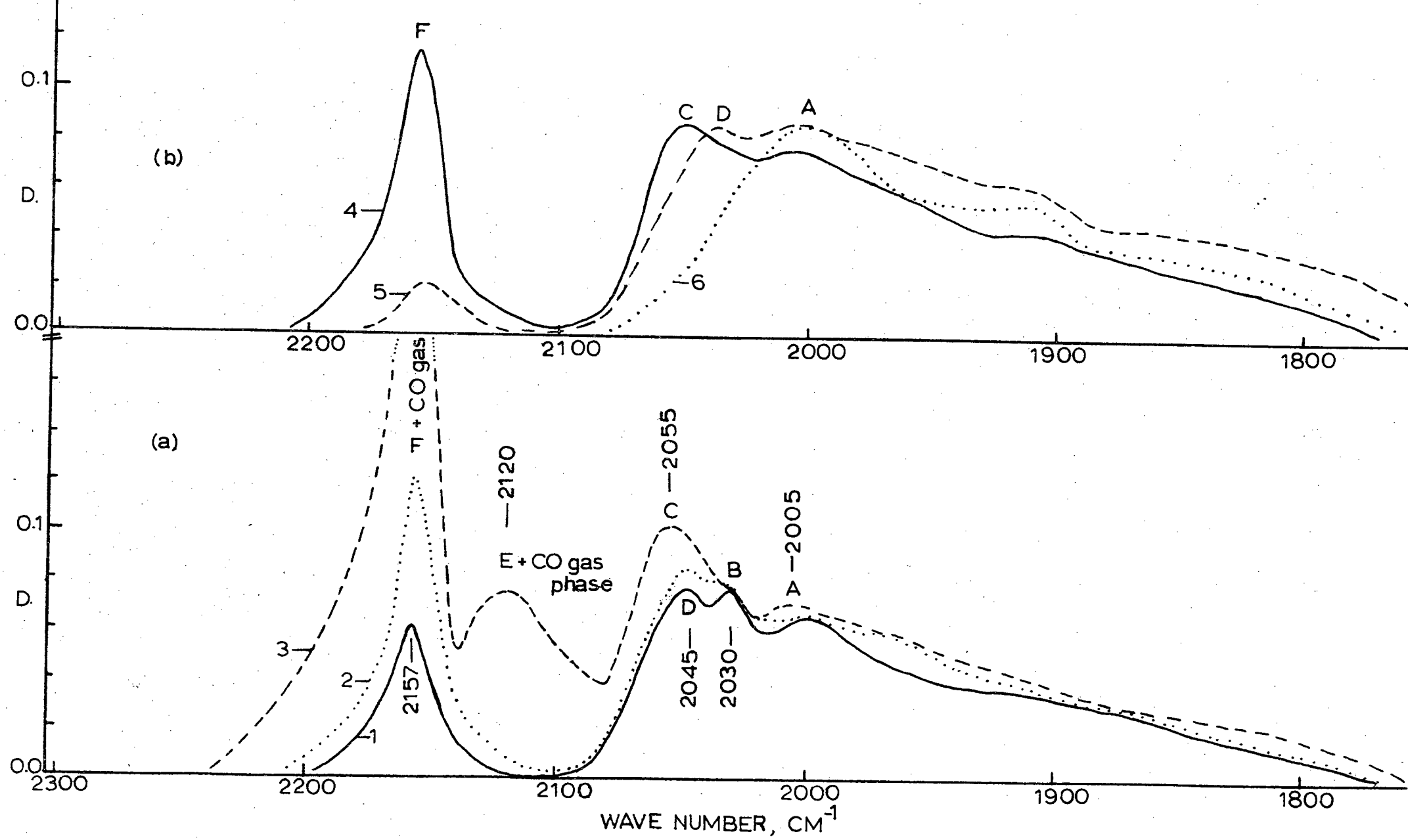

Fig. 57. Carbon monoxide chemisorbed on supported cobalt, promoted with 20:100 K:Co.
(a) Increasing pressures at 1) 3 torr, 2) 15 torr, 3) 80 torr.
(b) Decreasing pressures at 4) 15 torr, 5) 0.12 torr, 6) 2x10-5 torr.

Note: In general it was found that bands B and D become more ill-defined as the potassium concentration increased. This may be ascribed to increasing poisoning of the B and D sites, or to the fact that these two bands were more rapidly displaced to lower wave numbers, with increasing potassium concentration, relative to A. Therefore, bands B and D were possibly camouflaged by A.

REFERENCES

See Chapter 4.